MULTIDISCIPLINARY CENTER FOR EARTHQUAKE ENGINEERING RESEARCH
A National Center of Excellence in Advanced Technology Applications

ISSN 1520-295X

FEDERAL HIGHWAY ADMINISTRATION

A Risk-Based Methodology for Assessing the Seismic Performance of Highway Systems

by

Stuart D. Werner, Craig E. Taylor, James E. Moore III,
Jon S. Walton and Sungbin Cho
Seismic Systems & Engineering Consultants
8601 Skyline Boulevard
Oakland, California 94611

Technical Report MCEER-00-0014

December 31, 2000

This research was conducted by Seismic Systems & Engineering Consultants and was supported by the Federal Highway Administration under contract number DTFH61-92-C-00106.

NOTICE

This report was prepared by Seismic Systems & Engineering Consultants as a result of research sponsored by the Multidisciplinary Center for Earthquake Engineering Research (MCEER) through a contract from the Federal Highway Administration. Neither MCEER, associates of MCEER, its sponsors, Seismic Systems & Engineering Consultants, nor any person acting on their behalf:

a. makes any warranty, express or implied, with respect to the use of any information, apparatus, method, or process disclosed in this report or that such use may not infringe upon privately owned rights; or

b. assumes any liabilities of whatsoever kind with respect to the use of, or the damage resulting from the use of, any information, apparatus, method, or process disclosed in this report.

Any opinions, findings, and conclusions or recommendations expressed in this publication are those of the author(s) and do not necessarily reflect the views of MCEER or the Federal Highway Administration.

MCEER
MULTIDISCIPLINARY CENTER FOR EARTHQUAKE ENGINEERING RESEARCH
A National Center of Excellence in Advanced Technology Applications

A Risk-Based Methodology for Assessing the Seismic Performance of Highway Systems

by

Stuart D. Werner[1], Craig E. Taylor[2], James E. Moore III[3],
Jon S. Walton[4] and Sungbin Cho[5]

Publication Date: December 31, 2000

Technical Report MCEER-00-0014

Task Number 106-E-7.3.1

FHWA Contract Number DTFH61-92-C-00106

1 Principal, Seismic Systems & Engineering Consultants, Oakland, CA
2 President, Natural Hazards Management, Inc., Torrance, CA
3 Associate Professor, Department of Civil and Environmental Engineering and the School of Policy, Planning and Development, University of Southern California
4 Vice President, McFarland-Walton Enterprise, Pebble Beach, CA
5 Research Associate, School of Policy, Planning and Development, University of Southern California

MULTIDISCIPLINARY CENTER FOR EARTHQUAKE ENGINEERING RESEARCH
University at Buffalo, State University of New York
Red Jacket Quadrangle, Buffalo, NY 14261

Preface

The Multidisciplinary Center for Earthquake Engineering Research (MCEER) is a national center of excellence in advanced technology applications that is dedicated to the reduction of earthquake losses nationwide. Headquartered at the University at Buffalo, State University of New York, the Center was originally established by the National Science Foundation in 1986, as the National Center for Earthquake Engineering Research (NCEER).

Comprising a consortium of researchers from numerous disciplines and institutions throughout the United States, the Center's mission is to reduce earthquake losses through research and the application of advanced technologies that improve engineering, pre-earthquake planning and post-earthquake recovery strategies. Toward this end, the Center coordinates a nationwide program of multidisciplinary team research, education and outreach activities.

MCEER's research is conducted under the sponsorship of two major federal agencies, the National Science Foundation (NSF) and the Federal Highway Administration (FHWA), and the State of New York. Significant support is also derived from the Federal Emergency Management Agency (FEMA), other state governments, academic institutions, foreign governments and private industry.

The Center's FHWA-sponsored Highway Project develops retrofit and evaluation methodologies for existing bridges and other highway structures (including tunnels, retaining structures, slopes, culverts, and pavements), and improved seismic design criteria and procedures for bridges and other highway structures. Specifically, tasks are being conducted to:

- assess the vulnerability of highway systems, structures and components;
- develop concepts for retrofitting vulnerable highway structures and components;
- develop improved design and analysis methodologies for bridges, tunnels, and retaining structures, which include consideration of soil-structure interaction mechanisms and their influence on structural response;
- review and recommend improved seismic design and performance criteria for new highway systems and structures.

Highway Project research focuses on two distinct areas: the development of improved design criteria and philosophies for new or future highway construction, and the development of improved analysis and retrofitting methodologies for existing highway systems and structures. The research discussed in this report is a result of work conducted under the existing highway structures project, and was performed within Task106-E-7.3.1, "Risk Assessment of Highway Systems" of that project as shown in the flowchart on the following page.

The objectives of this task were twofold. The first objective was to investigate and demonstrate whether a network-based seismic risk assessment methodology could be developed and applied to a regional highway system. Then, assuming that this was the case, a formal set of methodologies and procedures for conducting a seismic risk assessment of highway networks and systems were to be developed, and applied to one or more examples. Post-earthquake function-

ality strongly depends on the characteristics of the highway system in question, such as its configuration, the locations of the individual components within the overall system and within specific links and subsystems, and the locations, redundancy, and traffic capacities and volumes of the links between key origins and destinations within the system. Consideration of the importance of each component to the overall system performance can provide a much more rational basis for establishing seismic strengthening priorities, defining seismic design and strengthening criteria, effecting emergency lifeline route planning, estimating economic impacts due to component or system-wide damage, and can also provide real-time information on how to get emergency response resources to a given location following a damaging event. The procedures contained in this report provide a basis for addressing the highway system seismic performance issues, and incorporate data and methodologies pertaining to engineering issues (structural, geotechnical, and traffic capacity), repair and reconstruction, system network and risk analysis, and socioeconomic considerations for impacts resulting from system damage. They also provide a mechanism to estimate system-wide direct losses and indirect losses due to reduced traffic flows and/or increased travel times. The programming of these methodologies into a future public-domain software package is currently underway; in addition, the current methodologies and procedures are being calibrated and validated, and component enhancements are being developed, via tasks in a subsequent contract with the Federal Highway Administration.

SEISMIC VULNERABILITY OF EXISTING HIGHWAY CONSTRUCTION
FHWA Contract DTFH61-92-C-00106

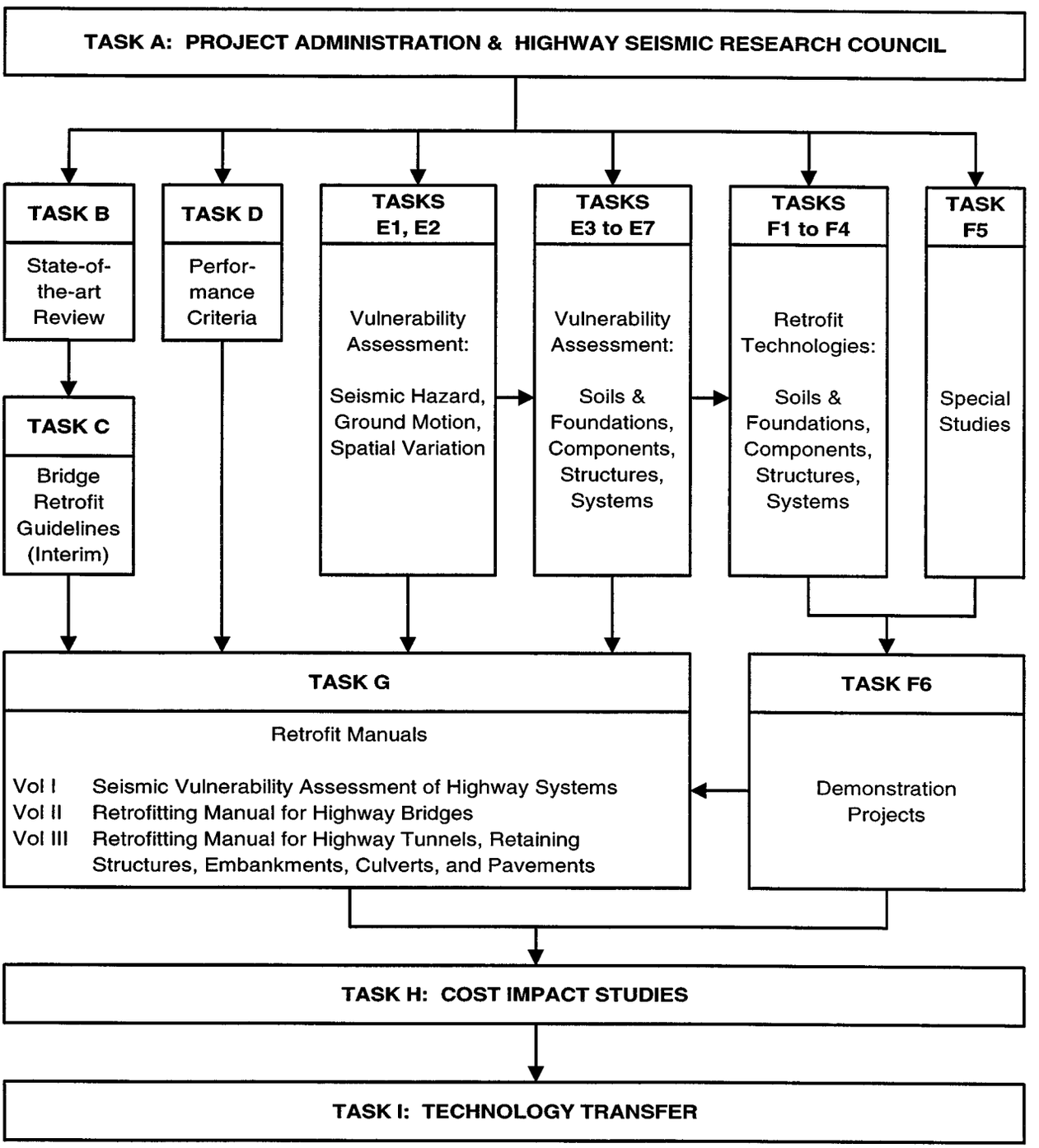

ACKNOWLEDGEMENTS

This report is based on seismic risk analysis (SRA) research performed under Task 106 E-7.3.1 of the project titled "Seismic Vulnerability of Existing Highway Construction". This overall project was carried out by the Multidisciplinary Center for Earthquake Engineering Research (MCEER) in Buffalo NY, under the sponsorship of the Federal Highway Administration.

This SRA research was performed by Mr. Stuart D. Werner of Seismic Systems & Engineering Consultants, Oakland CA (principal investigator and earthquake engineering), Dr. Craig E. Taylor of Natural Hazards Management Inc., Torrance CA (uncertainty and hazard analysis), Professor James E. Moore II and Mr. Sungbin Cho of the University of Southern California, Los Angeles CA (transportation network analysis), and Mr. Jon Walton of the City of San Jose, San Jose CA (programming). The following additional major contributors are also acknowledged:

- Dr. Ian Buckle of the University of Nevada, Reno NV, Mr. Ian Friedland of the Applied Technology Council, Washington D.C., and Professor Masanobu Shinozuka of the University of Southern California, Los Angeles CA for their encouragement and helpful suggestions throughout this research.

- Dr. John M. Jernigan of Ellers Oakley Chester and Rike Inc. of Memphis TN, for his major contributions to the bridge damage state models through his Ph.D. work at the University of Memphis, and for his assistance with estimating bridge repair requirements and traffic states.

- Professor Howard H.M. Hwang of the University of Memphis in Memphis TN, for his generosity in providing us with his extensive GIS data base for Shelby County area, and his contributions to the ground motion modeling and liquefaction screening for Shelby County.

- Dr. Wen David Liu and Ms. Michelle Chen of Imbsen & Associates Inc. in Sacramento CA, and Mr. Hae-In Kim of Caltrans in Sacramento CA, for their contributions to the development of fragility curves for the I-40 and I-55 crossings of the Mississippi River in Memphis.

- Ms. Sarah H. Sun and Esther Anderson of the Shelby County Office of Planning and Development (OPD), for their help in providing transportation/traffic data for Shelby County.

- Mr. Edward Wasserman of the Tennessee Department of Transportation in Nashville TN, for his assistance in providing us with data and drawings for bridges in Shelby County.

- Drs. David Perkins, Arthur Frankel, and Eugene (Buddy) Schweig of the United States Geological Survey, Denver CO and Memphis TN, and Dr. Arch Johnston of the University of Memphis, Memphis TN, for their earthquake modeling insights and guidance.

- Professors John Mander (State University of New York at Buffalo, Buffalo NY) and T. Leslie Youd (Bringham Young University, Provo UT), and Mr. Maurice Power (Geomatrix Consultants Inc., San Francisco CA) for their bridge- and hazards-modeling support.

TABLE OF CONTENTS

TABLE OF CONTENTS
(continued)

TABLE OF CONTENTS
(continued)

TABLE OF CONTENTS
(continued)

TABLE OF CONTENTS
(continued)

TABLE OF CONTENTS
(continued)

TABLE OF CONTENTS
(continued)

TABLE OF CONTENTS
(continued)

TABLE OF CONTENTS
(continued)

TABLE OF CONTENTS
(continued)

LIST OF FIGURES

LIST OF FIGURES
(continued)

LIST OF TABLES

LIST OF TABLES
(continued)

CHAPTER 1
INTRODUCTION

1.1 BACKGROUND

Past experience has shown that earthquake damage to highway components (e.g., bridges, roadways, tunnels, retaining walls, etc.) can go well beyond life safety risks and the costs to repair the component itself. Rather, such damage can also severely disrupt traffic flows and this, in turn, can impact the economy of the region as well as post-earthquake emergency response, repair, and reconstruction operations. Furthermore, the extent of these impacts depends not only on the seismic performance characteristics of the individual components, but also on the characteristics of the highway system that contains these components. System characteristics that will affect post-earthquake traffic flows include: (a) the highway system network configuration; (b) locations, redundancies, and traffic capacities and volumes of the system's roadway links; and (c) component locations within these links (Oppenheim and Anderson, 1981, Oppenheim and Hendrickson, 1987, Hobeika et al., 1991, Wakabayashi and Kameda, 1993 and Wakabayashi, 1999).

From this, it is evident that earthquake damage to certain components (e.g., those along important and non-redundant links within the system) will have a greater impact on the system performance (e.g., post-earthquake traffic flows) than will other components. Unfortunately, such system issues are typically ignored when specifying seismic retrofit priorities, performance requirements, and design/strengthening criteria for new and existing components; i.e., each component is usually treated as an individual entity only, without regard to how the extent of its damage from earthquakes may impact highway system performance. For example, current criteria for prioritizing bridges for seismic retrofit represent the importance of the bridge as a traffic-carrying entity only by using average daily traffic count, detour length, and route type as parameters in the prioritization process (Gilbert, 1993). These criteria do not account for the systemic effects associated with the loss of a given bridge, or for combined effects associated with the loss of other bridges in the highway system. However, consideration of these systemic and combined effects can provide a much more rational basis for establishing seismic retrofit priorities and performance requirements for bridges and other highway components.

1.2 OBJECTIVE

The Seismic Risk Assessment (SRA) methodology described in this report addresses the above system seismic performance issues. It incorporates data and models for seismology and geology, engineering (structural, geotechnical, and transportation), repair and reconstruction, system analysis, and economics, in order to estimate system-wide direct losses (i.e., costs for repair of damaged highway components) as well as indirect losses due to reduced traffic flows, increased travel times, and associated economic impacts of earthquake damage to the system. The programming of this methodology into a future public-domain software package is now underway (Walton et al., in press).

1.3 BENEFITS

Highway system SRA can be applied to the existing system as well as to modified systems in which various alternative seismic risk reduction measures are modeled. In this way, SRA can indicate the effectiveness of the alternative measures in reducing system-wide economic and traffic flow impacts of system damage due to earthquakes. For example, SRA can address the following issues in terms of system performance and risk reduction:

- *How should the System be Strengthened?* SRA can evaluate the relative effects of alternative system enhancements in improving post-earthquake seismic performance. For example, system enhancements that could be evaluated using SRA could include: (a) strengthening of individual components; (b) construction of additional roadways to expand system redundancy; and (c) alternative post-earthquake traffic-management strategies.

- *What Components should be Retrofitted?* SRA can incorporate system performance issues into the establishment of priorities for retrofit of bridges and other highway system components. This can be accomplished through comparisons of the relative degree to which seismic retrofit and improved seismic performance of certain individual components in the system would reduce system-wide traffic flow disruptions and associated economic losses, as well as system-wide repair costs.

- *How should the Components be Retrofitted?* SRA can also evaluate alternative retrofit strategies for the individual components and their relative impacts on seismic performance. For example, for those components selected for retrofit, SRA can assess the relative effectiveness of alternative levels and types of seismic strengthening in reducing system-wide traffic disruptions and economic losses, as well as overall repair costs.

- *What Post-Earthquake Response and Recovery (ER&R) Strategies should be Carried Out?* SRA results can guide the planning of ER&R strategies that would be most effective in the presence of potential damage to the highway system. Such results can also guide the prioritization of highway-system risk-reduction options that would optimize the effectiveness of ER&R operations after an earthquake.

- *How can Traffic best be Managed after an Earthquake?* The effectiveness of various post-earthquake traffic management strategies for reducing congestion can be tested using SRA.

- *What Level of Funding is Appropriate for Enhancing Highway System Seismic Performance?* Because SRA can estimate economic impacts of highway system damage, it can help to justify government funding levels for system-wide seismic strengthening programs.

Section 2.4 provides further discussion of how the SRA results can be used for seismic risk reduction decision making.

1.4 APPLICABILITY

The methodology described and applied in this report provides the framework for the future development of a public domain software package that is applicable to SRA of highway systems nationwide (Walton et al., in press). The results from this methodology are intended to guide decision makers from government, transportation agencies, and consulting firms in their establishment of rational seismic risk reduction strategies for highway systems.

To meet this objective, the methodology must, of course, be practical and efficient to apply, while still providing technically sound results. Toward this end, appropriate simplifications have been incorporated into the methodology wherever possible and technically justifiable. The introduction of additional technically plausible simplifications may be possible in the future, as further experience is gained in the application of this SRA methodology.

1.5 USERS

The SRA methodology is a multidisciplinary tool that encompasses the technical disciplines of the geosciences, geotechnical and structural earthquake engineering, transportation engineering and planning, and risk analysis. It is recognized that end users of the methodology (e.g., decision makers from government and transportation agencies) may not have a background in these areas. However, individuals actually applying the methodology for these end users should have fundamental knowledge in these fields, so that the SRA can be properly set up and implemented, and its results can be properly interpreted.

1.6 REPORT OUTLINE

This report contains eight main chapters and eight appendices. The eight chapters provide the basic framework and a demonstration application of the SRA methodology and its modules. In this, chapter 2 summarizes the main elements of the methodology, and chapters 3 through 6 describe its system, hazards, component, and economic modules, respectively. A demonstration application of the SRA methodology to the Shelby County, Tennessee highway system is provided in chapter 7. Chapter 8 provides concluding comments and recommended directions for further development of this methodology.

The eight appendices of this report provide additional technical detail on the material contained in the main chapters. In particular, they address the probabilistic framework for the SRA methodology (appendix A), the transportation network analysis procedures (appendix B), the scenario earthquake and ground motion hazards modeling for the demonstration SRA provided in chapter 7 (appendices C and D), the liquefaction hazard evaluation procedure built into the SRA methodology (appendix E), and the various bridge models built into the methodology. These bridge models address the development of fragility curves for standard bridges subjected to ground shaking hazards (appendix F), user-specified fragility curves for two Mississippi River crossings that are included in the demonstration SRA in chapter 7 (appendix G), and preliminary fragility curves for bridges subjected to permanent ground displacement hazards (appendix H).

CHAPTER 2
SEISMIC RISK ANALYSIS METHODOLOGY

2.1 OVERVIEW

The highway system SRA methodology is shown in figure 1. It can be carried out for any number of scenario earthquakes and simulations, in which a "simulation" is defined as a complete set of system SRA results for one particular set of input parameters and model parameters. The model and input parameters for one simulation may differ from those for other simulations because of random and systematic uncertainties.

For each earthquake and simulation, this multidisciplinary procedure uses geoseismic, geotechnical and structural engineering, repair/construction, transportation network, and economic models to estimate: (a) earthquake effects on system-wide traffic flows (e.g., travel times, paths, and distances); (b) economic impacts of highway system damage (direct and indirect losses); and (c) post-earthquake traffic flows along vital roadways (to facilitate emergency response planning). Key to this process is a modular GIS data base that contains the data and models needed to implement the system SRA.

This SRA methodology has several desirable features. First, it has a GIS framework, to enhance data management, analysis efficiency, and display of analysis results. Second, the GIS data base is modular, to facilitate incorporation of improved data and models as they are developed from future research efforts. Third, the results of the methodology can either be deterministic (for a few simulations and scenario earthquakes) or probabilistic (which will involve many simulations and earthquakes)[1]. This range of results facilitates the use of SRA for a variety of seismic risk reduction decision-making applications (some of which are discussed in section 2.4 of this chapter). Finally, the methodology's use of rapid engineering and network analysis procedures enhances its possible future application to real-time prediction of highway system states and traffic impacts after an actual earthquake.

2.2 GIS DATA BASE

The GIS data base contains four modules with data and models that characterize the system, seismic hazards, component vulnerabilities, and economic impacts of highway system damage. To facilitate analysis efficiency, these modules are pre-processors to the four-step SRA methodology shown in figure 1. They contain input data and modeling and analysis procedures provided by the user for the particular highway system to be analyzed.

2.2.1 SYSTEM MODULE

The system module contains input data and models needed to characterize the highway system and its seismic performance (traffic flows, travel times, etc.) at various times after an earthquake. This information should be provided by transportation and urban planning specialists who are knowledgeable about the highway system, traffic, and demographic characteristics of the region.

---

[1] The probabilistic framework for this SRA methodology is described in appendix A.

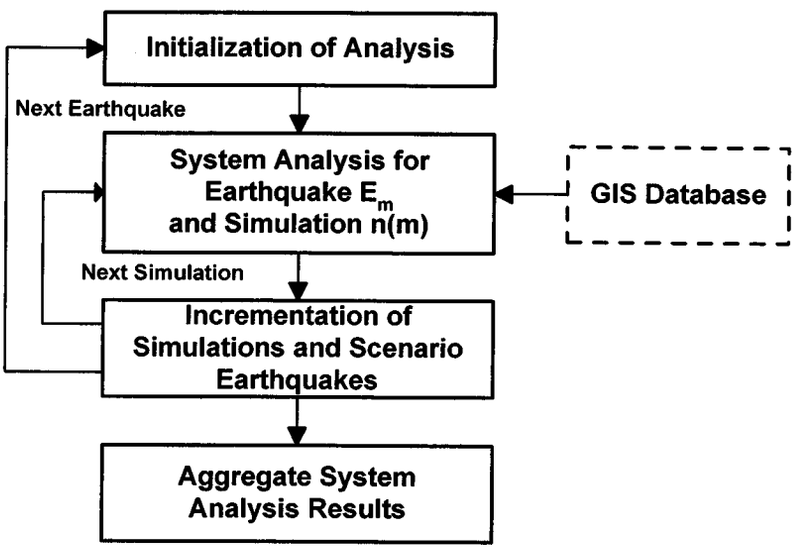

a) Overall Four-Step Procedure

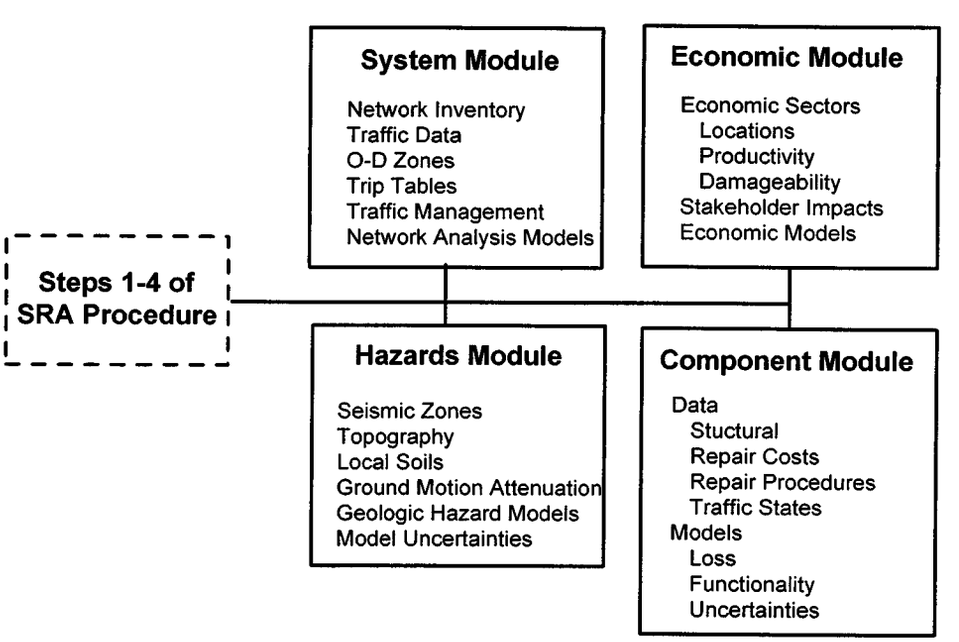

b) GIS Database

Figure 1. Seismic Risk Analysis for Highway Systems

2.2.1.1 Input Data

The user-specified input data contained in the system module should include: (a) system network configuration linkages, and component types and locations; (b) numbers of lanes, traffic flows, capacities, and congestion functions for each roadway link; (c) origin-destination zone locations and trip tables; (d) any in-place traffic management measures for modifying the system to ease post-earthquake traffic flows (e.g., detour routes, changing roadways from two-way to one-way traffic, etc.). and (e) any special system characteristics, such as certain roadways being critical for emergency response or national defense. Section 3.3 describes these system data in more detail.

2.2.1.2 Transportation Network Analysis Procedures

The transportation network analysis procedures contained in the system module estimate post-earthquake traffic flows throughout the highway system, for each simulation and scenario earthquake. The procedures have the following features: (a) they represent the latest well-developed technology for providing rapid and dependable estimates of flows in congested networks, for given changes in link configuration due to earthquake damage; (b) they are compatible with the GIS framework of this SRA methodology; and (c) they use system input data that are typically available from Metropolitan Planning Organizations (MPOs). These procedures are summarized in section 3.4, and are described in more detail in appendix B.

2.2.2 HAZARDS MODULE

The hazards module contains input data and models provided by geologists and geotechnical engineers for characterizing system-wide seismic hazards for each scenario earthquake and simulation considered in the SRA of the highway system. These seismic hazards include ground motion, liquefaction, landslide, and surface fault rupture.

2.2.2.1 Input Data

The input data contained in the hazards module should include: (a) the ensemble of scenario earthquake events to be considered, as specified by the user in the initialization phase of the SRA (see section 2.3.1 and appendix C); (b) locations and topography of slopes within the system that could be prone to landslide; (c) local soil conditions throughout the system, as needed to estimate local geologic effects on ground shaking and the potential for liquefaction and landslide; and (d) locations and characteristics of any faults within the system that have a potential for surface rupture. Charter 4 provides a further description of these input data.

2.2.2.2 Hazards Estimation Models

The hazards module also contains geoscience and engineering models for estimating ground shaking, liquefaction, landslide, and surface fault-rupture hazards to the highway system due to the various scenario earthquakes.

2.2.2.2(a) Ground Motion Hazards

For each scenario earthquake and simulation, ground motion hazards are estimated at the site of each component in the highway system. These estimates should incorporate the latest well-developed technology for estimating: (a) site-specific rock motions, and their rate of attenuation over the distance from the seismic source to the site; and (b) effects of local soil conditions in modifying the ground surface motions in the vicinity of the bridge or other highway component, relative to the underlying rock motions. The ground motion estimates for each simulation should also include the effects of uncertainties in rock-motion attenuation rates and soil amplification factors. These estimates may be provided as peak accelerations, response spectra, or time histories, depending on the requirements of the component damage-state model. Ground motion hazard models are further addressed in section 4.3. The particular ground motion hazard model that is used in the demonstration SRA of the Shelby County, Tennessee highway system is described in appendix D.

2.2.2.2(b) Liquefaction and Landslide Hazards

The liquefaction and landslide hazard models for the SRA should use rapid and well-established procedures for developing site-specific estimates of these hazards due to each scenario earthquake. For each component site, the models should incorporate: (a) an initial screening approach based on review of site soil conditions and topography to eliminate those sites that clearly will not be susceptible to liquefaction or landslide hazards; (b) for those sites not eliminated by step a, further evaluation of the susceptibility of the site to liquefaction or landslide hazards during each scenario earthquake; and (c) for those sites determined to have a potential for liquefaction or landslide hazards during a given scenario earthquake, estimation of liquefaction- or landslide-induced permanent ground displacement due to the given earthquake. The models should be based on accepted empirical, analytical, and/or experimental procedures, and should include effects of uncertainties in the liquefaction and landslide hazard estimates. These models are further addressed in sections 4.4 and 4.5, and the liquefaction model that is included in the SRA methodology is described in appendix E.

2.2.2.2(c) Surface Fault Rupture Hazard

For faults that could cause surface rupture and displacement within the highway system, potential displacements should be estimated from a procedure that includes: (a) an initial screening approach to eliminate those component sites that will clearly not be prone to surface fault rupture; (b) for those sites indicated by step a to be susceptible to surface fault rupture, estimation of potential surface displacements using (in most cases) applicable empirical models that correlate surface displacement with earthquake magnitude and fault-rupture length. However, if additional assessment is needed (e.g., where empirical data may not be sufficient, or if surface fault rupture could have a particularly significant impact on the seismic performance of the system), more detailed geologic investigations should be carried out. Uncertainties in the surface fault displacement estimates (e.g., due to technical limitations in available models and data or due to random effects of data scatter about the empirical correlations, etc.) should be estimated and considered in this fault displacement hazard assessment. Surface fault rupture models are further discussed in section 4.6.

2.2.3 COMPONENT MODULE

The component module contains input data and procedures provided by structural and geotechnical engineers to develop a "loss model" and a "functionality model" for each component in the system. The loss model estimates the component's direct losses (i.e., repair costs), and the functionality model estimates the component's "traffic state" (i.e., whether the component will be partially or fully closed to traffic during repair of the earthquake damage, the duration of the closure, and speed limits for traffic along the component during repair). Chapter 5 addresses SRA modeling issues for bridge, approach fill, and pavement components, and appendices F, G, and H describe bridge models now included in the SRA methodology.

The loss and functionality models are provided as fragility curves that include effects of uncertainties in input data and modeling procedures. These curves relate the probability of occurrence of a given level of repair cost or a given traffic state, to the level of ground shaking and permanent ground displacement at the component site. The fragility curves consider: (a) the component's seismic response to various levels of ground shaking and permanent ground displacement; (b) its "damage state", (i.e., the degree, types, and locations of any earthquake damage to the component); (c) how the damage will be repaired; (d) the costs of these repairs, whether the component will need to be fully or partially closed during the repairs, and the durations of these closures; and (e) the component's repair costs and traffic states at various times after the earthquake (to reflect the rate of traffic restoration over time as repairs proceed).

After each component's traffic states at various times after the earthquake are obtained, they are incorporated into the highway system network model to obtain the overall post-earthquake "system states" at each time. The post-earthquake system states are in the form of modified highway systems (relative to the pre-earthquake system) that now incorporate reduced traffic states of the various links in the system that have been damaged during the earthquake. These system states must also include the effect of each component's damage state on adjacent and underlying roadways. This, in turn, will depend on the level of damage to the component, and the component's location within the system as well.

2.2.4 ECONOMIC MODULE

The economic module contains models and data for evaluating broader economic impacts of earthquake-induced traffic flow disruptions. These impacts include direct losses (component repair costs), and indirect dollar losses (e.g., to commuters and businesses), and assessment of effects of these disruptions on stakeholders. This module should be developed by a team of engineers, transportation specialists, urban planners, and economists. Chapter 6 provides further discussion of the modeling of economic impacts of highway system damage.

2.3 ANALYSIS PROCEDURE

2.3.1 STEP 1 – INITIALIZATION OF ANALYSIS

Step 1 consists of the user's specification of whether the SRA is to be deterministic or probabilistic, input of the scenario earthquakes and number of simulations to be considered in the

SRA, and identification of sites within the highway system that may be prone to liquefaction, landslide, or surface fault rupture hazards.

The scenario earthquakes to be considered in the SRA are defined in terms of their magnitude, location, and frequency of occurrence. They should be developed using regional models that account for the seismologic and geologic characteristics of the region. To facilitate later estimates of probabilistic loss distributions and their variability over time, the earthquakes are represented in a form suitable for later use in a "walk-through" analysis (Daykin et al., 1994). In this, the user specifies a suitable time frame of interest. Then, for each year within this time frame, the number of earthquakes that occur in the region (i.e., zero, one, or more earthquakes) is established, along with the magnitude and location of each earthquake. Section 4.2 describes this process in more detail. Appendix C illustrates the use of the process to develop multiple scenario earthquakes for the Central United States.

If the user desires to carry out a probabilistic analysis that accounts for uncertainties in the SRA process and their effects on the analysis results, step 1 also includes the user's specification of the number of simulations to be considered for each scenario earthquake. This specification will depend on the user's desired confidence levels for the analysis results (see appendix A).

Prior to starting the SRA, the user should perform geologic screening to identify sites within the highway system that may be prone to liquefaction, landslide, or surface fault rupture hazards. Locations of these potentially hazardous sites are input during step 1 of the SRA methodology. Chapter 4 further discusses these geologic screening efforts, and appendix E provides a detailed description of geologic screening for liquefaction hazards.

2.3.2 STEP 2 – DEVELOPMENT OF SIMULATIONS FOR EACH EARTHQUAKE

Step 2 develops each simulation for each scenario earthquake from the following process:

- *Hazard Evaluation.* First, the data and models contained in the hazards module are used to estimate the earthquake ground motions and geologic hazards throughout the system.

- *Direct Loss and System State Evaluation.* Once the ground motions and geologic hazards are estimated, the data and models from the component module are used to evaluate direct losses and system states (defined at various times after the earthquake).

- *Transportation Network Analysis.* The data and transportation network analysis procedure from the system module are applied to each post-earthquake system state, in order to estimate system-wide travel times as well as access and egress times for key locations designated by the user (e.g., locations, of key medical, government, industrial, transportation, or residential facilities). Differences between these post-earthquake results and pre-earthquake travel times measure how earthquake damage to the system affects its ability to carry traffic.

- *Economic Impact Evaluation.* The data and models from the economic module are applied to the above post-earthquake travel times to estimate effects of the impeded traffic flows on the economy of the region.

2.3.3 STEP 3– INCREMENTATION OF SIMULATIONS AND SCENARIO EARTHQUAKES

Under step 3, the evaluations from step 2 are repeated, in order to develop multiple simulations for multiple scenario earthquakes (if the SRA is to be probabilistic).

2.3.4 STEP 4 – AGGREGATE SYSTEM ANALYSIS RESULTS

This final step in the SRA process is carried out after the system analyses for all simulations and scenario earthquakes have been completed. In this step, the results from all simulations and earthquakes are aggregated and displayed. Depending on user needs, these aggregations could focus on the seismic risks associated with the total system or with individual components. These deterministic or probabilistic results should be adapted and/or simplified to meet the particular requirements of each user audience. Examples of such results from a demonstration SRA of an actual highway system are provided in chapter 7.

2.3.4.1 Deterministic Results

Deterministic results can be developed for one or more earthquake events, which is termed a seismic vulnerability analysis. In this, for a given earthquake, the SRA can be developed using best-estimate values of uncertain parameters. Alternatively, several sets of deterministic results can be developed that incorporate randomly selected values of the uncertain parameters, in order to assess the sensitivity of the results to variations in these parameter values. Output from a deterministic SRA can include: (a) GIS displays of the spatial distribution of the seismic hazards, component damage states, and overall system states at various times after the earthquake; and (b) tabulations of economic losses and travel time increases (relative to pre-earthquake travel times) due to estimated highway system damage due to each designated earthquake.

2.3.4.2 Probabilistic Results

SRA results may also be developed for the broader (probabilistic) range of simulations, leading to loss statistics (e.g., average annualized loss), to loss distributions that show the severity of earthquake-induced system losses for different probability levels, and/or to random walk plots to visually display the temporal distribution of losses over exposure times of importance to the user[2]. For policy- and financial-planning purposes, the impacts of incorporating uncertainties into the SRA will be of considerable interest.

- *Loss Distributions.* Loss distributions are plots of the loss value vs. the probability that this value will be exceeded during a designated exposure time. They may be: (a) total loss distributions, which are computed from the loss values computed for all earthquakes and simulations; or (b) conditional loss distributions, which are loss vs. probability curves associated with a pre-condition specified by the user (e.g., losses due to the occurrence of earthquakes within a designated magnitude range). Appendix A describes how these loss distributions are developed.

---

[1]The "loss" can be defined in several ways, such as direct repair cost, travel time delays due to earthquake damage (between certain key origin-destination zones or aggregated over all zones), indirect losses due to travel time delays, or other adverse consequences.

- *Random Walk Plots.* A formal walk-through is used to visualize how earthquake losses vary over time, which can be helpful for decision-making. A visual display of results from a walk-through analysis, over a time segment equal to a designated exposure time, is termed a random walk plot. It shows the cumulative loss since the start of the time segment for each year in the segment. It is often desirable to show random walk plots for many different sets of these time segments (extracted from the total duration of the walk-through) to depict the variability of the losses from one time segment to the next.

2.4 USE OF SRA RESULTS FOR SEISMIC RISK REDUCTION DECISION-MAKING

SRA can be used to guide the selection of appropriate strategies for reducing seismic risks to a highway system (see table 1). An iterative approach for using SRA to assess seismic decision alternatives for a highway system is shown in figure 2 and is outlined below.

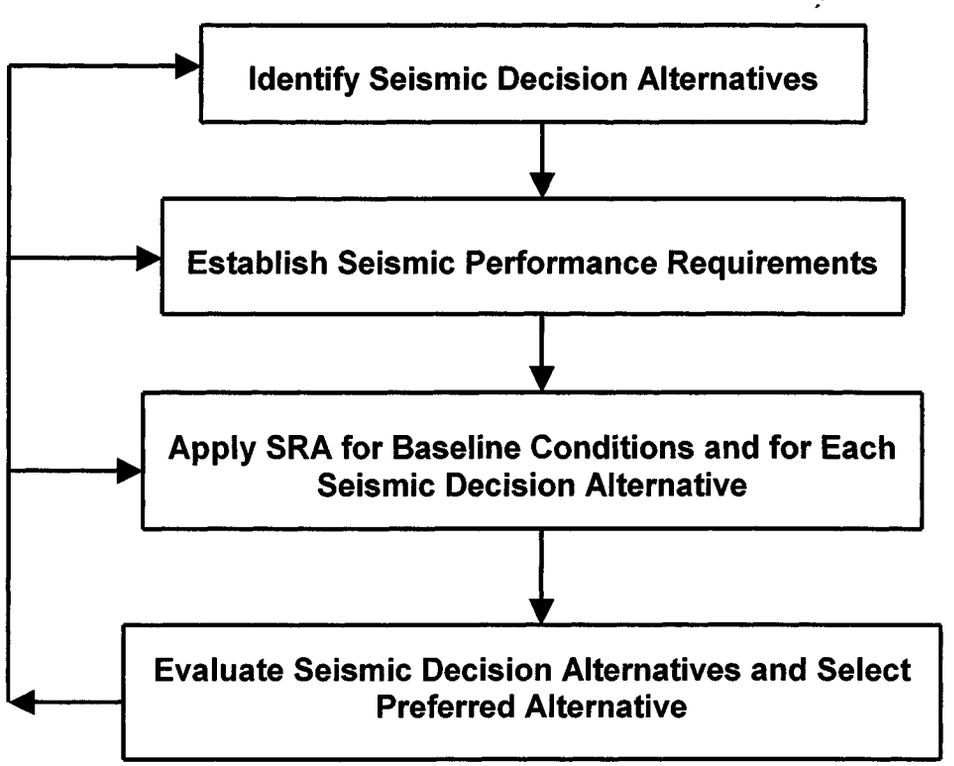

Figure 2. Use of SRA Results for Seismic Risk Reduction Decision Making

2.4.1 STEP 1. IDENTIFY SEISMIC DECISION ALTERNATIVES

Under step 1, the various options that are open to decision-makers as possible strategies for reducing seismic risks to the highway system are identified. In addition to the various measures listed in table 1, other measures could include (a) financial planning to ensure adequate funds for emergency response and recovery operations, and to establish appropriate funding levels for seismic risk reduction; and (b) coordination with FEMA and other federal agencies to streamline the post-earthquake procurement of funds for highway system repair and recovery.

Table 1. Example Uses of Highway System SRA for Seismic Risk Reduction Decision Making

Strategy	Description
Prioritization of Bridges for Seismic Retrofit	Evaluation of what retrofit sequence should be adopted for various bridges in the region, in order to optimize the benefits of the retrofit to the seismic performance of the highway system. SRA would be applied for alternative retrofit sequences, and would assess which of the sequences leads to the optimum seismic performance of the system.
Establishment of Design Acceleration Level for Bridge Design or Retrofit	Selection of which of several alternative design acceleration levels should be considered for design of a given new bridge or for retrofit of a given existing bridge. This evaluation process should consider the initial construction costs associated with each design acceleration level, as well as the potential for earthquake damage to the bridge and its consequence on the seismic performance of the highway system.
Emergency Response Planning	Evaluation of how various seismic decision alternatives would affect access times to and from key locations in the region such as hospitals, police and fire stations, airports, government command centers, centers of commerce, etc. This could serve as a basis for establishing special seismic retrofit priorities and design acceleration levels for components along routes essential to emergency response. SRA can also be used in real-time assessment of seismic performance of a highway system after an actual earthquake, to guide real-time emergency response operations.
Assessment of Available Repair Resources	Downtimes of roadway links due to earthquake damage will depend on the available equipment, material, and labor resources for repair of the links. SRA can assess how losses due to highway system damage are affected by downtimes, first for the currently existing repair resources, and then for increased resources to reduce these downtimes. Assessment of costs and benefits of various levels of repair resources can guide plans for future repair-resource deployment.
System Enhancement	Assessment of how construction of new roadways that are being planned could improve the seismic performance of the highway system, as well as the effectiveness of possible short term traffic management strategies (e.g., conversion of selected roadways from one-way to two-way traffic) in improving system performance.

2.4.2 STEP 2: ESTABLISH SEISMIC PERFORMANCE REQUIREMENTS

In step 2, decision makers should tentatively select relevant types and forms of results from the SRA that are to be used to evaluate the seismic decision alternatives. This selection should be based on collective input from other stakeholders in the seismic performance of the highway system. Such stakeholders can include: (a) federal, state, and local transportation officials -- who may wish to focus on performance requirements that minimize repair costs and downtimes of the overall highway system; (b) emergency response planners -- who may wish to include performance requirements that address acceptable levels of travel time delays to and from critical facilities; and (c) business and civic leaders -- who may wish to include performance requirements based on access to and egress from regional centers of commerce, education, etc.

The performance requirements may be either deterministic or probabilistic. For example, deterministic requirements could consist of acceptable levels of loss for a designated level 1 earthquake (a moderate and frequently occurring event), and for a level 2 earthquake (a severe and infrequently occurring event). Probabilistic requirements may consist of acceptable probabilities of exceedance for designated levels of loss due to highway system damage, or acceptable means and variances of total losses, as discussed subsequently. In this, the losses should be computed as the present value of the initial cost for implementing the seismic decision alternative (e.g., the initial construction cost associated with a given design acceleration level), the post-earthquake repair costs, and the post-earthquake losses due to increased travel times and reduced accessibility to key locations in the region.

The establishment of seismic performance requirements should recognize that it is not possible to achieve a "zero seismic risk"; i.e., regardless of what degree of seismic risk reduction is implemented, there will always be some finite residual risk of unacceptable seismic performance of the highway system. An "acceptable" level of seismic risk is that level for which the costs to further reduce these residual risks are no longer acceptable. When establishing acceptable risk levels and corresponding seismic performance requirements, one must consider initial implementation costs needed to meet such requirements (e.g., initial costs of construction for alternative levels of design acceleration for retrofit of an existing bridge) as well as potential losses due to earthquake-induced damage of the highway system.

A systematic approach for establishing an acceptable level of seismic risk involves valuation of means and variances of total life-cycle costs for various seismic decision alternatives (Taylor and Werner, 1995, Werner et al., 1999 and Ferritto et al., 1999). This includes the following:

- It is based on computation of total life-cycle cost for each seismic decision alternative which, as previously noted is computed as the present value of: (a) the initial cost for implementing the alternative (e.g., cost of construction associated with different design acceleration levels for a bridge); (b) post-earthquake repair costs; and (c) post-earthquake losses due to increases in travel time along the system, reduced access to key locations. Where higher-order economic losses can be estimated, they can also be included in this total cost computation.

- Mean values and variances of these life-cycle costs are computed through statistical analysis of the life-cycle costs associated with a given seismic decision alternative, as obtained from probabilistic SRA of that alternative for each scenario earthquake and simulation.

- Seismic decision alternatives are treated as "investments" in seismic risk reduction. One basis for evaluating an investment is in terms of its financial yield. In this SRA application, a higher "yield" of an investment in seismic risk reduction is viewed being analogous to minimizing the mean value of the total life cycle cost. In addition, a prudent investor evaluates his/her investments not only in terms of their yield but also in terms of their safety. In this, the safety (or reduction in volatility) of an investment in seismic risk reduction can be viewed in terms of lowering the variance of the life-cycle costs (or standard deviation of these costs, which is the square root of the variance) to an acceptable level.

- Figure 3 shows how this approach was used to establish a design acceleration level for a wharf structure in California. In this case, the decision-makers opted to use a design acceleration level of about 0.45 g, which is higher than the design acceleration at which the mean value of the life-cycle cost is minimized (which is about 0.25 g). This was based on their desire for reduced volatility in the seismic performance of this wharf facility (Werner et al., 1999).

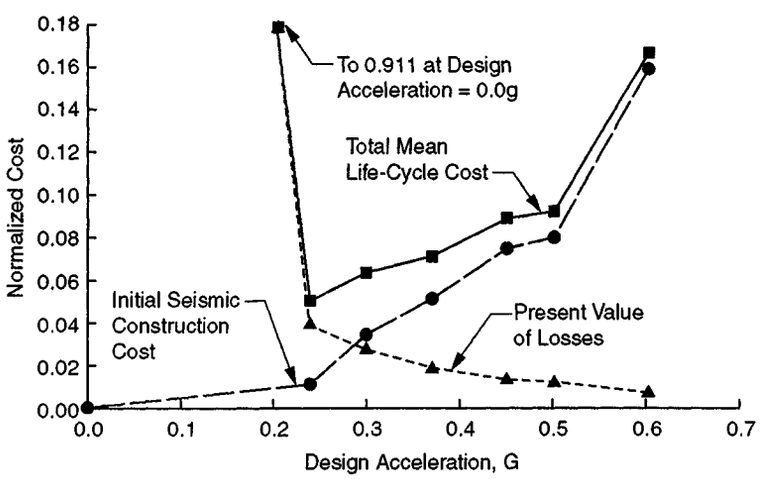

a) Mean Value of Total Life-Cycle Cost

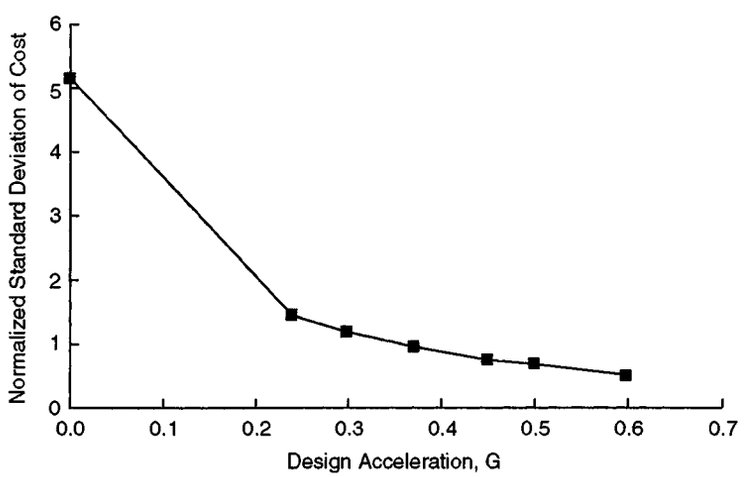

b) Volatility (Standard Deviation) of Total Life Cycle Cost

Figure 3. Selection of Design Acceleration Level for a Wharf Structure (Werner et al., 1999)

- Figure 4 illustrates how SRA results can be used to guide the establishment of priorities for retrofit of a several bridges within a highway system. In this, alternative priorities are evaluated in terms of the means and standard deviations of the resulting total costs. The dashed line in this figure shows those prioritization plans with the most favorable combinations of mean and variance (i.e., the lowest values of these quantities).

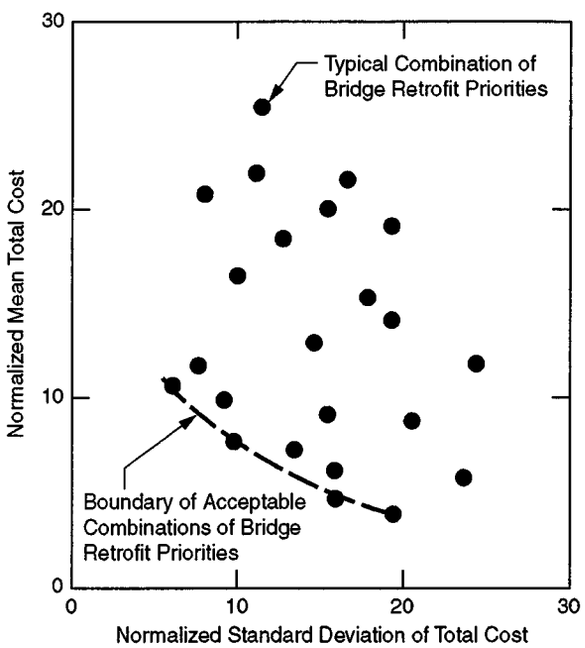

Figure 4. Illustrative Results for Evaluation of Alternative Bridge Retrofit Priorities

2.4.3 STEP 3. APPLY SRA FOR BASELINE CONDITIONS AND FOR EACH SEISMIC DECISION ALTERNATIVE

Under step 3, SRA of the highway system is carried out for each earthquake event and simulation identified for consideration under the seismic performance requirements for the system (from step 2).

2.4.3.1 Baseline System Performance

The first step in the SRA application is to develop a set of baseline system performance results. These baseline results should consist of:

- *Pre-Earthquake Performance of Existing Highway System.* The transportation network analysis procedures in the SRA methodology are used to assess the pre-earthquake traffic flows, travel times, and costs of travel for the existing (undamaged) highway system.

- *Post-Earthquake Performance of Existing Highway System.* Scenario earthquakes are applied to the existing highway system (before any seismic decision alternatives are considered), and SRA is carried out to evaluate post-earthquake traffic flows, travel times, and travel costs.

- *Baseline Results.* Comparison of the pre- and post-earthquake performance of the existing highway system will indicate the potential risks and losses that could occur in the absence of seismic risk reduction.

2.4.3.2 Post-Earthquake System Performance for Each Decision Alternative

Once the above baseline system performance results are developed, it remains to carry out SRA of the highway system after each seismic decision alternative is implemented. To illustrate this process, suppose that the objective of the SRA is to establish appropriate levels of design acceleration for the upgrade of a major bridge for which seismic retrofit is planned. Also, suppose that five different levels of design acceleration have been identified as seismic decision alternatives in step 1. Then, SRA of the highway system is carried out for cases in which the bridge is retrofitted to correspond to each of the alternative design acceleration levels. The resulting losses due to damage to the highway system after the bridge is retrofitted to each design acceleration level (due to repair costs, travel time delays, etc.), plus the initial cost of construction for that design acceleration level, are used in step 4 to evaluate the various design acceleration levels being considered.

2.4.4 STEP 4. EVALUATE SEISMIC DECISION ALTERNATIVES AND SELECT PREFERRED ALTERNATIVE

Under step 4, the SRA results for the baseline (existing) condition and for each seismic decision alternative are evaluated and compared. From this, a preferred alternative is selected. Stakeholder interaction in evaluating system performance goals relative to this overall decision-making process should be an important element of this step. On the basis of this interaction, it is possible that additional seismic decision alternatives may be identified, the seismic performance requirements for the highway system may need to be modified, and/or additional SRAs may need to be implemented for additional cases or decision alternatives. If this occurs, one or more of the previous steps of the procedure may need to be repeated (see figure 2).

2.5 CURRENT SCOPE OF METHODOLOGY

This SRA methodology is intended to serve as a modular framework for future software development and practical application to highway systems nationwide. However, not all elements of the methodology necessary to achieve this objective could be fully developed within the time frame and resources of this research program. SRA elements that have been excluded from the current scope but are prime candidates for future inclusion are as follows:

- *Earthquake Models.* The demonstration application of the SRA methodology that is described in chapter 7 has focused on the Shelby County, Tennessee highway system. In view of this, earthquake models currently included in the methodology are for the Central United States region only (see chapter 4 and appendix C). Plans are underway to include earthquake models for other regions nationwide where SRA of highway systems could be carried out in the future.

- *Seismic Hazard Models.* In view of the above-indicated focus of the demonstration application to the Shelby County system, a ground motion model that is applicable to this region has been included in the SRA methodology at this time. However, as noted above for the earthquake models, the future inclusion of ground motion models applicable to other regions of the country is essential to the nationwide focus of this methodology, and will be added in the future. In addition, only ground motion and liquefaction hazards are included at this time. Landslide and surface fault rupture hazards (which are addressed in sections 4.5 and 4.6 of chapter 4) will be included in the future.

- *Component Models.* The component modeling activities within the SRA methodology development have focused on bridges and approach fills subjected to ground shaking hazards (see chapter 5 and appendices F through H). However, a very preliminary model for bridges subjected to permanent ground displacement hazards is included in the methodology at this time (see section 5.3 and appendix H). In addition, a preliminary model for pavements subjected to permanent ground displacement hazards is described in section 5.5 of chapter 5. Further development of these models, and the addition of models for other highway components (retaining walls, tunnels, culverts, slopes, etc.) is being planned.

- *Transportation Network Analysis and Economic Losses.* As discussed in chapter 6, earthquake-induced damage to a highway system could affect the stricken region's economic productivity and capacity. Estimation of these effects requires the coupling of system, hazards, and component models with regional economic models, which is a formidable task. This is now an area of extensive research and development (see section 6.1 of chapter 6). Accordingly, the SRA methodology now includes only a very simple model of economic impacts of increased commute times due to earthquake damage to a highway system. It does not yet treat the effects of this damage on a region's post-earthquake economic recovery, nor does it treat how damage to the economic infrastructure may impact post-earthquake traffic demands on the system. When sufficiently developed, system/economic models that include these coupled effects should be incorporated into the SRA methodology.

CHAPTER 3
SYSTEM MODULE

3.1 OBJECTIVE

The systems module contains the data and models necessary to characterize the highway system for the SRA methodology described in chapter 2. This chapter summarizes fundamental transportation engineering concepts that are the basis for the system module, and then describes the two main elements of the module -- the system inventory and data requirements, and the transportation network analysis procedures.

3.2 FUNDAMENTAL CONCEPTS

3.2.1 LEVEL OF SERVICE PREDICTION

A fundamental objective of transportation engineering is to predict the level of service (delays, speeds, travel times) in large urban highway/roadway networks. These predictions make it possible to evaluate different network configurations or different operating policies. However, it is difficult to obtain reliable and accurate predictions of the level of service for several reasons:

- Congestion makes the time-cost of travel dependent on traffic flow, although it is the decisions of travelers that define flows. These decisions, in turn, affect the cost of travel (where the term "cost" is used herein to represent travel times within the network).

- Network paths overlap. They share links in common. Flows on one path influence the time-costs on overlapping paths that share links with the first path.

- Travelers have a choice of modes. The response of different groups of travelers to the attributes of different modes varies across groups and trip purposes. This can be treated as a choice of network. At the most basic level, this is a choice of transit or automobile travel.

- Travelers have a choice of destinations. The cost of reaching different destinations depends on the flows along the paths that connect origins and destinations. The choice of destination depends in part on the relative cost of reaching the destination.

- The demand for travel depends on the cost of travel. As the level of service on the network changes, the demand for travel to any destination changes.

3.2.2 TRANSPORTATION NETWORK ANALYSIS MODELS

The following sequence of models is typically used to estimate flows in urban networks:

- *Trip generation models* -- which estimate where the demand for travel is located, and the number of trips that originate and terminate in a given location.

- *Trip distribution models* -- which estimate the number of trips originating at a given location that terminate at another given location.

- *Mode choice models* -- which choose the networks along which flows between a given origin-destination pair will occur.

- *Network (or route) assignment models* -- which designate those routes within a network along which flows between a given origin-destination pair will occur.

Network assignment receives particular attention, in part because it is the most quantifiable aspect of the transportation network analysis process. This is the aspect of the problem that is most relevant to SRA objectives. How will flows occur in a network disrupted by an earthquake? Some links in the network will be partially or fully severed due to damage to transportation components caused by earthquake-induced ground shaking or permanent ground displacement. How will flows occur under these circumstances, and at what cost? The other aspects of the flow prediction problem are relevant, and will certainly bear on the performance of the transportation system following an earthquake. However, many of these other aspects will be strongly influenced by damage to the urban activity system, and by policies pursued after the event. Some of these impacts are unknown. If information exists to model them, they can be represented in the SRA methodology. These effects cannot be treated now, but much depends on the cost of traversing paths in the transportation network, and adequate treatment of network assignment following an earthquake. The costs implied by these flows are central to SRA of highway systems.

More importantly, the transportation modeling requirements associated with the SRA methodology are a departure from conventional transportation modeling objectives. The SRA procedure develops travel costs and related distributions that are conditioned on alternative seismic risk reduction strategies or policy assumptions. The number of alternative network states investigated as a result of multiple scenario earthquakes, simulations, and post-earthquake times is much larger than the number of network alternatives conventionally examined for transportation planning purposes. This requires a departure from standard transportation modeling procedures. However, the basic urban transportation modeling objective associated with SRA -- which is to predict the level of service as a function of the network configuration -- remains unchanged from that for conventional transportation analysis applications.

The SRA methodology applies an experimental procedure designed for rapid *estimation* of network flows. This estimation procedure is drawn from the connectionist computing literature. It is based on an association technique that rapidly and efficiently maps network conditions predicted by other components of the SRA to an approximation of the corresponding network flows. This is not a neural network procedure, but it is an artificial intelligence application that encodes the rules for associating inputs (stimulus vectors) with outputs (response vectors), and then remembers what rules to apply to new stimuli. In this case, the stimulus vector describes the state of the network. The target response vector is the set of transportation flows that would otherwise be predicted for such a network by a more exact, conventional network analysis. This technique implies substantial preprocessing cost before the tool can be used as part of the SRA

procedure. Once these preprocessing costs have been borne, very good approximations to closed form solutions conventionally used to represent the mathematics of competitive route choice in congested networks can be achieved very inexpensively and quickly for very large numbers of system states. This capability is essential to a basic SRA objective -- which is to carry out rapid and reliable analysis of many system states due to many scenario earthquakes and simulations, in order to develop probabilistic estimates of highway system performance (see chapter 2).

In summary, conventional analytical solutions are used to develop many (hundreds of) predictions of traffic flows for incrementally different network configurations. These solutions (termed "training cases" and "test cases") are then used to establish a highly generalized mapping that is then used to rapidly develop good approximations to the true traffic flows for new network configurations, such as might be associated with an earthquake. These good approximations of the true flow solutions and associated network costs are used in great numbers in the distributions generated by the SRA methodology. In this, the training cases for the SRA methodology are generated by computing user equilibrium flows for a systematically representative set of approximately 2,400 training cases.

3.3 SYSTEM INVENTORY AND DATA REQUIREMENTS

Highway system data needed to carry out the SRA includes the system's configuration, traffic flows and capacities, its component types and locations, its origin-destination zones and travel demands, and any special system characteristics and post-earthquake traffic management plans.

3.3.1 SYSTEM CONFIGURATION

The system configuration is modeled as a network of links and nodes that represent the highways and roads within the system. The important characteristics of these links are: (a) the numbers and locations (coordinates) of the end nodes for each link; (b) the link classification or facility type, i.e., whether the link is physical (i.e., classified as a freeway, major arterial, or other type of road element) or is a virtual link that associates trip demands from individual origin-destination zones to the nearest physical links in the highway system; (c) the length of each physical link; and (d) the number of lanes that comprise each physical link. A GIS map showing system links, nodes, and attributes should be developed for later use in the SRA.

3.3.2 TRAFFIC FLOWS

Traffic flows (also termed traffic volumes) represent the rate of travel along a given link in the system during a fixed time interval. The SRA methodology relies on traffic flow data available from Metropolitan Planning Organizations (MPOs) for the region. The methodology is designed to make use of MPO data resources, and assumes that the data from these resources are sufficiently current for use in these analyses.

The units of traffic flow are equivalent passenger-car-units (PCU)/hour. If MPO traffic-flow data for the highway system incorporates separate monitoring of automobile flows and flows from other types of vehicles (busses, trucks, etc.), the flows from these other vehicles may be expressed as a multiple of a single passenger-car-unit (PCU) (TRB, 1995). This requires separate origin-destination trip tables for passenger and freight flows. Most MPOs construct trip tables for passenger flows only. Larger MPO agencies may also construct trip tables for bus transit flows. Most agencies have very little data describing freight flows. Representative transportation data from an MPO are summarized in chapter 7, which describes a demonstration application of the SRA methodology to the Shelby County, Tennessee highway system.

Traffic flows are usually obtained from traffic counts, and are further characterized by the following data for each link: (a) whether the link is carrying one-way or two-way traffic; (b) the free-flow travel speed; (c) base-year traffic flow characteristics obtained from observed traffic counts[1], such as average daily traffic data, peak hour data, and average non-peak hour data; (d) similar traffic flow data for the past two-to-three years, as well as projected traffic flows for future years; (e) observed speed or travel time; and (f) speed class. The last element relates speed and capacity. Many cities have also real time data available. Real time data and periodic traffic counts are used to update transportation planning data.

3.3.3 TRAFFIC CAPACITY

The effective traffic capacity is a highway-design parameter that is about 2/3 to 3/4 of the theoretical maximum flow for the roadway link. As shown in the Transportation Research Board's Highway Capacity Manual (TRB, 1995), the capacity of a roadway link is often computed as the product of the number of lanes in the link and its capacity per lane (which varies by facility type, and is usually assumed to be 2,000 PCU/hour for freeways and 625 PCU/hour for local roads). The SRA methodology relies on local data to the extent such data are available.

3.3.4 CONGESTION FUNCTION

The congestion function models how delay varies with traffic flow. In this, there is no compelling model of the relationship between delay and flow. The literature has certain accepted models of link congestion, most notably the following Bureau of Public Roads (BPR) model:

$$t = t_o\left[1 + 0.15(v/c)\right]^4 \qquad (1)$$

where t is the link travel time, t_o is the travel time when the link is uncongested, and v/c is the ratio of the link's traffic flow to its (effective) design capacity (Sheffi, 1985). However, there is no substantive theoretical and little empirical foundation to this function; rather, it is a

[1]With respect to traffic counts, hourly counts leading to a time-of-day profile are viewed to be most desirable. Daily traffic counts are too aggregate for modeling peak hour performance. Time-series procedures are usually applied to raw traffic count data from the field, to remove cycle and trend components.

convenient form and an artifact of frequent use[2]. Other congestion models range from the simple Greenshields model (Greenshields, 1935) to more sophisticated follow-the-leader models in which vehicles are represented discretely.

3.3.5 COMPONENT TYPES AND LOCATIONS

The system module contains the locations and types of all components in the system that, if damaged, could impact the system's ability to carry traffic. These could include bridges, tunnels, retaining walls, pavements, approach fills, slopes, and culverts. Only bridges, pavements, and approach fills are included in the current version of the SRA methodology described here. The other components listed above may be incorporated in the future.

3.3.6 ORIGIN-DESTINATION ZONES

The area served by the highway system is divided into a series of Origin-Destination (O-D) zones for which demographic, economic, and emergency response data are compiled and used by transportation engineers for traffic flow analysis, future roadway planning, and traffic control planning. These Origin-Destination zones are also referred to as Traffic Analysis Zones (TAZ). Within the context of a system SRA, evaluation of travel times and flows to and from certain key zones can be used to assess post-earthquake impacts of highway system damage on the surrounding area. Data for each O-D zone in the region should include: (a) a GIS map of all O-D zones (plotted to the same scale as GIS map of the highway system map called out in section 3.3.1), which includes data to describe each zone's location, size, and shape; (b) the coordinate location of any key elements of the zone that may be important to post-earthquake response and recovery (such as fire stations, police stations, hospitals, airports, government centers, post-earthquake emergency command/coordination centers, major economic centers, or major residential centers; and (c) current and any future projected demographic information such as the number of households in the zone, population, vehicle types used for transportation, number of employed workers, and their types of employment (e.g., retail vs. non-retail).

3.3.7 TRIP TABLES

In the current practice for transportation modeling, it is assumed that the demand for travel between each O-D pair in the system is known by mode, either from observation or as the output of a travel demand forecast. These demands are represented as trip tables (also called "O-D matrices"), which are two-dimensional matrices that contain the total number of trips, by mode

---

[2] The BPR fourth degree polynomial shown in equation 1 is the standard congestion function used in transportation planning and engineering. This function was contained in FHWA's original urban transportation modeling codes, and then in the subsequent Urban Transportation Planning System updates (see section 3.4.1). Although research that supports this function is limited, it is the singly most widely used congestion function in the field.

and time of day, between all O-D zones in the region[3]. The trip table is a mode-specific function of the demographics of the region, and is usually developed from surveys of users of the highway system. Experience from recent earthquakes has shown that post-earthquake trip patterns may differ substantially from pre-earthquake patterns (Moore et al., 1997), although there is relatively little information or modeling experience for estimating post-earthquake trips. Post-earthquake trip generation rates will change because the objectives of travel will change. This remains a major uncertainty in the SRA process, and an important source of improvement that will require accounting for location specific damage to the activity system.

3.3.8 SPECIAL SYSTEM CHARACTERISTICS

Any special characteristics of the system and its roadways that may be important to post-earthquake response and recovery should be compiled, including all designated critical routes for national defense or emergency response.

3.3.9 TRAFFIC MANAGEMENT PLANS

Experience from past earthquakes has shown that sound traffic management plans can have an important impact on post-earthquake traffic flows and on the reduction of travel time delays while repair of the damaged highway system and components is proceeding (Gordon et al., 1996, Giuliano et al., 1996 and Caltrans, 1995). Therefore, it is important to include any post-earthquake traffic plans for the system that are currently in place. Such plans may include: (a) detour routes; (b) methods to enhance traffic flows along selected roadways (e.g., increase of traffic capacities through changes to one-way traffic, parking restrictions, traffic signal timing, etc.); and (c) enhancements of alternative modes of transportation, such as bus, train, and van modes. Public transit accounts for a small mode share under pre-earthquake conditions, but would likely become much more important (at least temporarily) after an earthquake. Mode choice is not modeled explicitly in this exercise. This is an important behavioral response that is likely to have a measurable impact on the level of service available from the transportation network; however, mode split would depend heavily on post-earthquake policy responses. The SRA methodology can be used to assess the effectiveness of existing post-earthquake traffic management plans, and how they may be modified to improve the ability of the damaged system to meet post-earthquake traffic demands, but no such policy responses have been assumed. If a public authority attempts to shift demand for transportation from private vehicles to public transit, the SRA procedure could account for this to some extent without modification. More careful assessments of this or other post-earthquake policies would likely require modification of the model.

---

[3]The trip table is most commonly estimated from surveys of users of the system. However, such surveys are usually very labor-, time-, and cost-intensive. By comparison, traffic counts are relatively inexpensive to obtain, and are routinely and automatically collected for many purposes. Therefore, there is considerable interest in developing procedures for estimating trip tables from traffic counts (Moore et al., 1997). As real time traffic data becomes available from telemetric sources, these options will become more important. However, good base O-D matrices are still required.

3.4 TRANSPORTATION NETWORK ANALYSIS PROCEDURES

This section summarizes two approaches for transportation network analysis. As a point of reference, the first approach is the network assignment element of the four-step Urban Transportation Modeling System. This represents the current practice used by Metropolitan Planning Organizations nationwide. However, conventional implementations of this approach have demonstrated limitations for application in SRA of highway systems. The basic UTMS approach to network assignment is sound, but commercial codes were too slow to support SRA modeling objectives. Therefore, two other approaches that are more suitable for SRA applications are instead built in to the SRA methodology. The first of these approaches -- a state of the art algorithm for computing User Equilibrium (UE) flows -- is a mathematically rigorous network assignment model of how users of the highway system choose a route for a given trip[4].

The second approach -- the Associative Memory (AM) method -- is a heuristic procedure for rapid estimation of user equilibrium traffic flows. This section summarizes each approach, and provides guidelines for choosing either the UE or AM method for a given SRA application. Appendix B of this volume provides further details on these two methods.

3.4.1 CURRENT PRACTICE – URBAN TRANSPORTATION MODELING SYSTEM

3.4.1.1 Overview

Current practice for urban transportation system analysis that is used by Metropolitan Planning Organizations in the United States is built around a large set of numerical models named the Urban Transportation Modeling System (UTMS). These models and their derivatives, which were developed over two decades ago by the U.S. Department of Transportation, are the standard planning tools in cities receiving Federal support for local transportation projects. They are typically used to compare benefits provided by alternative investments in network configuration or management, or to predict changes in the baseline level of service provided by the network due to changes in the urban activity system or demographic characteristics of urban settlements.

Input to the UTMS includes demographic information that describes the distribution of population with regard to travel behavior, aggregate economic information such as workforce participation and income, and land use information describing the spatial distribution and level of activities (figure 5). Then, the four steps of the UTMS for predicting traffic flows (which are trip generation, trip distribution, mode choice, and network assignment) are carried out. These steps are applied sequentially to estimate network Level of Service (LOS), or the system's ability to meet the traffic demands placed upon it by the surrounding urban area (Kim et al., 1997).

---

[4] Some Metropolitan Planning Organizations model user equilibrium flows with less exact tools, approximating user equilibrium flows with incremental assignment techniques. However, these have been largely replaced by convergent implementations of the Frank-Wolfe algorithm. The user equilibrium formulation available in the SRA methodology is an implementation of the Frank-Wolfe procedure written specifically for this research (see appendix B of this report).

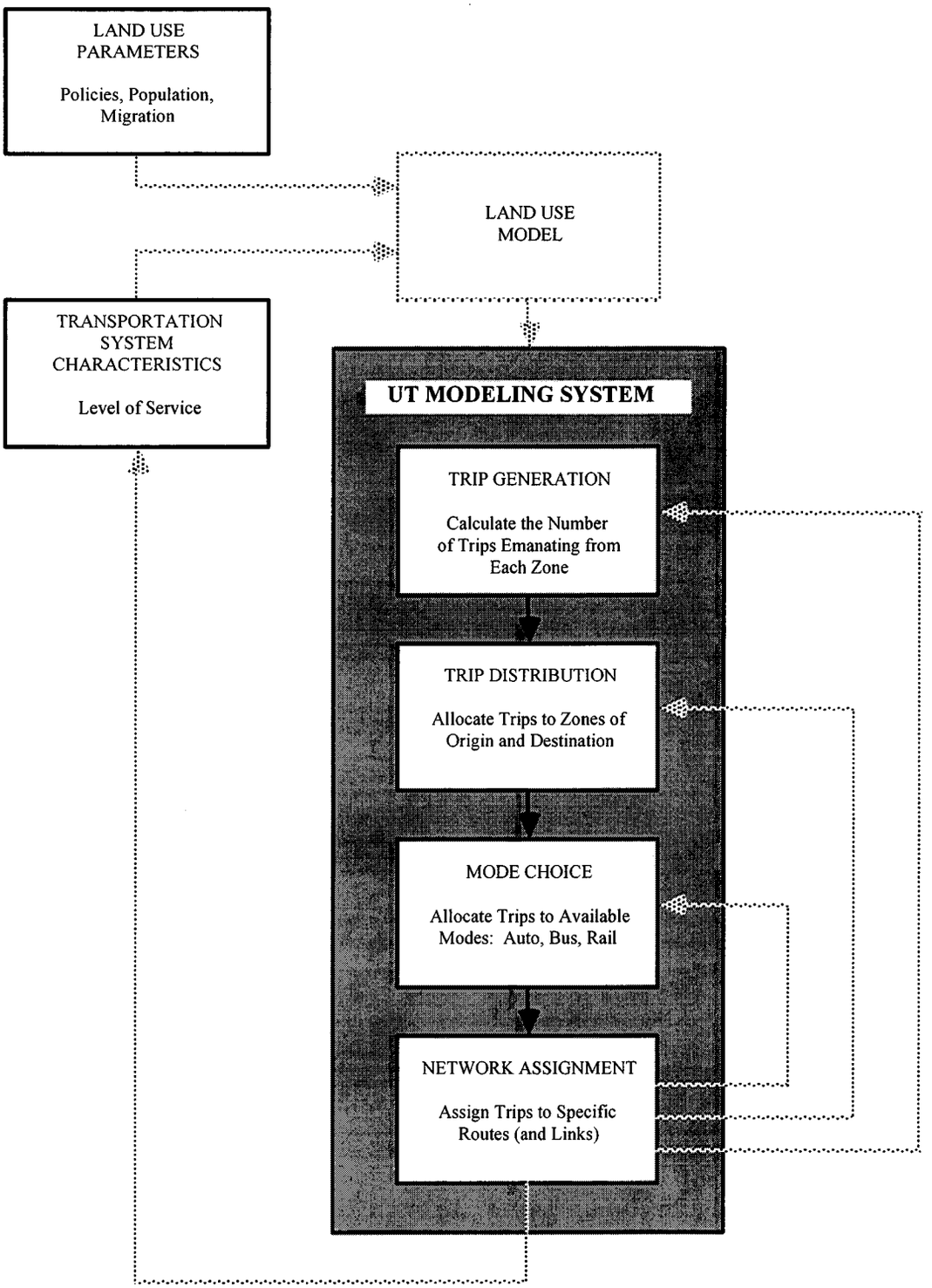

Figure 5. The Urban Transportation Modeling System (UTMS)

3.4.1.2 Applicability to SRA of Highway Systems

The transportation network analysis phase of the SRA methodology that is outlined in chapter 2 requires procedures that are rapid, efficient, and capable of analyzing highway system states that could exist after a major earthquake. The conventional UTMS transportation planning tools summarized above have the following deficiencies with respect to these requirements:

- It is costly to consider an adequate level of detail for representing the region served by the system (i.e., region boundaries and O-D zones) and the system network structure.

- LOS measures developed from network assignment models are inconsistent with the LOS assumptions associated with the other UTPS models. Although this deficiency could be addressed through iteration (as illustrated by the gray arrows in figure 5), such iteration would be difficult because: (a) there are no clear rules for iterative convergence in this context; (b) convergence is by no means assured; and (c) even if convergence were possible, such iteration would be extremely costly. Furthermore, there is no obvious basis for the sequencing of the various models as shown in figure 5. Considerable research has been and is being directed toward integrating the UTMS models into a single unified model, but no operationally better model has been developed.

- Behavioral shifts associated with major disasters such as large earthquakes are difficult to represent. In addition, land use interactions are almost always ignored.

- The UTMS procedure has very little capacity for considering the time dependence of the system performance characteristics. As a result, trip generation and trip distribution are usually assumed to be static (invariant over time). Separate four-step models must usually be estimated for different times of day.

At present, there are no readily accessible means for overcoming these limitations, regardless of whether earthquakes are involved or not. The SRA methodology does not overcome them. It inherits them. The methodology does, however, involve an important transportation modeling innovation that supports the stochastic nature of the SRA objectives. In this context, outputs consist of a sufficiently dense set of simulations that can be used to develop probability density functions for total costs. This requires a modeling capability that treats a much larger number of network states than would normally be modeled. Such a procedure is developed here. The key trade-off is to model many approximate solutions instead of one exact solution.

3.4.2 TRANSPORTATION NETWORK ANALYSIS FOR SRA APPLICATIONS

3.4.2.1 User Equilibrium Flows

Network flow problems are essentially route choice or traffic assignment problems. The question is how to determine how people, vehicles, and goods use the transportation network. The notion of equilibrium plays a central role in all attempts to construct mathematical models to traffic flow. Users are allocated to routes in a way that accommodates all trip requirements, and

for which all used paths between each origin-destination pair have the same time cost. This represents an "equilibrium" condition, since users are left with no incentives to change paths. The problem is complex because congestion ensures that link time costs are endogenous, and because paths overlap. Therefore, flows on one path influence the costs of traversing other paths.

From an economic perspective, traffic equilibrium is a special case of market equilibrium. The demand side of the market corresponds to the users of the network, and the supply side is represented by the network itself, with market prices represented as generalized travel costs, (i.e., travel times, monetary costs, risk, inconvenience, discomfort, etc. due to use of the network).

Mathematically exact equilibrium formulations have been developed for the following two idealizations of user behavior (Wardrop, 1952). Both formulations are static (steady state) and deterministic.

- *User Equilibrium (UE)* assumes that individual user travel times on all routes actually used are equal to or less than those user travel times that would be experienced on any unused route. That is, each (rational, perfectly informed) user is perceived to choose the route that minimizes his/her individual travel time. Average travel time is the same on all used routes.

- *System Equilibrium (SE)* is the set of flows under the condition that the average travel time throughout the entire system is minimized. This implies that: (a) each user behaves cooperatively, accepting a route assignment that ensures the most efficient use of the entire system; and (b) a network authority exists that is recognized and accepted by all users. Marginal travel time is the same on all used routes.

For either equilibrium condition, traffic flows are obtained as solutions to mathematical programming problems. Moore et al., (1997) provides algorithms for obtaining these solutions.

The UE condition is a much more practical and behaviorally meaningful outcome. SE flows cannot be sustained by competition between users, because a system-optimal set of flows leaves users with lower cost alternative routes. Flows cannot be optimized in a system wide sense unless users can be assigned to routes and assignment can be enforced. This is not the case in an urban network. For these reasons, the UE approach is built into the SRA methodology. Guidelines for applying the UE approach in SRA applications are provided in section 3.4.2.3.

Steady-state models of network equilibrium are approximations. In reality, travelers depart from different origins at different times, and attempt to arrive at their destinations within a narrow window of time. Demands for transportation services and equilibrium route costs are not constant. They change continuously over time of day. The SRA methodology does not incorporate a model of dynamic network equilibrium, because no computable formulation exists that is operational for urban applications.

3.4.2.2 Associative Memory Procedure

The Associative Memory (AM) procedure is a rapid flow prediction model for: (a) providing inexpensive and dependable estimates of flows in congested networks, given changes in link configuration due to possible earthquake damage; and (b) attaching these changes to the decision-making process for policies to reduce seismic risks due to highway system damage, e.g., establishing priorities for seismic retrofit, etc. This procedure integrates well with existing efforts in the field, because its flow estimates are inputs to both total transportation system cost and accessibility measures. The procedure is derived from the artificial intelligence field, and predicts changes in highway system flows by providing good approximate solutions to constrained optimization problems for representing economic determinants of these flows. In this case, an AM matrix is used to map given sets of system network configurations (stimulus) to lead to corresponding traffic flows (response). The AM is developed as follows (see figure 6):

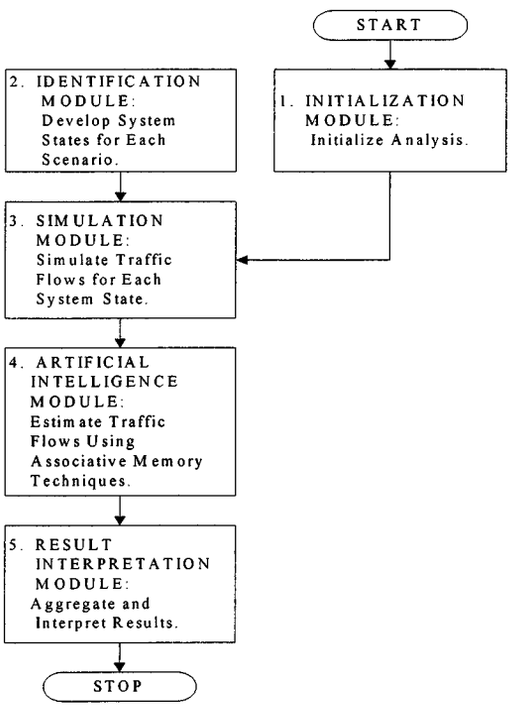

Figure 6. Flowchart for Associative Memory Procedure (Moore et al., 1997)

1. A UE model is used to develop an ensemble of UE traffic flows corresponding to various network configurations, all of which represent the same general type of network and traffic flow characteristics. This family of network problems and solutions correspond to the same set of origin-destination travel requirements. All are based on the same network, subject to incremental reductions in capacity and removals of links. Link removals can result from modeling of earthquake-induced failures of bridges or other highway components, or may be identified randomly. Most of these solutions are designated as "training cases", and the remainder are designated as "test cases".

2. The SRA methodology generates three types of training and test cases. First, each bridge is sequentially removed from the network, and UE flows are computed as a result of this removal. Capacity is eliminated in both directions. Second, pairs of bridge failures are identified. Each bridge in the neighborhood is considered in turn, where a "neighborhood" is defined in terms of the minimum number of network links that must be traversed to reach neighboring bridges, in this case ten. Pairs are formed between the first bridge and each other bridge in the neighborhood. Each pair is removed from the network. Capacity is eliminated in both directions. In the last set of training and test cases, bridge pairs identified in the second set of cases are permitted to fail one direction at a time. This is only feasible for roadway links where directional traffic flows occur along separate bridge structures. For each set of training and test cases, flows are computed for each link in each of the system states, as equivalent passenger-car-units per hour. This is an expensive preprocessing step that serves all subsequent analyses; however, if enough training cases are considered, it has the advantage of making the AM independent of the scenario earthquakes and simulations selected for investigation.

3. The training cases from step 2 are used to train the AM; i.e., to compute the elements of an AM matrix that minimizes the mean-square difference between the estimated and true UE traffic flows across all of the training cases. These true flows are the product of a conventional UE computational procedure.

4. The basic premise of this approach is that the training cases are representative of the relationships linking network configurations to UE flows. In other words, it is assumed that the AM matrix will provide a good estimate of traffic flows from other network configurations that represent conditions similar to those of the training cases, but which have not actually been used to train the AM. To check this, the AM matrix is used to predict traffic flows for each test case from step 2. These predicted flows are then compared to the UE flows for the various test cases.

5. Step 4 will usually lead to good comparisons between predicted and UE traffic flows, if an adequate number of training cases was considered in step 3. However, if needed, additional training cases can be developed in step 2 and used to further refine the AM matrix and the accuracy of its traffic flow predictions. This determination can be automated. The quality of the test estimates can be evaluated by computing the correlation coefficient between the predicted test flows and the UE flows. Correlation coefficients in the neighborhood of 0.98 indicate an excellent fit for test values. If this benchmark is not achieved or otherwise approached, additional training cases can be generated either by electing random deletion of links or by selecting additional system states from a list defined for the scenario earthquakes and simulations under investigation. In the demonstration SRA of the Shelby County highway system described in chapter 7, slightly less than 7,000 training cases were used to develop the multicriteria AM used in that analysis . This limit is largely a function of desktop computing limitations.

6. Like conventional approaches, the AM approach can rapidly and accurately predict aggregated (total system or subsystem) travel times to even a greater degree of accuracy than

its predictions of disaggregate travel times (along individual links). These aggregated travel times are the primary SRA results needed for subsequent estimation of economic losses or increases in travel times to key locations due to earthquake damage to the highway system (see chapters 6 and 7 of this manual).

Moore et al., (1997) and Kim et al., (1997) provide further background on the AM method, including past applications, basic concepts, and derivations for various types of AMs (i.e., simple, recurrent, and multi-criteria). Appendix B also provides additional information on this method.

3.4.2.3 Guidelines for System Analysis for SRA Applications

The UE and AM procedures included in the SRA methodology have the following benefits that make them particularly desirable for SRA applications: (a) they both represent the latest technology developed by experts in the field of transportation system analysis, and both circumvent many of the previously-noted limitations of the UTMS for SRA applications; (b) their analysis results are readily adaptable to GIS; (c) both are plausible for application to a highway system with possible substantial closures due to earthquake damage; and (d) they both use transportation system input data of the type that are readily available through MPOs.

Neither conventional calculation of UE flows nor use of an AM to approximate these flows updates O-D matrices. Travel is a derived demand. Changes in O-D matrices should reflect changes in demands for the goods and services made possible by travel. At a minimum, changes in demand should reflect changes in the cost of travel. Modeling these changes requires linking a model of the transportation network to a model of the activity system. If such a linked model is available, the AM procedure can be trained against the traffic flows that such a model associates with different network states.

The main difference between the two approaches is in the number of system states that they can readily handle. Conventional transportation planning applications require modeling of a relatively few alternative sets of network flows associated with different network investment or management options. If the user wishes to carry out deterministic estimates of losses for a limited number of scenario earthquakes, the UE approach should be used. Graphical results from a deterministic SRA for a particular scenario earthquake and simulation can include: (a) UE traffic volumes for roadway links in the network, shown as bandwidths along each link (figure 7); (b) minimum-time travel paths to one destination from all possible origins (figure 8); and (c) minimum-time travel paths between user-selected pairs of origins and destinations (figure 9).

These deterministic applications for a limited number of scenario earthquakes are fairly conventional network analyses that can be used to explore specific what-if questions associated with various pre- and post-earthquake seismic risk reduction options. However, suppose the user instead requires probabilistic estimates of losses for many scenario earthquakes and simulations (leading to many thousands of system states for which travel times and traffic flows must be estimated). The computational burden of providing these estimates as near-exact mathematical solutions for UE conditions is excessive, and is a new transportation engineering problem.

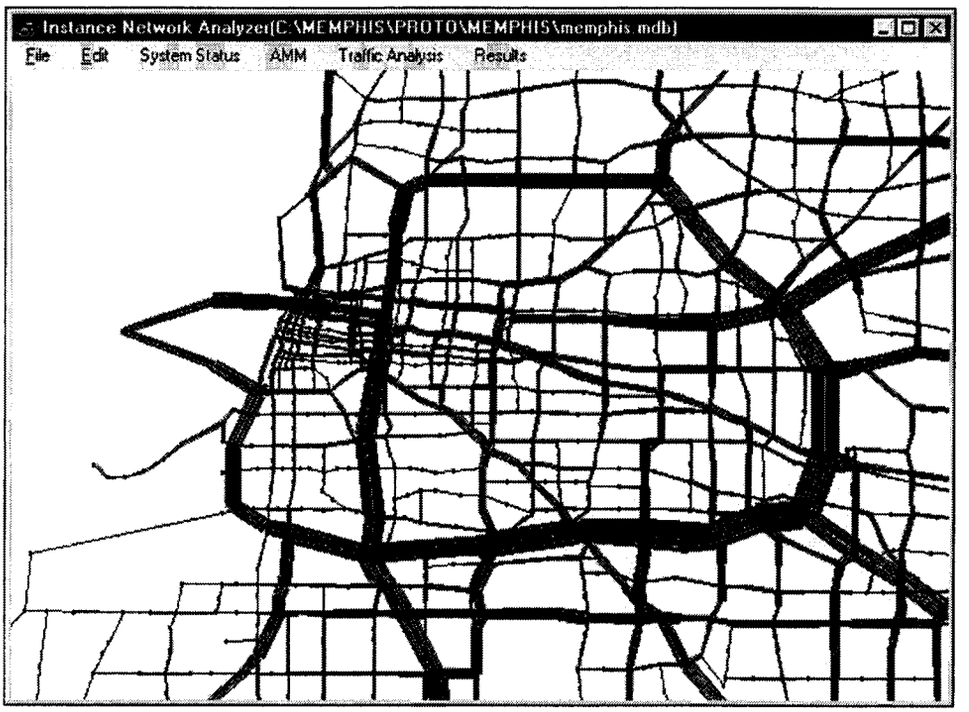

Figure 7. UE Traffic Volumes Shown as Bandwidths along each Link

Figure 8. Minimum-Time Travel Paths to One Destination (Circled) from all Origins

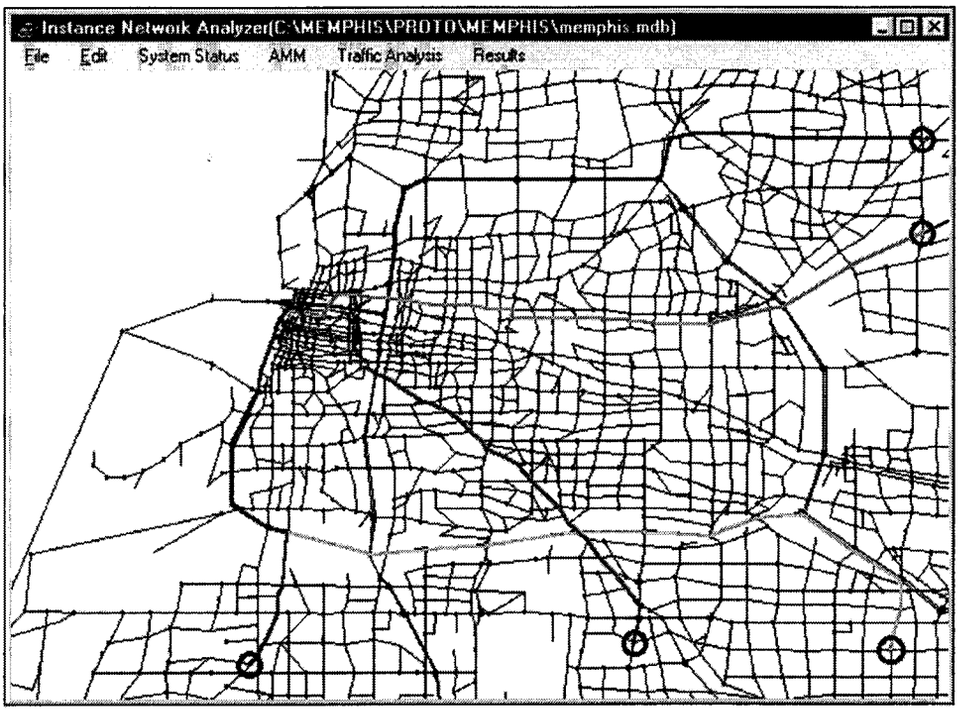

Figure 9. Minimum-Time Travel Paths between User-Selected Origin-Destination Pairs

For such probabilistic applications, the AM approach and its capacity for rapid prediction of network flows is particularly effective and efficient. In fact, a properly estimated AM procedure can readily provide rapid access to traffic flow and travel time estimates for thousands of system states, once initial costs and efforts for developing the AM matrix have been completed. To illustrate this, figure 10 provides a comparison of CPU times for the UE and AM method, as applied to the highway system model used for the demonstration SRA of the Shelby County, Tennessee highway system that is described in chapter 7. This figure shows that the AM procedure is clearly much more economical when it is necessary to analyze large numbers of system states as part of a probabilistic SRA.

The magnitude of the errors introduced by relying on an AM procedure to estimate UE traffic flows is routinely smaller than the differences between exact UE flows and observed flows (Moore et al., 1997). Therefore, since the ultimate objective of the SRA application is to estimate traffic flows that would otherwise be appearing in the real world, the error introduced by relying on AM procedures is inconsequential relative to that for conventional network modeling approaches. The quality of the match between exact UE results and the AM outputs is summarized in figures 11 and 12 for 2,460 test cases. These test cases are defined by 820 system states at each of three post-earthquake times 7, 60, and 150 days after the scenario earthquake. None of these test cases was used to train the AM. UE flows were computed for each case to test the quality of the results provided by the AM.

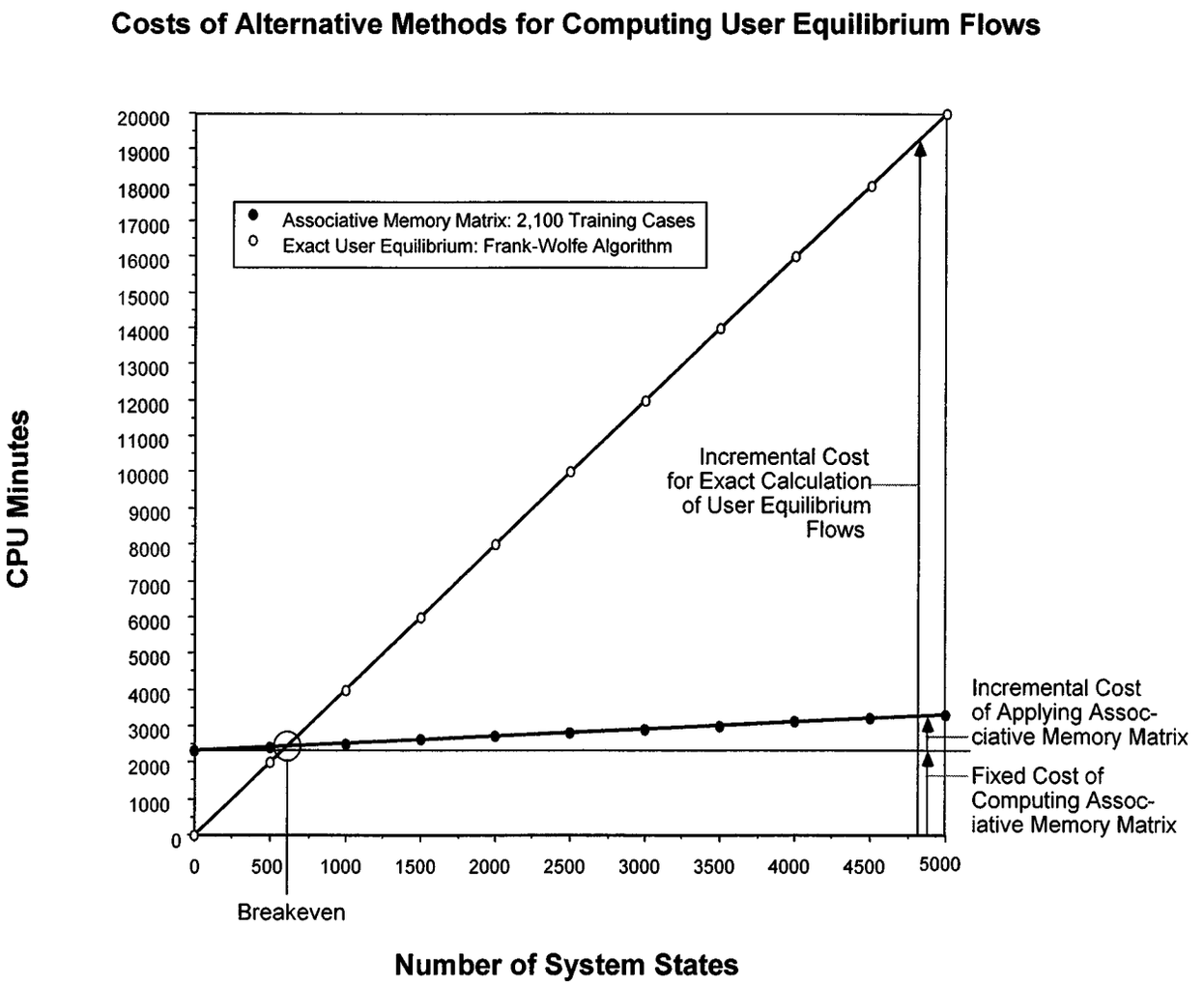

Figure 10. CPU Times for UE and AM Methods of Transportation Network Analysis

These figures show that the AM applied to thee test cases generally performs very well. Figure 11 is a scatter plot that relates AM average link traffic flows to UE traffic flows across each of the 2,460 test cases. The correlation coefficient (R^2) value reported in this figure is for individual link traffic volumes, not average link volumes. Basing this calculation of R^2 on individual link volumes is conservative, because there is a greater variance in individual AM estimates than in average AM estimates. Figure 12 summarizes the cumulative portion of cases for which the R^2 between AM and UE flows is less than or equal to a given value. For a small portion of the cases, R^2 is as low as 0.5. However, the great majority of the test cases demonstrate a very high correlation between UE traffic flows and the flows estimated by the AM.

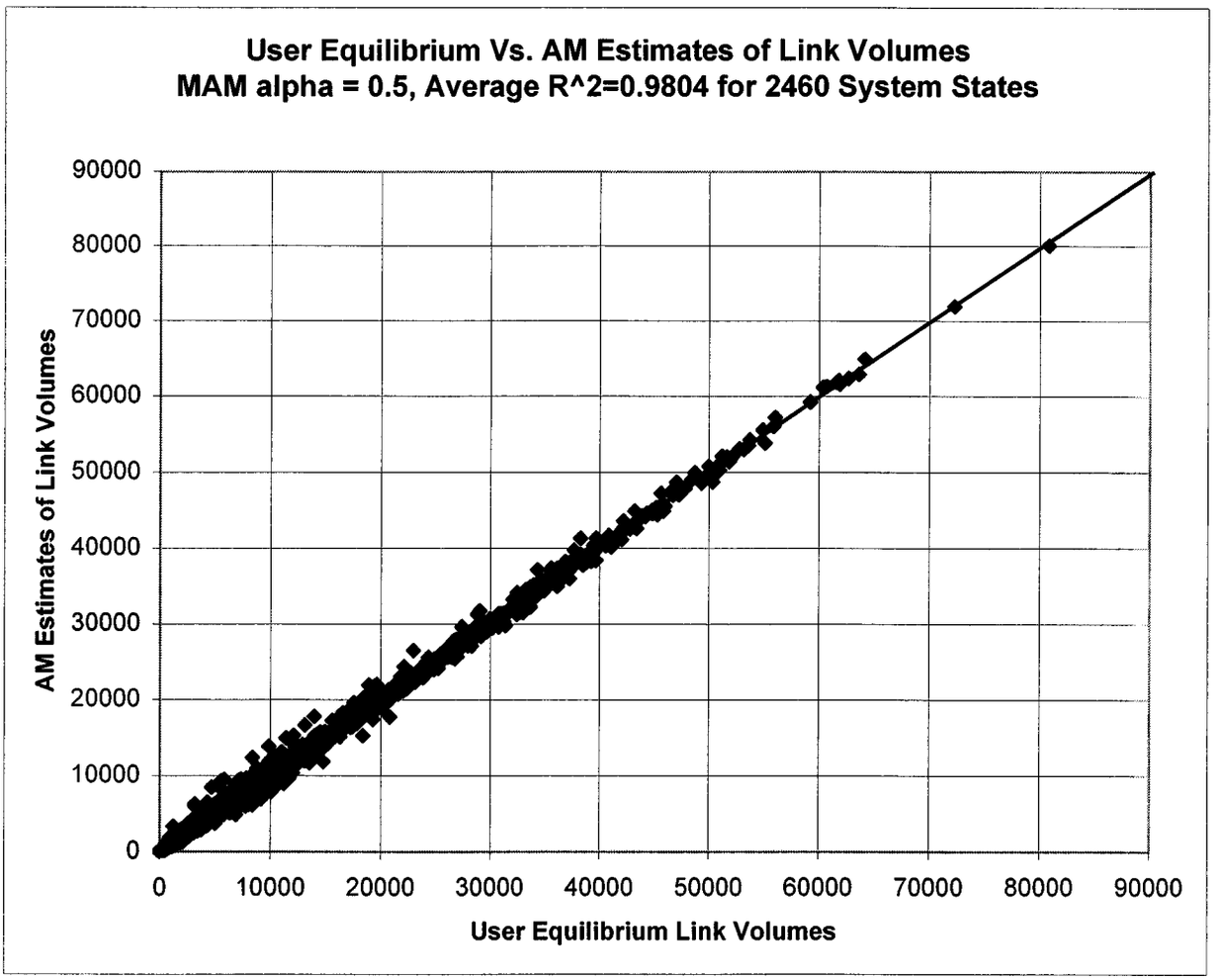

Figure 11. Scatter Plot of AM Estimates of Link Volumes to UE Link Volumes for 2,460 Test Cases at Post-Earthquake Times of 7, 60, and 150 Days

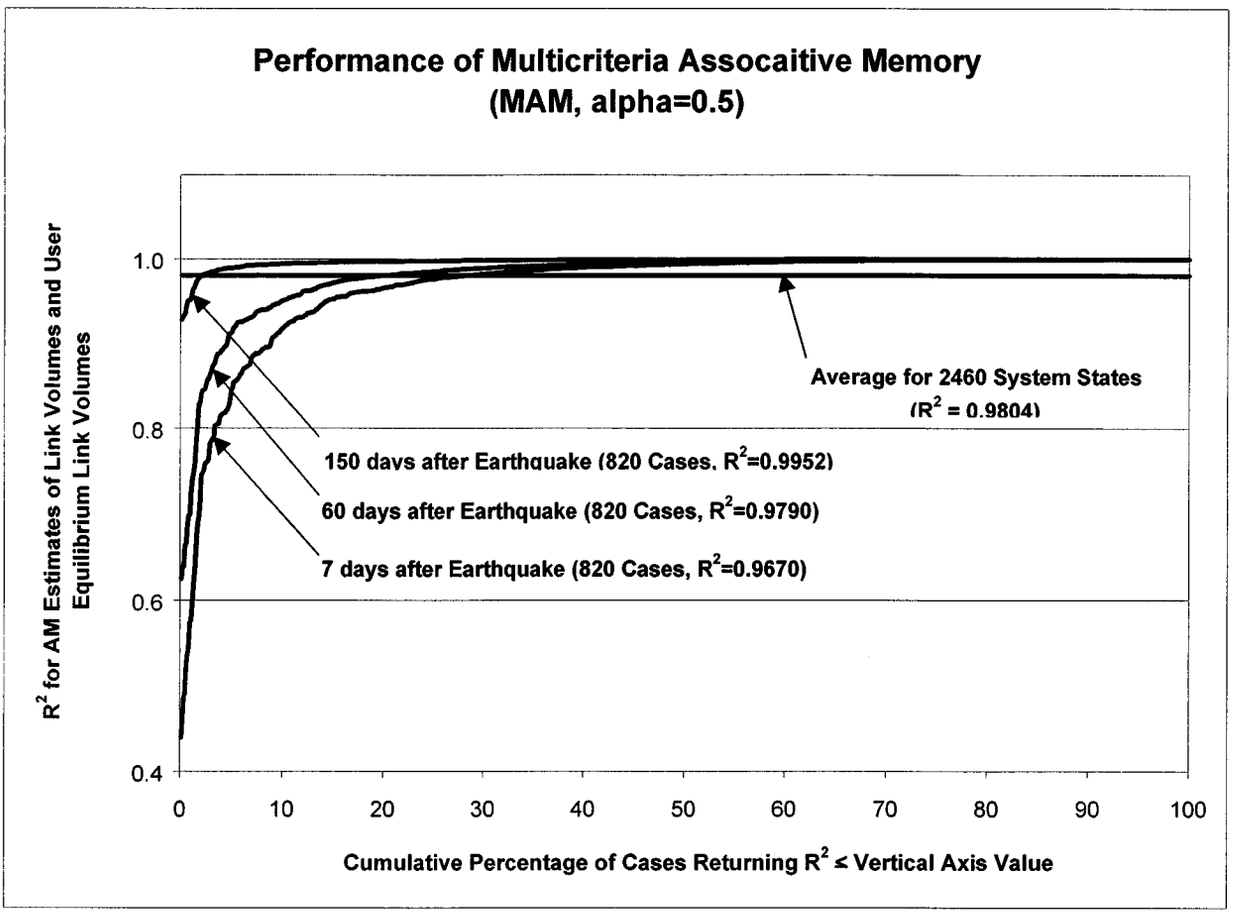

Figure 12. Cumulative Portion of Cases Returning a Given R^2 Between AM Estimates and UE Link Traffic Volumes

CHAPTER 4
EARTHQUAKE MODELING AND HAZARDS MODULE

4.1 OBJECTIVE

The seismic hazards imposed on a highway system will depend on the magnitudes, locations, and frequencies of occurrence of earthquakes in the region, and on the local geology and soil conditions throughout the system. This chapter summarizes how scenario earthquakes are modeled in the SRA methodology, using regional seismologic and geologic data within the framework of a walkthrough process. It also describes the elements of the hazards module, which contains the data and models necessary to characterize the seismic and geologic hazards throughout the highway system due to each scenario earthquake and simulation. These hazards include earthquake ground motions and liquefaction (which are incorporated into the SRA methodology), and landslide and surface fault rupture (which will be added in the future). For each hazard, the chapter summarizes: (a) the hazard and its possible effects on highway systems; (b) methods for evaluating the hazard at each component site; and (c) the input data needed to implement the hazard evaluation procedure.

4.2 SCENARIO EARTHQUAKES

4.2.1 OVERVIEW

In a SRA of a system with spatially dispersed components, individual scenarios are required to evaluate correlation effects of earthquakes, i.e., the simultaneous effects (including systemic consequences of damages) of individual earthquakes on components located at diverse sites.

As noted in section 2.3.1, scenario earthquakes for the SRA are developed by the user as part of the initialization phase of the SRA process. In this, regional earthquake source models are used to define an ensemble of earthquakes, in which each earthquake is most commonly defined in terms of its magnitude, location, and frequency of occurrence. In this SRA methodology, these earthquakes are represented in a form suitable for use in a walkthrough analysis (Daykin et al., 1994). This facilitates the development of loss distributions from the SRA results, the estimation of nominal confidence levels and limits of these loss results, and the display of their variability over time.

4.2.2 REGIONAL EARTHQUAKE SOURCE MODELS

The SRA methodology incorporates regional earthquake source models that have been adapted from models used by the United States Geological Survey (USGS) during their development of new seismic hazard maps for the conterminous United States (Frankel et al., 1996). The USGS models have been selected because of their development by recognized earth scientists and because of their subsequent extensive external review process. These models incorporate: (a) smoothed historical seismicity as one component of the hazard calculation; (b) a weighted combination of alternative models with different reference magnitudes, as well as large

background zones based on broad geologic criteria; and (c) the use of geologic slip rates to estimate earthquake recurrence times for faults in the Western United States.

Thus far, scenario earthquakes for the Central United States (CUS) have been included in the SRA methodology, as described in appendices A and C. These earthquakes are used in the demonstration SRA of the Shelby County, Tennessee highway system that is described in chapter 7. Future work will adapt the USGS models to other regions of the United States, so that the SRA methodology will contain a consistent and technically robust set of earthquake models nationwide.

4.2.3 WALKTHROUGH ANALYSIS

The SRA methodology requires that the ensemble of scenario earthquakes be represented in a form suitable for use in a walkthrough analysis. The walkthrough analysis facilitates the development of loss distributions and statistics, confidence levels and limits of these results, and the display of their variability over time. The steps that comprise a walkthrough analysis are described appendix A and are briefly summarized below.

4.2.3.1 Step 1 – Total Duration of Walkthrough

In step 1, the user selects the total time duration of the walkthrough. This duration may be in the tens, hundreds, or even thousands of years. The user's selection of the walkthrough duration should be based on his/her target confidence levels and limits for the SRA results.

4.2.3.2 Step 2 – Scenario Earthquakes during Each Year of Walkthrough

Step 2 establishes the scenario earthquakes for each year of the walkthrough. This is carried out first for year 1, and then for each succeeding year of the walkthrough. For each year, this process generates a series of uniform random numbers that are used with various earthquake probability distributions developed from regional earthquake source models (section 4.2.2), in order to establish: (a) the number of potentially damaging earthquakes (i.e., earthquakes with $M_w \geq 5.0$) that have occurred somewhere in the region during the year; and (b) the location and the magnitude of each of these earthquakes. Note that, for the demonstration SRA of the Shelby County, Tennessee highway system in the CUS that is described in chapter 7, it is assumed that up to two potentially damaging earthquakes can occur during a single year. For other regions of the United States that are more seismically active, the earthquake model should consider the possibility that more than two earthquakes with $M_w \geq 5.0$ could occur in a given year.

4.2.4 APPLICATION IN DEMONSTRATION SRA

For each year of the walkthrough, a uniform number of multiple simulations is selected by the user. A SRA of the highway system is carried out for each year and each simulation, and the results from all of these years and simulations are analyzed in order to develop loss statistics. The number of simulations considered in each year is selected to meet target confidence levels and limits established by the user. Appendix A describes how this number of simulations can be estimated, and also includes procedures for estimating loss statistics.

4.3 GROUND MOTION HAZARDS

4.3.1 HAZARD DESCRIPTION

Past earthquakes have shown that highway components can be susceptible to damage from strong ground shaking. The extent of this damage depends not only on the geometry and structural characteristics of the component, but also on the amplitude, frequency content, and duration of the ground shaking. Past earthquakes have also shown that the spatial distribution of ground shaking throughout a system will depend on the nature of the fault rupture process, the travel paths followed by the seismic waves as they propagate from the earthquake source and throughout the system, and the local soil conditions within the system. Furthermore, empirical studies of recorded ground motions have shown that this distribution of ground shaking is not random; rather, it tends to attenuate with increasing distance from the seismic source and is usually most severe in soft soil deposits. In addition, for a given source-site distance and site conditions, the ground motions tend to increase with increasing earthquake magnitude, except for large magnitude earthquakes where saturation of the ground motion amplitudes tends to occur. The estimation of ground shaking hazards is essential not only to evaluate the potential for system and component damage from these hazards, but also to assess other collateral hazards such as liquefaction and landslide.

4.3.2 HAZARD EVALUATION PROCEDURE

The procedure used to estimate earthquake ground motions for SRA of a highway system must account for the seismologic, geologic, and tectonic characteristics of the region, as well as local soil conditions at the component sites throughout the system. General descriptions of how these quantities can be considered in the ground motion evaluation process are well documented in the technical literature (e.g., Frankel et al., 1996, Howner and Jennings, 1982, Seed and Idriss, 1982, Werner, 1991, Kramer, 1996, and Dickenson, 1998).

As previously noted, the estimation of earthquake ground motions for a highway system SRA will differ from that for an individual component, because of the need to represent the spatial distribution of the ground shaking throughout the system due to each scenario earthquake. To represent this spatial distribution, the ground motion model must consider: (a) how the bedrock motions attenuate with increasing distance from the earthquake source, and how they are affected by the earthquake magnitude; and (b) how the local soil conditions amplify the bedrock motions as the seismic waves propagate through the subsurface soil layers and up to the ground surface.

The current version of the SRA methodology incorporates a ground motion model for the CUS only. Future work will incorporate models for other regions of the United States as well. The basic procedure for selecting an appropriate ground motion model for a given region is summarized in the following subsections.

4.3.2.1 Step 1 – Bedrock Motions

System-wide bedrock motions due to a given scenario earthquake event must be provided as spectral accelerations at the full range of natural periods that could have an effect on the seismic response of highway system components (including the zero-period spectral acceleration which is equal to the peak bedrock acceleration). The representation of how these bedrock motions vary with source-site distance and earthquake magnitude should be based on an existing bedrock-motion attenuation equation for the region that is accepted by the technical community.

Selection of an appropriate equation should consider such factors as the types of variables included in the equation, the range of variables over which the relationship is considered valid, the data base, and the functional form (e.g., Campbell, 1985 and Taylor, 1991). The selection should also consider that differences in geologic and tectonic characteristics between different regions of the United States can lead to different rates of attenuation of bedrock motions with increasing distance from the earthquake source, and also different dependencies of the bedrock motions on earthquake magnitude. Therefore, the attenuation equation that is used for a highway system SRA should be appropriate for the region where the system is located. This equation should be based on applicable regional data and attenuation rates, as derived from strong motion records or from historical information for regions where such records are not available. The development of such equations often includes simplified models of fault rupture and seismic wave propagation.

4.3.2.2 Step 2 – Soil Amplification Factors

In step 2, empirically- and/or analytically-based soil amplification factors (SAFs) are used to scale the bedrock motions and obtain period-dependent motions at the ground surface. To be consistent with current bridge- or building-design practice, these SAFs are typically established for different site categories that reflect different general site soil conditions (e.g., Dobry et al., 2000 and AASHTO, 1998). The SAFs should vary with the strength of the shaking, which occurs because of nonlinear stress-strain and energy dissipation characteristics of the soil materials.

SAFs for the CUS now included in the SRA methodology are based on the 1997 NEHRP site categories (Dobry et al., 2000). It is expected that default SAFs for other regions of the country that will be added to the SRA methodology at a later date will also be based on the NEHRP categories. However, there may be conditions within the highway system where such broad site categories and SAFs may not be adequate. For example, at sites where component damage could severely affect post-earthquake traffic flows (i.e., along major links with limited redundancy) and/or where soil amplification effects could be substantial, more detailed site-specific soil testing and analysis should be implemented to obtain more refined SAFs. Therefore, the SRA methodology provides the user with an option to override the default SAFs with these more detailed site-specific factors. However, it is recommended that any overriding of the default factors be peer reviewed by a panel of qualified geotechnical engineers, whose assessment of the new SAFs would be submitted to the cognizant state or federal highway transportation authorities.

4.3.3 INPUT DATA

Input data for modeling earthquake ground motion hazards at a given site in the highway system consist of: (a) the earthquake magnitude; (b) the distance from the site to earthquake source; and (c) the local soil conditions at the site. The earthquake magnitude is specified as part of the scenario earthquake designation, and the source-site distance is obtained from the coordinates of the site (specified as part of the highway component input data as described in chapter 5) and the coordinates of the earthquake location (specified as part of the scenario earthquake designation). Input data for modeling local soil conditions are discussed below.

As noted in section 4.3.2.2, the SAFs for representing local soil effects on ground shaking can usually be specified for various NEHRP soil categories, and based on available soil-category maps for the region. In the absence of such maps, the soil categories should be based on: (a) compilation of a topographic map, quaternary geology map, and a map of depth to bedrock contours throughout the system area; and (b) use of available soil test data obtained along or near the system, to correlate the geologic units from these maps with the various soil categories. At critical sites within the highway system, the SAFs should instead be based on site-specific soil test data and analysis. The soil test data obtained at these critical sites should include index properties, strength properties, SPT or CPT profiles, and downhole shear wave velocity profiles.

4.3.4 UNCERTAINTIES

The estimation of site-specific ground motions will be affected by uncertainties in the bedrock motion attenuation relationships, and in the soil properties and associated soil amplification factors throughout the system. These uncertainties should be included in the ground motion estimation process, as distributions of the data values and model predictions about their estimated mean values. Appendix D describes how uncertainties have been included in the ground motion model for the CUS that is used in the demonstration SRA of the Shelby County, Tennessee highway system (which is described in chapter 7).

4.3.5 GROUND MOTION MODELS IN SRA METHODOLOGY

The SRA methodology currently includes a model for estimating ground motions in the CUS only. As previously noted, models procedures for estimating ground motions in other parts of the country will be incorporated into the methodology in the future, and will be based on the principles outlined in section 4.3.2.

The CUS ground motion model that is now included in the SRA methodology consists of the bedrock motion attenuation equations and the SAFs for different soil categories that have been developed for the region by Hwang and his associates at the University of Memphis (Hwang and Huo, 1997 and Hwang et al., 1997). This model was selected because: (a) the assumptions used to develop these attenuation equations and SAFs are internally consistent (e.g., consistent definitions of "bedrock", etc.) and, as a result, they can be used together to compute ground surface spectral accelerations (as the product of the bedrock accelerations from the attenuation equations and the SAFs for the appropriate soil category); (b) the attenuation equations and SAFs

were specifically developed for the CUS region; (c) bedrock motions estimated from the attenuation equations by Hwang and his associates compare well with motions estimated using other well-established equations for the CUS (Hwang and Huo, 1997); (d) the Hwang et al. SAFs are developed from statistical compilations of results from state-of-the-practice analytical procedures (Hwang et al., 1997); and (e) effects of uncertainties are considered. The adaptation of this ground motion model for use in this SRA methodology is further described in appendix D.

4.4 LIQUEFACTION HAZARDS

4.4.1 HAZARD DESCRIPTION

Liquefaction is a process that occurs in loose, saturated, granular soil materials subjected to earthquake ground shaking. If this shaking is of sufficient strength and duration, the soils tend to decrease in volume due to a collapse of the soil "skeleton". This volume change is restricted by the rate at which the pore water can flow out of the soil, thereby resulting in a dramatic increase in pore water pressure and a temporary loss of stiffness and shear strength of the soil when the pore water pressure approaches the in situ vertical effective stress. Liquefaction-induced soil failure can result in lateral spread displacement and vertical settlement, reduced bearing strength, increased lateral pressures against retaining structures (e.g., abutment walls) that are in contact with the liquefied soils, and a loss of frictional resistance of pile elements at their interface with liquefied soils layers. If these effects are sufficiently large, they can cause substantial damage to highway structures.

4.4.2 HAZARD EVALUATION PROCEDURE

The SRA methodology uses an adaptation of a screening procedure by Youd to estimate liquefaction hazards throughout the highway system due to a given scenario earthquake (Youd, 1998). The steps that comprise this procedure are summarized below, and are described in more detail in appendix E.

4.4.2.1 Step 1 – Initial Screening

Step 1 consists of initial screening based on review of geologic data and prior liquefaction evaluations in the region, to establish which sites in the system have a sufficiently low potential for liquefaction to enable them to be eliminated from further analysis under the subsequent steps of the process. This screening is to be carried out by the user prior to the start of the SRA, and should be based on the screening guidelines provided in appendix E. The results of this screening are input to the SRA, in the form of designations of those sites within the system where liquefaction analysis would be warranted for each scenario earthquake and simulation. All other sites are eliminated from further evaluation. The remaining steps in the process are carried out only for the sites that have not been eliminated by the geologic screening, and after the ground shaking hazard at each site is estimated for each scenario earthquake and simulation.

4.4.2.2 Step 2 – Further Screening

In step 2, each remaining site is further screened by use of a simplified and conservative assessment of the ground shaking hazard at the site, due to each scenario earthquake and simulation. This additional screening identifies those sites whose liquefaction potential for this particular earthquake and simulation is sufficiently low to eliminate them from further consideration.

4.4.2.3 Step 3 – Liquefaction Susceptibility Evaluation

For those sites not eliminated by the further screening under step 2, step 3 uses procedures by Seed and Idriss to further evaluate the liquefaction susceptibility of each remaining site (Seed and Idriss, 1982). For those sites determined from step 3 to be susceptible to liquefaction under the given scenario earthquake and simulation, steps 4 and 5 are used to estimate liquefaction-induced permanent ground displacements.

4.4.2.4 Step 4 – Calculation of Lateral Spread Displacement

For those sites with a gently sloping or free face condition that have been shown from step 3 to be susceptible to liquefaction due to the given earthquake and simulation, step 4 computes lateral spread displacements using recent models by Youd and his associates (Youd et al., 1999).

4.4.2.5 Step 5 – Calculation of Vertical Settlement

For those sites that have been shown from step 3 to be susceptible to liquefaction under the given earthquake and simulation, step 5 computes liquefaction-induced vertical ground settlement using the Tokimatsu-Seed procedure (Tokimatsu and Seed, 1987).

4.4.3 INPUT DATA

The input data for system-wide liquefaction hazard evaluation under the SRA methodology are summarized below (Youd, 1998).

4.4.3.1 Geologic Data

To implement the initial geologic screening of the sites throughout the highway system (step 1 above), detailed information from geologic maps and/or reports on Quaternary geologic or sedimentary units should be obtained, with a particular emphasis on units from the Holocene and late Holocene eras. This information should include the locations of these units within the highway system, the types of soil deposits that are characteristic of these units, the general distribution of cohesionless sediments in the deposits, and the depths of the sediments. In addition, these geologic data should be correlated with soil boring data within the system.

4.4.3.2 Water Table

Expected water table levels should be obtained from boring logs at highway component sites or at nearby sites. If such boring logs are not available, regional water table maps or information from local engineers or hydrologists familiar with local soil conditions may be used.

4.4.3.3 Soil Properties

Properties to be obtained for classifying the soils include the fines content, Atterberg limits, clay content, natural moisture content, and sensitivity. In addition, evaluation of liquefaction susceptibility (under step 3 of the liquefaction hazard evaluation procedure as indicated in section 4.4.2.3) requires Standard Penetration Test (SPT) corrected blowcounts[1]. These corrected blowcounts, denoted as $(N_1)_{60}$, include corrections of the measured blowcounts to account for overburden pressure, hammer energy ratio, borehole diameter, rod length, and samplers with or without liners (Youd, 1998). Finally, material properties required for estimation of lateral spread displacements using the Youd et al., (1999) models (under step 4 of the hazard evaluation procedure, as indicated in section 4.4.2.4) are (a) T_{15}, which is the cumulative thickness (in meters) of saturated granular layers with $(N_1)_{60}$ less than 15; (b) F_{15}, which is the average fines content (in percent) for the granular layers comprising T_{15}; and (c) $(D_{50})_{15}$, which is the average mean grain size (in millimeters) for granular layers comprising T_{15}. At sites within the highway system where past test data are lacking, the above properties should either be estimated from correlations of regional geologic data with soil data from other sites in the region, or should be measured during a new test program at the site. At links within the system where the geologic screening shows a potential for liquefaction and where closures due to earthquake damage could cause significant disruption of post-earthquake traffic flows, site-specific field and laboratory testing should be conducted to obtain any missing soil data needed for liquefaction evaluation.

4.4.4 UNCERTAINTIES

The liquefaction hazard evaluation procedure currently incorporated into the SRA methodology includes effects of model uncertainties in the permanent ground displacement calculations only (see appendix E). There is interest in the modeling of uncertainties in other elements of the liquefaction hazard evaluation process, and research for developing such models is being implemented (TRB, 1999). Therefore, as liquefaction uncertainty models are developed in the future, they should be incorporated into the SRA methodology.

---

[1] In addition to the SPT, the Cone Penetrometer Test (CPT) is widely used in foundation engineering investigations. Therefore, the screening procedures by Youd evaluate liquefaction susceptibility in terms of CPT data as well as SPT data, and lists input data requirements for such evaluations.

4.5 LANDSLIDE HAZARDS

4.5.1 HAZARD DESCRIPTION

Strong earthquakes have often caused landslides that are most commonly small, but have also caused major slides that have caused widespread damage and loss of life. The potential for landslide depends on the geologic, hydrologic, topographic, geometric, and material characteristics of a given slope. Slopes become unstable during an earthquake when the shear stresses required to maintain equilibrium under combined in situ (static) and seismic (dynamic) conditions exceed the available shearing resistance on some potential failure surface. The most common types of landslides that have occurred during historic earthquakes are rock slides, disrupted soil slides, and rock falls -- which have usually occurred in steep terrain and can produce rapid movements and major devastation. Other types of landslides are classed as: (a) coherent slides (e.g., rock and soil slumps and block slides, and slow earth flows) which typically consist of a few coherent blocks that move on relatively deep failure surfaces and slow velocities; and (b) lateral spreads and flows, which occur in soils with low residual strength (e.g., liquefiable soils and sensitive clays) and therefore can occur on flat slopes and can have high velocities of movement (Kramer, 1996). Significant landslides have occurred during major earthquakes in San Francisco (1906), Alaska (1964), Peru (1970), Japan (numerous earthquakes), and China (1920), and more recently during the Loma Prieta (1989), Northridge (1994), and Taiwan (1999) events. During the 1989 Loma Prieta earthquake, a large landslide led to extended closure of Highway 17 -- the major highway that links the city of Santa Cruz with San Jose and the San Francisco Bay area.

4.5.2 HAZARD EVALUATION PROCEDURE

The evaluation of landslide hazards within a highway system during a given scenario earthquake should include the following steps (e.g., Power et al., 1994 and Kennedy/Jenks Consultants, 1995).

4.5.2.1 Step 1 – Landslide Inventory

In step 1, a landslide inventory for the region containing the highway system is compiled and mapped. The objective of this inventory is to correlate landslide density with slope steepness and geology. The inventory should be mapped at an appropriate scale for use in subsequent steps of the evaluation procedure (e.g., 1:24,000). It should be based on existing landslide hazard maps and interpretation of existing aerial photographs, and may be supplemented by field reconnaissance of areas within the system that could have a high landslide susceptibility.

4.5.2.2 Step 2 – Landslide Susceptibility Classes

In step 2, landslide susceptibility classifications are developed from consideration of geology, slope steepness, and density of existing slides. Example landslide susceptibility classifications developed for a lifeline SRA in a region of Northern California is shown in table 2a. This table shows that, for a given set of subsurface conditions, the susceptibility classification may range

from "Very High" for steeply sloped areas with a large slide density to "Very Low" for areas with a moderate to small slope and with a small slide density. An appropriate susceptibility classification would then be assigned to each landslide area inventoried and mapped in step 1.

4.5.2.3 Step 3 – Threshold Ground Motions

For each of the above susceptibility classes, step 3 estimates threshold levels of earthquake ground shaking that would trigger earthquake-induced landslide. These threshold ground motion levels should be estimated using appropriate simplified analytical procedures and should be guided by any available empirical data on movements of slopes with comparable geologic conditions during past earthquakes (e.g., Keefer, 1984). Best-estimate ground shaking levels, together with an appraisal of possible uncertainties in these best estimate values, should be developed. Appropriate state-of-the-practice analytical procedures for estimating threshold ground motions are well summarized in the technical literature (e.g., Kramer, 1996 and Dickenson, 1998). The threshold ground motion levels estimated for each susceptibility class should be incorporated into the landslide inventory and map compiled under step 1, for each landslide area defined in that step.

4.5.2.4 Step 4 – Ground Displacements

Step 4 estimates potential ground displacements due to earthquake-induced landslide, as a function of the level of earthquake ground shaking and the landslide susceptibility class (e.g., see table 2b). Again, appropriate state-of-the-practice analytical procedures (e.g., Kramer, 1996 and Dickenson, 1998) should be used for these ground displacement evaluations.

4.5.2.5 Step 5 – Landslide Hazard Estimation

In step 5, the ground shaking at each potential landslide site due to each earthquake and simulation (estimated by procedures outlined in section 4.3.2) is compared to the threshold ground shaking level for slope failure at that site, as estimated in step 3. If the earthquake-induced ground shaking level exceeds the threshold level, landslide is assumed to occur. Then, the results from step 4 are used to estimate the site-specific ground displacement due to landslide.

4.5.3 INPUT DATA

The data and models that should be incorporated into the hazards module in order to carry out the above approach for estimating earthquake-induced landslide hazards are summarized below.

Table 2. Landslide Hazard Evaluation
(Kennedy/Jenks Consultants et al., 1995)

Slope Steepness	Resistant Sandstone or Chert Bedrock (Kjfs or Kjch)			Melange Bedrock (Kjfm) or Thick Colluvium over Bedrock (Qc)		
	SLIDE DENSITY			SLIDE DENSITY		
	0 -3/km (<10%)	3-13/km (<25%)	>13/km (>25%)	0-3/km (<10%)	3-13/km (<25%)	>13/km (>25%)
	Susceptibility Rating			Susceptibility Rating		
>60%	M	H	VH	H	H-VH	VH
30 - 60%	L	M	M-H	M	H	VH
15 - 30%	VL	L-M	M-H	VL	L-M	M-H
<15%	VL	VL	L	VL	L	M

a) Example Lifeline Susceptibility Ratings

PGA, g	Slope Failure Susceptibility Class				
	VH	H	M	L	VL
< 0.1	0.1 m	0.5 m	--	--	--
0.1-0.2	0.1 m	0.1 m	0.05 m	--	--
0.2-0.3	0.5 m	0.25 m	0.25 m	0.05 m	--
0.3-0.4	1 m	1 m	0.5 m	0.25 m	0.05 m
0.4-0.5	1.7 m	1.5 m	1 m	0.5 m	0.25 m
> 0.5	2.5 m	2 m	1.5 m	1 m	

b) Example Estimates of Ground Displacements

4.5.3.1 Landslide Inventory and Susceptibility Classes

The mapped landslide inventory data compiled under step 1 and the susceptibility classes established for each area from step 2 should be incorporated directly into the hazards module.

4.5.3.2 Data Needed for Seismic Analysis

The hazards module should include the soil properties and topographic data needed to estimate: (a) the threshold ground motion levels for the onset of liquefaction, as computed under step 3 above; and (b) the landslide-induced ground displacements for the range of potential earthquake-induced ground motion levels and landslide susceptibility classes within the system. Although these data vary somewhat among the various analysis procedures that can be used for the above computations, they will generally include: (a) topographic data, including the steepness of the various slopes being evaluated; (b) the depth, thickness, mass density, cohesion, and angle of internal friction of the various layers that comprise each slope; and (c) fines content, water table locations, and depths to rock at the various slopes being evaluated. Additional material properties required for estimation of lateral spread displacements using the current procedures by Youd and his associates (Youd, 1998 and Youd et al., 1999) are listed in section 4.4.3. For those sites with landslide susceptibilities of "High" to "Very High", and for which landslide could have significant impacts on the seismic performance of the highway system, further testing of the soil materials at the sites should be used to obtain the above properties. However, for sites with lower landslide susceptibilities and where landslide would not significantly impact the system's seismic performance, the above properties can be estimated using correlations with geologic data.

4.5.4 UNCERTAINTIES

Where possible, uncertainties associated with the above data and models should be characterized for defining the simulations as described in chapter 2. These characterizations should be provided in terms of estimated distributions of the data values and model predictions about the estimated mean values. However, there are currently no widely accepted procedures to characterizing uncertainties in the estimation of landslide hazards. Further research into the development of such procedures is recommended.

4.6 SURFACE FAULT RUPTURE HAZARDS

4.6.1 HAZARD DESCRIPTION

Highway components can be damaged by permanent displacement of the ground surface due to fault rupture. Such displacements may be vertical and/or horizontal, with associated tension fissures or compression bulging. The direction and amount of ground movement will depend on the type of faulting, the magnitude and depth of the earthquake, and the complexity of the fault zone. For strike-slip faults, the zone of deformation often includes one or more primary fault strands that contain most of the ground displacement. For thrust or reverse faults, the width of the deformation zone may vary from a single fault strand to a broad zone of primary/secondary deformation on the hanging wall (i.e., the rock and soil above the fault) in excess of 300 ft.

The surface fault rupture hazard will be limited to locations where the rupture approaches and reaches the ground surface and, as a result, this hazard to a spatially distributed highway system will be much more localized than will ground shaking hazards. Also, this surface rupture hazard is most likely to occur in regions whose earthquakes typically have a shallow focal depth, such as California and the Wasatch Fault zone in Utah. Surface fault rupture is unlikely in regions of the Eastern and Central United States where the major faults are typically deeply buried.

4.6.2 HAZARD EVALUATION PROCEDURE

For highway systems that are located in regions where surface fault rupture is possible, this hazard should be evaluated by applying the following steps.

4.6.2.1 Step 1 – Initial Screening

Step 1 consists of a review of relevant geologic and tectonic data for the region. These data should be obtained from: (a) available geologic reports, aerial photographs, and maps; (b) technical reports and papers that address the tectonics and earthquake activity of the region and its individual faults; and (c) applicable regressions for displacement levels as a function of earthquake magnitude and/or various fault characteristics (e.g., length, fault length, fault type, etc.). Following this, potential surface fault displacement hazards to the highway system should be evaluated in terms of: (a) fault location, length, and width; (b) fault activity -- i.e., whether the fault is characterized as active or potentially active; (c) fault geometry -- i.e., whether the fault is strike-slip, normal, reverse, or thrust, and assessment of the fault's potential rupture areas, dip angles, and slip directions for its main traces and any secondary strands; (d) best-estimate values and uncertainty estimates of fault displacement per event, as obtained from past detailed displacement studies for the fault or, in the absence of such studies, from applicable magnitude vs. displacement and displacement vs. length regressions (e.g., Wells and Coppersmith, 1994); and (e) recurrence intervals, as estimated using slip rate data from past studies of the fault or from the technical literature.

4.6.2.2 Step 2 – Detailed Evaluation

The above screening step is usually sufficient to characterize the surface fault rupture hazard. However, in some cases, faults could exist with a potential for surface fault displacements that could severely impact post-earthquake system traffic flows. For such faults, additional evaluation should be carried out to adequately characterize the surface rupture hazard. This could include field reconnaissance by qualified geologists to map fault scarps, study relationships between geologic units and bedrock structure, and assess fault activity. Results of this evaluation should be used with data obtained under step 1, in order to characterize the potential fault displacement hazards in terms of the characteristics listed in the previous paragraph.

4.6.3 INPUT DATA

To evaluate the surface fault displacement hazard using the above procedure, the available data, maps, aerial photographs, technical literature, etc. reviewed under step 1 -- and the additional detailed evaluations carried out if needed under step 2 -- should include the following:

- *Geology.* The lithology, stratigraphy, and other relevant regional geologic characteristics.

- *Tectonics.* Tectonic characteristics of the region including fault dimensions, locations, dip angles, and potential rupture areas.

- *Earthquake History.* The past earthquake history of the region, particularly including earthquakes attributed to the faults whose rupture could directly damage the highway system.

- *Slip Rate Data.* Data for characterizing slip rates, such as age data for geologic units offset by the fault rupture, etc.

- *Empirical Models.* Applicable empirical models that relate fault displacement to earthquake magnitude and to rupture length.

4.6.4 UNCERTAINTIES

Where possible, uncertainties associated with the above data and models should be characterized for use in the SRA application. These characterizations should be provided as estimated probability distributions of data values and model predictions. However, there is currently only very limited information that is available for guiding the estimation of these distributions. Further research along these lines is recommended.

CHAPTER 5
COMPONENT MODULE

5.1 INTRODUCTION

This chapter describes the process for characterizing the seismic performance of components for a given scenario earthquake and simulation. The process involves three main steps. First, the component's seismic response is estimated from fragility curves that represent the probability that the component will be in a given damage state, as a function of the level of ground shaking and permanent ground displacement at the site for the earthquake and simulation. These fragility curves are typically developed from mechanics-based analytical models and/or empirical data describing component performance during past earthquakes. The probabilities provided by the fragility curves represent effects of uncertainties in component input data and analytical models.

Once the damage state is established, the next step in the process is to evaluate how the damage will be repaired, how much it will cost, how long it will take, and how traffic will be affected during repair. Models for carrying out this second step are developed from regional construction data. Finally, after the traffic impacts during repair are established (which will vary with time after the earthquake), the final step incorporates these "traffic states" into a highway network model, to establish corresponding system states at various times after the earthquake.

The remainder of this chapter is organized into five main sections. These sections describe general model types (section 5.2), and modeling methods for bridges, approach fills, roadways, and other components (sections 5.3 to 5.6 respectively).

5.2 MODEL TYPES

Two types of component models are developed for SRA applications -- loss models and functionality models. Loss models estimate direct losses to the damaged component, in terms of the costs of post-earthquake repair or reconstruction, as a function of the level of ground shaking and permanent ground deformation at the component site. Functionality models estimate the ability of the damaged component to carry traffic, as a function of the level of ground shaking and ground movement at the site, and also as a function of time after the earthquake (reflecting the time required for repair and reconstruction).

Both models depend on: (a) the seismic response of the component (in terms of the type and extent of component damage) as a function of the ground shaking and permanent ground displacement at the site; and (b) the type and degree of repair and reconstruction that is needed. However, the two models use this information differently. The loss models use the information to estimate repair costs for all components, which are then summed to obtain total system-wide direct losses. The functionality models, on the other hand, use the information to establish "traffic states" for each component -- i.e., whether the component and its adjacent and underlying roadways are fully open, partially open, or fully closed to traffic after the earthquake and, if fully or partially open, the acceptable traffic speed limits. In addition, durations of any traffic restrictions due to earthquake damage are specified.

Another distinction between the loss and functionality models is how their results are used in the overall SRA process (as described in chapter 2). The traffic state results from the functionality models are used to assemble post-earthquake system states, and these system states are then analyzed using network analysis procedures (see chapter 3 and appendix B) to estimate effects of earthquake damage on system-wide traffic flows and travel times. Indirect and induced economic losses due to these increased travel times are then estimated using economic models (see chapter 6). These losses are added to the direct losses from the loss models in order to estimate overall losses due to earthquake damage to the highway system.

5.3 BRIDGES

5.3.1 INPUT DATA

5.3.1.1 Data Needs

Ideally, input data for analysis of the seismic response of a bridge should include information on: (a) bridge geometry, including lengths, widths, overall heights, relative heights of various bents along the length of the bridge, and skew; (b) materials of construction; (c) member sizes, reinforcement, and detailing; (c) bearings, joints, and seat widths; (d) foundations and soil conditions; and (e) abutments. Although this information can be obtained from as-built drawings for individual bridges, this can be a laborious task when many bridges are involved (e.g., for SRA of a highway system). Furthermore, such data are usually not available in a computerized database that can be rapidly accessed for seismic evaluation of large numbers of bridges.

5.3.1.2 Current Databases and Bridge Management Systems

The only available nationwide computerized database for bridges is the National Bridge Inventory (NBI) database that is required by the National Bridge Inspection Standards established by the Federal Highway Administration. This database serves to facilitate inspection, to provide information for aggregation into a report to Congress on the number and state of the nation's highway bridges, and to identify and classify the Strategic Highway Corridor Network and its connectors for defense purposes (FHWA, 1995b). The database has not been developed to provide information for evaluation of bridge performance during earthquakes or other natural or man-made hazards. Therefore, although the NBI database includes some relevant bridge attributes, it does not include sufficient data for detailed seismic vulnerability evaluation.

In addition to the NBI database, bridge management systems -- which include PONTIS (initiated by the FHWA) and BRIDGIT (initiated through the National Cooperative Highway Research Program) -- are being implemented by a number of states. The objective of these systems is to provide analytical methods that facilitate efficient and cost-effective allocation of resources for maintenance, repair, and upgrading of the nation's highway bridges. These systems do not currently address seismic risk issues and, as a result, the data fields contained in these systems do not include most of the attributes that would be needed for seismic vulnerability assessment of a bridge. In recognition of this need, the feasibility of including seismic

vulnerability evaluation in the PONTIS bridge management system is being assessed (Small, 1997 and 1999).

5.3.1.3 Recent Developments

Research to address data needs for seismic evaluation of bridges has included: (a) the work by Jernigan et al., (1996) to develop a comprehensive database of structural attributes for seismic evaluation of bridges in Shelby County, Tennessee; and (b) the work by Mander and his co-workers (Dutta and Mander, 1998 and Mander and Basoz, 1999) to use the NBI database to infer structural attributes for seismic evaluation.

The objectives of the work by Jernigan et al. were to: (a) develop structural attribute data for bridges in Shelby County that can be used in demonstration SRAs of the county's highway system; (b) develop a framework for guiding the future development of structural attribute databases for SRA of highway systems nationwide; and (c) provide data that can be used by state, county, and city government agencies for seismic risk evaluation and risk reduction planning. To accomplish this, extensive spatial and structural data were compiled from the NBI database, engineering drawings, inspection reports, and visual observations of 452 bridges and culverts in Shelby County. These data were incorporated into a GIS database developed at the Center for Earthquake Research and Information at the University of Memphis (see table 3).

Detailed computerized bridge structural-attribute databases of the type developed by Jernigan et al. are not available at most local, county, and state transportation departments. Instead, bridge attribute databases used by most transportation departments are drawn from the NBI database summarized in section 5.3.1.2. Therefore, Mander and his associates developed a simplified procedure for estimating bridge fragility curves by: (a) using information from the NBI database to infer certain structural attributes related to skew and three-dimensional effects; and (b) using these inferences to modify fragility curves developed for various "standard" bridges, in order to develop curves for the actual bridge (see table 4). This "rapid pushover method" is summarized in section 5.3.2.2, and its incorporation into the SRA methodology is described in appendix F (Dutta and Mander, 1998).

5.3.1.4 Approach for SRA of Highway Systems

In view of the above limitations of the structural data in current federal databases and bridge management systems, the user of the SRA methodology has two options -- to either infer such structural attributes from the current NBI and bridge management databases, or to develop such attributes directly from bridge drawings.

Of these two options, the inferences from the NBI database are a much more practical approach and, as concluded by Mander et al., appear to provide sufficient accuracy for most conventional bridges (Dutta and Mander, 1998). The second option is impractical for use with the large numbers of bridges that will be involved in SRA applications. However, in highway systems, there will invariably be some special or unique bridges whose seismic performance could have a major impact on post-earthquake traffic flows and travel times throughout the

system (e.g., long bridges along non-redundant links with large traffic volumes). For such bridges, the user may need to develop structural data by using the second option -- i.e., directly from the bridge drawings.

Table 3. Jernigan et al., (1996) Database for Bridges in Shelby County, Tennessee

File Number	Description	Structural Attributes
B-1	Relevant Information from NBI Database	Bridge ID number, route, location (log mile), feature crossed by bridge, maximum span length, total length, roadway width, bridge width, average daily traffic, year built, skew angle, superstructure types (main span and approach span), number of main spans, and number of approach spans.
B-2	Abutment Attributes	Bridge ID number, abutment type (material, type, and fixity), abutment bearing and expansion type, seat width, foundation type, and whether seismic retrofit was implemented.
B-3	Bent File No. 1	Bridge ID number, bent type and material, superstructure to substructure connectivity, bent bearing and expansion type, seat width, number of columns per bent, maximum column height, and minimum column height.
B-4	Bent File No. 2	Bridge ID number, column fixity (to bent cap and to pile cap or footing), column size (at top and bottom), column shape, vertical reinforcement, transverse reinforcement, and foundation type.

5.3.2 DAMAGE STATES DUE TO GROUND SHAKING

5.3.2.1 General Evaluation Procedure

This SRA methodology includes the following three options for estimating bridge damage states due to ground shaking: (a) the above-indicated rapid-pushover method (Dutta and Mander, 1998 and Mander and Basoz, 1999), which is the preferred method for application to conventional bridges; (b) a second method for conventional bridges which consists of an elastic demand-capacity approach similar to that described in previous FHWA seismic retrofit manuals for bridges (FHWA, 1995a) but specifically tailored to bridges in the Central United States (Jernigan, 1998 and Jernigan and Hwang, 1997); and (c) user-specified fragility curves. The rapid-pushover method is summarized in section 5.3.2.2. Appendix F provides additional background on both the rapid-pushover and elastic demand-capacity approaches.

Table 4. Fields in NBI Database used by Mander et al. to Infer Bridge Fragility Curves (Dutta and Mander, 1998 and Mander and Basoz, 1999)

NBI Data Item	Definition	Skew Factor	3-D Response Factor	Use in Inferring Bridge Fragility
1	State		X	To infer seismic design code used.
8	Structure Number			General ID Number.
27	Year Built		X	Infer whether seismic or conventional design.
34	Skew	X		
42	Service Type			To select highway bridges.
43	Structure Type		X	To infer which type of "standard" bridge to use as basis for fragility curve development.
45	Number of Spans in Main Unit		X	To infer whether single- or multiple-span bridge.
46	Number of Approach Spans			To infer if bridge is a major bridge (as defined in NIBS, 1997).
48	Length of Maximum Span		X	To also infer if bridge is a major bridge (as defined in NIBS, 1997).
49	Structure Length		X	To infer average span length. To compute replacement value.
52	Deck Width			To compute replacement value.

Because the rapid-pushover and elastic demand-capacity approaches are oriented toward the rapid analysis of the large numbers of bridges in a highway system, they incorporate certain simplifications for estimating the damage throughout a bridge. Although these simplifications will be of only secondary importance for most conventional bridges, they could be more important for special or unique bridges whose performance could have a significant impact on

the highway system. Therefore, to enable the user to apply a more refined modeling approach for such bridges, the SRA methodology includes an option for user-specified fragility curves. However, the user should recognize that this option is more time consuming than the other two bridge modeling approaches and is impractical for application to large numbers of bridges. Appendix G provides examples of user-specified fragility curves for two major long-span bridges in Shelby County, Tennessee that cross the Mississippi River.

5.3.2.2 Rapid Pushover Method

In the SRA methodology, the rapid-pushover method is the preferred method for modeling of large numbers of conventional bridges because: (a) it provides rapid estimation of damage states; (b) it incorporates a simplified but rational engineering procedure based on principles of mechanics; and (c) it uses readily available information on each bridge that is contained in the NBI database to infer input parameters needed for damage state evaluation.

Table 5. Damage States considered in Rapid Pushover Method
(Dutta and Mander, 1998 and Mander and Basoz, 1999)

Damage State Designation		Description
Number	Level	
1	None	First yield.
2	Slight	Minor cracking and spalling of the abutment, cracks in shear keys at abutment, minor spalling and cracking at hinges, minor spalling of column requiring no more than cosmetic repair, or minor cracking of deck.
3	Moderate	Any column experiencing moderate shear cracking and spalling (with columns still structurally sound), moderate movement of abutment (< 5.1 cm) (< 2 inches), extensive cracking and spalling of shear keys, connection with cracked shear keys or bent bolts, keeper bar failure without unseating, rocker bearing failure, or moderate settlement of approach.
4	Extensive	Any column degrading without collapse (e.g., shear failure) but with column structurally unsafe, significant residual movement of connections, major settlement of approach fills, vertical offset or shear key failure at abutments, or differential settlement.
5	Complete	Collapse of any column, or unseating of deck span leading to collapse of deck. Tilting of substructure due to foundation failure.

This section summarizes the adaptation of the rapid pushover method to establish bridge damage states (as defined in table 5) for each earthquake and simulation in the SRA methodology. This adaptation is described in more detail in appendix F.

5.3.2.2(a) Development of Pushover Capacity Spectrum

The pushover capacity spectrum is a plot of equivalent five-percent damped spectral acceleration vs. spectral displacement (which is related to drift). Spectral displacements (drifts) that represent the onset of each damage state are also defined. Mander et al. establish capacity spectra and the limiting drifts for each damage state for each of each of six "standard" bridges, defined as long, unskewed bridges that represent six different commonly occurring bridge types.

The capacity spectrum for each standard bridge type (which includes effects of strength degradation and hysteretic energy dissipation) is obtained as the sum of the capacity contributions of the piers and the three-dimensional arching action of the deck (Dutta and Mander, 1998 and Mander and Basoz, 1999).

- *Pier Contribution to Bridge Capacity.* The strength capacity of a bridge pier will usually decay as the earthquake shaking proceeds. The magnitude and rate of this decay will depend on the design details at potential plastic hinge zones -- particularly connection details such as lap splices and anchorage zones -- and on the shear capacity of the columns and the column-to-cap connections. Although sophisticated energy-based procedures are available to evaluate these sources of strength decay, a simplified displacement-based analysis method is used instead, to increase the speed of the evaluation. The method uses a simplified strength degradation model for the bridge pier, where the total pier capacity consists of: (a) diagonal strut (or arch) action to represent the concrete resistance; and (b) resistance contributions of the longitudinal and transverse reinforcing steel. These contributions to the pier capacity are expressed in terms of geometric factors obtained or inferred from the NBI database.

- *Deck Contribution to Bridge Capacity.* The deck's contribution to the bridge's total base shear capacity has been systematically overlooked in most capacity analyses. This contribution is due to the resistance of the deck resulting from plastic moments that are mobilized by the bearings working as a group. This action occurs because, as the deck rotates, the resulting lateral displacements are resisted by frictional forces in each bearing and by arching action of the deck. These effects are evaluated for bridges with multiple simply-supported spans and with continuous spans, by using a plastic mechanism analysis to establish the deck capacity as the lowest capacity of all possible postulated failure mechanisms. These failure mechanisms depend on the geometry of the deck spans, the relative flexibility of the pier bents, and the resistance and capacities of the bearings.

5.3.2.2(b) Median Spectral Acceleration Capacities for each Damage State – Standard Bridges

Mander et al. use the following steps to establish median acceleration capacities for each standard bridge type and each damage state:

- The capacity spectrum is overlaid onto a smoothed five-percent damped spectrum shape for rock sites, whose spectral accelerations at a period of 1.0 sec. and 0.3 sec. are assumed to be equal to the peak ground acceleration (PGA, or zero-period spectral acceleration) and 2.5 x PGA respectively. This assumption is also a basis for the ground motion spectrum shape

developed under the National Earthquake Hazard Reduction Program (NEHRP) (Dobry et al., 2000, Dutta and Mander, 1998, and Mander and Basoz, 1999).

- This smoothed spectrum shape is scaled by alternative PGA values until it intersects the capacity spectrum at the drift (spectral displacement) level that corresponds to the onset of a given damage state. The PGA level at which this occurs is defined as the median PGA for the onset of the given damage state.

- Using the above relationships between spectral acceleration and PGA for the smoothed spectrum shape, the above median PGA capacities are converted to corresponding spectral acceleration capacities at periods of 1.0 sec. and 0.3 sec. At this stage, these capacities correspond to rock site conditions. Corrections to account for the actual site soil conditions are provided later.

5.3.2.2(c) Median Acceleration Capacities for each Damage State – Actual Bridge

The acceleration capacities for each damage state at the actual bridge being evaluated (for rock site conditions) are obtained by multiplying the corresponding acceleration capacities for the appropriate standard bridge (see section 5.3.2.2 (b)) by factors that correct for the effects of skew and three-dimensional arching action of the actual bridge.

5.3.2.2(d) Estimation of Bridge Damage State for Each Scenario Earthquake

The operations and results described in the above subsections are initial steps that are carried out once for each bridge in the highway system prior to carrying out the SRA for each scenario earthquake and simulation. It then remains to summarize the operations that utilize the results of these initial steps to estimate each bridge's damage state for each earthquake and simulation. These steps are summarized below, and are further described in appendix F:

- *Demand Ground Motions for each Earthquake and Simulation.* For each scenario earthquake and simulation included in the SRA, the ground motion model from the hazards module (chapter 4) establishes: (a) demand spectral accelerations at periods of 1.0 sec. and 0.3 sec. at the actual bridge site; and (b) the soil amplification factors used to convert the site-specific bedrock spectral accelerations at these periods to corresponding spectral accelerations at the ground surface. These spectral accelerations and soil amplification factors include effects of uncertainties in ground motion attenuation rates and local soil conditions.

- *Spectral Acceleration Capacities Including Uncertainties and Local Soil Conditions.* The median spectral acceleration capacities previously established for each bridge (see section 5.3.2.2(c)) are for NEHRP type B rock conditions. In this step, NEHRP soil amplification factors (which represents soil amplification relative to type B conditions) are used to modify these capacities to correspond to the local soil conditions at the site. Effects of uncertainties in structural material properties and analysis procedures are introduced at this stage, using uncertainty factors defined in Jernigan (1998). The end result of this step is a simulation-specific value of spectral acceleration capacity at periods of 1.0 sec and 0.3 sec. that is used

in the following step to estimate the bridge damage state for the given scenario earthquake and simulation.

- *Estimation of Bridge Damage State.* The demand spectral accelerations at periods of 1.0 sec. or 0.3 sec. (depending on whether long-period or short-period response governs for this particular bridge and damage state) are compared to the corresponding spectral acceleration capacities for each damage state, in order to establish the bridge damage state for this particular scenario earthquake and simulation (as further described in appendix F).

5.3.3 DAMAGE STATES DUE TO PERMANENT GROUND DISPLACEMENT

In addition to ground shaking, bridges can be damaged by permanent ground displacement from earthquake-induced liquefaction, landslide, or rupture of a fault located beneath the bridge.

Only limited research has been carried out to estimate potential bridge damage states due to permanent ground displacement. As a result, the SRA methodology now includes only a very simplified algorithm from the HAZUS software (NIST, 1997) for estimating such damage states. Future research to develop improved algorithms is encouraged. The following subsections outline the main features of the HAZUS algorithm. The algorithm is further described in appendix H.

5.3.3.1 Bridge Classification

The HAZUS algorithm classifies bridges by type, whether or not they have been seismically designed, and whether they are "high risk" bridges.

5.3.3.1(a) Bridge Type

Bridge types modeled in the HAZUS algorithm are: (a) major bridges, defined as having span lengths greater than 500 ft; (b) continuous bridges, which have continuous spans less than 500 ft long; and (c) simply supported bridges, with simply supported spans less than 500 ft long. As noted below, simply supported bridges with more than one span are designated as "high risk".

5.3.3.1(b) Seismic Design

In the HAZUS algorithm, bridges are also classified based on whether or not they have been seismically designed or retrofitted. This classification is shown in table 6a. The various ages of bridges that are shown in this table represent editions of the Caltrans and AASHTO bridge design standards when improvements in seismic design provisions have been included (NIST, 1997).

5.3.3.1(c) High Risk Bridges

Bridges that have any attributes that increase their seismic vulnerability are classified by HAZUS as "high risk". These attributes include: (a) an irregular shape of the superstructure (i.e., if it is substantially curved or skewed); (b) bridges with no seismic design; or (c) simply-

supported bridges with more than one span. In the bridge shape classifications given in Table 6b, a bridge with a type 3 shape factor is designated as "high risk" in the HAZUS algorithm.

Table 6. HAZUS Bridge Classification based on Design Specification and Superstructure Shape (NIST, 1997)

Site Condition	Age of Bridge		High Risk
	Caltrans Design Specification	AASHTO Design Specification	
1	1981-	1984-	No
2	1973-1980	1975-1983	No
3	1940-1972	1958-1974	Yes
4	before 1940	before 1958	Yes

a) Classification of Design Specifications

Shape	Superstructure Shape	High Risk
1	Straight	No
2	20°-45° skewed or 45°-90° curved	No
3	More than 45° skewed or 90° curved	Yes

b) Classification of Shape of Superstructure

5.3.3.2 Damage State Definitions

The HAZUS algorithm uses the following four damage state definitions: (a) *Slight/Minor:* Minor cracking and spalling at the abutments, at columns (where damage requires no more than cosmetic repair), or at the deck; (b) *Moderate:* Moderate cracking and spalling of columns (columns still structurally sound), any connection having cracked shear keys or bent bolts, or moderate settlement of an approach; (c) *Extensive:* Any column degrading without collapse (column structurally unsafe), any connection losing some bearing support, or major settlement of approach; and (d) *Complete:* Any column collapsing and connection losing all bearing support, which may lead to imminent deck collapse.

5.3.3.3 Damage Algorithms

HAZUS fragility curves for damage states of bridges subjected to permanent ground displacement are assumed to correspond to a lognormal distribution with median and standard deviation (β) parameters that are given in table 7 (NIST, 1997).

Table 7. HAZUS Damage Algorithms for Bridges subjected to Permanent Ground Displacement (NIST, 1997)

Bridge Type	HAZUS Damage State	Median PGD, cm. (in.)	β**
Seismically Designed*	Slight/Minor	12.7 (5)	0.6
	Moderate	20.3 (8)	0.6
	Extensive	40.6 (16)	0.6
	Collapse	61.0 (24)	0.7
Conventionally Designed*	Slight/Minor	12.7 (5)	0.6
	Moderate	17.8 (7)	0.6
	Extensive	30.5 (12)	0.6
	Collapse	45.7 (18)	0.7
High Risk (see table 6)	Slight/Minor	10.2 (4)	0.6
	Moderate	15.2 (6)	0.6
	Extensive	25.4 (10)	0.6
	Collapse	35.6 (14)	0.7

*Major, continuous, or simply-supported bridges.

**Logarithm of standard deviation, which is used as measure of dispersion of fragility curves (NIST, 1997).

5.3.3.4 Incorporation into SRA Methodology

Step-by-step procedures for incorporating these algorithms into the SRA methodology – including uncertainty estimates -- are provided in appendix H.

5.3.4 POST-EARTHQUAKE REPAIR

After a bridge's damage state is estimated for a given scenario earthquake and simulation, the next step is to assess how the damage will be repaired, how much the repairs will cost, how long they will take, and how traffic along the bridge will be affected during repair. The duration and extent of any partial or complete traffic closure along each bridge (i.e., the bridge's traffic states)

at specified times after the earthquake are input into a network model for the highway system, in order to establish post-earthquake system states at these times. Transportation network analysis procedures described in chapter 3 are then applied to each post-earthquake system state, as well as the system's pre-earthquake system state, in order to assess the effects of earthquake damage on system-wide traffic flows and travel times at various times after the earthquake.

5.3.4.1 Repair Cost

The costs for bridge repair will depend on the bridge type, location, and accessibility, on the type, extent, and location of the damage, and on region-specific construction practices and unit costs for bridge repair and construction. These costs are added to the indirect losses due to disruption of traffic flows throughout the highway system in order to estimate overall economic impacts of earthquake damage to the system.

Table 8. Bridge Repair Cost Algorithm
(Mander and Basoz, 1999)

Damage State (NIST, 1997)	Best Mean Repair Cost Ratio	Range of Repair Cost Ratios
Slight Damage	0.03	0.01 to 0.03
Moderate Damage	0.08	0.02 to 0.15
Extensive Damage	0.25	0.10 to 0.40
Complete Damage	= 1.0 (if $n < 3$) = 2.0 x (bridge replacement cost)/n (if $n \geq 3$) (where n = number of spans.)	0.30 to 1.0

The SRA methodology provides default values of bridge repair cost ratios (i.e., ratio of repair cost to replacement cost) which can be overridden by the user. These default values are shown in table 8 (Mander and Basoz, 1999). The repair cost estimates shown in this table should be further developed in the future (e.g., through use of empirical data compilation and/or expert-opinion surveys).

5.3.4.2 Traffic State and Duration

5.3.4.2(a) Default Estimates

Tables 9 and 10 show default traffic states for bridges damaged by ground shaking and permanent ground displacement. For each damage state defined in table 5, these tables provide estimates of repair procedures and durations, and corresponding traffic states along the bridge and any underlying roadways. Table 11 contains estimates of the number of lanes closed along and beneath the bridge, as a function of its damage state and total number of lanes. Estimates of bridge reconstruction durations are provided in table 12. Instead of the default traffic states shown in tables 9 and 10, the user will have the option of specifying his/her own traffic states.

Table 9. Default Traffic States for Bridges Damaged by Ground Shaking

Damage State[1] (see table 5)	Repair Procedure		Traffic State	
	Description	Duration[2]	Bridge	Underlying Roadway
None	None.	None	Fully Open	Fully Open
Slight	Epoxy injection of cracks.	2-3 weeks.	Fully Open	Fully Open
Moderate (Repairable structural damage)	1. Close bridge for inspection and shoring. 2. Repair columns, i.e., remove damaged concrete, design/implement repair (e.g., increase lap splice, add transverse steel, grouting, jacketing). 3. Repair abutments, bearings, etc.	1-3 days. 3-span bridge: 2-4 weeks. 4-span bridge: 2½-5 weeks. 5-span bridge: 3-6 weeks.	Closed. Partially open to reduced traffic during duration of repairs (see table 11).	Partially closed (one lane each direction) during cleaning, shoring, column repair operations (2-3 weeks). Open to emergency vehicles.
Extensive (Severe damage to structural elements but no overall collapse mechanism)	1. Close bridge for inspection and shoring. 2. Repair or replace columns, i.e., remove damaged concrete, design/implement repair (e.g., increase lap splice, add transverse steel, grouting, jacketing). 3. Repair abutments, repair or replace bearings, etc.	1 week 3-span bridge: 4- 8 weeks[3]. 4-span bridge: 5 - 10 weeks[3]. 5-span bridge: 6 - 12 weeks[3].	Closed. Partially open to reduced traffic during duration of repairs (see table 11).	Partially closed (one lane each direction) during cleaning, shoring, column repair operations (3-4 weeks). Open to emergency vehicles.
Collapse (Severe structural damage leading to overall collapse mechanism, or Unseating of deck leading to collapse of deck)[1,4]	Replace bridge for case of severe structural damage. See table 12 for breakdown of repair procedure. Replace fallen deck span, replace bearings, and repair or replace damaged substructure.	3-span bridge: 3 - 6 months[3]. 4-span bridge: 4 - 8 months[3]. 5-span bridge: 5 - 10 months[3]. 3-6 months.	Closed during duration of reconstruction of bridge. Closed during duration of bridge repair, replacement.	Fully closed during demolition & cleaning (3-6 days). Partially closed (one lane each direction) during cleaning, shoring, column repair operations (4-8 weeks).

[1]Refers to column, wall, and/or footing damage states. [2] All repair durations assume full availability of all necessary repair resources. [3]For extensive or collapse damage state, bridge replacement durations can be cut in half if repair schedule is based on incentive bonus and 24-hour/day and 7-days/week contract.

[4]For a deck span that unseats from its bearing but falls onto substructure (no deck collapse), the repair procedure would involve jacking of the deck, replacing the bearing, and repairing any substructure damage. The minimum duration of these repairs, including time for inspection and mobilization of equipment, is estimated to be 2 -4 weeks. The bridge itself and any roadway beneath the bridge will be fully closed during the repair.

Table 10. Default Traffic States for Bridges Damaged by Permanent Ground Displacement

Damage State (see table 5)	Repair Procedure		Estimated Traffic State	
	Description	Duration*	Bridge	Underlying Roadway
None	None	None.	Fully Open	Fully open.
Slight	1. Inspection. 2. Epoxy inject cracks.	2-4 hours. 1-2 weeks.	Closed. Fully open.	Fully open. Fully open.
Moderate	1. Inspection, shoring. 2. Repair columns. 3. Repair abutments, bearings, etc.	1-3 days. 3-span bridge: 2-4 weeks. 4-span bridge: 2½-5 weeks. 5-span bridge: 3-6 weeks.	Closed. Partially open to reduced traffic during duration of repairs (see table 11).	One lane closed each way during cleaning, shoring, column repairs (2-3 weeks).
Extensive	1. Inspection, shoring. 2. Repair/replace columns. 3. Repair abutments, repair/replace bearings.	1 week. 3-span bridge: 4- 8 weeks. 4-span bridge: 5 - 10 weeks. 5-span bridge: 6 - 12 weeks.	Closed. Partially open to reduced traffic during duration of repairs (see table 11).	One lane closed each way during cleaning, shoring, column repairs (3-4 weeks).
Collapse	Replace bridge. See table 12 for replacement process.	3-span bridge: 3 - 6 months. 4-span bridge: 4 - 8 months. 5-span bridge: 5 – 10 months.	Closed for duration of reconstruction of bridge.	Fully closed during demolition, cleaning (3-6 days). One lane closed each way during cleaning, shoring, column repairs (4-8 weeks).

* All repair durations assume full availability of all necessary repair resources. For extensive or collapse damage state, cut repair duration in half if repair schedules are based on incentive bonus and 24-hour per day and 7-days per week schedule.

Table 11. Definition of "Partially Opened" Bridge in Tables 9 and 10

Damage State (see table 5)	Total Number of Lanes Each Way before Earthquake				
	1	2	3	4	5
	Number of Lanes Each Way Open to Traffic after Earthquake				
None	1	2	3	4	5
Slight	1	2	3	4	5
Moderate	0	1	2	3	4
Extensive	0	1	1	2	2
Collapse	0	0	0	0	0

Table 12. Estimated Bridge Reconstruction Durations under Emergency Conditions

Task	Duration, Days
1. Mobilization and Demolition	10
2. Obtain Piles and Load Test	5
3. Analyze Load Test Results	1
4. Drive Piles	
a. Abutment No. 1	3
b. Bent No. 2	5
c. Bent No. 3	5
d. Abutment No. 4	3
5. Form and Pour Abutments and Wingwalls	4
6. Form and Pour Caps	5
7. Form and Pour Columns	5
8. Form and Pour Column Cap	6
9. Set Girders	6
10. Form and Pour Bridge Deck	15
11. Form and Pour Bridge Rails	5
12. Construct Approach Roadway	10
13. Install Bridge End Guardrails	2
TOTAL	90

a) Construction Time for Four-Lane, Three-Span Bridge with Length of 76.2 m (250 ft.)

Task	Duration, Days
1. Pile Load Test	5
2. Analyze Load Test Results	1
3. Drive Piles	5
4. Form and Pour Caps	3
5. Form and Pour Columns	3
6. Form and Pour Column Cap	3
TOTAL	20

b) Construction Time for Center Bent in Open Roadway

5.3.4.2(b) Basis for Estimates

Repair durations will not only depend on the bridge's damage state and accessibility, but also on such issues as: (a) potential competition for scarce repair and reconstruction resources (i.e., materials, equipment, and labor) in the event of widespread damage to a region's overall infrastructure; (b) environmental regulations and costs associated with repair vs. replacement of severely damaged bridges; and (c) public reactions and politics (which had an important influence on the contrasting times for repair of collapsed or severely damaged bridges after the Loma Prieta Earthquake, as compared to bridge damage repair times after the Northridge Earthquake). The extent of these issues can differ for different regions of the United States.

In view of this, the development of a general model for estimating post-earthquake bridge repair durations throughout the country is an exceedingly difficult task. Therefore, a different approach has been adapted here, in which the default repair durations and traffic states given in tables 9 and 10 are intended to represent near lower-bound estimates realized under ideal conditions of: (a) immediate availability of all necessary resources to complete the bridge repairs in the most efficient manner possible; and (b) no environmental or political issues to delay bridge repairs. These default repair durations and traffic states may be overridden by the user. Actual repair durations may be much longer than those given in these tables.

As noted in chapter 2, SRA results can guide the establishment of an appropriate level of dedicated equipment, material, and labor resources that would reduce post-earthquake bridge repair durations to an acceptable level. This process can involve: (a) estimation of bridge repair durations based on currently available repair resources; (b) use of the SRA methodology to estimate total losses in conjunction with these durations; (c) if these losses are not acceptable, identification of additional repair resources that would be needed to reduce the bridge repair durations; (d) estimation of additional costs for procuring these additional repair resources; (e) use of the SRA methodology to re-estimate the total losses based on these reduced repair times; (f) comparison of costs (for mobilizing and storing the increased repair resources) and benefits (reduction in post-earthquake losses) of this decision; and (g) repeating steps (c) through (f) until a suitable balance between costs and benefits is achieved.

5.4 APPROACH FILLS

If approach fills alongside bridge abutments have not been adequately compacted during construction, they are vulnerable to damage from earthquake-induced differential settlement. These differential settlements are often localized due to the rigidity of the abutment wall, and the difficulty in manipulating large compactors near walls. This maximizes their potential for damage.

This procedure for modeling earthquake-induced settlement of bridge approach fills is based on the model for dry soils is described in Youd, (1999). This settlement is computed separately for each scenario earthquake and simulation, once the magnitude and location of the earthquake are specified and the level of ground shaking is estimated throughout the system.

5.4.1 INPUT DATA

Two sets of input data are required to estimate approach fill settlement. The first consists of bridge-dependent data and the second consists of earthquake- and simulation-dependent data.

5.4.1.1 Bridge-Dependent Data

The bridge-dependent data needed to estimate approach fill settlement are as follows: (a) the bridge number and location within the highway system; (b) the relative compaction of the approach fill soils (standard Procter density) (RC); and (c) the maximum thickness of the approach fill (T_{AF}).

The bridge number and location are specified as part of the input provided under the system module (see section 3.3.5). Also, in the absence of actual RC and T_{AF} data at a bridge site, the following values of these parameters may be used: (a) RC = 95%; and (b) T_{AF} = minimum vertical clearance + 1.52 m (5 ft). It is noted that the NBI database specifies the minimum vertical clearance for each bridge.

5.4.1.2 Earthquake- and Simulation-Dependent Data

The earthquake- and simulation-dependent data needed to compute approach fill settlement are: (a) the moment magnitude of scenario earthquake (M_w); and (b) the peak ground acceleration at bridge site (PGA). The moment magnitude is obtained from the scenario earthquake designation, and the PGA is computed for each scenario earthquake and simulation, using ground motion models contained in the hazards module (see sections 2.2.2 and 4.3).

5.4.2 EVALUATION PROCEDURE

The evaluation of approach fill settlement for each bridge, scenario earthquake, and simulation consists of the following steps:

- For the M_w of the scenario earthquake, the site-specific PGA for the earthquake and simulation, and the RC of the approach fills, use table 13 to estimate the volumetric strain of the approach fill materials (ε_{AF}) .

- Compute the total settlement of the approach fill (S_{AF}) as:

$$S_{AF} = \varepsilon_{AF} T_{AF} \tag{2}$$

- Obtain corresponding traffic state due to approach fill settlement, by using either the default traffic states given in table 14 or alternative values specified by the user. Table 14 provides traffic impacts (in terms of lane restrictions and speed limit reductions) and repair durations, as a function of the level of approach fill settlement. As for the bridges, these default repair durations and traffic states assume that equipment, materials, and labor resources are immediately available to efficiently implement the repairs. They also assume the absence of conditions that could increase repair methods, costs, and times, such as: (a) substantial lateral movement and slip-out; and (b) unusual foundation problems.

- If full repair resources are available, it can be assumed that repairs to the approach fill will be carried out concurrently with the repairs of any bridge damage due to ground shaking or liquefaction. Therefore, the largest of these various repair durations will govern the total duration of traffic disruption at the bridge, for the given scenario earthquake and simulation.

5.5 ROADWAY PAVEMENTS

Flexible or rigid roadway pavements are susceptible to damage and closure due to earthquake-induced ground displacement hazards. These hazards include differential settlement of dry or moist soils, lateral spreading and settlement of liquefiable soils, sliding of embankments or slopes due to instability of the embankments or the underlying soil materials, and surface fault rupture. Methods for evaluating the vulnerability of pavements to these hazards are also addressed in Youd, (1999). Procedures to estimate the extent of these hazards are summarized below.

Table 13. Best-Estimate Value of Maximum Volumetric Strain in Dry Soil due to Seismic Shaking (Youd, 1999)

Scenario Earthquake and Simulation Data		Volumetric Strain (%)		
Earthquake Magnitude (M_w)	Peak Ground Acceleration (PGA), (g)	Loose Fill (RC ≤ 90%)	Moderately Dense Fill (90% < RC < 95%)	Dense Fill (RC ≥ 95%)
$M_w \geq 7.0$	PGA ≥ 0.4 g	10%	5%	1%
	0.2 g < PGA < 0.4 g	5%	2%	0.5%
	PGA ≤ 0.2 g	2%	0.5%	0.1%
$5.0 < M_w < 7.0$	PGA ≥ 0.4 g	6%	3%	0.5%
	0.2 g < PGA < 0.4 g	2%	1%	0.2%
	PGA ≤ 0.2 g	1%	0.2%	0.05%
Mw ≤ 5.0	PGA ≥ 0.4 g	3%	1%	0.2%
	0.2 g < PGA < 0.4 g	1%	0.2%	0.05%
	PGA ≤ 0.2 g	0.5%	0.1%	0.01%

Table 14. Default Traffic States due to Approach Fill Settlement

Approach Fill Settlement	Repair Process	Traffic State				
		Description	Lanes Open: Partial Closure during Off Hours (Each Way)**			
			Lanes Open before EQ (Each Way)			
			1	2	3	4
Less than 15.2 cm (6 in)	Minor regrading and resurfacing. Duration of repairs = 1 day.	No closure of traffic. Reduce speeds during repairs.	-	-	-	-
15.2 to 30.5 cm (6 to 12 in)	Clear debris. Repair cracks, and build differential settlement ramps or add rock and A/C asphalt over it.	Fully closed for 2 days. Then, fully reopened.	-	-	-	-
30.5 to 61.0 cm (12 to 24 in)	Clear debris. Temporary repairs consist of adding new rock and A/C over it. Permanent repairs consist of adding new structural sections and drainage where needed.	Full closure for 1 week to make temporary repairs. Then, reopen traffic during peak hours. Partial closure of traffic during off hours (midnight to 5 am) to make permanent repairs. Duration of operations to make permanent repairs = 2 to 4 weeks.	0	1	2	3
Greater than 61 cm (24 in)	Clear debris and build temporary lanes for traffic. Demolish existing roadway, fill, and regrade. Permanent repairs will require survey, new design, new drainage, and addition of new structural sections where needed.	Full closure for 1 to 2 weeks for temporary lane construction. Fully reopen traffic along temporary lanes at restricted speeds* to complete permanent repairs of roadways. Permanent repairs will involve partial closure during off hours. Duration of rebuilding effort will range from 1 to 2 months, depending on extent of damage to roadway and fills.	0	1	2	3

*Restricted speeds for roadways will be about half of normal speed limit and, for highways, will be about 30 mph.

**Keep non-redundant roadways open to emergency vehicles when partially closed to permanent traffic and, if possible even when fully closed.

- *Differential Settlement Hazards.* Settlement of dry or moist soils beneath a pavement should be estimated using methods described in section 5.4 for approach fills.

- *Liquefaction Hazards.* Liquefaction-induced lateral spread and vertical displacement of soils beneath a pavement should be estimated by methods described in section 4.4 and appendix E.

- *Sliding Hazards.* The potential for roadway hazards due to sliding of underlying soils should be evaluated using methods summarized in section 4.5.

- *Fault Rupture Hazards.* Potential displacement of active faults that cross a pavement segment should be evaluated using procedures summarized in section 4.6.

Once the level of displacement from these hazards is estimated, the next step is to estimate the potential extent and duration of traffic impacts due to these displacements. The user may apply either the default traffic states given in table 15 or alternative traffic states that he or she designates. Where both horizontal and vertical ground displacement may occur (e.g., in the presence of liquefaction, sliding, or surface fault rupture), the displacement value used in table 15 should be the vector sum of the two displacement components. As for the bridges and approach fills, these estimated traffic states and repair durations are intended to represent near lower-bound estimates assuming immediate availability of repair resources. Circumstances that could affect these estimates include: (a) the presence of significant lateral movement or slip-out of underlying soils; (b) severe damage to concrete pavements (e.g., major longitudinal cracking and warping of the pavement plane) which could require new design and substantial replacement of the existing roadway; and (c) unusual foundation problems.

5.6 OTHER COMPONENTS

In addition to bridges, approach fills, and roadways, the seismic performance of a highway system can be affected by damage to retaining structures, slopes, tunnels, and culverts. Guidelines for seismic hazard screening, evaluation, and retrofit of these components are provided in Youd, 1999. Damage state and traffic state models for these components will be developed during future research efforts.

Table 15. Default Traffic States due to Permanent Ground Displacement at Roadway Pavements

Permanent Ground Displacement*	Repair Process	Traffic State				
		Description	Lanes Open: Partial Closure during Off Hours (Each Way)***			
			Lanes Open before EQ (Each Way)			
			1	2	3	4
Less than 15.2 cm (6 in)	Minor regrading and bresurfacing. Duration of repairs = 1 day.	No closure of traffic. Reduce speeds during repairs.	-	-	-	-
15.2 to 30.5 cm (6 to 12 in)	Clear debris. Repair cracks, and build differential settlement ramps or add rock and A/C asphalt.	Fully closed for 4 to 8 days. Then, fully reopened.	-	-	-	-
30.5 to 61.0 cm (12 to 24 in)	Clear debris. Temporary repairs consist of adding new rock and A/C over it or, for settlement only, constructing differential settlement ramps. For permanent repair of damage, add new structural sections and drainage where needed.	Full closure for 1-2 weeks to make temporary repairs. Then, reopen traffic along these limited lanes under restricted speeds** to make permanent repairs under traffic conditions. Duration of operations to make permanent repairs under reduced traffic = 1 to 4 months, depending on length of roadway to be repaired.	0	1	2	3
Greater than 61 cm (24 in)	Clear debris and build temporary lanes for traffic. Demolish existing roadway, fill, and regrade. Permanent repairs will require survey, new design, new drainage, and addition of new structural sections where needed.	Full closure for 2-4 weeks for temporary lane construction. Reopen traffic along temporary lanes at restricted speeds** to complete rebuilding of roadways. Rebuilding will also involve full closure during off hours (e.g., midnight to 5 am). Duration of rebuilding effort will range from 2 to 6 months, depending on length of roadway to be rebuilt.	0	1	2	3

*Ground displacement = Vector sum of horizontal and vertical components of displacement.

** Restricted speeds for roadways will be about half of normal speed limit and, for highways, will be about 30mph.

*** Keep non-redundant roadways open to emergency vehicles when partially closed to permanent traffic and, if possible even when fully closed.

CHAPTER 6
ECONOMIC MODULE

6.1 BACKGROUND

One set of important end results from SRA of highway systems is the estimation of economic impacts of earthquake damage to the system. These effects can be conceptualized by considering that, in addition to damaging the highway system, earthquakes can also damage buildings, contents, and lifeline infrastructure. Building, content, and infrastructure damage will reduce the region's industrial capacity to produce goods and services. This will affect the traffic demands placed on the highway system after the earthquake. At the same time, the highway system damage will reduce the system's capacity to transport materials, equipment, employees, and other personnel essential to the productivity of firms and households in the region.

These factors together will affect the stricken region's economic productivity and capacity. Estimation of these effects requires the coupling of system, hazards, and component models, with regional economic models, which is a formidable task. Although progress has been made in this area in recent years (e.g., Moore et al., 1999a and 1999b), this is still an area of extensive research and development. This is because most regional economic models are aspatial. These models may treat interactions between economic sectors in considerable detail, but not in a spatially dis-aggregate way. Spatial dis-aggregation is needed to make the link between economic performance and access to lifeline services, including transportation. Furthermore, since access to transportation facilities is unpriced, the value of transportation services is not adequately represented in most regional economic models. Even if a spatially dis-aggregate model of the regional economy is available, it is still necessary to model economic responses to transportation network damage. These responses include changes in the propensity to travel, choice of destination, and choice of route.

Another important factor when using economic loss results for decision making is evaluation of impacts of the highway system damage on stakeholders. Future development of economic models should include assessment of who gains (e.g., construction industry) and who loses (e.g., business sectors heavily dependent on trucking to distribute goods) in the event of such damage.

6.2 OBJECTIVE

The objective of the economic module is to provide the input data and models necessary to estimate economic losses due to highway system damage. However, as noted above, no practical and theoretically sound models addressing these requirements are currently available. It was beyond the scope and resources of the research under this FHWA project to develop such models. Therefore, it was necessary to instead incorporate existing simplified models to provide first-order estimates of economic losses due to commute time increases only. These costs account for the decreases in level of service expected on a damaged network, but not on other effects. The broader set of effects of highway system damage on a region's economic productivity summarized above are not estimated by these models.

This SRA methodology has been designed to provide a framework for future inclusion of extended economic models that do address a broader range of economic effects. This framework includes an economic module within which improved models can be included in the future. It also includes a walk-through procedure that will enable users to assess economic losses over time -- which is an important factor for future economic and budgetary decision-making based on the SRA results. Future research is recommended to develop practical economic loss models and input data for extended models that can be incorporated into the SRA methodology.

6.3 PROCEDURE

With this as background, the economic loss model that is currently incorporated into the SRA methodology is taken from the procedure described in the Caltrans Policy and Procedure Circular P78 Revised (Caltrans, 1994). As noted above, this model addresses economic impacts of increased commute times due to earthquake damage to the highway system, but does not treat the effects of this damage on a region's economic productivity. The following sections summarize the input parameters and application for this model.

6.3.1 INPUT PARAMETERS

The input parameters for this economic loss model, together with default values that can be overridden by the user, are as follows:

a) *Increase in Total System-Wide Travel Time (in units of hours) over a 24-Hour Time Period, at a given Time after the Earthquake (denoted as X_1)*. This will be one of the outputs from the transportation network analysis of the highway roadway system, as described in the previous chapters of this volume.

b) *Percentage of Total Traffic that is Trucks (denoted as X_2).* For example, for the demonstration SRA of the Shelby County TN highway system that is described in chapter 7, X_2 was specified to be 30 percent . This means that the remaining portion of the total traffic (i.e., automobile traffic) = 100 - X_2 = 70 percent.

c) *Vehicle Occupancy Rate for Automobile Traffic (denoted as X_3).* For example, in the above Shelby County TN demonstration SRA, X_3 was specified to be 1.4 persons per vehicle.

d) *Economic Costs of Delay for Trucks (X_4) and for Person-Hours in Automobiles (denoted as X_5).* For example, in the Shelby County TN SRA, these input parameters were specified as X_4 = \$19.20 per truck hour and X_5 = \$6.00 per person-hour in automobile.

e) *Cost of Excess Fuel per Gallon (denoted as X_6).* In this, it is assumed that one gallon of fuel is used per vehicle per hour of travel time delay. In the Shelby County TN demonstration SRA, X_6 was specified to be \$1.20 per gallon.

6.3.2 COMPUTATION OF ECONOMIC LOSSES AT EACH POST-EARTHQUAKE TIME

For each post-earthquake time at which system states were developed and travel times were obtained, economic losses due to increased commute times (over a 24-hour time period) are computed from the following steps (where the quantities X_1 to X_6 are defined in section 6.3.1).

- Compute the costs due to truck traffic time delays, C_1, from equation 3:

$$C_1 = X_1 * [\frac{X_2}{100}] * X_4 \tag{3}$$

- Compute the cost due to automotive traffic time delays, C_2 from equation 4:

$$C_2 = X_1 * [\frac{100 - X_2}{100}] * X_3 * X_5 \tag{4}$$

- Compute costs of increased fuel due to travel time delays, C_3, from equation 5:

$$C_3 = X_1 * X_6 \tag{5}$$

- Compute the economic loss due to increased commute time that is caused by earthquake damage to the highway system (over a 24-hour period and for each designated post-earthquake time), as the sum of the costs of increased truck-traffic time delays, increased automotive-traffic time delays, and increased fuel due to overall time delays, i.e.,

$$C_{TOT} = C_1 + C_2 + C_3 \tag{6}$$

6.3.3 COMPUTATION OF AGGREGATED ECONOMIC LOSSES

To use the above results for estimation of the total aggregated economic loss due to the given scenario earthquake and simulation, the following steps can be implemented:

- The above calculations should be carried out for several post-earthquake times ranging from early times (when daily losses may be relatively large) to late times (when daily losses will be small).

- Once this is completed, the losses for each post earthquake time can be plotted vs. time. A curve of loss vs. time can then be obtained (e.g., by connecting successive data points with a straight line). This curve can then be extrapolated out to estimate a maximum time at which the losses per day finally vanish.

- The total aggregated economic loss for the scenario earthquake and simulation is then obtained as the area beneath this curve.

CHAPTER 7
DEMONSTRATION SEISMIC RISK ANALYSIS

7.1 OBJECTIVE AND SCOPE

This chapter describes a demonstration SRA of the highway system in Shelby County, Tennessee. The objective of this analysis is to illustrate the applicability of the SRA methodology described in this volume, and the types of results that can be obtained.

This demonstration SRA is probabilistic, using multiple scenario earthquakes and a single simulation for each earthquake. The analysis includes bridge and approach fill components and ground shaking hazards only, for which random values of the uncertain parameters are estimated from the algorithms and fragility curves described in chapters 4 and 5 and appendices D and F. Results of the SRA show effects of earthquake damage to the highway system in terms of: (a) ground motions, damage states and traffic states for selected earthquakes; (b) economic losses due to increased commute times; and (c) increased access and egress times to and from selected origin-destination zones. These results are provided in the following forms: (a) GIS plots for selected scenario earthquakes; (b) probabilistic total loss distributions; (c) random walk plots; (d) tabulations of results for selected scenario earthquakes; and (e) confidence level estimates.

The demonstration SRA described in this chapter is a significant update of a prior SRA of the Shelby County highway system that was carried out early in this research to evaluate current models and to identify and prioritize research needs (Werner et al., 1997). This use of the demonstration SRA process for this purpose is continuing. Since the SRA described in this chapter was completed, new SRA of the Shelby County highway system has been initiated under a follow-on research project. The purpose of this new SRA is to evaluate the most recent improvements to the current SRA methodology (Werner et al., 2000). These include liquefaction hazards modeling, inclusion of the rapid-pushover model for bridges subjected to ground shaking, and modeling of the effects of closures to the two Mississippi River crossings in Shelby County and how trips that use these crossings can be detoured. Because their evaluation is still in progress, these latest improvements are not included in this chapter. They will, however, be documented in a future report when the evaluations are completed.

7.2 SYSTEM

Shelby County (whose county seat is Memphis) is located in the southwestern corner of Tennessee, just east of the Mississippi River and just north of the Tennessee-Mississippi border. Because of its proximity to the New Madrid seismic zone, the potential seismic risks to the Memphis and Shelby County area are well recognized and have been studied extensively.

The Shelby County highway system (figure 13) includes a beltway of interstate highways that surrounds the city of Memphis, two major crossings of the Mississippi River within the Memphis city limits (at Interstate Highways 40 and 55), major roadways within the beltway, and highways and roadways just outside of the beltway that extend to important transportation, residential and commercial centers to the south, east, and north.

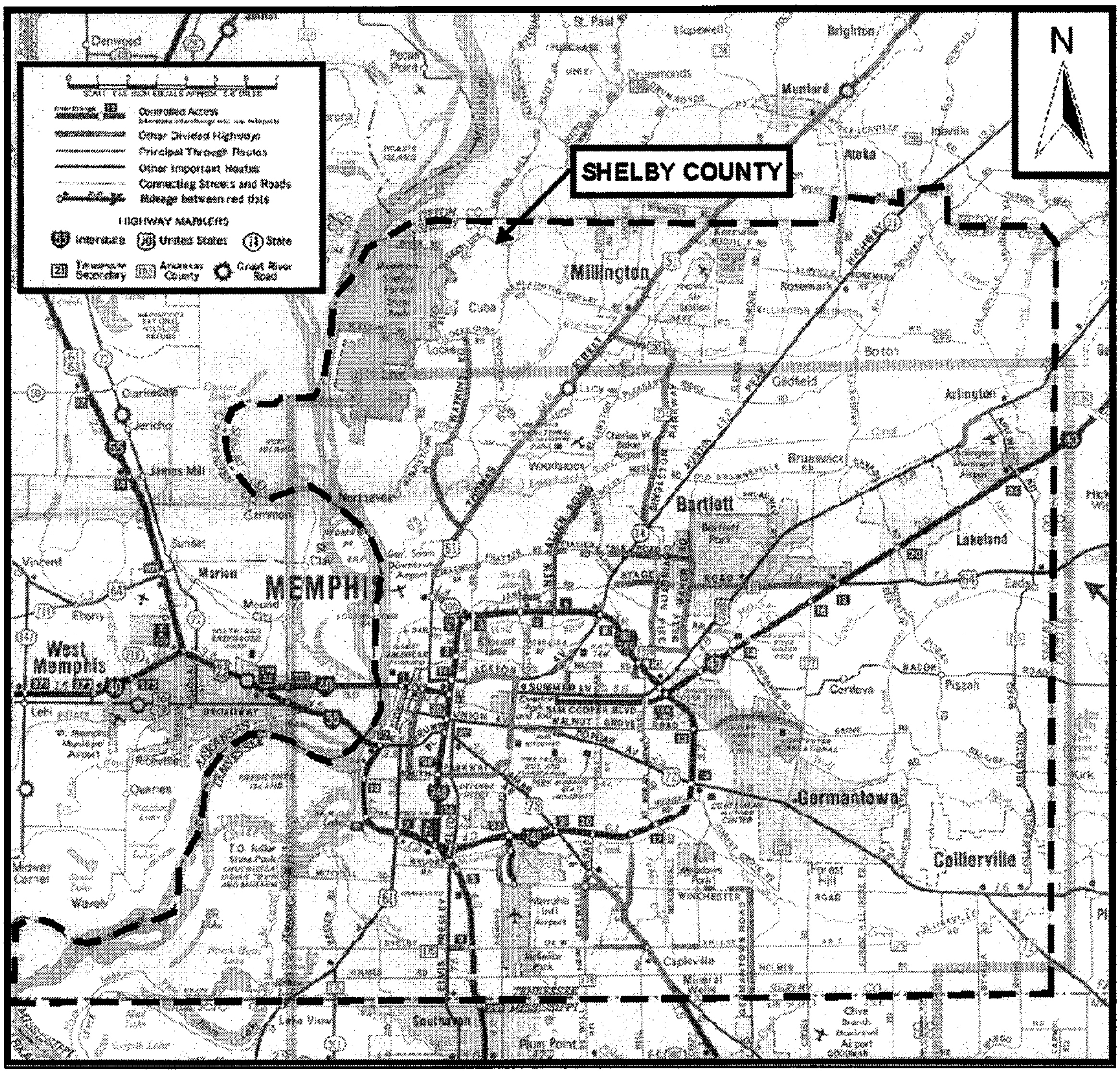

Figure 13. Shelby County, Tennessee

The demographics of the county are represented in terms of the Origin-Destination (O-D) zones shown in figure 14. This figure also shows locations of key government, transportation, medical, education, commercial, and residential areas for which post-earthquake access and egress times were monitored in this demonstration SRA.

7.3 INPUT DATA

7.3.1 SYSTEM

The modeling of the Shelby County highway system network and origin-destination zones was based, in part, on data describing the system, traffic, and origin-destination zones. These data were provided by the Shelby County Office of Planning and Development (OPD), who is the Metropolitan Planning Organization (MPO) for the region.

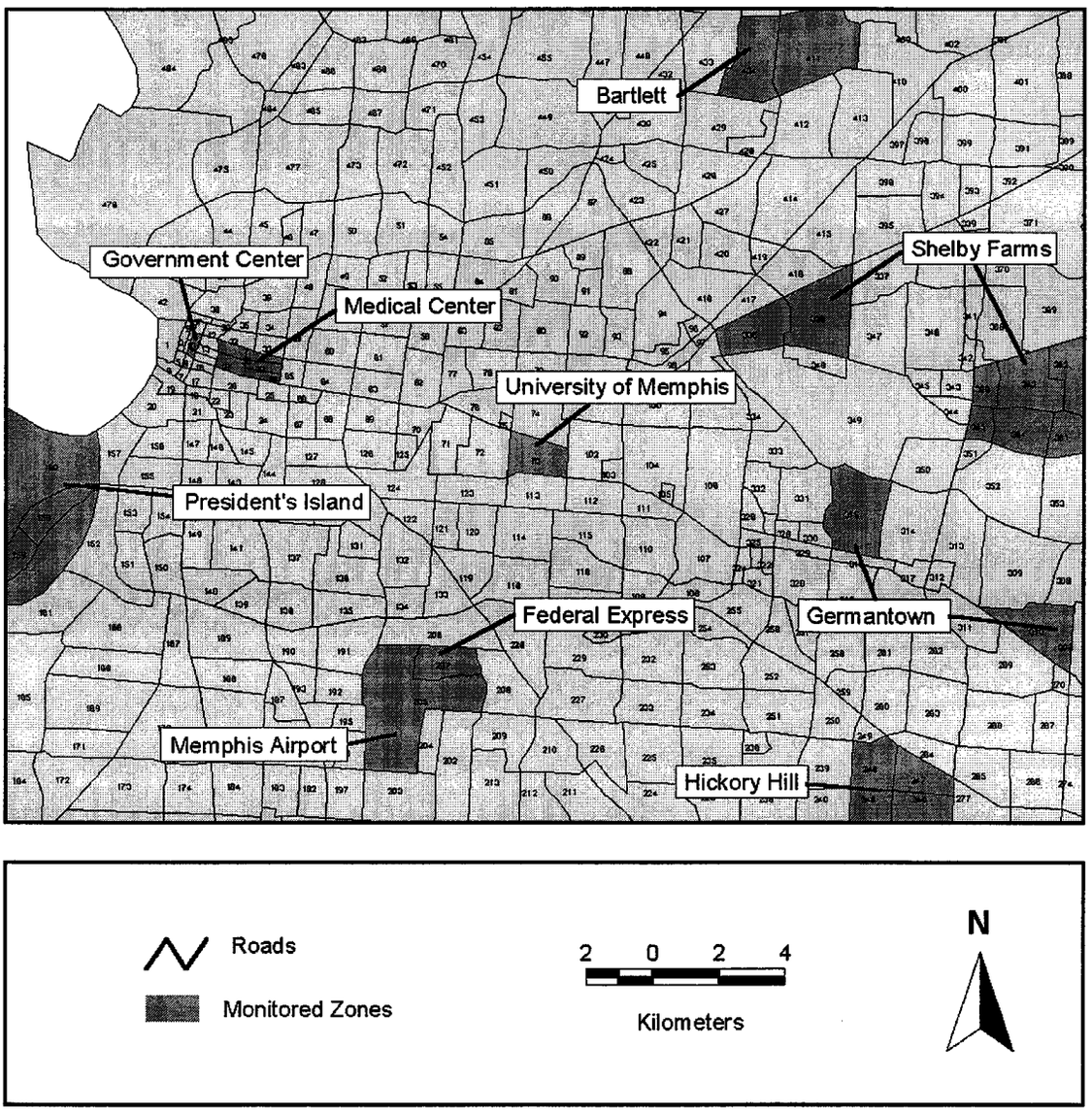

Figure 14. Origin-Destination Zones

Although the data provided by OPD were helpful and essential to this analysis, they contained certain shortcomings for application to SRA of the Shelby County highway system. Because of these shortcomings, special measures were needed to adapt these data for this demonstration SRA. These measures were achieved at some cost, and with some trial and error. The following summary of these measures is intended to provide insight into complexities that can arise when carrying out SRA with real-world data previously developed to meet MPO traffic management and forecasting objectives that did not include SRA.

7.3.1.1 The Problem

The database provided by OPD contains roadway traffic and O-D zone trip-table data that are essential for analysis of post-earthquake traffic flows in Memphis and Shelby County. These

data are tied to a roadway network and array of origin-destination (O-D) zones. In addition, the data were tied into a software package named MINUTP (Comsis, 1994) that, at this time, is being used by OPD for their county-wide transportation analyses and projections. These data corresponded to a working file for OPD's projected network for the year 2020, which was the most current file available from OPD at the time of this SRA.

As is the case for most transportation planning networks, these roadway network and O-D zone representations were not designed for used by a GIS, nor do they use a standard GIS coordinate system (e.g., state-plane coordinates). Therefore, this transportation planning network representation could not be used to establish roadway segment lengths and bridge locations, or to graphically display the roadway network and post-earthquake road closures. Similarly, the O-D zone representation could not be used to graphically display the roadway network and post-earthquake impacts on travel times to and from particular O-D zones. Even more important, the O-D zone trip table supplied by OPD was inconsistent with this set of O-D zones.

7.3.1.2 The Solution

7.3.1.2(a) Multiple Database Development

To solve this problem, it was necessary to obtain a detailed GIS database of the Shelby County highway system that was based on a state-plane coordinate system. This database was then incorporated into the input file for the SRA of this system. From this, all roadway segment locations and lengths were established, and locations of all bridges were input into this network database. In addition, the trip table was estimated numerically by imputing changes in O-D requirements from link volumes. This involved the updating of a uniform set of interzonal flows based on empirical link flows and a maximum likelihood estimation procedure. This is a nonstandard step for the SRA, but could easily be replicated in other venues if transportation planning data are available in a form that involves multiple zone systems.

To address the issue with the O-D zones, a map of O-D zones for Shelby County that had been provided by OPD was scanned. This map had a physical scale, and included major roadways in the system. The OPD database of O-D zones (which contains a graphical representation of the shape of each O-D zone and an identification number for that zone) was then compared to the O-D zones in the above GIS database. Fortunately, there was a one-to-one correspondence between the zones in these two databases.

At this stage, two system databases were available -- each of which had some but not all of the attributes needed for SRA of a highway system. The OPD database contained the roadway attributes and traffic data and O-D trip table data needed to carry out the post-earthquake transportation network analysis. However, it did not contain a physical scale that would be needed to establish locations of damaged bridges and restricted roadways after a given scenario earthquake, and to graphically display pre-and post-earthquake damage states, traffic states, system states, and travel times between O-D zones. On the other hand, the GIS database contained a physical scale, but did not incorporate the roadway, traffic, and trip table data needed for the network analysis.

7.3.1.2(b) Implementation

The GIS model of the Shelby County highway system uses 7,807 links and 15,614 nodes to represent all roadways in the system ranging from interstate highways down to low-speed ramps, as well as each of the 384 bridges in the system (figure 15). Prior to carrying out the SRA of this system, a special relational table between the GIS and OPD databases was developed. This table was needed to map the post-earthquake system states from the GIS links to the modified OPD transportation planning network used to compute user equilibrium (UE) flows. After this mapping was carried out for each scenario earthquake and simulation, the post-earthquake travel times and traffic flows could be estimated. This OPD planning network consisted of 11,699 links (including virtual links that connected O-D demand to physical links), and 3,917 nodes.

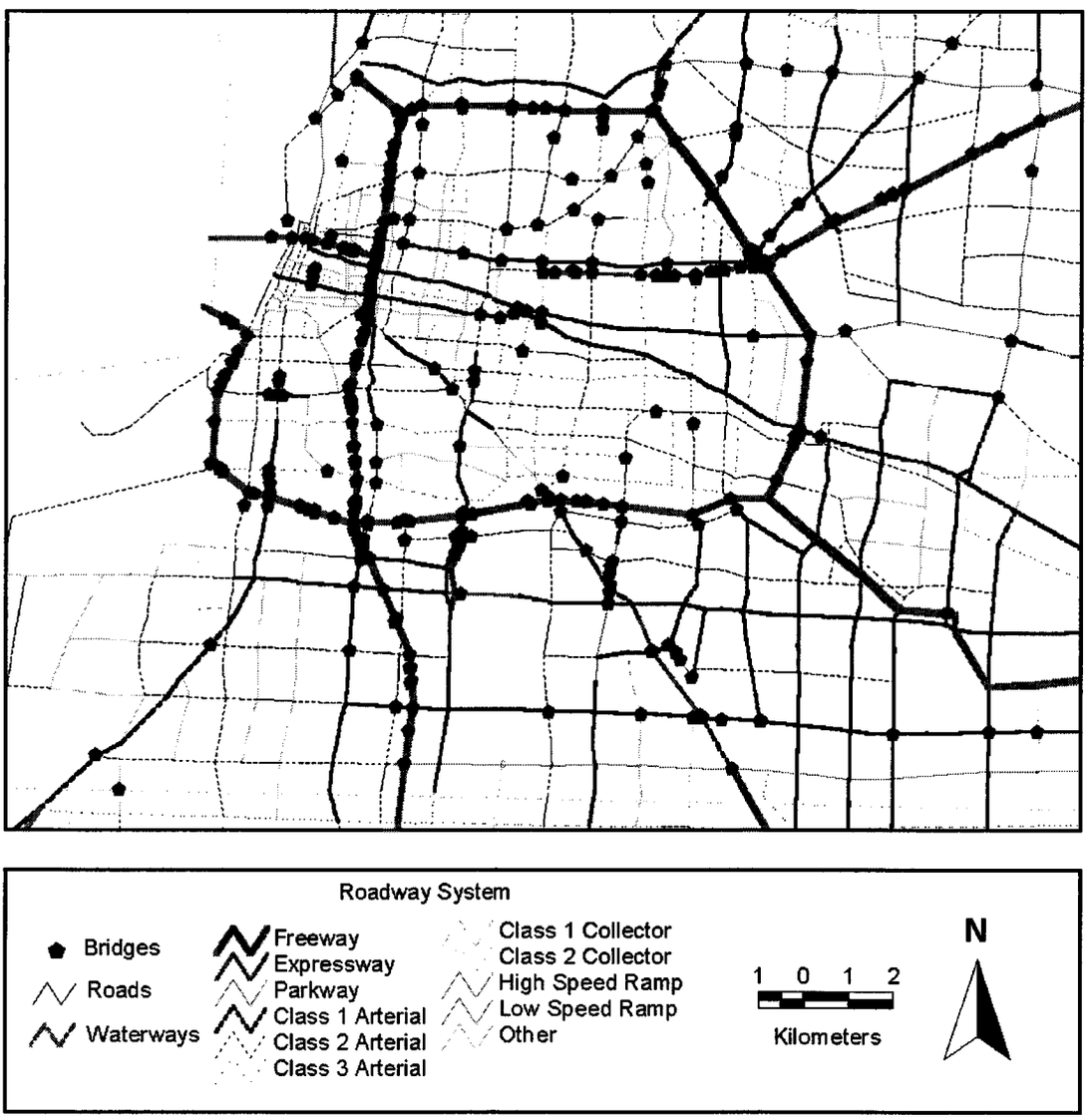

Figure 15. GIS Model of Shelby County Highway System

7.3.2 SOIL CONDITIONS

Soil conditions in Shelby County were estimated from prior mapping of local geology by the Center for Earthquake Research and Information at the University of Memphis (Ng et al., 1989). This mapping involved: (a) analysis of about 8,500 boring logs from the area; (b) division of the County into cells with sizes of 760 m by 915 m (2,500 ft. by 3,000 ft.); and (c) use of the boring logs from sites in each cell to develop a representative boring log for that cell. Soil conditions in cells with no boring logs were estimated from logs in nearby cells with similar surface geology. In this way, a NEHRP site classification was assigned to each cell (see figure 16). Geologic screening procedures were also applied to the representative boring log for each cell to identify those cells with a potential for liquefaction. Figures 16 and 17 show that soils along the Mississippi River and other waterways in Shelby County are classed as NEHRP soil type E and liquefiable, whereas all other soils in the county are classed as NEHRP soil type D and non-liquefiable.

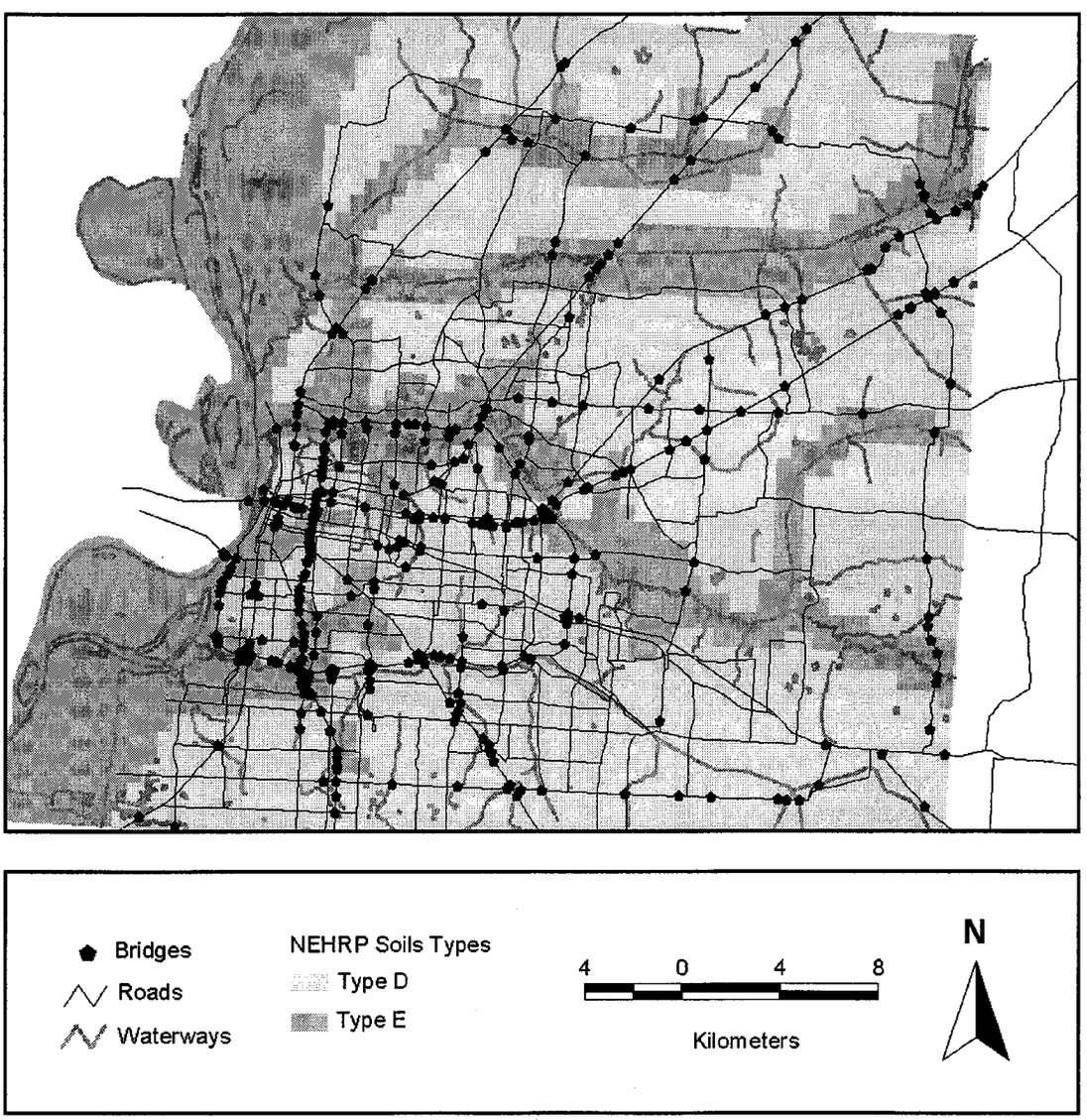

Figure 16. NEHRP Soil Types in Shelby County

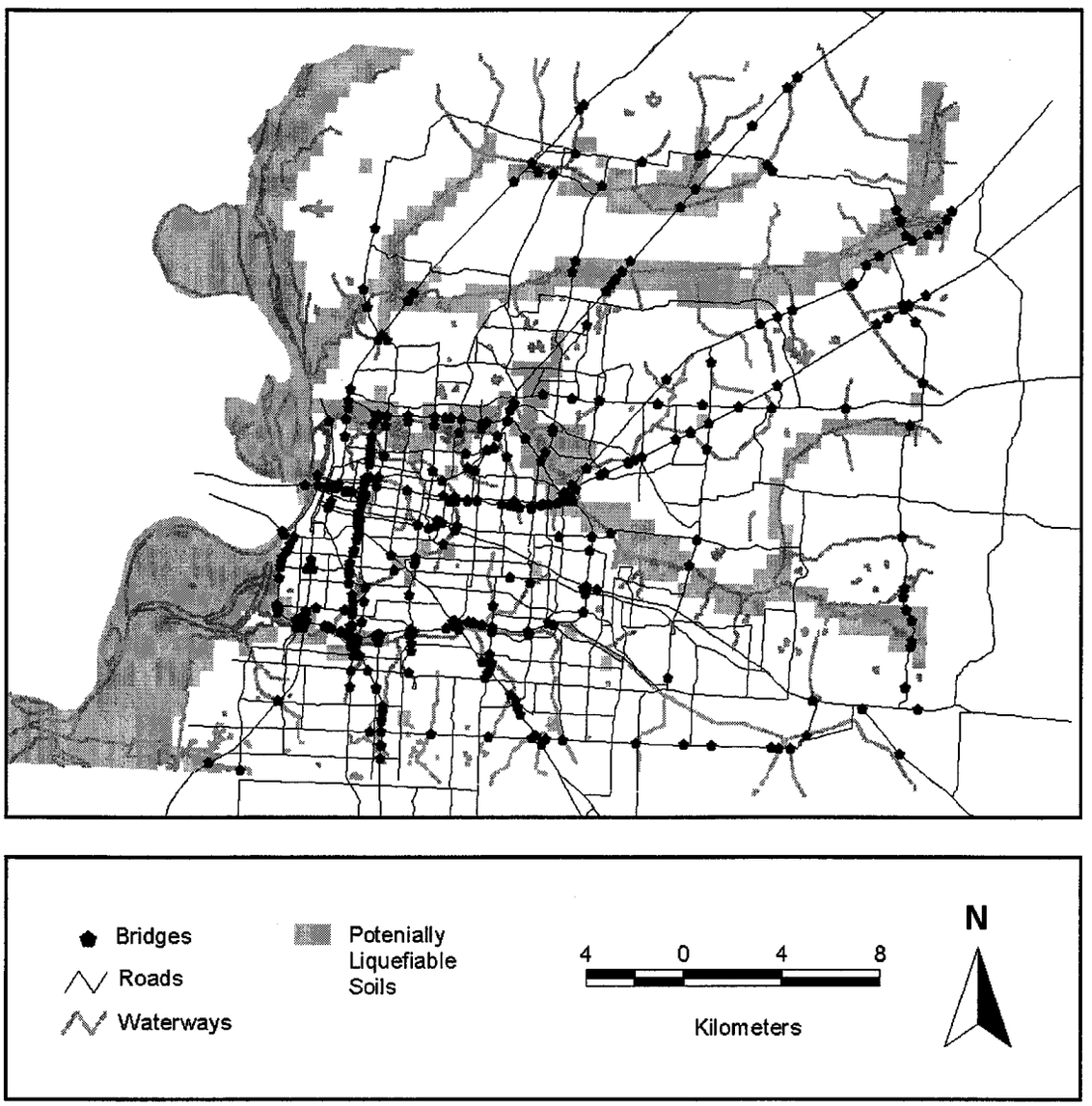

Figure 17. Geologic Screening for Potentially Liquefiable Soils in Shelby County

7.3.3 COMPONENTS

This demonstration SRA considers bridges and approach fills, subjected to ground shaking hazards only. Fragility curves developed from the elastic capacity-demand approach are used to model the bridges.

7.3.3.1 Bridges

The fragility curves for bridges subjected to ground shaking hazards that are used in this demonstration SRA were developed by Jernigan (1998) from an elastic-capacity demand approach applied specifically to bridge types from Shelby County. Appendix F summarizes this

procedure and provides the resulting fragility curves. As noted in that appendix, Jernigan grouped each of the 382 bridges in Shelby County (excluding the Mississippi River crossings) into one of six bridge groupings. These groupings distinguished the bridges according to whether they are continuous or simply supported, whether they have a steel or concrete superstructure, whether their substructure consists of pile bents or multi-column bents, and whether the bridge has a single span or multiple spans. The models were developed by using dynamic analysis, random combinations of uncertain parameter values, and assumed limiting values of capacity-demand ratios leading to the onset of various levels of damage to the bridge.

Modeling of the Shelby County bridges for this demonstration SRA encountered certain issues for which the following interim resolutions were required:

- Because of the previously noted need to work with separate OPD and GIS databases, it was necessary to tie the links in the GIS database (which contains the bridge data) to the links in the OPD database (which contains the traffic and trip data). The links in the OPD database often have lengths that contain several bridges. Therefore, it was necessary to relate traffic states along each of these links to the worst-case traffic state for any of the bridges along that link. This leads to a conservative (over-estimation) of the traffic state for the overall link.

- Special fragility curves for the I-40 and I-55 crossings of the Mississippi River have been developed, as described in appendix G. However, these crossings are not included in this demonstration SRA because of the need to first investigate procedures for rerouting trips across these non-redundant bridges, if the bridges are closed due to earthquake damage. These effects and associated modeling procedures are now being investigated as part of a follow-on research project (Werner et al., 2000).

7.3.3.2 Approach Fills

Approach fills have been modeled using the procedure summarized in section 5.4. In the absence of detailed information on the approach fills for each bridge in the Shelby County highway system, the relative compaction of the fills was assumed to be equal to 95 percent, and the height of the fills was assumed to be equal to the minimum vertical clearance of the bridge plus 1.52 m (5 ft). In this, the minimum vertical clearance for each bridge is specified in the NBI database for each bridge in the system (FHWA, 1995b).

7.3.4 SCENARIO EARTHQUAKES

This SRA was conducted as a walk-through analysis procedure that encompassed a duration of 50,000 years. Scenario earthquakes occurring during each year of this duration were estimated by adapting the earthquake models for the Central United States that were developed under the United States Geological Survey (USGS) National Hazard Mapping Program (Frankel, 1996), and by also making use of results from other relevant earthquake studies of the region (Johnson, 1996, Johnson and Schweig, 1996 and Crone, 1998). This adaptation is described in appendix C of this report.

This process generated a total of 2,321 earthquakes with moment magnitudes ranging from 5.0 to 8.0. Each earthquake was located into one of the 1,763 microzones (with dimensions of about 11.1 km in length and width) that encompassed the surrounding area. The locations of these earthquakes (broken down into different magnitude ranges) are shown in appendix C. Either zero, one, or two earthquakes were assumed to occur during any year of the walk-through.

In this SRA, it was assumed that an earthquake would not lead to damage if it causes peak ground accelerations that do not exceed 0.05 g anywhere in the system. On this basis, it was determined that only 925 of the 2,321 earthquakes could be classified as damaging (for which post-earthquake system states and network analyses would be required). In addition, because of cataloging difficulties, it was necessary to exclude the second damaging earthquake during the relatively few years when more than one earthquake occurred. This excluded an additional 44 damaging earthquakes, resulting in a total of 871 damaging earthquakes for which system states and network analyses were developed. These cataloguing difficulties have since been resolved, and the total ensemble of generated earthquakes is now being considered in the updated SRA of the Shelby County highway system that is now being carried out.

7.4 TRANSPORTATION NETWORK ANALYSIS

The transportation network analysis process for this current demonstration SRA initially used simple associative memories (SAM) and multi-criteria associative memories (MAM) that are described in appendix B. The SAM results were found to be insufficiently accurate, and the MAM application was too computationally intensive. Therefore, it was necessary to use other convergent algorithms to compute user equilibrium (UE) traffic flows for the post-earthquake system states developed for this SRA. The results shown in subsequent sections of this chapter are based on these UE flows. Since these results were developed, the MAM process was modified to improve its computational efficiency, and this enabled the MAM to be successfully applied to post-earthquake system states developed for the a new SRA now being conducted under a follow-on research project (Werner et al., 2000).

7.4.1 AM PERFORMANCE TARGETS

Ideally, an appropriately specified and trained associative memory would exactly replicate user equilibrium flows in networks. This is not the case, but AM outputs can provide excellent estimates of exact UE flows in distressed networks.

The zeroth level prediction of flows in a distressed transportation network consists of UE flows for an intact network. The simple correlation coefficient between these values is typically in the neighborhood of 0.88 to 0.90 in networks damaged by the earthquakes represented in this demonstration SRA. Thus, AMs only offer real improvements relative to this zeroth level prediction to the extent that the simple correlation coefficients for test comparisons between AM outputs and corresponding UE flows used to train the AM matrix exceed about 0.90. The target value is 0.98-0.99. Correlation coefficients that are this high imply AM predictions that are a very good estimate of UE flows.

7.4.2 PERFORMANCE OF SIMPLE ASSOCIATIVE MEMORY

In this demonstration SRA, a SAM matrix estimated against 200 training cases returned correlation coefficients of about 0.94. This performance is inadequate for estimating the traffic flows and travel times needed to support the SRA. Much larger training sets produce marginally better SAM estimates, but it is unlikely a SAM exercise will approach the target given above.

7.4.3 INITIAL PERFORMANCE OF MULTI-CRITERIA ASSOCIATIVE MEMORY

A prior investigation of the Los Angeles (LA) highway network showed that a multi criteria associative memory (MAM) consistently outperforms a SAM (Moore et al., 1997). The quality of the SAM estimates obtained for the LA flows are commensurate with the quality obtained for the Shelby County highway network. The Shelby County network includes fewer physical links than the LA network. However, the Shelby County network model was much more detailed, containing an order-of-magnitude more links. As a result, calculating a MAM matrix for the Shelby County network involved generating the pseudo inverse for a matrix of about 100 million elements. Standard methods for evaluating the pseudo inverse that were in place during this initial MAM application to the Shelby County network were found to be too computationally intensive to carry out this inversion within practical time and computer storage limits.

7.4.4 NETWORK ANALYSIS FOR THE DEMONSTRATION SRA

For each of the 871 damaging earthquakes considered in this demonstration SRA (with one simulation per earthquake), system states were developed across three post-earthquake times, resulting in a total of 2,613 network system states. Repairs proceed with time after an earthquake. Capacity returns incrementally. Under the reconstruction models used in this SRA, the system is assumed to approach its pre-earthquake transportation capacity at about five months (150 days) after the earthquake, regardless of the state immediately after the event. Thus, only about one-third of these system states showed substantial reductions in network capacity.

In view of the above difficulties with the SAM and initial MAM applications, UE flows for this demonstration SRA were computed for each system state by using a carefully implemented convergent algorithm that differed from the associative memory. This approach involves too great a computational burden to be applied routinely for a large number of system states. It was used here solely to facilitate the demonstration SRA that is described in this chapter.

7.4.5 RECENT DEVELOPMENTS

7.4.5.1 Modifications and Improved Performance of MAM

Once estimated, a MAM matrix is no more difficult to apply than a SAM matrix, and leads to much better estimates of UE traffic flows. Therefore, after the demonstration SRA was completed, efforts focused on how to reduce the computational intensity of the MAM approach. These efforts led to replacing the standard methods for generating the pseudo matrix in the MAM approach by the Choleski decomposition. This reduced memory storage requirements by an

order of two and computation times by an order of six, relative to standard approaches such as Gaussian elimination.

This modification enabled the MAM to be successfully applied to the post-earthquake system states for the Shelby County highway system (Werner et al., 2000). As noted in chapter 3, this MAM application led to correlation coefficients that range from 0.97 (at seven days after the earthquake) to 0.99 (at 150 days after the earthquake), with an average across all 2,613 cases of 0.98. This meets the AM performance target given in section 7.4.1. It means that a mechanism now exists to rapidly estimate traffic flows as part of a seismic risk analysis treating any number of additional damaging earthquakes and resulting system states.

7.4.5.2 New MAM Training Strategy

It is tempting to train associative memories with network flows corresponding to system states generated by the same process that will generate new observations, i.e., by damaging earthquakes. Training associative memories with UE flows for system states that have been generated by the other SRA modules might logically produce associative memory matrices that perform particularly well with respect to the new system states likely to result from earthquakes. However, computational experience shows that it is better to select training sets in a way that provides a systematically representative collection of all possible network states. Training AMs with a set of systematically representative system states and associated UE flows produces an associated memory matrix with a greater capacity to generalize across network topologies.

Best test results were obtained for a multi-criteria associated memory ($\alpha = 0.5$) trained against system states selected on the basis of systematic representation. Each case is defined by removing a different combination of links containing bridges, and computing a set of convergent, user equilibrium flows for each resulting version of the Shelby County network. One of the training cases consists of the undamaged Shelby County network and associated UE flows. In addition, approximately 2,700 MAM training cases were generated. Appendix B describes this updated training process in more detail.

7.5 RESULTS

7.5.1 GIS PLOTS

Figures 18 to 22 contain GIS plots developed from the SRA to represent system-wide seismic hazards, component vulnerabilities, and post-earthquake system states for selected earthquakes and simulations. These particular results are for Earthquake 41789 -- a large earthquake (M_w = 8.0) located about 142 km north-northeast of downtown Memphis. They show: (a) peak ground accelerations (PGAs) at the bridge sites throughout the Shelby County highway system; (b) damage states for the bridges in the system; and (c) post-earthquake system states at times of 7 days, 60 days, and 150 days after the earthquake. Such plots can be developed for any earthquake considered in the SRA. It is noted that the large variability in the spatial distribution of the ground shaking within Shelby County that is shown in figure 18 was investigated using methods of standardized residuals, and found to be generally consistent with the large intra-event

uncertainties exhibited in many currently accepted strong ground motion models (Boore et al., 1997, Abrahamson and Silva, 1997, and Sommerville et al., 1997).

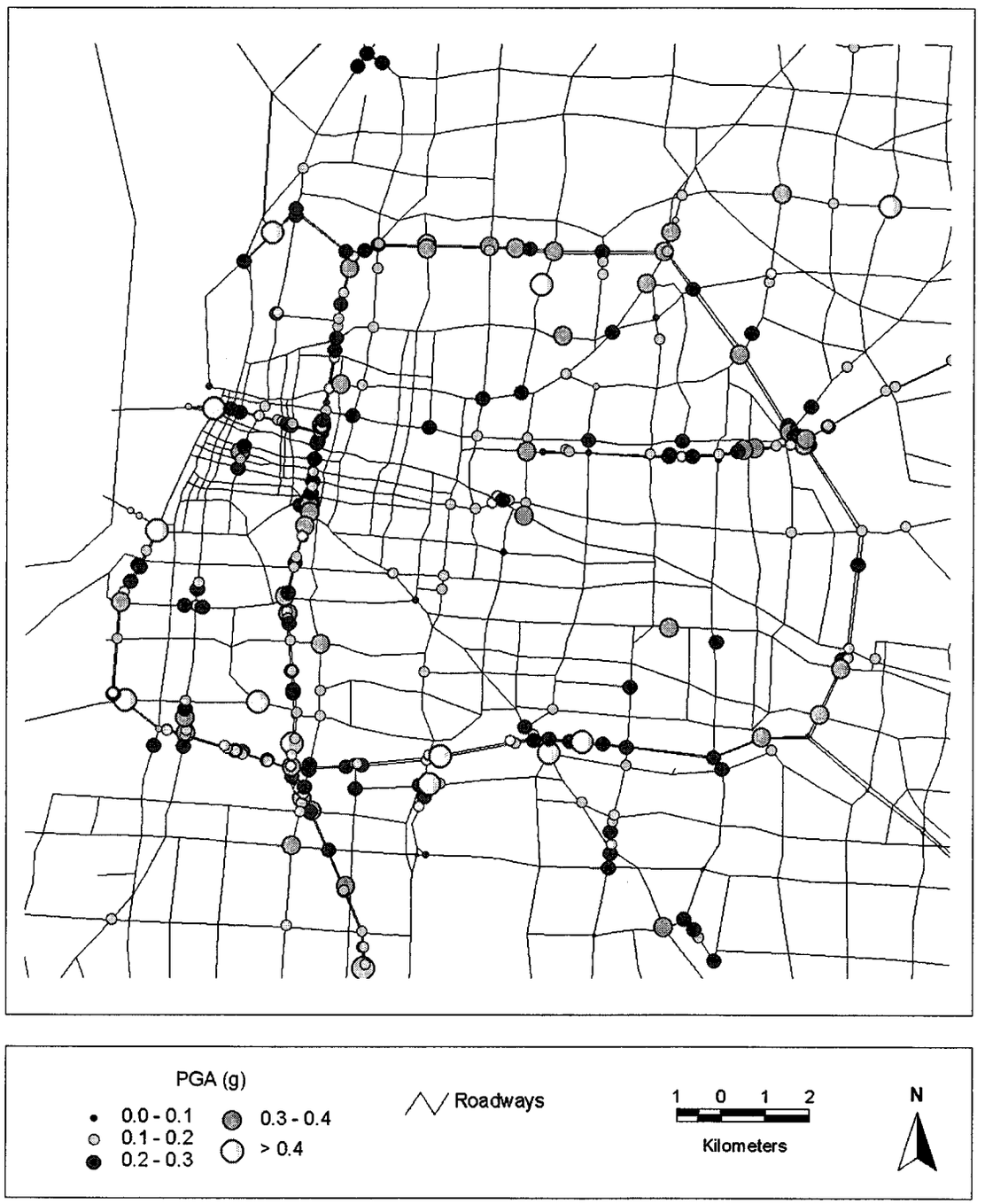

Figure 18. Peak Ground Accelerations at Bridge Sites due to Earthquake 41789

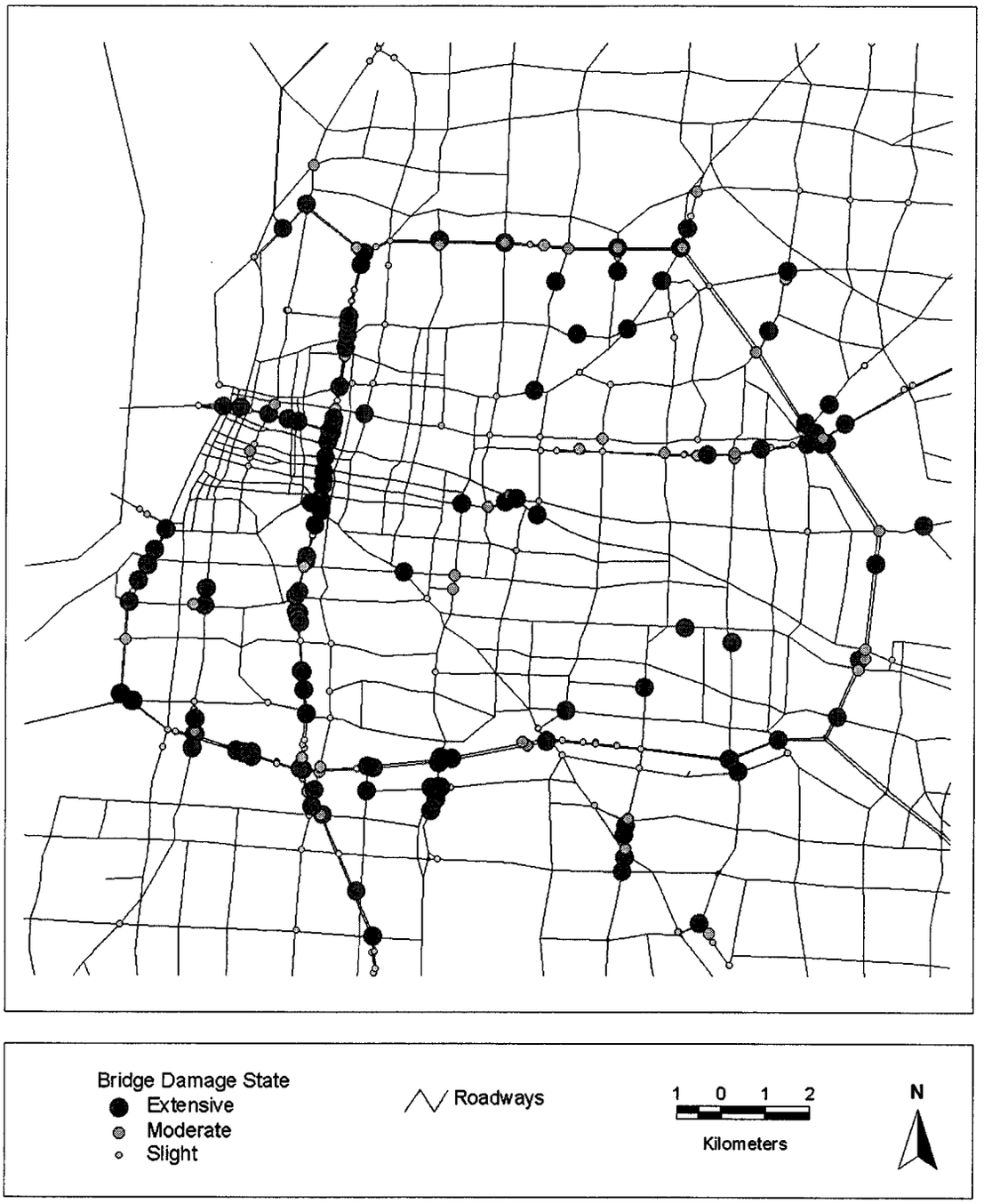

Figure 19. Bridge Damage States due to Earthquake 41789

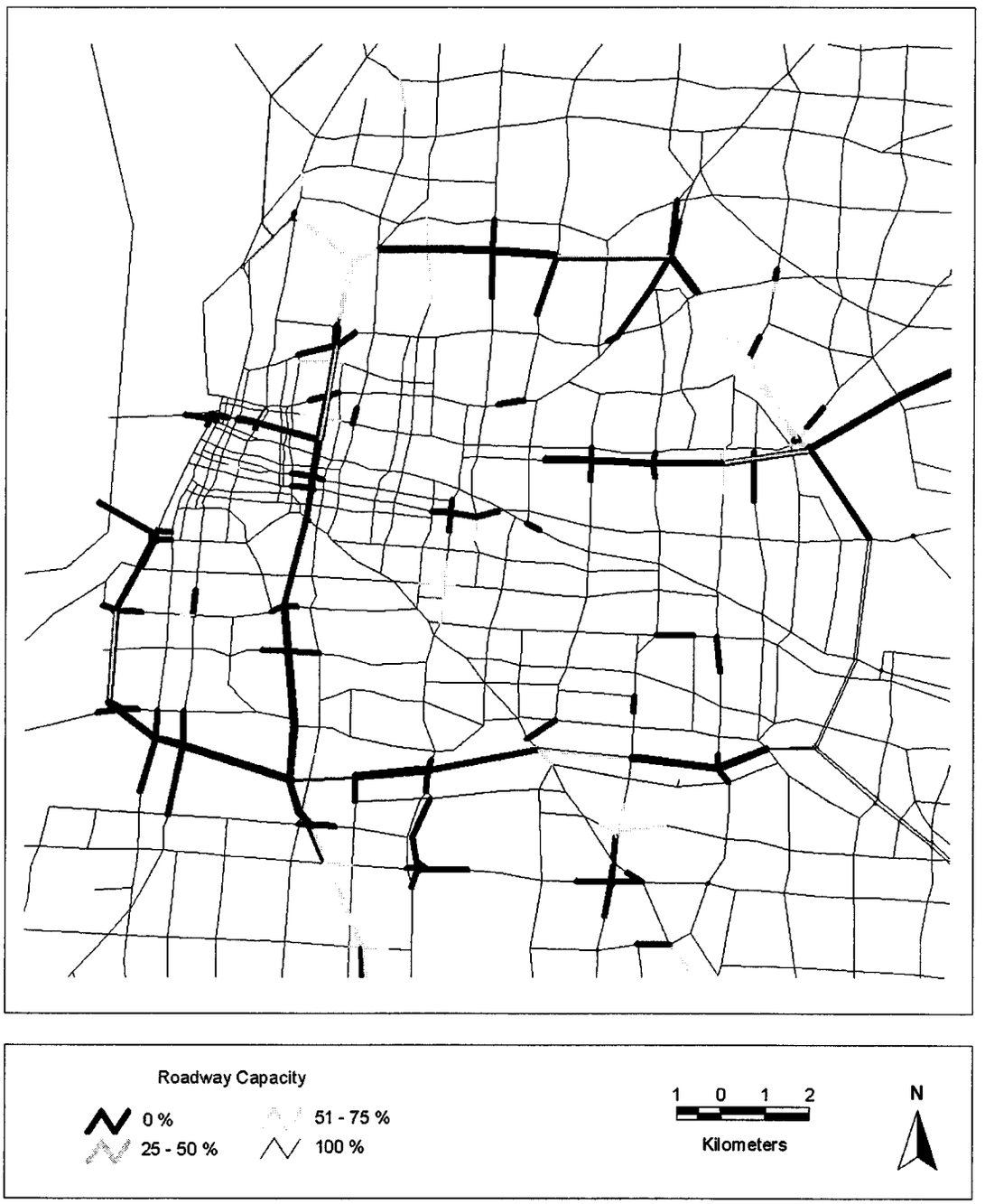

Figure 20. System State at 7 Days after Earthquake 41789

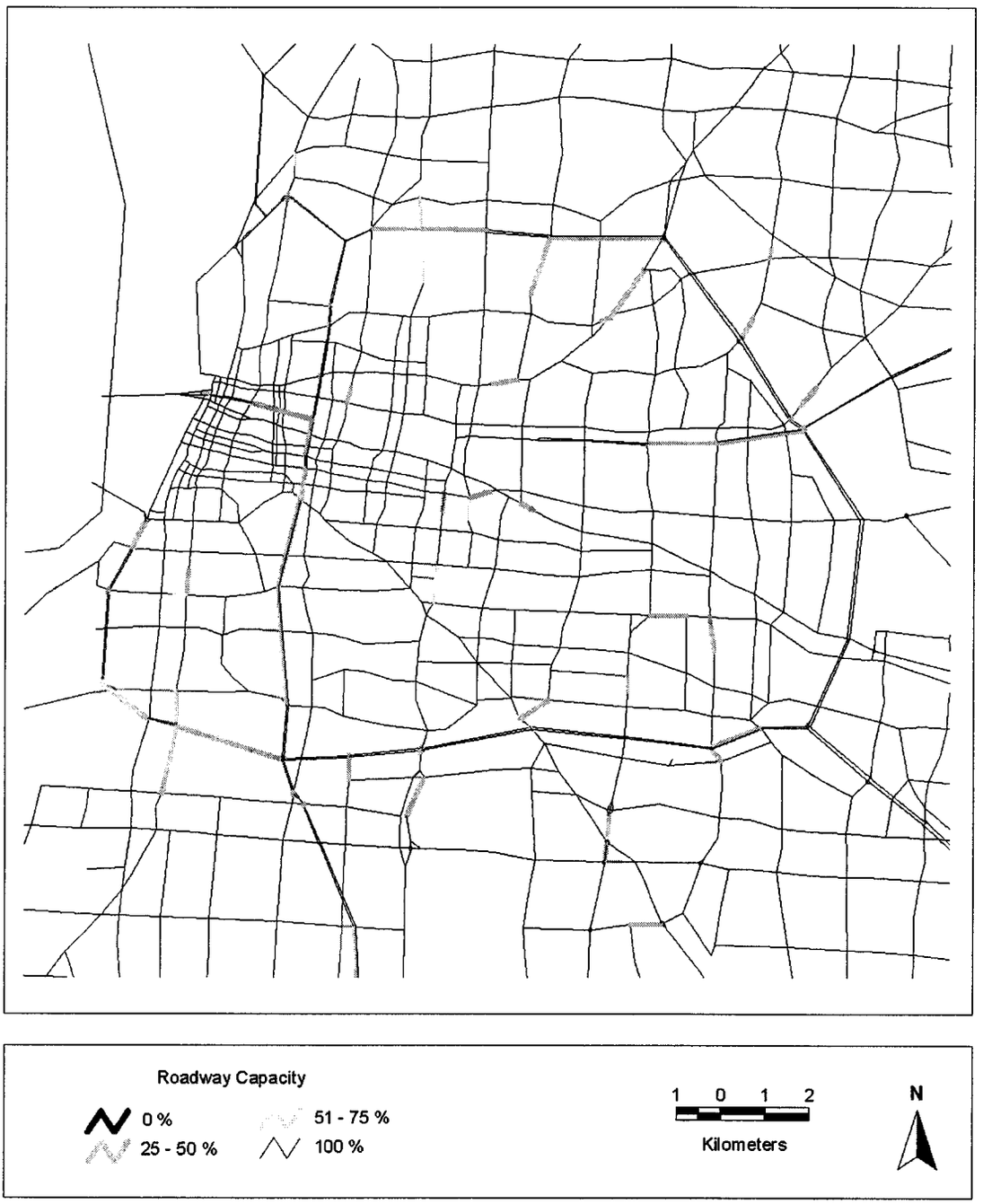

Figure 21. System State at 60 Days after Earthquake 41789

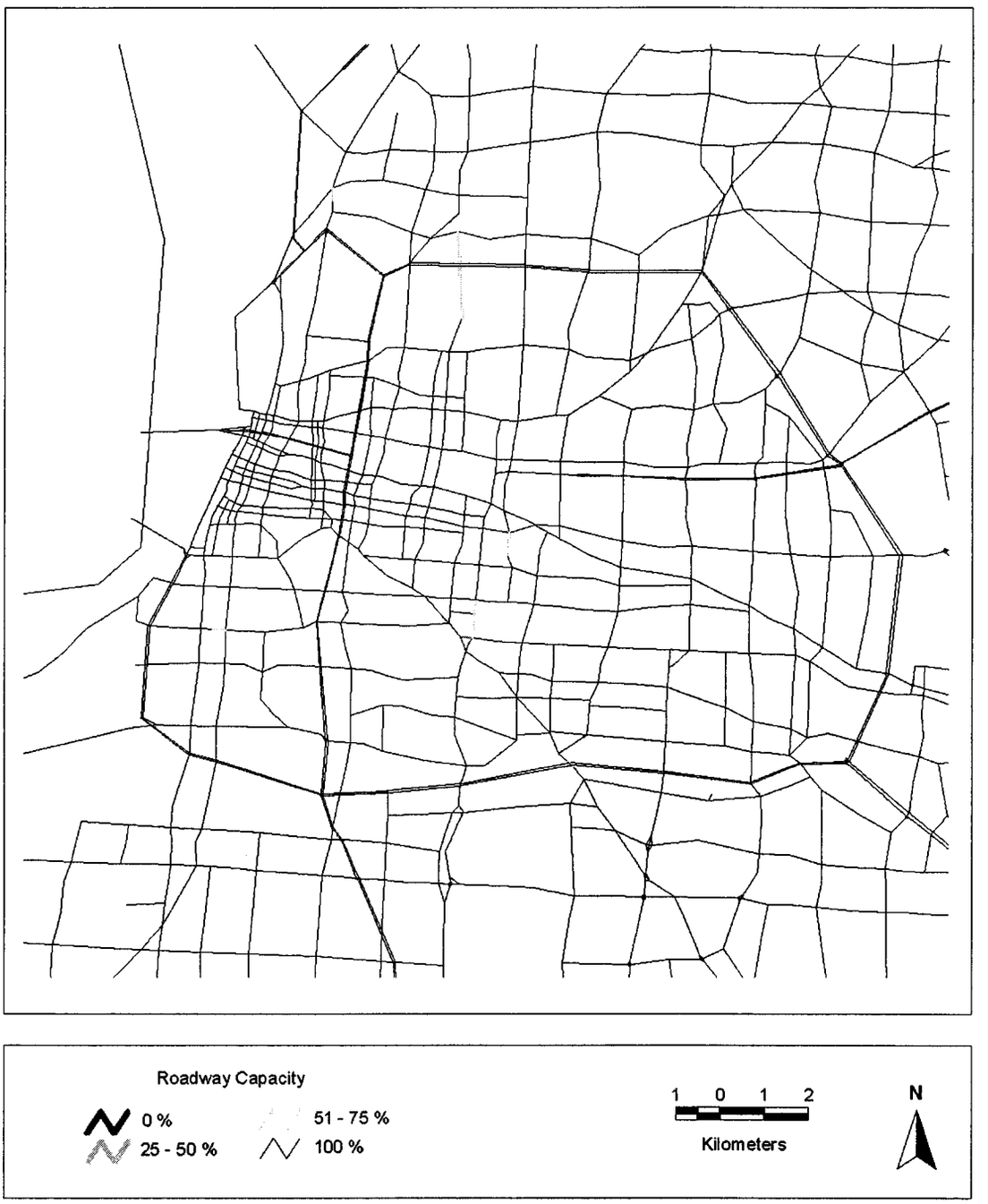

Figure 22. System State at 150 Days after Earthquake 41789

7.5.2 ECONOMIC LOSSES

7.5.2.1 Total Loss Distributions

Figure 23 shows economic loss distributions (for exposure times of 1, 10, 50, and 100 years) caused by damage to the Shelby County highway system from the array of 871damaging earthquakes occurring over 50,000 years that are considered in this SRA. These losses are due to increases in commute times only. They are computed by applying the simplified models from chapter 6 to the travel time increases computed for the highway system from each earthquake. Economic losses per 24-hour day are estimated at post-earthquake times of 7, 60, and 150 days.

These results show economic losses due to earthquake-induced commute time increases of about $80 million and $300 million, for probabilities of exceedance of 50-percent in 50 years and 10-percent in 50 years respectively. These estimates are based on the lower-bound repair times from chapter 5 that assume availability of dedicated repair resources (labor, equipment, and materials) to complete system repairs as efficiently as possible. If such resources are not available, repair times and traffic disruptions could extend over a longer time, and the economic losses for these probability levels would be larger. The SRA methodology can assess the relative effectiveness of alternative strategies in reducing these losses (e.g., seismic retrofit of certain bridges, increasing repair resources for reducing post-earthquake repair times, etc.).

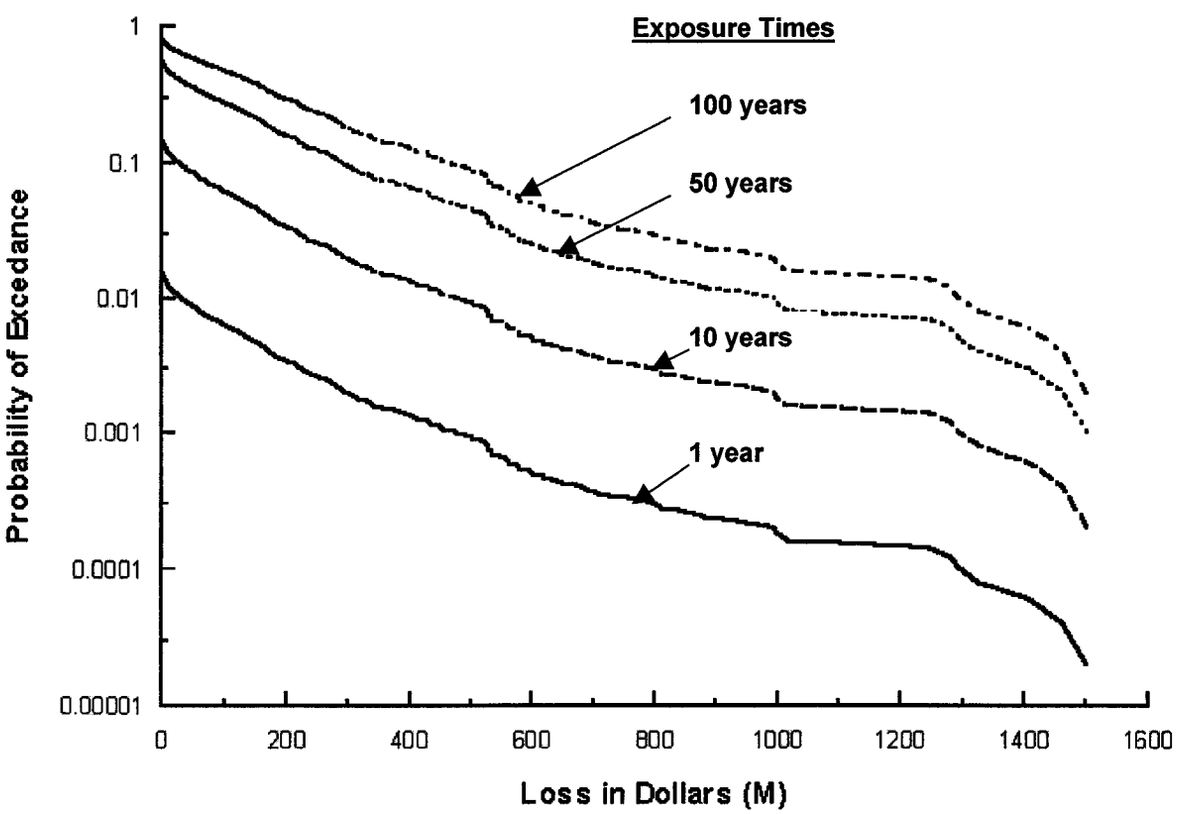

Figure 23. Economic Losses due to Earthquake-Induced Increases in Commute Time

7.5.2.2 Random-Walk Plots

Figure 24 shows random walk plots for several 1,000-year time segments selected from the 50,000 year walk-through. Each plot shows the distribution of cumulative economic loss over time, which can be important to decision-makers. The distributions are seen to vary substantially for the different 1,000-year segments.

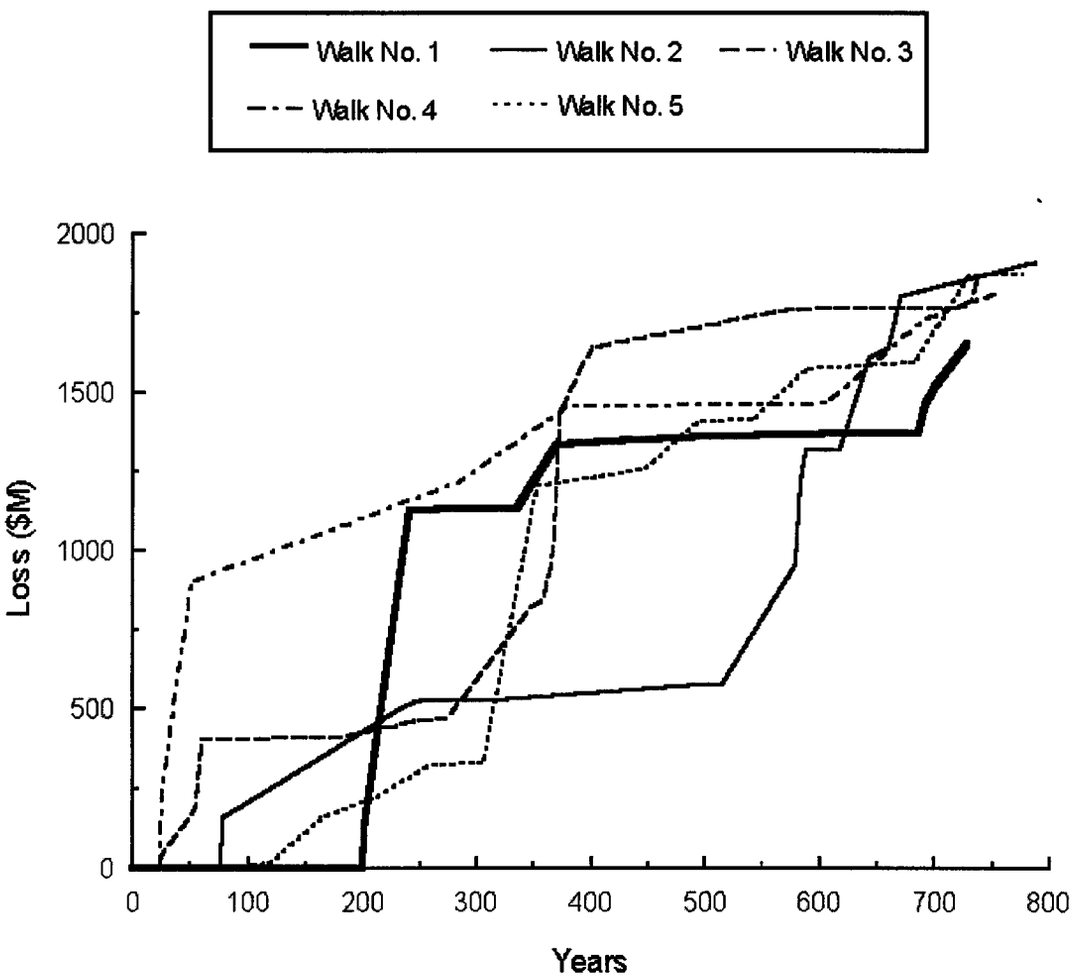

Figure 24. Random Walk Plots showing Variations of Cumulative Economic Losses Over Different 1000-Year Time Segments

The selection of the time segment for the random walk plots should reflect user needs. For example, federal or state transportation agencies planning the construction of a major bridge with an estimated design life of 100 years may wish to examine potential risks to the bridge over multiple 100-year time segments. Financial institutions holding or evaluating 30-year bonds for financing a highway construction project would be interested in examining potential losses over 30-year time segments. Loss statistics can be readily obtained from the multiple random walk data compiled for any selected time segments.

7.5.2.3 Losses from Individual Earthquakes

Table 16 shows economic losses for the single simulation considered for each of the four earthquakes whose locations are shown in figure 25. These losses will depend on the size and location of the earthquake, and also on the values of the uncertain parameters used to establish the seismic hazards and component vulnerabilities for the simulation. For this reason, probabilistic estimates of losses that account for these uncertainties (by considering multiple scenario earthquakes and simulations) are highly desirable to provide a proper perspective for interpreting loss estimation results and making rational seismic risk reduction decisions.

Table 16. Economic Losses due to Selected Scenario Earthquakes

Earthquake (See figure 25 for location)			Economic Loss per 24-Hour Day (Dollars x 10^6)			Total Economic Loss (Dollars x 10^6)
ID Number	Moment Magnitude	Distance from Government Center, km	7 Days after Earthquake	60 Days after Earthquake	150 Days after Earthquake	
11140	6.8	66 km NW	$31.44	$3.94	$1.16	$1,409.73
13773	5.8	77 km NE	$17.45	$2.98	$0.83	$849.33
30474	6.4	70 km NNE	$17.87	$3.17	$0.92	$883.39
41789	8.0	142 km NNE	$30.16	$5.87	$1.27	$1,503.03

7.5.3 ACCESS AND EGRESS TIMES TO KEY LOCATIONS

The SRA methodology can provide results describing how earthquake damage to the highway system affects access and egress times to and from key centers of government, commerce, transportation, medical care, and education, residential centers, etc. These results can include total loss distributions and tabulations of losses for individual earthquake events (where "loss" is now defined in as earthquake-induced increases in access and egress time for the key zones). Such results can be valuable to emergency response planners , and can also be considered when planning and prioritizing seismic risk reduction measures for a highway system.

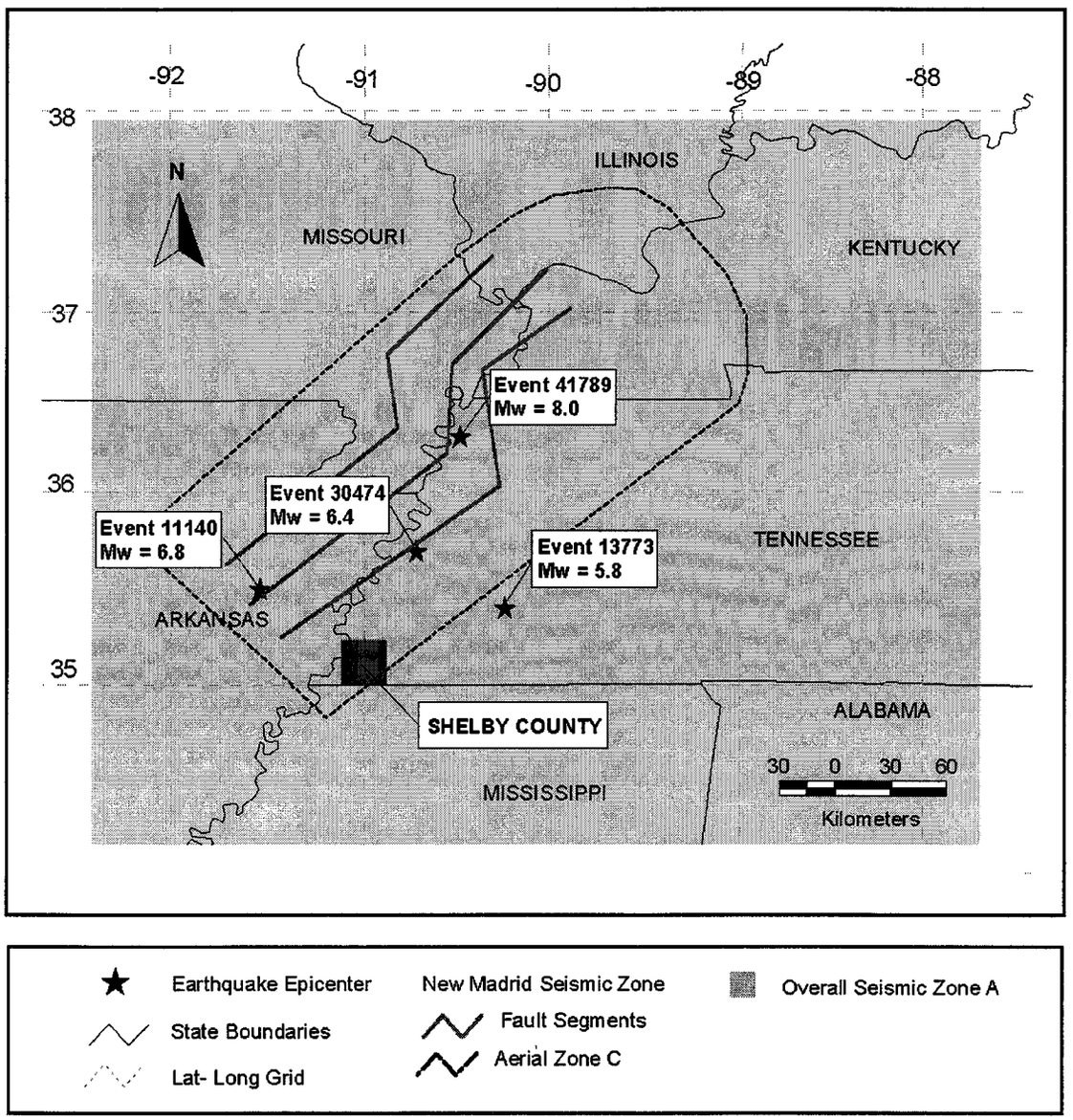

Figure 25. Scenario Earthquakes Considered in Tables 16 and 17

7.5.3.1 Loss Distributions

Figures 26 through 28 provide loss distributions for average access times to the following locations in Shelby County: (a) the Memphis Airport and Federal Express Center located south of the beltway; (b) the major hospital and medical center located just east of downtown Memphis; and (c) the Germantown residential center located east of the beltway. For each of these areas, the loss distributions are provided for post-earthquake times of 7 days and 60 days. Such distributions can also be provided for egress times from these locations.

These figures show how access to each of these areas is affected by earthquake damage to the highway system., including effects of uncertainties in the estimation of the earthquake, the

seismic hazards, and the component vulnerabilities. For example, figure 26a shows that, at 7 days after an earthquake, there is a 10-percent probability of exceedance that access to the Memphis Airport and Federal Express south of the beltway will increase by about 10 percent due to earthquake damage to the system. Figure 26b shows that these increased access and egress times will reduce rapidly at later times after an earthquake, but only if the repair times assumed in chapter 5 on the basis of readily available and sufficient repair resources can be realized.

Figures 26 to 28 also show how earthquake effects on access times can be affected by differences in location and trip demands to and from the various zones. For example, earthquake effects on access times are seen to be relatively low for the Germantown area (figures 28) as compared to the hospital and medical center (figure 27) and for the Memphis Airport and Federal Express area (figure 26).

7.5.3.2 Losses from Selected Earthquakes

Tables 17a through 17d provide information on access and egress time increases for each of the four earthquakes whose locations are shown in figure 25. These results are provided for the three locations listed in section 7.5.3.1 plus the following additional six locations: (d) the government center in downtown Memphis; (e) the University of Memphis in east-central Memphis; (f) President's Island, which is the location of the Port of Memphis along the Mississippi River; (g) Hickory Hill, a commercial area located southeast of the beltway; (h) Shelby Farms, a residential area located northeast of the beltway; and (i) Bartlett, a residential area located north of the beltway. These results show that access and egress to and from all of these zones are substantially affected by the location of the zone, the trip demands to and from the zone, and the location and size of the earthquake. The results, together with the loss distributions discussed in section 7.5.3.1, also show the wide variety of stakeholders in the performance of the Shelby County highway system during earthquakes.

7.5.4 NOMINAL CONFIDENCE LEVELS AND LIMITS

Appendix A describes a procedure that has been developed to estimate nominal confidence levels and limits for the mean value of the total losses, also called the average annualized loss (AAL). This procedure is based on the assumptions that: (a) the results from the walkthrough process considered in an SRA constitute multiple Bernoulli trials; and (b) the sampling distribution of the AAL is normally distributed in accordance with the central limit theorem. For this SRA of the Shelby County TN highway system, which is based on a walkthrough with a duration of 50,000 years and only one simulation per scenario earthquake, the procedure described in appendix A results in 95-percent confidence limits for the AAL that are $\$(2.17 \pm 0.274) \times 10^6$. This corresponds to a 95-percent confidence that the true value of the AAL will be within about ± 12.6 percent of the computed AAL of $2.17 million.

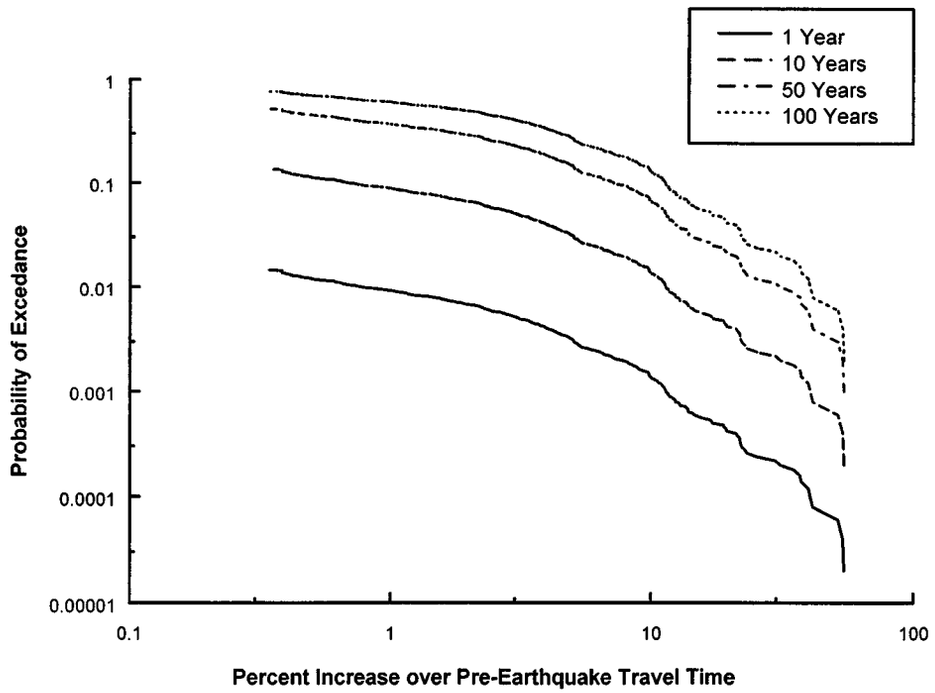

a) Time after EQ = 7 Days

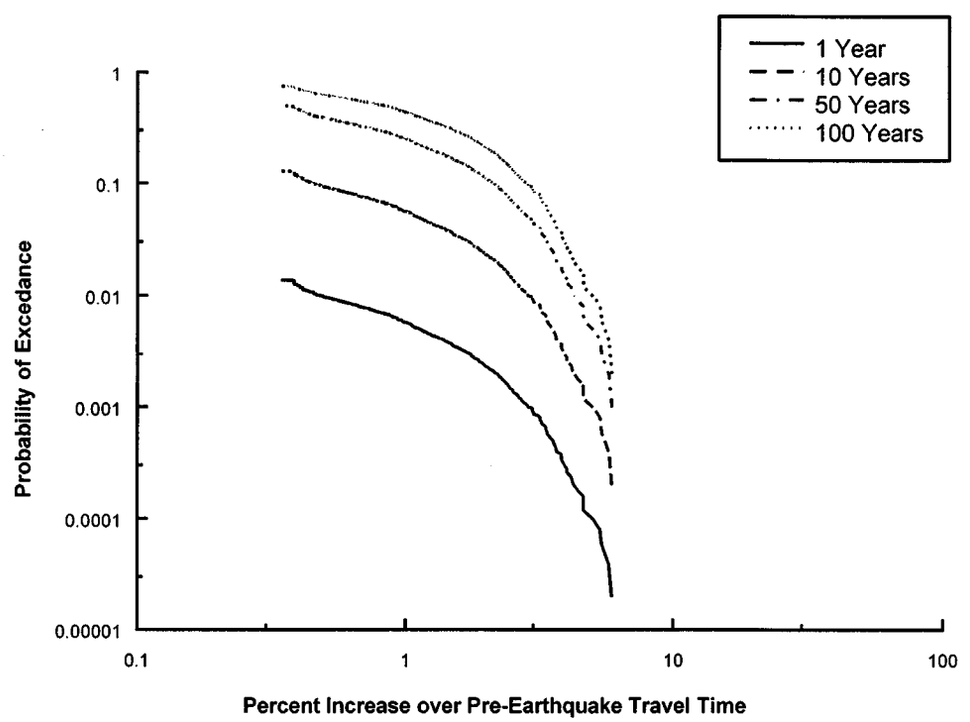

b) Time after EQ = 60 Days

Figure 26. Access Times to Memphis Airport and Federal Express

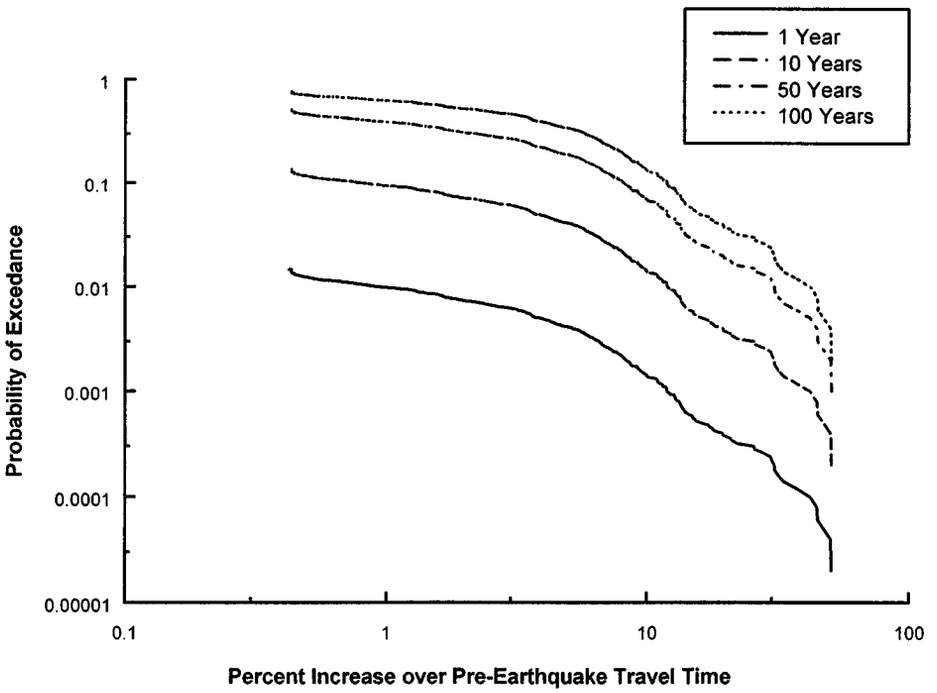

a) Time after EQ = 7 Days

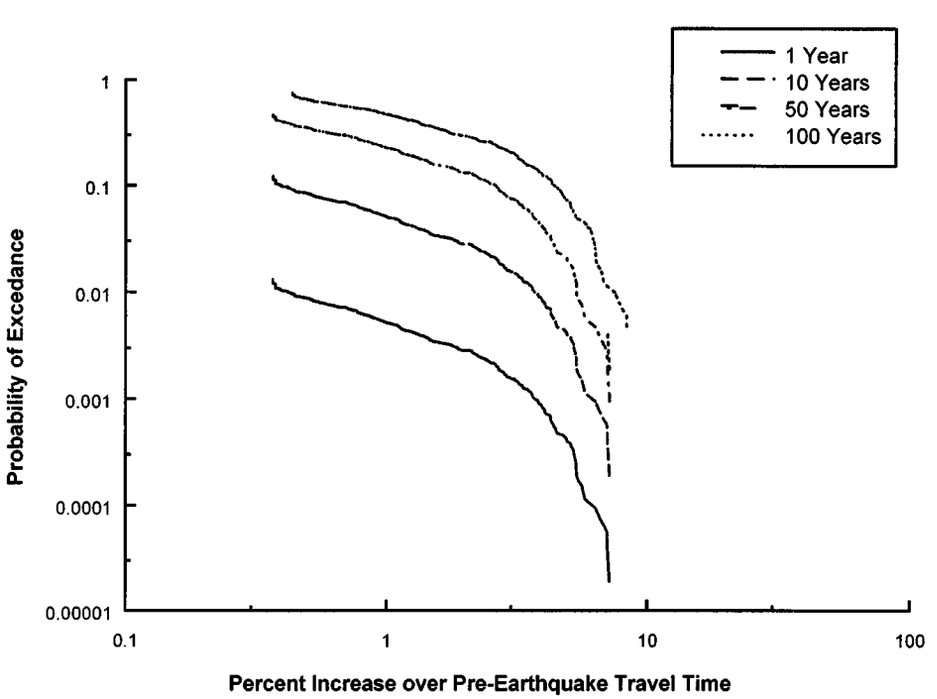

b) Time after EQ = 60 Days

Figure 27. Access Times to Memphis Medical Center

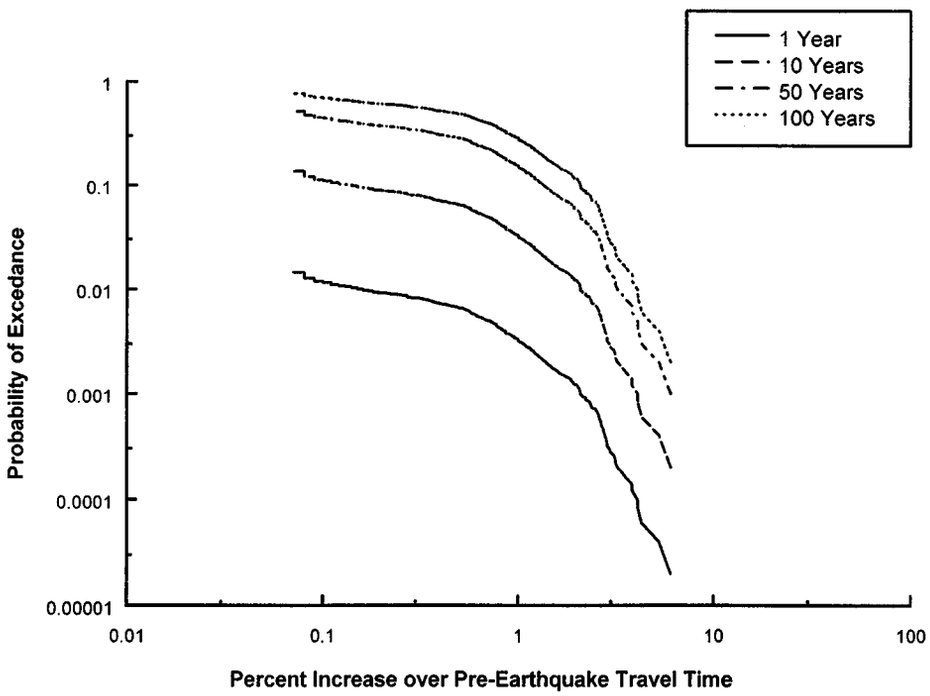

a) Time after EQ = 7 Days

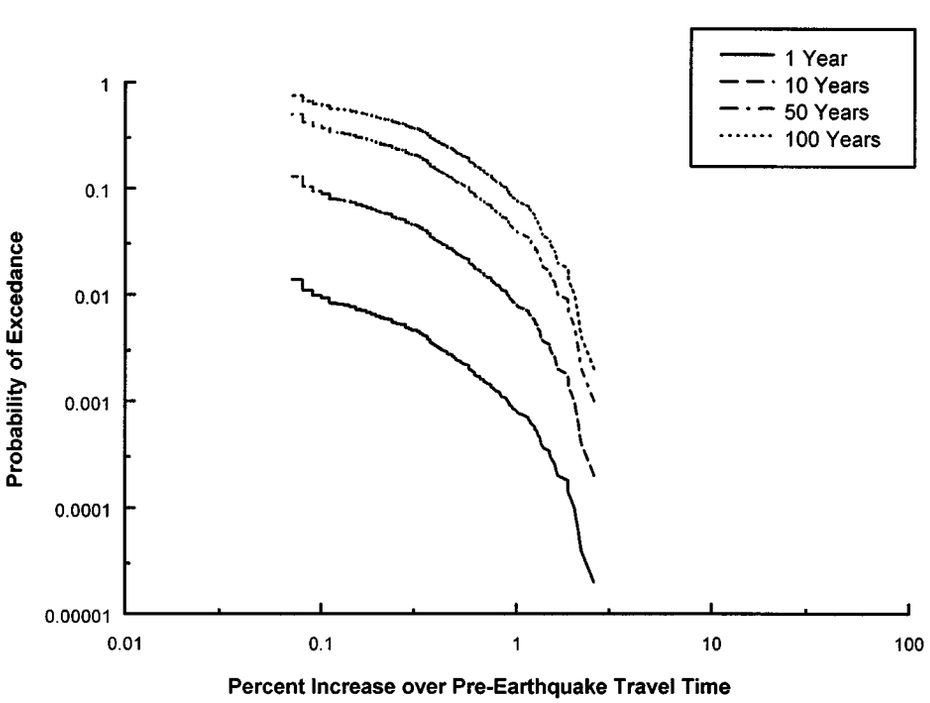

b) Time after EQ = 60 Days

Figure 28. Access Times to Germantown Residential Area

Table 17. Percent Increase in Access and Egress Times for Selected Locations in Shelby County, Tennessee due to Earthquake Damage to Highway System

a) Earthquake 11140, M_w = 6.8 centered 65.8 km NW of Government Center (Fig. 25)

Origin-Destination Zone	Post-Earthquake Access Time			Post-Earthquake Egress Time		
	7 Days after EQ	60 Days after EQ	150 Days after EQ	7 Days after EQ	60 Days after EQ	150 Days after EQ
9 (Government Center in downtown Memphis)	43.8%	5.8%	2.0%	57.4%	5.9%	2.3%
28 (Major Hospital Center, just east of downtown Memphis)	44.6%	6.7%	2.0%	58.9%	8.2%	2.3%
205 (Memphis Airport and Federal Express transportation center, south of beltway)	53.7%	4.0%	1.6%	53.4%	4.9%	1.6%
73 (University of Memphis campus in central Memphis)	21.6%	4.3%	1.5%	29.2%	4.7%	1.6%
310 (Germantown, residential area east of beltway)	2.9%	0.9%	0.4%	5.5%	1.0%	0.4%
160 (President's Island, Port of Memphis at Mississippi River)	34.9%	6.1%	1.6%	44.5%	7.5%	2.5%
246 (Hickory Hill, commercial area southeast of beltway)	3.9%	1.9%	1.1%	7.3%	2.2%	1.2%
335 (Shelby Farms residential area northeast of beltway)	28.4%	4.8%	1.6%	28.4%	5.0%	1.6%
412 (Bartlett, residential area north of beltway)	13.2%	3.0%	1.3%	16.9%	3.3%	1.6%

Table 17. Percent Increase in Access and Egress Times for Selected Locations in Shelby County, Tennessee due to Earthquake Damage to Highway System (continued)

b) Earthquake 13773, M_w = 5.8 centered 76.8 km NE of Government Center (Fig. 25)

Origin-Destination Zone	Post-Earthquake Access Time			Post-Earthquake Egress Time		
	7 Days after EQ	60 Days after EQ	150 Days after EQ	7 Days after EQ	60 Days after EQ	150 Days after EQ
9 (Government Center in downtown Memphis)	34.5%	5.2%	1.8%	33.4%	3.2%	1.5%
28 (Major Hospital Center, just east of downtown Memphis)	37.2%	6.7%	2.0%	37.4%	5.9%	2.0%
205 (Memphis Airport and Federal Express transportation center, south of beltway)	41.3%	3.2%	1.5%	41.2%	2.6%	1.2%
73 (University of Memphis campus in central Memphis)	14.1%	3.4%	1.1%	15.1%	2.8%	0.9%
310 (Germantown, residential area east of beltway)	2.4%	0.6%	0.3%	2.4%	0.7%	0.3%
160 (President's Island, Port of Memphis at Mississippi River)	30.1%	2.9%	1.2%	33.0%	3.1%	1.4%
246 (Hickory Hill, commercial area southeast of beltway)	3.4%	1.5%	0.9%	3.9%	1.5%	1.0%
335 (Shelby Farms residential area northeast of beltway)	11.5%	3.5%	1.1%	12.5%	6.2%	2.1%
412 (Bartlett, residential area north of beltway)	7.5%	3.4%	1.4%	7.8%	4.7%	1.7%

Table 17. Percent Increase in Access and Egress Times for Selected Locations in Shelby County, Tennessee due to Earthquake Damage to Highway System (continued)

c) Earthquake 30474 M_w = 6.4 centered 69.9 km NNE of Government Center (Fig. 25)

Origin-Destination Zone	Post-Earthquake Access Time			Post-Earthquake Egress Time		
	7 Days after EQ	60 Days after EQ	150 Days after EQ	7 Days after EQ	60 Days after EQ	150 Days after EQ
9 (Government Center in downtown Memphis)	27.7%	5.4%	1.9%	29.1%	3.7%	2.0%
28 (Major Hospital Center, just east of downtown Memphis)	30.6%	6.3%	2.0%	32.4%	5.7%	2.5%
205 (Memphis Airport and Federal Express transportation center, south of beltway)	36.9%	3.2%	1.5%	33.0%	4.3%	1.6%
73 (University of Memphis campus in central Memphis)	12.6%	4.2%	1.4%	14.3%	4.1%	1.4%
310 (Germantown, residential area east of beltway)	2.6%	1.0%	0.3%	2.6%	0.7%	0.3%
160 (President's Island, Port of Memphis at Mississippi River)	23.4%	4.1%	1.3%	24.0%	3.3%	1.6%
246 (Hickory Hill, commercial area southeast of beltway)	3.3%	1.4%	0.7%	3.5%	1.1%	0.7%
335 (Shelby Farms residential area northeast of beltway)	37.9%	5.9%	1.7%	33.4%	4.1%	1.2%
412 (Bartlett, residential area north of beltway)	8.6%	2.3%	1.0%	8.9%	2.9%	1.2%

Table 17. Percent Increase in Access and Egress Times for Selected Locations in Shelby County, Tennessee due to Earthquake Damage to Highway System (continued)

d) Earthquake 41789, M_w = 8.0 centered 141.8 km NNE of Government Center (Fig. 25)

Origin-Destination Zone	Post-Earthquake Access Time			Post-Earthquake Egress Time		
	7 Days after EQ	60 Days after EQ	150 Days after EQ	7 Days after EQ	60 Days after EQ	150 Days after EQ
9 (Government Center in downtown Memphis)	48.6%	8.4%	2.2%	43.5%	7.6%	2.0%
28 (Major Hospital Center, just east of downtown Memphis)	50.6%	8.5%	2.3%	47.9%	7.7%	2.3%
205 (Memphis Airport and Federal Express transportation center, south of beltway)	54.4%	5.4%	1.6%	50.9%	4.9%	1.5%
73 (University of Memphis campus in central Memphis)	25.3%	5.2%	1.6%	28.4%	5.0%	1.7%
310 (Germantown, residential area east of beltway)	5.2%	2.1%	0.5%	5.0%	2.0%	0.6%
160 (President's Island, Port of Memphis at Mississippi River)	37.1%	6.4%	1.6%	38.0%	7.7%	1.8%
246 (Hickory Hill, commercial area southeast of beltway)	7.0%	2.9%	1.2%	7.9%	3.1%	1.3%
335 (Shelby Farms residential area northeast of beltway)	35.9%	3.3%	1.0%	35.8%	4.8%	1.4%
412 (Bartlett, residential area north of beltway)	18.0%	5.3%	1.6%	19.0%	6.2%	2.0%

CHAPTER 8
CONCLUDING COMMENTS

This report has described and illustrated a new methodology for SRA of highway systems that has been developed under this research project. This concluding chapter of this report summarizes the advances in SRA technology that have been made under this project, and outlines recommended directions for further development and programming of the SRA methodology.

8.1 NEW ADVANCES

8.1.1 OVERVIEW

This SRA methodology integrates data and models for geosciences (seismology and geology), structural and geotechnical engineering, transportation engineering and planning, and economics in order to

- Evaluate the ability of the highway-roadway system to accommodate traffic demands at various times after an earthquake.

- Estimate economic losses due to earthquake-induced damage and disruption of the system.

- Develop information that can be used by engineers, administrators, and planners for making decisions pertaining to priorities, levels, and types of seismic risk reduction measures that would most effectively serve the needs of the public and other stakeholders in the seismic performance of the highway-roadway system.

8.1.2 DECISION GUIDANCE TOOL

As noted in chapter 2, decisions that can be guided by SRA results include:

- Prioritization of existing bridges and other components for seismic retrofit.

- Establishment of appropriate levels of seismic design for new and existing bridges and other components.

- Development of post-earthquake response plans, including assessment of post-earthquake traffic management options and establishment of appropriate levels of post-earthquake repair resources.

- Assessment of how various system-enhancement options (e.g., construction of new roadways) would affect the seismic performance of the overall highway system.

8.1.3 FEATURES

The SRA methodology is now being programmed into a software package named REDARS (Risks from Earthquake DAmage to Roadway Systems). When development of this software is completed, it will be publicly disseminated for use by transportation and engineering personnel to assess seismic risks to highway systems nationwide and to facilitate decision making. An initial (beta) version of this software (REDARS 1.0) is now being developed (Walton et al., 2000). This modular software now includes the following technical features that are described in this report:

- *Deterministic or Probabilistic Analysis.* There is an option to carry out either a probabilistic SRA considering multiple scenario earthquakes and simulations, or a deterministic SRA for a limited number of user-selected earthquake events.

- *Earthquake Modeling.* Multiple scenario earthquakes developed from regional seismologic and geologic data can be incorporated.

- *Hazards Module.* Ground motion attenuation and soil amplification models appropriate to the region where the highway system is located can be readily incorporated. A state-of-the-practice model for estimation of liquefaction hazards is also included.

- *Component Module.* Simplified but rational procedures based on principles of mechanics are incorporated for evaluating the vulnerability of conventional bridges subjected to ground shaking hazards. For a unique or special purpose bridge subjected to ground shaking, there is an option to provide a user-specified vulnerability model for that bridge. A first-order model to estimate the vulnerability of bridges subjected to liquefaction hazards is also included. In addition, the software features a methodology to estimate earthquake-induced settlement of bridge approach fills.

- *System Module.* Efficient state-of-the-art methods are used to carry out transportation network analysis in order to estimate post-earthquake traffic flows. For the probabilistic SRA option, an Associative Memory approach is used for rapid analysis of large numbers of system states from multiple scenario earthquakes and simulations. If the deterministic SRA option is selected, the User Equilibrium approach is used for analysis of limited numbers of system states from user-selected earthquake events.

- *Economic Losses.* A simplified model for estimation of economic losses due to increases in user commute times is included at this time.

8.2 FUTURE RESEARCH DIRECTIONS

The long-range goal of this research is to develop a technically sound, user friendly, and efficient methodology that can be readily applied to SRA of highway-roadway systems nationwide. This section provides recommendations for building on the procedures and modules described in this report in order to achieve this goal.

8.2.1 ECONOMIC MODULE

The SRA methodology should be extended to address how damage to the highway-roadway system will affect the productivity of economic sectors in the region. The current SRA methodology -- with its incorporation of walk-through procedures and its linked models for estimating seismic hazards, component vulnerabilities, network flows, and aggregate economic losses -- provides an excellent framework for addressing this problem. However, further development is needed. As noted in chapter 6, damage to buildings and contents will reduce the demand for transportation services. Damage to the highway-roadway network will reduce transportation supply. How the regional economy responds to these changes requires a detailed model that is disaggregate in terms of both economic sectors and geographic space. Developing and packaging such a model is challenging. A sophisticated user interface is needed to link user needs with a set of interacting models and a substantial, site-specific data bank. Such models should also include assessment of economic losers and gainers due to earthquake damage to the system and due to policies implemented to mitigate this damage.

8.2.2 INPUT DATABASE

As described in chapters 3 through 7, significant input data are needed to implement this SRA methodology. Although some of these data are available through computerized databases at transportation department and metropolitan planning agency offices, much are not. Efforts to develop these data may be formidable. Therefore, a coordinated effort involving national and state transportation agencies should be initiated to expand existing transportation databases to include data needed for SRA of highway systems. Where appropriate, this should be coordinated through the PONTIS and/or BRIDGIT bridge management systems.

8.2.3 SCENARIO EARTHQUAKE MODELING

The SRA methodology should include models for estimating scenario earthquakes nationwide. The current methodology incorporates earthquake models for the Central United States that are based on models developed under the USGS National Hazards Mapping Program. Such models should be adapted to other regions of the country as well.

8.2.4 HAZARDS MODULE

Further development of the hazards module should include: (a) adaptation of ground motion models that are applicable nationwide; (b) investigation of a probabilistic basis for estimating the significant input data needed to estimate liquefaction-induced lateral spread displacements using the procedure described in appendix E; and (c) adaptation of models for estimating landslide and surface fault rupture hazards. The modular structure of the SRA methodology facilitates the inclusion of new and enhanced hazards models, as they are developed in the future.

8.2.5 COMPONENT MODULE

The Component Module now includes rational analytical methods to develop fragility curves for bridges subjected to ground shaking hazards, as well as initial models for approach-fill settlement and roadway pavements (see chapter 5 of this volume). Continued development of these models should focus on: (a) an improved basis for estimation of repair costs and downtimes of bridges, as a function of the bridge's damage state; (b) estimation of damage states, repair costs, and downtimes for other highway components (e.g., retaining structures, slopes, tunnels, culverts, and pavements); and (c) an improved basis for estimating damage states, repair costs, and downtimes for bridges and other highway components subjected to permanent ground displacement.

8.2.6 SYSTEM MODULE

In addition to estimation of post-earthquake travel demands as discussed in section 8.2.1, other modeling issues associated with the transportation network analysis element of the SRA methodology require further development. For example, research is needed to develop simplified network modeling procedures that retain acceptable accuracy in the results, methods for modeling of a highway subsystem extracted from a larger system, and procedures for addressing detour routes when non-redundant links are closed due to earthquake damage. In addition, the objective function for the Associative Memory (AM) transportation network analysis procedure is based on total system travel time, as computed from individual link travel times computed using User Equilibrium methods. This assumes that all trips in the system by all users have equal importance. It would be desirable to modify this approach to also consider the possibility of a higher importance of certain post-earthquake trips, such as trips that are essential for life safety (e.g., to and from medical centers) and for emergency response and recovery (e.g., the delivery of supplies and equipment that were transported to the damaged region via air).

8.2.7 SIMULATIONS

Research should be directed toward further development of the procedures described in section A.5 of appendix A for estimating nominal confidence levels and limits pertaining to calculative precision of the number of simulations relative to SRA input data and models.

8.2.8 RISK REDUCTION MODULE

An explicit module that addresses costs, times, traffic impacts, etc. associated with alternative seismic risk reduction decisions for the highway system should be developed and incorporated into the SRA methodology. The purpose of this module would be to guide decision-makers as they consider the implementation of alternative seismic risk reduction strategies.

8.3 SOFTWARE DEVELOPMENTAND LICENSING ISSUES

To facilitate the continued development of the programming of the SRA methodology into the REDARS software, the following development and licensing issues should be addressed.

8.3.1 DEVELOPMENT

The current beta version of REDARS has been developed as a one-tier Windows-based application in which the program, program processes, program code, and data all reside locally on the user's personal computer (PC). This has facilitated the programming and testing of the REDARS software and its SRA models and algorithms. However, as the software expands and the user base grows and diversifies, it would be wise to consider the migration of the REDARS software to run as a true three-tier, client/server application. A three-tier application is one in which the application and database are located on a server, and all processing of the programming takes place on the server. The user would then have a client window on their PC on which they would enter input information and view results; however, the PC is only a viewing tool. Benefits to implementing REDARS as a three-tier application are as follows:

- *Computations.* The intensive computation required during the SRA application could be totally handled on the server side of the system. This allows the proper scaling of the server to minimize user wait times while running simulations.

- *Maintenance.* The software could be maintained on the server, ensuring that all the users would be applying the same software version. This would ensure that all problems reported by users can be quickly and efficiently addressed without users having to wait for a new release of the software.

- *Database.* The default database could be maintained on the server, ensuring that the data are valid and current at all times for all users. In addition, a Database Administrator could ensure the integrity of the data base at all times, and could grant database privileges to individual users or user groups based on their individual needs.

- *Programming.* By programming in a cross-platform language (such as Java), the program could be useful to a much larger group of users. Furthermore, it is easier to maintain complex multiple-program links on a server than on a PC.

- *Costs.* By creating the next version of REDARS in this fashion, the cost of the software could be significantly reduced without sacrificing functionality. In the current one-tier architecture, the licensing costs for the use of REDARS would probably run close to $5,000 per seat. The licensing cost for the same use in a three-tier architecture could possibly be as low as $30,000 for an unlimited number of users.

8.3.2 LICENSING

REDARS includes GIS elements and plotting functions that are currently addressed through links to the ArcView 3.0 GIS software and the KYPLOT plotting software respectively (although these may be changed in the future). This decision to use off-the-shelf (OTS) software for GIS and plotting functions has allowed the SRA team to generate the necessary results and output while minimizing programming costs. However, if this same approach is adapted for releases of future versions of REDARS, licensing costs for use of this and other OTS software will need to be considered as a possible additional cost of distribution of REDARS to its end users.

CHAPTER 9
REFERENCES

Abrahamson, N.A. and Silva, W.J., "Empirical Response Spectral Acceleration Relations for Shallow Crustal Earthquakes", *Seismological Research Letters*, Volume 68, Number 1, January/February 1997, pp 94-127.

American Association of State Highway and Transportation Officials (AASHTO), *Standard Specifications for Highway Bridges*, Washington D.C., 1998.

Ayyub, B.M. and McCuen, R.H. (1997). *Probability, Statistics, and Reliability for Engineers*, CRC Press, Boca Raton FL.

Bartlett, S. F. and Youd, T. L., *Empirical Analysis of Horizontal Ground Displacement Generated by Liquefaction-Induced Lateral Spreads*, Report NCEER-92-0021 prepared for National Center for Earthquake Engineering, Buffalo NY, 1992.

Bartlett, S. F. and Youd, T. L., "Empirical Prediction of Liquefaction-Induced Lateral Spread", *Journal of the Geotechnical Engineering Division, American Society of Civil Engineers*, Volume 124, Number 4, April 1995, pp 316-329.

Benjamin, J.R. and Cornell, C.A., *Probability, Statistics, and Decision for Civil Engineers*, McGraw Hill Book Company, New York NY., 1970, 684 pp.

Boore, D.M., Joyner, W.B., and Fumal, T.E, "Equations for Estimating Horizontal Response Spectraand Peak Acceleration from Western North America Earthquakes: A Summary of Recent Work", *Seismological Research Letters*, Volume 68, Number 1, January/February 1997, pp 128-153.

Boyce, D. E., Janson, B.N., and Eash, R.W., "The Effect on Equilibrium Trip Assignment of Different Link Congestion Functions," *Transportation Research A.*, Volume 15A, Number 3, 1981, pp. 223-232.

California Department of Transportation (Caltrans), "Appendix B, Northridge Earthquake Traffic Recovery Study, Procedure for Simulating Areawide Delay/ Economic Cost of Delay", *Interstate 10 Recovery Report, Northridge Earthquake Recovery*, Caltrans District 7, Office of Operations, Los Angeles CA, September 15, 1994.

California Department of Transportation (Caltrans), *Northridge Earthquake Recovery, Final Comprehensive Transportation Analysis,* Caltrans District 7, Office of Operations, Los Angeles CA, August 1995.

Campbell, K.W., "Strong Ground Motion Attenuation Relations: A Ten-Year Perspective", *Earthquake Spectra*, Volume 1, Number 4, pp 759-804, 1985.

Comsis Corporation, *MINUTP Technical Users Manual*, Silver Springs MD, July 1994.

Crone, A.J., "Defining the Southwestern End of the Blytheville Arch, Northeastern Arkansas: Delimiting a Seismic Source Zone in the New Madrid Region", *Eastern Section Seismological Research Letters*, Volume 69, Number 4, July/August 1998, pp 350-358.

Daykin, C.D., Pentikainen, T., and Pesonon, M., *Practical Risk Theory for Actuaries*, Chapman & Hall, London, England, 1994.

Der Kiureghian, A. and A. H-S. Ang, 1977, "A Fault Rupture Model for Seismic Risk Analysis," *Bulletin of the Seismological Society of America*, Volume 64, Number 4, August 1977, pp 1173-1194.

Dickenson, S.E., "Seismic and Geologic Hazards", *Seismic Guidelines for Ports* (edited by S.D. Werner), Technical Council on Lifeline Earthquake Engineering Monograph No. 12, American Society of Civil Engineers, Reston VA, pp 4-1 to 4-65, March 1998.

Dobry, R., Borcherdt, R.D., Crouse, C.B., Idriss, I.M., Joyner, W.B., Martin, G.W., Power, M.S., Rinne, E.E., and Seed, R.B., "New Site Coefficients and Site Classification System used in Recent Building Seismic Code Provisions", *Earthquake Spectra*, Volume 16, Number 1, pp 41-68, February 2000.

Dutta, A. and Mander, J.B., "Seismic Fragility Analysis of Highway Bridges", *Proceedings of the INCEDE-MCEER Center-to-Center Project Workshop on Earthquake Engineering Frontiers in Transportation Systems*, Tokyo Japan, June 22-23 1998.

Eash, R. W., Janson, B.N., and Boyce, D.E.,"Equilibrium Trip Assignment: Advantages and Implications for Practice," *Transportation Research Record*, Number 728, 1971, pp. 1-8.

Efron, B. and Tibshirani, R.J., *An Introduction to the Bootstrap*, Chapman & Hall, New York NY, 1993.

Federal Highway Administration, *Seismic Retrofitting Manual for Highway Bridges*, Report No. FHWA-RD-94-052 (Edited by I.G. Buckle and I.M. Friedland), Office of Engineering and Highway Operations, Research and Development, McLean VA, May 1995a.

Federal Highway Administration., *Recording and Coding Guide for the Structure Inventory and Appraisal of the Nation's Bridges*, Report FHWA-PD-96-001, Office of Engineering, Bridge Division, Bridge Management Branch, Washington D.C., December 1995b.

Ferritto, J., Dickenson, S., Priestley, N., Werner, S., and Taylor, C., *Seismic Criteria for Marine Oil Terminals, Volume 1*, Technical Report TR-2103-SHR, Naval Facilities Engineering Service Center, Port Hueneme CA, July 1999.

Frankel, A., Mueller, C., Barnhard, T., Perkins, D., Leyendecker, E.V., Dickman, N, Hanson, S., and Hopper, M., *National Seismic Hazard Maps, Documentation June 1996*, Denver: United States Geological Survey, Open-File Report 96-532, June 1996.

Gilbert, A., "Developments in Seismic Prioritization of Bridges in California," *Proceedings of Ninth Annual US/Japan Workshop on Earthquake and Wind Design of Bridges, Tsukuba Science City, Japan*, May 1993.

Giuliano, G., Golob, J., Bahl, D., Lee, W., and Liao, Y.C., *Impacts of the Northridge Earthquake on Transit and Highway Use*, Research Report No. LCRI-96-03R, Lusk Center Research Institute, University of Southern California, Los Angeles CA, March 1996.

Gordon, P., Richardson, H.W., and Davis, B., *Transport-Related Business Interruption Impacts of the Northridge Earthquake*, Lusk Center Research Institute, University of Southern California, Los Angeles CA, March 1996.

Greenshields, B., *Proceedings of the Highway Research Board, Washington D.C.*, 1935.

Hobeika, A.G., Manchikalapudi, L.N., and Kim, S. *Transportation Problems Faced after Big Earthquakes: A Case Study of the Loma Prieta Earthquake*, Prepared by Center for Transportation Research, Virginia Polytechnic Institute and State University, Blacksburg VA for National Science Foundation, Washington D.C., May 15, 1991.

Hogg, R.V. and Klugman, S.A., *Loss Distributions*, New York: John Wiley & Sons, New York NY, 1984.

Housner, G.W. and Jennings, P.C., *Earthquake Design Criteria*, Earthquake Engineering Research Institute, Berkeley CA, September 1982.

Hwang, H.H.M and Huo, J.-R., "Attenuation Relations of Ground Motion for Rock and Soil Sites in Eastern United States", *Soil Dynamics and Earthquake Engineering*, Volume 16, pp 363-372, 1997.

Hwang, H.H.M., Lin, H., and Huo, J.-R., "Site Coefficients for Design of Buildings in Eastern United States, *Soil Dynamics and Earthquake Engineering*, Volume 16, pp 29-40, 1997.

Imbsen & Associates, Inc. (IAI), *Final Retrofit Strategy Report, Seismic Vulnerability Project, I-40 Mississippi River Bridge Tennessee/Arkansas*, Report prepared for Tennessee Department of Transportation, Nashville TN by IAI in collaboration with Howard Needles Tammen & Bergendoff, Kansas City MO and Woodward Clyde Consultants, Oakland CA, April 2 1993.

Jernigan, J.B. and Hwang, H.H.M., *Inventory and Fragility Analysis of Memphis Bridges*, Center for Earthquake Research and Information, University of Memphis, Memphis TN, Sept. 15 1997.

Jernigan, J.B., *Evaluation of Seismic Damage to Bridges and Highway Systems in Shelby County, Tennessee*, Ph.D. Thesis, University of Memphis, Memphis TN, December 1998.

Jernigan, J.B., Werner, S.D., and Hwang, H.H.M., *Inventory of Bridges using GIS for Seismic Risk Assessment of Highway Systems*, Center for Engineering Research and Information, University of Memphis, Memphis TN, March 1996.

Johnston, A.C. and Schweig, E.S., "The Enigma of the New Madrid Earthquakes of 1811-1812", *Annual Review Earth Planetary Science*, Vol. 24, 1996, pp 339-384.

Johnston, A.C., "Seismic Moment Assessment of Earthquakes in Stable Continental Regions – III. New Madrid 1811-1812, Charleston 1886, and Lisbon 1755", *Geophys. J. Int.*, Vol. 126, 1996, pp 314-344.

Kalaba, R., and Tesfatsion, L., "Obtaining Initial Parameter Estimates for Nonlinear Systems Using Multicriteria Associative Memories", *Computer Science in Economics and Management*, Volume 4, 1991, pp. 237-259.

Kalaba, R., and Udwadia, F., "An Adaptive Learning Approach to the Identification of Structural and Mechanical Systems", *Computers and Mathematics with Applications*, Volume 22, 1991, pp. 67-75.

Kalaba, R., Kim, M., and Moore II, J. (1991). "Linear Programming and Associative Memories", *Applied Mathematics and Computation*, Volume 40, 1991, pp. 203-214.

Kalaba, R., Kim, M., and Moore II, J., "Linear Programming and Recurrent Associative Memories", *International Journal of General Systems,* Volume 20, 1992, pp.177-194.

Kalaba, R., Lichtenstein, Z., Simchnoy, T., and Tesfatsion, L.,"Linear and Nonlinear Associative Memories for Parameter Estimation", *Information Sciences*, Volume 61, 1990, pp. 177-194.

Kalaba, R., Moore II, J., Xu, R., and Chen, G., "Nonlinear Estimation with Associative Memories and Machine Evaluation of Derivatives: An Application to Calibrating Spatial Interaction Models", *Environment and Planning A,* Volume 31, 1999, pp. 441-457.

Keefer, D.K., "Landslides caused by Earthquakes", *Bulletin of the Geologic Society of America*, Volume 95, Number 2, pp 406-421, February 1984.

Kennedy/Jenks Consultants, Dames & Moore, and William Lettice & Associates, *Integrated Water System Reliability Study*, Report prepared for Marin County bMunicipal Water District, Corte Madera CA, September 1995.

Kim, G., Cho, S., and Moore, J.E. II, *A Manual for Rapid Estimation of Traffic Flows in Seismic Risk Analysis of Highway Systems*, Report VKC-351, MC-0042, School of Urban Planning and Development, University of Southern California, Los Angeles CA, Prepared for National Center for Earthquake Engineering Research, Buffalo NY under Task 106-E-7.3.1, February 1997.

Kohonen, T., *Self-Organization and Associative Memory*, Third edition, New York NY: Springer-Verlag, 1989.

Kramer, S.L., *Geotechnical Earthquake Engineering*, Prentice-Hall, Inc., 653 pp., 1996.

Law, A.M. and Kelton, W.D., *Simulation Modeling and Analysis*, New York: McGraw-Hill, Inc., New York NY, 1991.

Liu, W.D., Imbsen, R.A., LeBeau, R.J., Nobari, F.S., and Mejia, L.H., "Seismic Evaluation of Tied-Arch Bridges across the Mississippi River on I-40", *Proceedings of ASCE Structures Congress XII at Atlanta GA, Volume 1*, (Baker, N.C. and Goodno, B.J., editors), American Society of Civil Engineers, New York NY, April 24-28 1994, pp 355-360.

Mander, J.B. and Basoz, N., "Seismic Fragility Theory for Highway Bridges", *Optimizing Post-Earthquake Lifeline System Reliability, Proceedings of the Fifth U.S. Conference on Lifeline Earthquake Engineering, Seattle WA*, Technical Council on Lifeline Earthquake Engineering Monograph No. 6 (Edited by W. M. Elliot and P. McDonough), American Society of Civil Engineers, Reston VA, pp 31-40, August 1999.

Mirza, S.A. and McGregor, J.G., "Variability of Mechanical Properties of Reinforcing Bars", *Journal of Structural Division, American Society of Civil Engineering*, Volume 105, Number ST5, May 1979, pp 921-937.

Mirza, S.A., Hatzinikolas, M., and MacGregor, J.G., "Statistical Description of Strength of Concrete", *Journal of Structural Division, American Society of Civil Engineering*, Volume 105, Number ST6, June 1979, pp 1021-1036.

Moore II, J., Kim, M., Seo, J., and Kalaba, R., "Obtaining Initial Parameter Estimates for Nonlinear Systems: Comparing Associative Memory and Neural Network Approaches", *Mathematical Modeling and Scientific Computing*, Volume 1, 1994a, pp. 89-115.

Moore II, J., Kalaba, R., Kim, M., Seo, J. and Kim, G., "Time Series and Turning Point Forecasts: A Comparison of Feedforward Neural Networks, Associative Memories, and Bayesian Econometric Techniques", *Mathematical Modeling and Scientific Computing,* Volume 2, 1994b.

Moore II, J., Kim, M., Seo, J., Wu, Y., and Kalaba, R., "Linear Programming, Recurrent Associative Memories, and Feed-Forward Neural Networks", *Computers and Mathematics with Applications*, Volume 22, 1991, pp. 71-90 .

Moore, J.E. II, Chang, S., Gordon, P., Richardson, H.W., and Shinozuka, M., "Integrating Transportation Network and Regional Economic Models to Estimate the Costs of a Large Earthquake", *Proceedings of National Meeting of Transportation Network Equilibrium Institute for Operations Research and Management Science, Cincinnati OH*, Transportation Science Section /1F, May 2-5, 1999a.

Moore, J.E. II, Chang, S., Gordon, P., Richardson, H.W., Shinozuka, M., Cho, S., Cho, S., and Dong, X., "Integrating Transportation and Economic Models", *Optimizing Post-Earthquake Lifeline System Reliability, Proceedings of the Fifth U.S. Conference on Lifeline Earthquake Engineering, Seattle WA*, Technical Council on Lifeline Earthquake Engineering Monograph No. 6 (Edited by W. M. Elliot and P. McDonough), American Society of Civil Engineers, Reston VA, pp 621-633, August 1999b.

Moore, J.E. II, Kim, G., Xu, R., Cho, S., Hu, H-H, and Xu, R., *Evaluating System ATMIS Technologies via Rapid Estimation of Network Flows: Final Report*, California PATH Report UCB-ITS-PRR-97-54, December 1997.

National Institute for Building Sciences (NIBS) (1997)., *HAZUS Earthquake Loss Estimation Methodology, Technical Manual, Volumes 1 and 2*, Washington D.C., 1997.

Ng, K.W., Chang, T.S., and Hwang, H.H.M., *Subsurface Conditions of Memphis and Shelby County*, Technical Report NCEER-89-0021, National Center for Earthquake Engineering Research, Buffalo NY, July 26, 1989.

Oppenheim, I.J. and Anderson, R. "Economic Effects of Transportation System Damage", *Earthquakes and Earthquake Engineering: The Eastern United States*, Ann Arbor Science, Ann Arbor MI, pp 563-576, 1981.

Oppenheim, I.J. and Hendrickson, C. "Seismic Risk to Transportation Systems", *Abatement of Seismic Hazards to Lifelines: Proceedings of a Workshop on Development of an Action Plan, Volume 2, Papers on Transportation Lifelines and Special Workshop Presentations*, Report No. FEMA 136, Federal Emergency Management Agency, Washington D.C., pp 83-92, July 1987.

Power, M.S., Taylor, C.L., and Perman, R.C., "Evaluation of Regional Landsliding Hazard Potential for a Utility District -- Eastern San Francisco Bay Area", *Proceedings of the Fifth U.S. National Conference on Earthquake Engineering Chicago IL*, Earthquake Engineering Research Institute, Volume 4, pp 839-848, July 10-14, 1994.

Priestley, M.J.N., Seible, F., and Calvi, G.M., *Seismic Design and Retrofit of Bridges*, John Wiley & Sons, New York NY, 1996, 686 pp.

Seeber, L. and Armbruster, J.G., *The NCEER-91 Earthquake Catalogue: Improved Intensity Based Magnitudes and Recurrence Relations for U.S. Earthquakes East of New Madrid*, Technical Report NCEER-91-0021, National Center for Earthquake Engineering Research, Buffalo NY, August 28, 1991.

Seed, H. B. and Idriss, I. M., *Ground Motions and Soil Liquefaction during Earthquakes*, Earthquake Engineering Research Institute, Berkeley CA., 1982.

Sheffi, Y., *Urban Transportation Networks: Equilibrium Analysis with Mathematical Programming Methods*, Prentice Hall, Englewood Cliffs NJ., 1985.

Small, E.P., "Alternatives for the Integration of Seismic Vulnerability Assessment within the Pontis Bridge Management System", *Proceedings of the National Seismic Conference on Bridges and Highways, Sacramento CA*, Federal Highway Administration and California Department of Transportation, pp 53-64, July 8-11 1997.

Small, E.P., "Examination of Alternative Strategies for Integration of Seismic Risk in Bridge Management Systems", *Proceedings of the International Bridge Management Conference*, Transportation Research Board, Washington D.C., April 1999.

Sommerville, P.G., Smith, N.F., Graves, R.V., and Abrahamson, N.A., "Modification of Empirical Strong Ground Motion Attenuation Relations to Include the Amplitude and Duration Effects of Rupture Directivity", *Seismological Research Letters*, Volume 68, Number 1, January/February 1997, pp 199-222.

Taylor, C. E. and Werner, S.D., "Proposed Acceptable Risk Procedures for the Port of Los Angeles 2020 Expansion Program," *Proceedings of the Fourth U. S. National Conference on Lifeline Earthquake Engineering, San Francisco CA,* Technical Council on Lifeline Earthquake Engineering Monograph 6 (Edited by M. O'Rourke), American Society of Civil Engineers, New York NY: pp 64-71, August 1995.

Taylor, C. E., Legg, M. R., Haber, J. M., and Wiggins, J.H., "New Lifeline Multiscenario Seismic Risk Techniques with a Model Application," *Civil Engineering Systems: Decision Making and Problem Solving*, Volume 2, June 1985, pp 77-83.

Taylor, C.E. (editor), *Seismic Loss Estimates for a Hypothetical Water System*, Technical Council on Lifeline Earthquake Engineering Monograph No. 2, American Society of Civil Engineers, New York NY, August 1991.

Taylor, C.E., Eguchi, R.T, and Chang, S., "Updating Real-Time Earthquake Loss Estimates: Methods, Problems, and Insights," *Proceedings of the Sixth U. S. National Conference on Earthquake Engineering, Seattle, WA,* Earthquake Engineering Research Institute, Oakland CA, May 31–June 4, 1998, 484pdf CD ROM.

Tokimatsu, K. and Seed, H B, "Evaluation of Settlements in Sands due to Earthquake Shaking", *Journal of the Geotechnical Engineering Division, American Society of Civil Engineers*, Volune 113, Number 8, pp 861-878, August 1987.

Transportation Research Board (TRB), *Proceedings of TRB Workshop on New Approaches to Liquefaction Analysis, Washington D.C.*, January 10, 1999.

Transportation Research Board (TRB). *Highway Capacity Manual*, Washington D.C., 1995.

Van Vliet, D., "The Frank-Wolfe Algorithm for Equilibrium Traffic Assignment Viewed as a Variational Inequality," *Transportation Research B*, Volume 21, Number 1, 1987, pp. 87-89.

Wakabayashi, H. and Kameda, H., "Network Performance of Highway Systems under Earthquake Effects: A Case Study of the 1989 Loma Prieta Earthquake", *Proceedings of U.S.-Japan Workshop on Earthquake Disaster Prevention for Lifeline Systems*, Public Works Research Institute, Tsukuba Science City, Japan, pp 215-232, October 26-27, 1993.

Wakabayashi, H., "Highway Network Reliability Assessment and Importance Analysis: Lessons Learned from the 1995 Kobe Earthquake", *Earthquake Engineering Frontiers in Transportation Systems, Proceedings of the Center-to-Center Workshop, June 22-23, 1998, Tokyo, Japan*, Edited by H. Kameda and I.M. Friedland, INCEDE Report 1999-05, pp 151-166, December 1999.

Walton, J., Cho, S., Werner, S.D., and Moore, J.E. II, *User Manual for REDARS 1.0*, Multidisciplinary Center for Earthquake Engineering Research, Buffalo NY, in press.

Walton, J.S., Cho, S., Werner, S.D., Moore, J.E. II, and Taylor, J.E., *User Manual for REDARS 1.0 -- A Computer Program for Evaluation of Risks from Earthquake Damage to Roadway Systems*, Report prepared for Multidisciplinary Center for Earthquake Engineering Research, Buffalo NY by Seismic Systems & Engineering Consultants, Oakland CA, December 2000.

Wardrop, J., "Some Theoretical Aspects of Road Traffic Research", *Proceedings of Institute of Civil Engineers*, Volume 1, Number. 2, pp 325-378, 1952.

Wells, Donald L. and Kevin J. Coppersmith, "New Empirical Relationships Among Magnitude, Rupture Length, Rupture Width, Rupture Area, and Surface Displacement Area," *Bulletin of the Seismological Society of America*, Volume 84, Number 4, pp. 974-1002, August 1994.

Werner, S.D., "Earthquake Ground Motions", *Earthquake Resistant Concrete Structures, Inelastic Response and Design SP-127*, American Concrete Institute, Detroit MI, pp 21-66, 1991.

Werner, S.D., Taylor, C.E., and Ferritto, J.M., "Seismic Risk Reduction Planning for Ports Lifelines", *Optimizing Post-Earthquake Lifeline System Reliability, Proceedings of the Fifth U.S. Conference on Lifeline Earthquake Engineering, Seattle WA*, Technical Council on Lifeline Earthquake Engineering Monograph 16 (Edited by W. M. Elliot and P. McDonough), American Society of Civil Engineers, Reston VA, pp 503-512, August 1999.

Werner, S.D., Taylor, C.E., and Moore, J.E. II, "Loss Estimation due to Seismic Risks to Highway Systems", *Earthquake Spectra*, Volume 13, Number 4, November 1997, pp 585-603.

Werner, S.D., Taylor, C.E., Moore, J.E. II, Walton, J.S., and Cho, S, *Year 1 Report for Task B1-2 -- Modeling Issues for Seismic Risk Analysis of Highway Systems*, Report prepared for Multidisciplinary Center for Earthquake Engineering Research, Buffalo NY by Seismic Systems & Engineering Consultants, Oakland CA, December 2000.

Youd, T. L. and Perkins, D. L., "Mapping of Liquefaction Induced Ground Failure Potential", *Journal of the Geotechnical Engineering Division, American Society of Civil Engineers*, Volume 104, Number GT4, April 1978, pp 433-446.

Youd, T. L., *Screening Guide for Rapid Assessment of Liquefaction Hazard at Highway Bridge Sites,* Technical Report MCEER-98-0005, Multidisciplinary Center for Earthquake Engineering Research, Buffalo NY, June 16, 1998.

Youd, T.L., "Chapter 6, Pavements", *Seismic Retrofitting Manual for Highway Systems -- Volume III, Screening, Evaluation, and Retrofitting of Retaining Structures, Slopes, Tunnels, Culverts, and Pavements*, Multidisciplinary Center for Earthquake Engineering Research, Buffalo NY, May 1999 Draft.

Youd, T.L., Hansen, C.M., and Bartlett, S.F., "Revised MLR Equations for Predicting Lateral Spread Displacement", *Proceedings of Seventh U.S.-Japan Workshop on Earthquake Resistant Design of Lifeline Facilities and Countermeasures against Soil Liquefaction, Seattle WA, August 15-17, 1999*, Multidisciplinary Center for Earthquake Engineering Research Technical Report.

APPENDIX A
PROBABILISTIC FRAMEWORK

A.1 OBJECTIVE AND SCOPE

A walkthrough procedure -- the calculation of random walks over time[1] -- is incorporated into the SRA methodology. This appendix provides the probabilistic framework for this procedure as it is implemented in the SRA methodology, and describes how it is used to develop loss distributions and to estimate nominal confidence levels and limits of these distributions.

The remainder of this appendix contains four main sections. Section A.2 provides an overview of the walkthrough procedure. Subsequent sections describe in more detail how scenario earthquakes are developed (section A.3), how loss distributions are developed from the SRA results for each scenario earthquake and simulation (section A.4), and guidelines for estimating a constant number of simulations for each earthquake to achieve a desired nominal confidence level for the loss results (section A.5).

A.2 OVERVIEW

A.2.1 WALKTHROUGH PROCEDURE

The walkthrough procedure is carried out for a user-specified duration (in years) that is established in accordance with basic principles discussed in section A.2.5. The user then also specifies a constant number of "simulations" to be considered for each scenario earthquake (where a simulation is defined and discussed in section A.2.2). The procedure then establishes scenario earthquakes for each year of the walkthrough, carries out SRA for each specified simulation for each earthquake during each year, develops probabilistic loss distributions and statistics from the SRA results for each simulation, and evaluates confidence levels and limits for these results These elements of the process are further discussed in the paragraphs that follow.

A.2.1.1 Scenario Earthquakes

A set of independent uniform random numbers is generated and used with regional seismicity and tectonics models to establish whether any potentially damaging earthquakes occur in the surrounding region during each year of the walkthrough (i.e., for years 1, 2, etc.) For many of the years, no damaging earthquakes will be found to occur, particularly for moderately seismic regions. For other years, it will be determined that one or more potentially damaging earthquakes occur. Additional series of uniform random numbers are then used to establish the magnitude, location, rupture center, and rupture length of each of these earthquakes. This is provided in tabular form (for each year of the walkthrough) as input data for the subsequent SRA calculations. Section A.3 describes the development of scenario earthquakes in more detail.

---

[1] A random walk over time is defined as a random process that is implemented for each year of a designated time frame of interest . The results of this random process from each of these years are then aggregated and analyzed probabilistically to obtain loss distributions for user-specified exposure times and/or statistical parameters that characterize these distributions.

A.2.1.2 Summary of SRA Process

Once a potentially damaging earthquake has been postulated for a given year, and its location and magnitude have been determined, a random process is then used to define seismic hazards (level of ground shaking and permanent ground displacement) at each component site, and the damage state of each component in the system due to its seismic hazards[2]. These seismic hazards and component damage states are obtained by first using random sampling to obtain a value of each designated "uncertain" parameter in the seismic hazard and component vulnerability models. Once values for all uncertain parameters are thereby obtained, they are input into the hazard and component models, in order to establish corresponding levels of seismic hazard and component damage. Then, the following steps are used to complete the SRA of the highway system for the given set of uncertain parameter values:

- Damage repair models are used to establish repair costs, downtimes of the component during repair, and whether partial traffic can be accommodated on the roadway during repair of the component damage. These are termed roadway "traffic states".

- These "traffic states" are incorporated into a roadway network model, in order to obtain overall post-earthquake system states (that differ from the pre-earthquake system states because some roadway links are now fully or partially closed due to earthquake damage). Such system states are obtained at several times after the earthquake, to reflect the rate of restoration of traffic-carrying capacities throughout the system as the repairs proceed.

- A transportation network analysis procedure is applied to each system state, in order to evaluate how the earthquake damage modifies system-wide traffic flows and travel times relative to pre-earthquake values.

- Losses due to earthquake damage to the highway system are assessed. In this, the term "loss" denotes economic loss, increases in travel times to/from any designated locations in the region, or any other adverse consequence of earthquake damage to the highway system.

A.2.1.3 Nominal Confidence Levels and Limits

Procedures summarized in section A.5 are used to estimate nominal confidence levels and limits for the above results. If the user determines that these nominal confidence levels/limits are inadequate, new simulations are added to the existing simulations. New SRA results are then developed for each of the additional simulations, revised loss distributions are obtained from this now-expanded set of SRA results, and new nominal confidence levels and limits are estimated. This process is repeated until the nominal confidence levels and limits are judged to be acceptable to the user.

---

[2] In theory, a random process would also be used to define post-earthquake travel times and traffic flows throughout the damaged highway system. However, the transportation network analysis procedure used in the SRA methodology is currently deterministic; i.e., it does not yet account for uncertainties in input data, network modeling and analysis procedures, etc (see chapter 3). In the future, this procedure may be extended to accommodate such uncertainties.

A.2.2 MULTIPLE SIMULATIONS

The above process for carrying out a SRA for a given set of randomly sampled uncertain model parameters is defined as a "simulation". The development of a constant number of multiple simulations for each scenario earthquake can be used to evaluate the sensitivity of various SRA results to the uncertainties in the seismic hazards and component vulnerabilities, through the use of conditional loss distributions. In addition, use of an increased number of simulations per scenario earthquake will increase the reliability of the probabilistic SRA loss results. This is because the reliability of these results will increase with increasing numbers of trials. In general, the number of trials for developing the loss distribution is obtained as the product of the number of years of the walkthrough and the number of simulations per scenario earthquake (with only a slight caveat that is discussed in section A.2.4). These trials are assumed to be Bernoulli trials (section A.2.4), to facilitate the establishment of loss distributions (section A.4) and the estimation of nominal confidence levels in the SRA loss results (section A.5).

To illustrate the simulation process, let us first assume that one simulation per earthquake is considered for a walkthrough with a duration of 50,000 years. A total of 50,000 "trials" is developed for use in obtaining the loss distribution (where, for this case, the number of trials equals the number of years in the walkthrough). However, if two simulations per earthquake are instead used, a total of 100,000 trials is developed. Of these, the first 50,000 trials represent the first simulation for each earthquake occurring during the 50,000-year walkthrough (in which, particularly for a moderately seismic region, many of the years will have no potentially damaging earthquakes). The next 50,000 trials are a repeat of the first 50,000 trials, except that the second simulation for each earthquake is now considered. In this, the earthquake occurrence or non-occurrence during each trial in the second set of 50,000 trials is the same as the earthquake occurrence or non-occurrence for the corresponding trial in the first set. If more than two simulations are considered the above process is repeated for each additional simulation.

A.2.3 RANDOM SAMPLING

As noted above, random sampling is used to establish whether one or more potentially damaging earthquakes have occurred during each year of the walkthrough and, if so, the magnitude and rupture location of each earthquake. In this, the random value of each uncertain parameter for each simulation is selected independently of the random value of all other uncertain parameters. This method for establishing the earthquakes that occur during each year and the multiple simulations for each earthquake is a form of "random sampling" of the multiple uncertain parameters associated with the SRA. Modern statistical theory has shown that the use of such random sampling methods for a relatively small number of samples can greatly increase statistical accuracy relative to that for non-random sampling[3].

[3] For example, in the 1936 presidential election, a straw poll of three million respondents (without random sampling) predicted that Alf Landon would be a clear winner over Franklin Roosevelt. Currently, random sampling of about one thousand (rather than three million) respondents would be used in modern polling procedures, and is deemed much more accurate than a straw poll of a biased sample of respondents. Therefore, modern random sampling methods of polling would have reduced the required number of respondents by a factor of 3,000 (i.e., 3,000,000/1,000) and would have achieved vastly superior accuracy (Taylor et al., 1998).

A.2.4 BERNOULLI TRIALS

The concept of Bernoulli trials is fundamental to the above random sampling process and the establishment of confidence levels and limits for the SRA results. A Bernoulli trial is a statistical sampling process in which: (a) each sample is independent of all other samples; and (b) the probability remains constant for each sample. It is assumed here -- with some caveats as discussed below -- that the ensemble of SRA results developed from the above walkthrough process can be treated as Bernoulli trials. Section A.5 describes how this assumption facilitates the establishment of nominal confidence levels and limits which, in turn, serve to guide the user's selection of the number of simulations to consider for each scenario earthquake.

To illustrate the Bernoulli trial concept, suppose that 10,000 years with one simulation per earthquake are randomly sampled in order to estimate earthquake losses. As indicated in appendix C, this would lead to about 430 potentially damaging earthquakes in the vicinity of Shelby County, Tennessee (which are earthquakes in the general region that have a moment magnitude ≥ 5.0), and probably about 80 simulated non-zero losses due to damage to the Shelby County highway system.

Assuming that the random sampling process summarized in section A.2.3 is used to establish each scenario earthquake and simulation, each of these 80 simulated non-zero losses are equally probable; i.e., each of these losses has an equal probability of occurrence of 1/10,000. In addition, no special dependencies are assumed to exist between the losses during one year and the losses during any other year of the walkthrough. Therefore, each year of the walkthrough is considered to be a Bernoulli trial. As noted above, this facilitates the establishment of confidence levels and limits for the loss results, and is an important benefit of the walkthrough procedure. In contrast to the walkthrough process, other probabilistic loss estimation methods may generate losses with varying probabilities and/or frequencies of occurrence.

There is a caveat in this approach when multiple simulations per earthquake (rather than a single simulation) are used. This is because, for this case, there will be some slight correlation among losses estimated for different years. Strictly speaking, this slight correlation implies that the trials will not be perfectly independent and, as a result, multiple simulations will not yield Bernoulli trials. However, for most purposes, this degree of correlation will be slight, and is expected to lead to only a very slight diminution of confidence levels relative to those for the same number of fully independent trials. Therefore, for application with the SRA methodology, the effects of these slight correlations will be neglected. Future research should be conducted to sort out the effects of these correlations on overall estimates of confidence levels and limits.

A.2.5 TIME VARIABLES

As noted above, this walkthrough process is carried out for a user-specified duration (in years). To establish this total duration, the user should first determine the exposure time of interest for his/her particular needs. For example, if the SRA results are to provide guidance for prioritization of seismic retrofit of various bridges with a design life of 100 years, then an exposure time of 100 years would be selected. As a second example, if the SRA results are to be used to evaluate whether or not to float 25-year bonds to finance a highway system seismic

retrofit program, an exposure time of 25 years would be used. For each of these examples, the user may postulate many random walks for the limited exposure times of interest[4].

Rather than (or in addition to) evaluating statistics for multiple exposure times of interest, the user may wish to focus on statistics of the overall random process, such as average annualized loss. This statistic is required for cost-benefit evaluation and other similar analyses. For this case, a single random walk over an extended duration is desirable. In general, the duration and number of random walks should be selected in accordance with objectives of the analysis and the desired confidence levels and limits.

A.3 ESTIMATION OF EARTHQUAKE OCCURRENCE

This section describes how earthquake occurrence is established for each year of the walkthrough, together with the magnitude, rupture location, and rupture length for each postulated earthquake. This description is in the form of a numerical example drawn from the demonstration SRA of the Shelby County, Tennessee highway system that is described in chapter 7. This region has moderate seismicity but a low probability, high catastrophic loss potential. The earthquake model described in appendix C, has been used to establish the scenario earthquakes for this demonstration SRA. In this, earthquakes are considered to occur randomly either in one of 1,763 areal zones or along three virtual faults used to model for the New Madrid fault zone (whose earthquake potential is represented in terms of an earthquake with a characteristic moment magnitude of 8.0).

The various steps for establishing the characteristics of each earthquake during each year of the walkthrough are summarized below. In this, it is assumed that: (a) there are estimates of magnitude-frequency relationships for both areal and linear (fault related) earthquake sources in the region; (b) the "b" value in the Gutenberg-Richter magnitude recurrence relationship is constant for all areal sources; and (c) earthquakes with a moment magnitude ≥ 5.0 can be designated as potentially damaging.

A.3.1 STEP 1 – DETERMINE NUMBER OF EARTHQUAKES DURING EACH YEAR

This first step determines: (a) the number of earthquakes that occur during each year of the walkthrough; and (b) whether each of these earthquakes is centered in an areal zone or along one of the virtual line sources that model the New Madrid fault zone. In this, it is assumed that, during any year, up to two potentially damaging earthquakes can occur in an areal zone and one potentially damaging earthquake can occur along a line source. (For a more seismically active region, additional potentially damaging earthquakes may be considered.) It is also assumed that the occurrence of earthquakes can be modeled using a Poisson process. Finally, in what follows, the occurrence of earthquakes in an areal zone and along a line source are treated separately during each year of the walkthrough.

---

[4] To illustrate, the demonstration SRA of the Shelby County, Tennessee highway system that is described in the chapter 7 was based on a walkthrough with a total duration of 50,000 years. This amounts to 500 random walks for a 100-year exposure period and to 2,000 random walks for a 25-year exposure period.

On this basis, the probability of occurrence of i earthquakes during a given year of the walkthrough, $P(i)$, is expressed as

$$P(i) = \frac{\lambda^i \exp(-\lambda)}{i!} \tag{7}$$

where λ is the mean rate of occurrence of potentially damaging earthquakes (i.e., earthquakes in the region with moment magnitude ≥ 5.0) along an areal or linear source. Therefore, the probability of zero or one potentially damaging earthquake during each year -- as obtained by setting $i = 0$ and 1 respectively into equation 7 -- are obtained from the following expressions:

$$P(0) = \exp(-\lambda) \tag{8}$$

$$P(1) = \lambda \exp(-\lambda) \tag{9}$$

From this, the probability of occurrence of one or more earthquakes and two or more earthquakes during a given year -- denoted as $P(i \geq 1)$ and $P(i \geq 2)$ respectively -- is calculated as

$$P(i \geq 1) = 1 - P(0) = 1 - \exp(-\lambda) \tag{10}$$

$$P(i \geq 2) = 1 - P(0) - P(1) = 1 - (1 + \lambda)\exp(-\lambda) \tag{11}$$

The calculation of $P(i \geq 1)$ and $P(i \geq 2)$ can be illustrated by considering the earthquake model of the central United States in the vicinity of Shelby County, Tennessee that is described in appendix C. This model leads to $\lambda = 0.0441$ for areal sources in the region, and $\lambda = 0.002$ for the virtual line sources used to represent the New Madrid fault zone. The resulting values of $P(i \geq 1)$ and $P(i \geq 2)$ are given in table 18.

Table 18. Probabilities of Earthquake Occurrence in Areal Source and along Linear Source

Probability	Earthquakes in Areal Source ($\lambda = 0.0441$)	Earthquakes along Linear Source ($\lambda = 0.002$)
$P(i \geq 1)$	0.043	0.002
$P(i \geq 2)$	0.000944	negligible

The above probabilities are used to determine the number of earthquakes that occur along an areal source during a given year by using a uniform random number generator to generate a number between 0 and 1. Depending on the value of this random number, one of the following possibilities can occur: (a) if the number is greater than 0.043, no earthquake occurs in any of the areal zones during the given year; (b) if the number is between 0.043 and 0.000944, one earthquake occurs along one of the areal zones during the year; or (c) if the number is less than 0.000944, two earthquakes occur in the areal zones during the year.

This process is then repeated to determine the number of earthquakes that occur along one of the virtual linear sources within the New Madrid fault zone during the same year. In this, the uniform random number generator is used to generate a second random number between 0 and 1. Depending on the value of this number, the following possibilities are considered: (a) if the number exceeds 0.002, no earthquake occurs along any of the linear sources during the given year; or (b) if the number is equal to or less than 0.002, one earthquake occurs along one of the linear sources during the year.

Table 19 shows how the walkthrough is used to determine whether a potentially damaging earthquake has occurred during a given year. In this, the walkthrough begins with year 1. For this year, a uniform random number generator is used to produce a number between 0 and 1, in order to determine how many earthquakes occur in an areal zone. Let us suppose that this number is 0.67. Then, no earthquake occurs in an areal zone within the region during year 1, since $0.67 > 0.043$. Following this, a second random number between 0 and 1 is generated to determine if an earthquake occurs along a line source in the New Madrid fault zone during year 1. Suppose this number is 0.138. Then, no earthquake occurs along a line source during the year, since $0.138 > 0.002$. This process is repeated for each year of the walkthrough.

Now, let us assume that similar results occur for years 2 through 24. Then, in year 25, suppose the first random number that is generated has a value of 0.036, and the second random number has a value of 0.083. Since the value of the first random number is between 0.043 and 0.000944, and the second random number exceeds 0.002, one potentially damaging earthquake occurs in an areal source and no earthquakes occur along a line source during year 25.

As this process proceeds for each subsequent year of the walkthrough, table 19 shows that during year 165 the first random number has a value of 0.0002, which is less than 0.000944. Therefore, during that year, two potentially damaging earthquakes occur in an areal zone. In addition, during year 373, table 19 shows that the second random number has a value of 0.0018, which is less than 0.002. Since this number is less than 0.002, a potentially damaging earthquake is considered to have occurred during that year, along one of the virtual line sources used to model the New Madrid fault zone.

A.3.2 STEP 2 – DETERMINATION OF EARTHQUAKE LOCATION

A.3.2.1 Earthquake Location in Areal Zone

If step 1 shows that one or two earthquakes have occur within the 1,763 areal zones for the region, the next step is to identify the location (i.e., the particular areal zone) of each earthquake.

To assess this, the models from appendix C are used to establish cumulative conditional probabilities of occurrence of a potentially damaging earthquake in each zone, (conditional on the premise that a potentially damaging earthquake has occurred in one the zones).

Table 19. Determination of Number of Potentially Damaging Earthquakes During Given Year

Year	Areal Zone		Linear Source	
Year	Random Number	Number of Earthquakes	Random Number	Number of Earthquakes
1	0.670	0	0.138	0
2	0.483	0	0.835	0
--	--	0	--	0
25	0.036	1	0.083	0
29	0.005	1	0.482	0
67	0.023	1	0.857	0
144	0.016	1	0.078	0
165	0.0002	2	0.621	0
187	0.003	1	0.711	0
249	0.033	1	0.183	0
282	0.023	1	0.268	0
308	0.027	1	0.177	0
313	0.036	1	0.915	0
329	0.019	1	0.093	0
373	0.428	0	0.0018	1

To illustrate the procedure for identifying the areal zone associated with a potentially damaging earthquake, table 20 shows illustrative conditional cumulative probabilities for a hypothetical set of 20 zones. This table indicates that the cumulative conditional probability of occurrence of a potentially damaging earthquake (i.e., an earthquake of moment magnitude $\geq$ 5.0) in zone 1 is 0.045. This table also shows that the cumulative conditional probability of occurrence of such an earthquake in zones 1 or 2 is 0.098, in zones 1, 2, or 3 is 0.137, and so on.

To use these cumulative probabilities to assign the earthquake to an areal zone, a random number generator is used to generate a number between 0 and 1. Then, this random number is compared to the range of cumulative conditional probabilities that are shown for each zone in table 20, in order to establish the zone where the earthquake occurs. For example, suppose that a random number with a value of 0.43 is generated. Then, table 20 shows that this corresponds to a potentially damaging earthquake that occurs in areal zone 10. The centroid of that zone is assumed to represent the coordinates of the location of this particular earthquake.

Table 20. Illustrative Cumulative Conditional Probabilities of Occurrence of Potentially Damaging Earthquake in Hypothetical Set of 20 Areal Zones

Zone	Cumulative Conditional Probability	Zone	Cumulative Conditional Probability
1	0.000 – 0.045	2	0.046 – 0.098
3	0.099 – 0.137	4	0.138 – 0.167
5	0.168 – 0.212	6	0.213 – 0.267
7	0.268 – 0.313	8	0.314 – 0.360
9	0.361 – 0.404	10	0.405 – 0.446
11	0.447 – 0.491	12	0.492 – 0.540
13	0.541 – 0.593	14	0.594 – 0.645
15	0.646 – 0.699	16	0.700 – 0.753
17	0.754 – 0.811	18	0.812 – 0.877
19	0.878 – 0.933	20	0.934 – 1.000

A.3.2.2 Earthquake Location along Linear Source

In this example, table 19 has indicated that, in year 373, an earthquake has occurred along a linear source in the New Madrid seismic zone. As described in appendix C, this seismic zone is modeled by three virtual fault traces. To determine which of these traces is the source for this earthquake (assuming an equal probability of earthquake occurrence along each of these faults), the cumulative conditional probabilities given in table 21 are established.

To use table 21 to establish which virtual fault trace is the source for this particular earthquake, a uniform random number generator is used to generate a number with a value between 0 and 1. This number is then compared to the cumulative conditional probabilities in table 21. For example, if the random number has a value of 0.45, then the earthquake is centered along trace 2. In step 3, the location of the rupture zone along this trace is established concurrently with the estimation of the moment magnitude of the earthquake (see section A.3.3).

Table 21. Cumulative Conditional Probabilities of Earthquake Occurrence along Virtual Fault Traces used to Model New Madrid Fault Zone

Virtual Fault Trace	Cumulative Conditional Probability of Earthquake Occurrence
1	0.00 – 0.33
2	0.34 – 0.67
3	0.68 – 1.00

A.3.3 STEP 3 – DETERMINATION OF EARTHQUAKE MAGNITUDE

A.3.3.1 Areal Sources

Appendix C indicates that the scenario earthquake modeling for the SRA of the Shelby County highway system leads to a historical seismicity (Gutenberg-Richter) representation for the surrounding region with a "b" coefficient of 0.95 for all areal zones. Therefore, once the total number of all earthquakes of moment magnitude ≥ 5.0 that occurs in all of the areal zones (denoted below as N_{TOT}) is established, the cumulative probability of occurrence of earthquakes with a moment magnitude in excess of M_i (denoted below as $P(M \geq M_i)$) is computed as:

$$P(M \geq M_i) = \frac{N(i)}{N_{TOT}} \tag{12}$$

where $N(i)$ is the total number of earthquakes of moment magnitude $M \geq M_i$ in all of the areal zones. Table 22 shows the conditional cumulative probabilities established for 21 magnitude increments ranging from 5.0 to 7.0 that was established for the region surrounding Shelby County using the modeling procedure described in appendix C. In this, $M_i = 7.0$ is the maximum moment magnitude considered to occur in the areal zones.

To establish the magnitude of the earthquake in the areal zone, a uniform random number generator is used to generate a number between 0.0 and 1.0. This number is then compared to the cumulative conditional probability ranges for each magnitude increment in that is given in table 22. For example, suppose this number has a value of 0.508. Then, table 22 shows that the earthquake has a magnitude of 5.3.

A.3.3.2 Linear Sources

A linear source may have a characteristic rupture length corresponding to the fault trace length, or it may have a shorter rupture length distributed within the overall fault trace. The modeling of this latter situation is accomplished from the following substeps:

- Assume the total rupture length, L_R can be obtained from the following relationship

$$\ln L_R = \ln L_{med} + \varepsilon \tag{13}$$

where L_{med} is the median (deterministic) rupture length, and ε is an uncertainty factor which is typically assumed to have a Gaussian distribution (in log space) with a median value of 0 and a standard deviation, σ_R that usually ranges from about –3 to +3.

Table 22. Cumulative Conditional Probabilities for Earthquake Magnitude Occurrences in Random Areal Zone with b = 0.95

Moment Magnitude, M_i	Cumulative Conditional Probability of Occurrence of Earthquake with Magnitude ≥ M_i	Moment Magnitude, M_i	Cumulative Conditional Probability of Occurrence of Earthquake with Magnitude ≥ M_i
5.0	1.000 – 0.802	5.1	0.801 – 0.642
5.2	0.641 – 0.514	5.3	0.513 – 0.411
5.4	0.410 – 0.328	5.5	0.327 – 0.262
5.6	0.261 – 0.208	5.7	0.207 – 0.165
5.8	0.164 – 0.131	5.9	0.130 – 0.103
6.0	0.102 – 0.081	6.1	0.080 – 0.063
6.2	0.062 – 0.049	6.3	0.048 – 0.037
6.4	0.036 – 0.028	6.5	0.027 – 0.020
6.6	0.019 – 0.014	6.7	0.013 – 0.009
6.8	0.008 – 0.006	6.9	0.006 – 0.002
7.0	0.001 – 0.000		

- Select an appropriate empirical relationship between earthquake magnitude and rupture length (e.g., Wells and Coppersmith, 1994) to obtain L_{med} and σ_R, which typically has the form

$$L_{med} = \exp(c + dM_i) \tag{14}$$

where c and d are regression coefficients and M_i is the earthquake's moment magnitude.

- Estimate the uncertainty factor ε from the following polar method for generating a normally distributed uncertainty factor in log space (Law and Kelton, 1991):

  a) Using an operational random number generator, select three uniformly distributed random numbers -- U_1, U_2, and U_3 -- each between 0 and 1.

  b) Let $V_1 = 2 * U_1 - 1$ and $V_2 = 2 * U_2 - 1$.

  c) Calculate $W = (V_1)^2 + (V_2)^2$. If $W > 1$, start over at Step a). Otherwise, if $W \leq 1$, calculate $Z = \sqrt{\frac{-2\ln W}{W}}$

d) Let $X_1 = V_1 * Z$ and $X_2 = V_2 * Z$. If $U_3 < 0.5$, set $X = X_1$. Otherwise, set $X = X_2$.

- Compute the total rupture length, including uncertainties, as

$$L_R = \exp(\ln L_{med} + X\sigma_R) \tag{15}$$

- Check to see if L_R exceeds the total length of the fault F_{TOT}. If so, set $L_R = F_{TOT}$.

- Otherwise, assume that the position of the rupture along the fault is represented by a parameter

$$P_R = U_4 * \Delta \tag{16}$$

where P_R is the distance from the start of the rupture zone along the fault to the start of the fault trace (figure 29), $\Delta = F_{TOT} - L_R$, and U_4.is a uniform random number with a value between 0 and 1.

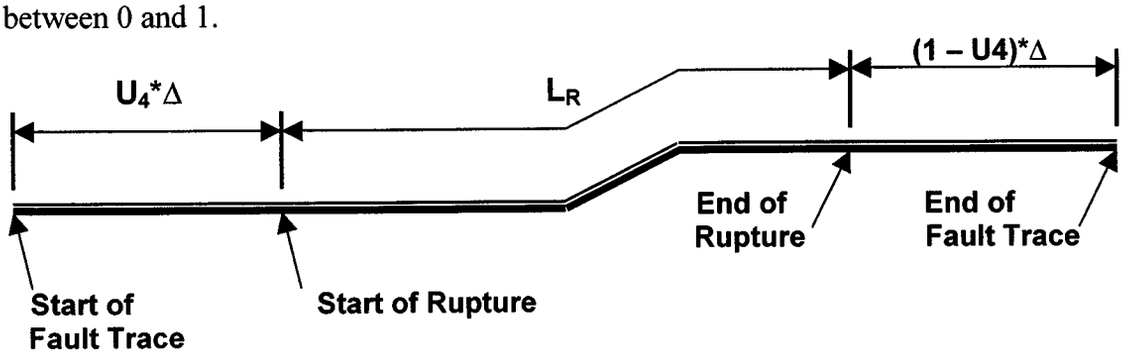

Figure 29. Location of Fault Rupture along Total Fault Trace

- Fix the position of the start of the rupture along the length of the fault trace by using a uniform random number generator to select a random value of U_4 between 0 and 1 and then substituting this into equation 16 (Taylor et al., 1985 and Der Kiureghian and Ang, 1977).

- Construct the extent of the fault rupture along the remainder of the length of the fault trace, accounting for any offsets in the trace as shown in figure 29.

- On this basis, the location of the earthquake's rupture zone along virtual line source 2 is established (e.g., extending from latitudes and longitudes of -90.98/35.20 to –89.91/36.00).

- As described in appendix C, the New Madrid fault zone is modeled as a series of three parallel linear sources with a characteristic earthquake magnitude of 8.0. For this case, the constant or characteristic moment magnitude of 8.0 has been used in equation 14 for all earthquakes occurring in the New Madrid fault zone. Of course, if the earthquakes along a linear source are instead represented using a Gutenberg-Richter model with a designated "b" value, the procedure described earlier for estimating the magnitude of an earthquake in an areal zone is used to estimate the earthquake magnitude for a linear source as well.

A.3.4 END RESULT

The end result of the above steps is a tabular representation of the earthquake occurrence during each year of the walkthrough. As illustrated in table 23, this table would include the magnitude and coordinates of each potentially damaging earthquake during each year where one or such earthquakes has been determined to occur.

Table 23. Illustrative 373-year Walkthrough for Shelby County SRA

Year	First Earthquake			Second Earthquake		
	Source	Moment Magnitude	Latitude and Longitude (deg)	Source	Moment Magnitude	Latitude and Longitude (deg)
1	--	none	--	--	none	--
2	--	none	--	--	none	--
--	--	none	--	--	none	--
25	Areal	5.2	-88.16/37.30	--	none	--
29	Areal	5.4	-89.96/37.70	--	none	--
67	Areal	5.4	-88.88/36.90	--	none	--
144	Areal	5.1	-89.60/35.00	--	none	--
165	Areal	6.7	-89.24/35.80	Areal	5.8	88.31/36.59
187	Areal	5.2	-88.04/37.10	--	none	--
249	Areal	5.2	-88.28/36.40	--	none	--
282	Areal	5.3	-89.00/35.90	--	none	--
308	Areal	6.0	-89.72/37.30	--	none	--
313	Areal	5.8	-87.32/37.40	--	none	--
329	Areal	5.2	-90.80/37.90	--	none	--
373	Linear	8.0	-90.98/35.20 to –89.91/36.00	--	none	--

A.4 DEVELOPMENT OF LOSS DISTRIBUTIONS

Once the SRA results are obtained within the walkthrough analysis framework summarized above, they can be used to develop either total loss distributions or conditional loss distributions, as described below.

A.4.1 TOTAL LOSS DISTRIBUTION

A total loss distribution is a plot of loss value vs. the probability that this value will be exceeded during a designated exposure time. The process for establishing a total loss distribution from the SRA walkthrough results is summarized below, for the general case of E earthquakes that occur over Y years, with S simulations developed for each earthquake. As previously described in section A.2.1.3, this corresponds to a total of $Y' = Y \times S$ assumed Bernoulli) trials for estimation of the total losses.

- The results of the walkthrough analysis are given as an output matrix with Y' rows and two columns. In each row, the first column contains the trial number, and the second column contains the value of the total loss for that trial. In this matrix, most of the Y' rows will have no potentially damaging earthquake occurrence (particularly for a region of moderate-to-low seismicity).

- Each of these Y' loss-severity estimates is treated as a statistical sample of the loss due to earthquake damage to the highway system. Each sample is assumed to be equally probable, with a frequency of occurrence of $1/Y'$.

- The Y' loss values are arranged in decreasing order with the highest value first, the next highest value second, and so on. Then, the i^{th} loss value L_i in this sequence is considered to have a frequency of exceedance of X_i, which is the number of occurrences of loss values equal to or greater than L_i. For example, the frequency of exceedance of the first (highest) loss value is $1/Y'$, and the frequencies of exceedance of subsequent loss values in the sequence are $2/Y'$, $3/Y'$, and so on.

- For an exposure time of T years, the probability P_i that the loss L will equal or exceed the i^{th} loss value, L_i is computed from the following Poisson equation:

$$P_i = P(L \geq L_i) = 1 - \exp(-TX_i) \qquad (17)$$

A.4.2 CONDITIONAL LOSS DISTRIBUTION

A procedure very similar to that outlined above for development of total loss distributions can also be used to develop conditional loss distributions. For example, suppose that it is desired to develop loss distributions that are conditional on the occurrence of a particular earthquake event with a designated magnitude and location. Also suppose that S simulations are to be considered for development of this conditional loss distribution. Then, the user carries out the SRA and loss estimation for these S simulations and the fixed earthquake event. Finally, for this reduced set of results, the user repeats the above procedure for development of a total loss distribution. This involves: (a) forming a loss matrix with S rows and two columns; (b) assuming all of the loss values have an equal probability of 1/S; (c) ordering the loss results for each simulation in decreasing order; and (d) adapting equation 17 to estimate the probability of exceedance for each loss value.

A.5 NOMINAL CONFIDENCE LEVELS AND LIMITS

A.5.1 OVERVIEW

When implementing a probabilistic SRA of a highway system, it is important to have guidelines for selecting an appropriate number of simulations to consider for each scenario earthquake, as well as the number of years to be modeled. This section provides such guidelines, in the form of procedures that relate the number of simulations and years modeled to nominal confidence levels and limits in the results. This will enable a user of the SRA methodology to select a sufficient number of simulations and years to meet a given target nominal confidence level. The procedures summarized in this section are based on the following considerations:

- As a preliminary method, the central limit theorem is used to evaluate the accuracy of mean estimates of loss. The overall accuracy of the various SRA models does not itself permit precise loss estimates. However, this use of the central limit theorem shows that reasonable estimates of mean (average annualized) losses can be developed from a manageable number of simulations and years modeled (Law and Kelton, 1991, and Hogg and Klugman, 1984).

- As a first approximation, a binomial distribution can be used to develop nominal confidence levels and limits for other loss estimates (e.g., for loss estimates with an annual probability of 0.01). This is briefly discussed in section A.5.3. In this, it is noted that achieving a given accuracy of other loss estimates will require more simulations and years modeled than required to achieve the same level of accuracy for the mean loss.

- Additional procedures for addressing this issue are summarized later in this chapter, together with a discussion of possible directions for further development of improved methods for estimating nominal confidence limits in the future.

A.5.2 NOMINAL CONFIDENCE LEVELS FOR AVERAGE ANNUALIZED LOSSES

Estimates of the mean value of the losses, also termed the average annualized loss (AAL), can be essential for use of SRA results. AAL estimates are required for cost/benefit, risk/benefit,

and mean/variance evaluations of proposed alternatives for reducing seismic risks to a highway system. Therefore, this section summarizes how to choose a number of simulations in this SRA process to attain a desired nominal confidence level for the AAL estimates.

To evaluate AAL nominal confidence levels, one may initially assume that the sampling distribution of the mean is normally distributed (in accordance with the Central Limit Theorem)[5]. From this, it turns out that the nominal confidence limit interval for an AAL estimate is defined from the following formula (e.g., page 67 of Hogg and Klugman (1984), and pages 286-289 of Law and Kelton (1991)):

$$AAL \pm \frac{t_o \sigma_A}{\sqrt{n-1}} \tag{18}$$

where

n = number of Bernoulli trials ($n-1$ = number of degrees of freedom).

t_o = value of Student's t distribution corresponding to any designated nominal confidence. level and value of n (see table 24 for values for a 95% nominal confidence level).

σ_A = adjusted standard deviation of the loss distribution $= \dfrac{\sum_i (x_i - AAL)^2}{n-1}$ (19)

x_i = loss value during the i^{th} year of the walkthrough.

Using table 24 and equations 18 and 19, one may define how the nominal confidence limits vary with the number of Bernoulli trials used (which as noted earlier, corresponds to the number of years in the walkthrough). Table 25 shows such a finding at the 95% nominal confidence level in terms of how, at this confidence level, the accuracy of the AAL increases with increasing number of years in the walkthrough. In this, the selection of an appropriate level of numerical accuracy of the AAL should consider how much accuracy is warranted in view of the degree of crudeness of the models used in the overall walkthrough procedure.

To illustrate the use of these results to estimate nominal confidence levels, consider the demonstration SRA of the Shelby County Tennessee highway system described in chapter 7. In this SRA, a walkthrough with a duration of 50,000 years and one simulation per earthquake is used. Chapter 7 shows that the resulting AAL (mean value of the total loss) due to increased commute time caused by earthquake damage to the highway system is \$2.17 million, and the adjusted standard deviation of these losses (σ_A) is \$30.96 million. To estimate the 95-percent nominal confidence limits for the AAL estimate, these quantities are substituted into equation 18 (where, from table 24, $t_o = 1.96$ for a 50,000 year walkthrough), i.e.

$$AAL \pm \frac{t_o \sigma_A}{\sqrt{n-1}} = \left(\$2.17 \pm \frac{1.96 * \$30.96}{\sqrt{50{,}000-1}} \right) x10^6 = (\$2.17 \pm \$0.274) x10^6$$

[5] The sampling distribution of the mean is the distribution of means of all possible samples of any size which can be drawn from a given population (whether with or without replacement).

Table 24. Values of t_0 for 95-Percent Nominal Confidence Level Relative to Number of Degrees of Freedom[6] (Law and Kelton, 1991; and Hogg and Klugman, 1984)

Degrees of Freedom (n-1)	t_0
1	12.706
5	2.571
10	2.228
20	2.086
30	2.042
40	2.021
50	2.009
60	2.000
70	1.994
80	1.990
90	1.987
100	1.984
∞	1.960

Therefore, for this example, a walkthrough duration of 50,000 years (and one simulation per year) results in a 95 percent nominal confidence that the true AAL will be within about ± 12.6 percent of the computed AAL of $2.17 million. Multiple simulations per scenario earthquake would produce even tighter nominal confidence limits, in spite of the previously-noted slight caveats about their strict application in producing Bernoulli trials. At the same time, it must be recognized that distributions for moderately seismic regions with high catastrophic loss potential will invariably produce very high coefficients of variations (the standard deviation divided by the mean). This will not necessarily be true for more highly seismic regions such as California and Alaska, primarily because these regions produce a larger number of potentially damaging earthquakes. As a result, fewer trials (years) will be needed in more highly seismic regions in order to produce comparable nominal confidence limits.

[6] Note that the use of table 24 does not imply that the original distribution is normal. Rather, in accordance with the Central Limit Theorem, the use of equation 18 and table 23 merely imply that the sampling distribution of the mean is normally distributed (Law and Kelton, 1991).

Table 25
Variation in AAL Nominal Confidence Limits vs. Number of Years in Walkthrough (Bernoulli Trials) for 95-Percent Nominal Confidence Level

Number of Years in Walkthrough (Bernoulli Trials)	AAL Confidence Limits
10	$\pm 0.70\sigma_A$
100	$\pm 0.20\sigma_A$
1,000	$\pm 0.062\sigma_A$
10,000	$\pm 0.020\sigma_A$
100,000	$\pm 0.0062\sigma_A$
1,000,000	$\pm 0.0020\sigma_A$
10,000,000	$\pm 0.00062\sigma_A$
100,000,000	$\pm 0.00020\sigma_A$
1,000,000,000	$\pm 0.000062\sigma_A$

A.5.3 NOMINAL CONFIDENCE LEVELS FOR OTHER LOSS ESTIMATES

One of the major benefits of the walkthrough procedure as defined is that it permits a fairly straightforward application of the binomial distribution in order to provide nominal confidence limits and levels for diverse loss levels (e.g., the 500-year loss, or the loss with a probability of 0.002). This benefit does not exist when a typical earthquake loss distribution generated by loss estimates for earthquake scenarios of diverse probabilities (and/or frequencies) of occurrence is used. Such typical loss distributions do not satisfy the requirements for the application of a binomial distribution. In particular, for a typical earthquake loss distribution, loss estimates and events (trials) are not equally probable.

The development of procedures for obtaining reliable estimates of the mean (average annualized) loss has been a major thrust of the SRA methodology development efforts to date. As a result, the actual application of a binomial distribution to estimate nominal confidence levels and limits for other loss estimates (e.g., the loss with a 0.002 probability of occurrence) is not included here. However, procedures that use a binomial distribution to develop nominal confidence levels and limits for these other loss estimates are well known in statistics. Such procedures should be further developed under future research efforts.

A.5.4 FURTHER CAVEATS IN ESTIMATING NOMINAL CONFIDENCE LEVELS FOR AVERAGE ANNUALIZED LOSS ESTIMATES

The use of the Central Limit Theorem to estimate confidence levels and limits for AALs provides a convenient means to show that reasonable accuracy can be provided with relatively few trials. There are, however, theoretical difficulties with this application that should be considered in future investigations -- even though these investigations will refine rather than revise this conclusion regarding reasonable achievable accuracy with relatively few trials.

Section A.2.4 has already noted one caveat in this application -- the slight difficulties in assuming that the use of multiple simulations per scenario earthquake produces Bernoulli trials. In addition, Law and Kelton (1991) (op. cit., pp. 280-285) contends that another problem with this application of the Central Limit Theorem is that it assumes that the variance is known. In fact, estimates of the variance can be very unstable. Law and Kelton (1991) defines a discrete-time stochastic process as being "covariance stationary" if simulated (or empirical) estimates of mean and variance from relatively few trials equal, respectively, simulated (or empirical) estimates of mean and variance from further trials in a discrete-time stochastic process. The covariance of two successive trials is also constant in a covariance-stationary process.

Law and Kelton (1991) contends, however, that simulation output data are always correlated. This leads them to define a standard deviation estimator σ_A' from the following expression

$$\sigma_A' = \sqrt{A * \frac{\sigma_A^{\,2}}{n}} \tag{20}$$

where n is the total number of trials, σ_A is the adjusted standard deviation of the loss distribution, as defined by equation 19, and

$$A = 1 + 2.0 * \sum_{j=1}^{n-1} \frac{\rho_j * (1 - j/n)}{n} \tag{21}$$

$$\rho_j = \frac{C_j}{\sigma_A^{\,2}} \tag{22}$$

$$C_j = \frac{\sum_{i=1}^{n-j} [x_i - x_{mean}(n)][x_{i+j} - x_{mean}(n)]}{n - j} \tag{23}$$

in which $x_1 \ldots x_n$ are trials. After σ_A' is obtained from equation 20, it is then used in place of σ_A in equation 18 in order to obtain an improved estimate of the AAL nominal confidence levels.

An alternative to the above simplified methods for estimating nominal confidence levels is to use bootstrap theory (Efron and Tibshirani, 1993). Bootstrap theory involves sampling with replacement. Sample distribution data can be used instead of distribution families (e.g., lognormal, beta, gamma, normal). (The imposition of distribution families on extant data itself often yields numerical errors that can be large.) The bootstrap approach does not require the assumption of the Central Limit Theorem. This implies that one does not need to begin with the assumption that a stable and known estimate of the standard deviation has been obtained. This approach should be further developed and evaluated in future research.

APPENDIX B
TRANSPORTATION NETWORK ANALYSIS PROCEDURES

As noted in chapter 3, the SRA methodology uses both the User Equilibrium (UE) and Associative Memory (AM) procedures for analysis of traffic flows and travel times in highway networks. The UE method is used to generate training and test cases for the AM procedure, and is also used for post-earthquake transportation network analysis when deterministic analyses for only a limited number of system states (for a limited number of scenario earthquakes and simulations) are to be considered. The AM method is used for transportation network analyses when the user wishes to carry out probabilistic analyses of large numbers of system states (for large numbers of scenario earthquakes and simulations). This appendix provides further information on these methods, which are described in more detail in Moore et al., (1997) and in Kim et al., (1997).

B.1 ASSUMPTIONS

The assumptions in the application of both the UE and the AM analysis procedures are as follows:

- Each analysis zone is unique, and serves as both an origin and destination of trips.
- Traffic flows are static; i.e., they do not change with time of day or time of year.
- Drivers have perfect traffic information; i.e., their behaviors are predictable.
- There is only one transportation mode (using roadway vehicles such cars, buses, and trucks); i.e., there is no mass transit.
- The transportation network consists of highway and roadway links, with no delays at signalized intersections or due to waiting to turn at intersections.
- The links are directed, in which adjacent nodes are connected by two links -- one in each direction.
- The links are congestable; i.e., the time cost of traffic increases with volume of flow.
- Travel demand is inelastic; i.e., origin-destination requirements do not change even if the network changes, unless earthquake-induced link failures make travel to some zones impossible.

B.2 USER EQUILIBRIUM FLOWS IN TRANSPORTATION NETWORKS

This research employs the static UE model to simulate traffic flows given network configurations for different link-failure system states. The standard link flow formulation for the static user equilibrium model is:

$$\text{Minimize} \quad \sum_a \int_0^{v_a} t_a(w)dw \tag{24}$$

subject to

$$v_a = \sum_s v_a^s \qquad \text{for all links } a \tag{25}$$

$$\sum_{a \text{ in Out(r)}} v_a^s - \sum_{a \text{ in In(r)}} v_a^s = Demand^{r-->s} \quad \text{for all origin-destination pairs } (r,s) \tag{26}$$

$$v_a^s \geq 0 \qquad \text{for all links } a, \text{ and destinations } s \tag{27}$$

where

w = the variable of integration,
v_a = the total flow on link a,
$t_a(w)$ = the link travel cost function for link a,
v_a^s = the total flow on link a bound for destination s
$Out(r)$ = the set of link flows outbound from node r, and
$In(r)$ = the set of link flows inbound to node r.

This is a nonlinear minimization problem with a convex objective function subject to two sets of linear constraints and two sets of non-negativity conditions (Eash et al., 1971). Equation 24 is the objective function. The objective function is to minimize the area under the link travel cost function $t_a(w)$, by satisfying the equilibrium conditions stated by Wardrop (1952). Equation 25 represents the flow conservation rule that the flows on each link is equal to the sum of the flows from all zones i to zone j passing the link. Equation 26 represents the trip conservation rule that the total number of trips from zone i to zone j over all paths is equal to the specified number of trip demand. Equation 27 ensures that all flows are non-negative.

The Bureau of Public Roads (BPR) link travel cost function is used to describe link travel costs as a function of link flows in the static user equilibrium model (Sheffi, 1985). The BPR link travel cost function is

$$t = t_0 \times [\, 1 + 0.15\, (v/c)^4 \,], \tag{28}$$

where

t = the link travel cost,

t_0 = the link travel cost when the link is not congested (free flow link travel costs)

and

v/c = ratio of the link volume v to the design link capacity ratio c.

The Frank-Wolfe algorithm is the standard method for solving the above convex mathematical programming problem. The application of the Frank-Wolfe algorithm involves the following steps (Boyce et al., 1981, Van Vliet, 1987 and Kalaba et al., 1990):

1. Compute the travel cost on each link corresponding to link flows in the current solution.

2. Trace minimum skim trees from each origin to all destinations using the link travel costs computed in step 1.

3. Assign all trips from each origin to each destination to the minimum cost paths computed in step 2 (all-or-nothing assignment). Call this link flow as w_a.

4. Linearly combine the current solution's link flows (v_a) and the new all-or-nothing assignment's link flows (w_a) to obtain a new current solution (v_a') so as to minimize the objective function. The two flows are combined by the following equation:

$$v_a' = (1-\lambda))v_a + \lambda w_a \qquad (29)$$

where λ is the value between 0 and 1.

5. If the solution has converged sufficiently, stop. Otherwise, return to step 1.

Modeling UE flows in this requires at least three kinds of data. These are origin-destination (O-D) trip requirements (a trip interchange matrix), link design capacities, and free-flow link travel times. The Shelby County OPD provided link design capacities and free flow travel times in the form of a MINUTP file for purposes of the demonstration SRA. An O-D matrix was imputed from link volumes by assuming that these values were occurring under user equilibrium conditions.

The UE model is used to simulate post-earthquake traffic flows with respect to link-failure system states due to different scenario earthquakes. Post-earthquake total system travel times can be computed by using post-earthquake traffic flows and UE link travel times. These calculations can be the foundation of an SRA procedure, or these can be used as to train associative memories.

Link-failure states are based on the assumption that links can be severed without damaging the opposite directional link. Network configurations for link failures are represented discretely. Collapsed links are coded as "2," and unaffected links are coded as "1. " Intermediate capacity

associated with damaged links can be represented as a real number on this interval. All link-failure system states are assumed to reflect the same pattern of travel demand. This is unrealistic, because origin destination requirements will certainly change following an earthquake. Pre-earthquake trip tables are used as a first approximation.

The total number of possible link-failure system states can be calculated combinatorically. Combinations are defined by the number of subsets of size ***r*** that can be constructed from the population of ***n*** objects with no concern for the arrangement or order of the ***r*** objects. The general combinatorial formula is

$$ {}_nC_r = \frac{n!}{r!(n-r)!} \tag{30} $$

where ***n*** is the total objects and ***r*** is the number of subsets to be taken. This function grows rapidly with n, implying a huge number of possible system states. Even in a small network, it is impossible to simulate all of these system states. Fortunately, there are other ways to generate system states. We are interested in system states associated with earthquakes. The SRA methodology provides these system states.

B.3 ASSOCIATIVE MEMORY METHODS

Associative memories are a subset of artificial intelligence approaches. These approaches mimic human memory processes. The associative memory (AM) approach is a heuristic method that addresses the pair association problem between stimulus and response matrices.

The AM approach requires a procedure for computing AM matrices (training) and evaluating the performance of these memory matrices (testing). AMs are computed from paired sets of training input data such that the application of a given stimulus produces the desired response. After training, the AM matrix is used to estimate response outputs for a set of new stimulus inputs that have not been used to train the AM matrix. The performances of different AM matrices are evaluated by comparing the estimated outputs with known test response outputs.

Researchers at the University of Southern California have experimented with the AM approach to various regional modeling problems. The group has successfully applied various versions of AM matrices to difficult parameter identification problems (Kalaba et al., 1990, Kalaba and Tesfatsion, 1991, Kalaba and Udwadia, 1991, Moore et al., 1994a, 1994b, and Kalaba et al., 1999), including constrained optimization problems (Kalaba et al., 1991, 1992 and Moore et al., 1991).

This SRA research uses the AM approach to estimate changes in network flows (response vectors) with respect to given network configurations (stimulus vectors) of post-earthquake system states resulting from different scenario earthquakes. The research employs three AM models. These are: (a) simple associative memories; (b) recurrent associative memories; and (c) multicriteria associative memories. Details of the three AM models are described below.

B.3.1 SIMPLE ASSOCIATIVE MEMORIES

Does there exist an associative memory $\boldsymbol{M}$ (Kohonen, 1989) that will map a finite set of arbitrarily selected stimulus vectors to the corresponding set of system response vectors? The stimulus- response notion is crucial. For each of K training cases, let the stimulus vector $\boldsymbol{s}_k$ of dimension $p \times 1$, and the system response vector $\boldsymbol{r}_k$ of dimension $q \times 1$, be specified (figure 30).

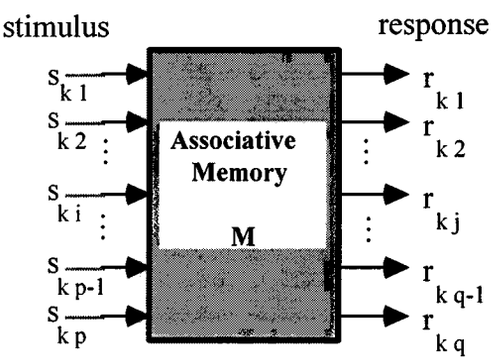

Figure 30. Ideal Associative Memory

The objective is to determine an AM matrix $\boldsymbol{M}^*$ of dimension $q \times p$, so that $\boldsymbol{M}^* \boldsymbol{s}_k$ will equal $\boldsymbol{r}_k$ as nearly as possible for $k = 1, 2, \ldots, K$. Following Kohonen (1989), we take this to mean that if we form the stimulus matrix $\boldsymbol{S}$ of dimension $p \times K$, whose $k^{\underline{th}}$ column is $\boldsymbol{s}_k$, and the response matrix $\boldsymbol{R}$ of dimension $q \times K$, whose $k^{\underline{th}}$ column is $\boldsymbol{r}_k$, then the matrix $\boldsymbol{M}^*$ is to be determined by minimizing the L_2 norm of the difference matrix $\boldsymbol{R} - \boldsymbol{MS}$,

$$\boldsymbol{M}^* = \arg\min_{\boldsymbol{M}} \|\boldsymbol{R} - \boldsymbol{MS}\|^2 \tag{31}$$

The hope is, then, that even if $\boldsymbol{s}$ is not in the training set, $\boldsymbol{M}^* \boldsymbol{s}$ will provide a good approximation to the system's response to stimulus $\boldsymbol{s}$. Clearly, minimizing the L_2 norm minimizes mean square error. Noting that

$$\|\boldsymbol{M}\| = \left(Trace(\boldsymbol{M}^T \boldsymbol{M})\right)^{1/2} \tag{32}$$

it follows that

$$\begin{aligned} \|\boldsymbol{R} - \boldsymbol{MS}\|^2 &= Trace\left((\boldsymbol{R} - \boldsymbol{MS})^T (\boldsymbol{R} - \boldsymbol{MS})\right) \\ &= Trace\left(\boldsymbol{R}^T \boldsymbol{R} - \boldsymbol{R}^T \boldsymbol{MS} - \boldsymbol{S}^T \boldsymbol{M}^T \boldsymbol{R} + \boldsymbol{S}^T \boldsymbol{M}^T \boldsymbol{MR}\right) \end{aligned} \tag{33}$$

Minimizing Equation 31 over $\boldsymbol{M}$,

$$\partial \|\boldsymbol{R} - \boldsymbol{MS}\|^2 / \partial \boldsymbol{M} = Trace\left(2\boldsymbol{M}^* \boldsymbol{SS}^T - 2\boldsymbol{RS}^T\right) = 0 \tag{34}$$

and, assuming $\boldsymbol{S}\boldsymbol{S}^T$ to be nonsingular, it follows that

$$\boldsymbol{M}^* = \boldsymbol{R}\boldsymbol{S}^T(\boldsymbol{S}\boldsymbol{S}^T)^{-1} \tag{35}$$

More generally, the solution to this problem is

$$\boldsymbol{M}^* = \boldsymbol{R}\boldsymbol{S}^+ \tag{36}$$

where $\boldsymbol{S}^+$, dimension $K \times p$, is the Moore-Penrose generalized inverse of the rectangular matrix $\boldsymbol{S}$. $\boldsymbol{S}^+$ can be calculated even if $\boldsymbol{S}$ is not of full rank. Codes for calculating this generalized inverse are available in standard software packages such as Mathematica, Matlab, and SAS.

B.3.2 RECURRENT ASSOCIATIVE MEMORIES

For constrained optimization (Kalaba et al., 1991 and 1992) and certain types of deterministic parameter identification problems (Kalaba and Tesfatsion, 1991), a recurrent extension of the AM approach has been shown to provide much improved estimates of response vectors. A recurrent AM matrix $\boldsymbol{M}^{**}$ is estimated by extending each original training stimulus vector $\boldsymbol{s}_k$ with $f(\boldsymbol{r}_k^*)$, a nonlinear damping transformation of the simple AM estimate corresponding to training response vector $\boldsymbol{r}_k$. Given $\boldsymbol{M}^*$, a simple AM matrix of dimension $q \times p$, and $\boldsymbol{R}^*$, an estimated training response matrix of dimension $q \times K$, the recurrent extension updates the training stimulus matrix to be

$$\boldsymbol{S}_r = \begin{vmatrix} \boldsymbol{S} \\ f(\boldsymbol{R}^*) \end{vmatrix} \tag{37}$$

dimension $(p+q) \times K$. The recurrent AM matrix is computed thus

$$\boldsymbol{M}^{**} = \boldsymbol{R}\boldsymbol{S}_r^+ = \boldsymbol{R}\begin{vmatrix} \boldsymbol{S} \\ f(\boldsymbol{R}^*) \end{vmatrix}^+ \tag{38}$$

The procedure is summarized in figure 31. Note that the procedure subsumes the calculation of a simple AM.

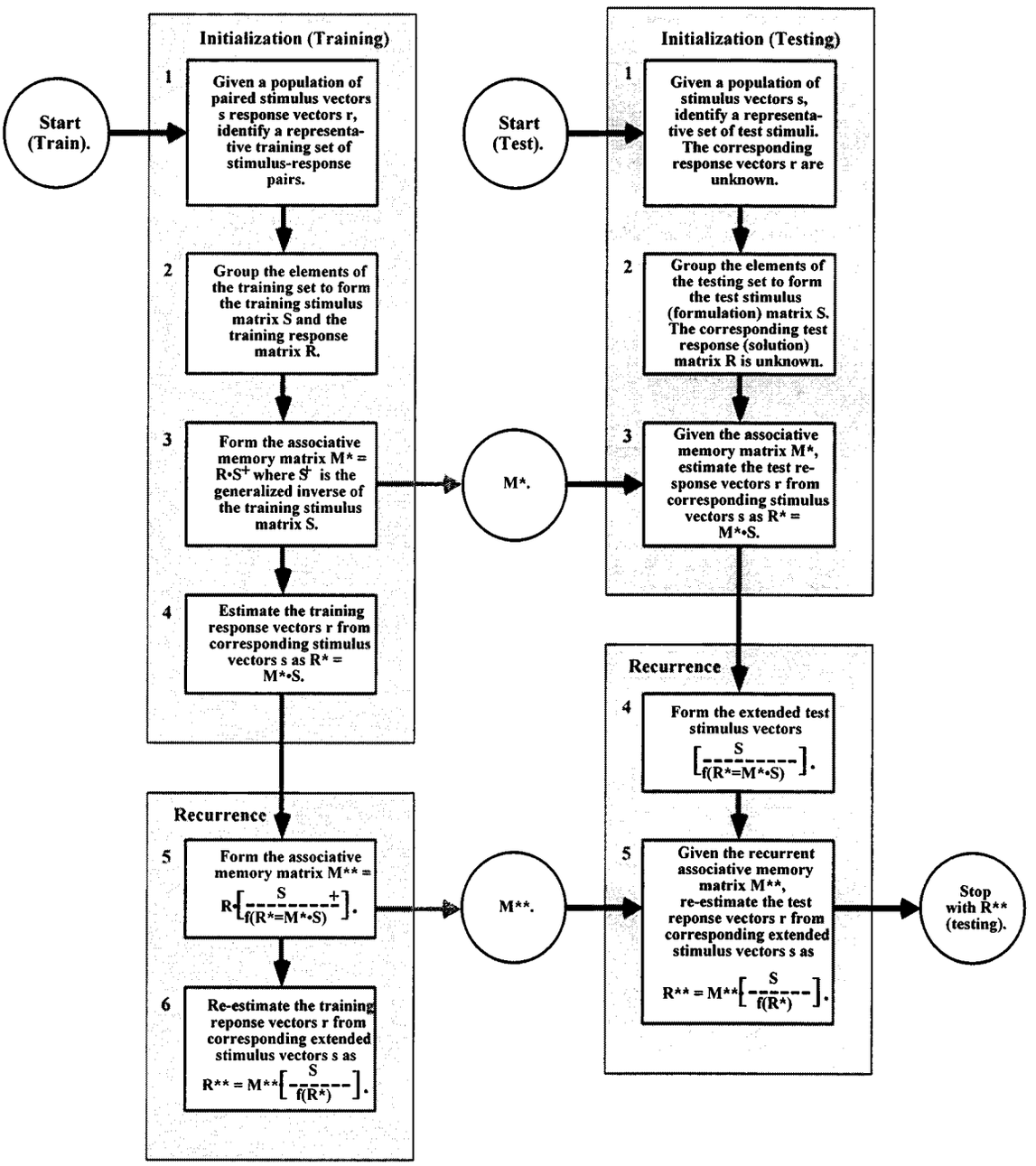

Figure 31. Computing Recurrent Associative Memory: Nonlinear Transformation of R* is Appended to the Stimulus Matrix S. Associative Memory is Recomputed.

B.3.3 MULTI-CRITERIA ASSOCIATIVE MEMORIES

Unfortunately, AMs are known to be particularly sensitive to noise (Kalaba et al., 1990, and Kalaba and Tesfatsion, 1991). Noise can produce scaling problems in the matrices $\boldsymbol{M}^*$ and $\boldsymbol{M}^{**}$. The numerical problems posed by relatively large matrix elements can be addressed in a number of ways. For example, equation 31 can be modified by attaching a penalty to the size of the elements in the AM matrix (Kalaba and Tesfatsion, 1991, and Kalaba and Udwadia, 1991).

Computing such a multicriteria AM matrix, $\hat{M}$, involves a trade-off. The objective is to find a matrix that replicates the training data as closely as possible, but minimizes the magnitudes of the elements necessary to achieve the best approximation. If α is defined to be a coefficient describing the relative importance of the first criteria, i.e., the importance of fitting the training data, equation 31 becomes

$$\hat{M} = \arg\min_{M} \left(\alpha \| R - MS \|^2 + (1-\alpha) \| M \|^2 \right) \tag{39}$$

Expanding,

$$\begin{aligned} & a \| R - MS \|^2 + (1-a) \| M \|^2 \\ & = Trace\left(a(R - MS)^T (R - MS) + (1-a) M^T M \right) \end{aligned} \tag{40}$$

Minimizing equation 39 over M,

$$\begin{aligned} & \partial \left(a \| R - MS \|^2 + (1-a) \| M \|^2 \right) / \partial M \\ & = Trace\left(2a \hat{M} S S^T - 2a R S^T + 2(1-a) \hat{M} \right) = 0 \end{aligned} \tag{41}$$

It follows that

$$\hat{M} = \alpha R S^T [\alpha S S^T + (1-\alpha) I]^{-1} \tag{42}$$

In the special case of a simple AM

$$\alpha = 1 \tag{43}$$

and equation 42 reduces to equation 35.

In general, the optimal value of α is unknown. However, Kalaba and Tesfatsion (1991) reports low sensitivity to values on the interval [0.1, 0.9]. Our previous research shows that the estimation performance of the multicriteria AM matrices are not sensitive to the value of α in predicting network flows. The general procedure of finding the best α value is to incrementally increase the value of α from 0.1 to 0.9. The multicriteria AM approach often provides better estimates of test data sets compared to the simple AM and recurrent AM approaches.

B.3.4 APPLICABILITY OF ASSOCIATIVE MEMORIES

The AM approach is applied to cases in which there seems to be a strong association between stimulus and response vectors. Regardless of whether the association is described by a linear or complex nonlinear function, the prospect of association between vector pairs constituting stimulus and response vectors is essential to the AM approach.

How to select an appropriate number of training cases is often unclear. Past computational experience indicates AMs capture the information in training cases quickly, but generalize less well than more complex connectionist techniques such as neural networks. If empirical data is used for training, it will include outcomes related to both structural relationships and system noise. The objective is to identify and predict structure, not noise. Noise, by definition, cannot be predicted. Neural networks, like other statistical techniques, can be accidentally trained to replicate noise. This degrades the use of a trained network as a predictive tool. One way to avoid this outcomes is to train connectionist heuristics against a set of validation response vectors defined by the same pair association rules as the training vectors, but distinct from the training vectors. Training stops when the outputs of the connectionist model offer no improvement against the validation set. The rationale is that the noise in the validation set is different from the noise in the training set. Thus, over-fitting by training noise can be avoided.

Multicriteria AMs appear to be less subject to over-fitting than neural networks. They are intended to be, but the same validation concept can be used to decide how much empirical information should be used to define the training set. The question of how large the training set should be is a question of what information the AM needs to identify the structural relationships driving the outcomes in the system under investigation. The question is more difficult to answer if the training set entirely synthetic. If the synthetic data used for training is almost noise free, then there is no risk of over-fitting to noise. The training of the AMs in SRA applications described in this volume has been deliberately conservative. The training sets used in these SRA applications are relatively small, and have been incrementally enlarged to see how quickly the estimation performance of the AMs is improved.

Over the past few years, research at the University of Southern California has focused on the application of AM models to various constrained optimization problems. Their research experience has revealed that AM models cost-effectively provide approximate solutions to constrained optimization problems, including network equilibrium problems. The estimation performance of the three AMs described here (simple, recurrent, and multicriteria AMs) varies according to the nature of the constrained optimization problems to which they are applied. They have tried to apply all three AM models to find the most accurate AM matrix for predicting network flows. The best results identified thus far have been provided by the MAMs.

B.3.5 TRAINING AND TESTING PROCESS

B.3.5.1 Basic Principles

Section 3.4.2 of chapter 3 has summarized the basic principles for training and testing of the AM matrices. The following training and testing process was described:

- *User Equilibrium Traffic Flows.* Develop an ensemble of "target" UE traffic flows corresponding to various network configurations that represent the same type of post-earthquake network, traffic flow, and origin-destination travel requirements as considered in the user's SRA application. Most of these solutions are designated as "training cases", and

the remainder are designated as "test cases". The development of these training and test cases is further described in section B.3.5.2.

- *Training of AM.* Compute the elements of an AM matrix that minimizes the mean-square difference between the flows estimated by the AM matrix and target UE flows.

- *Testing of AM.* The basic premise of this approach is that the AM matrix trained in this way will provide a good estimate of traffic flows from other network configurations that represent conditions similar to those of the training cases, but have not actually been used to train the AM. To check this, the AM matrix is used to predict traffic flows for each test case as designated above. These predicted flows are then compared to the target UE flows from the test cases. These comparisons can be evaluated by computing the correlation coefficient between the predicted and target traffic flows. Correlation coefficients in the neighborhood of 0.98 indicate an excellent comparison.

- *Refinement of AM.* The above step will usually lead to good comparison between predicted and target UE traffic flows, if a sufficient number of training cases were considered during the training of the AM. However, if this comparison is not satisfactory (as indicated by a correlation coefficient less than about 0.98), additional training cases can be developed and used to further refine the AM and the accuracy of its traffic flow predictions.

B.3.5.2 Training Cases

The training of the AM can be accomplished by using training cases selected from: (a) the earthquake-induced system states developed from the SRA procedures described in chapter 2; or (b) hypothetical system states developed by systematically and incrementally closing individual links or pairs of links. The SRA methodology uses the latter approach because of its much greater efficiency. This approach develops UE flows for the following four sets of system states: (a) baseline; (b) full closure of individual bridges; (c) full closure of pairs of neighboring bridges; and (d) partial closure of pairs of bridges. These system states are described below.

B.3.5.2(a) Baseline

The baseline system state represents pre-earthquake traffic flows that will be the basis for comparison with traffic flows from all post-earthquake traffic flows. Accordingly, this baseline is a system state with no link closures.

B.3.5.2(b) Full Closures of Individual Bridges

This is a set of system states in which each link in the system that contains a bridge is incrementally closed (one at a time). The total number of system states in this set is equal to the number of bridges in the highway system.

B.3.5.2(c) Full Closures of Pairs of Neighboring Bridges

This set of system states involves full closure of one central bridge and its link in the system model, plus one additional bridge on links within a "tenth-order neighborhood" of the first bridge. In this, a "first-order neighborhood" is defined as consisting of those links whose end node is the same as the start node of the central link[1]. Accordingly, the link flow on the central link is a function of the flows on its first-order neighborhood links. A "second-order neighborhood" consists of those links whose end nodes are the same as the start nodes of all links in the first-order neighborhood. A "tenth-order neighborhood" is established by successive extensions of this process. A "third-order neighborhood" is illustrated in figure 32.

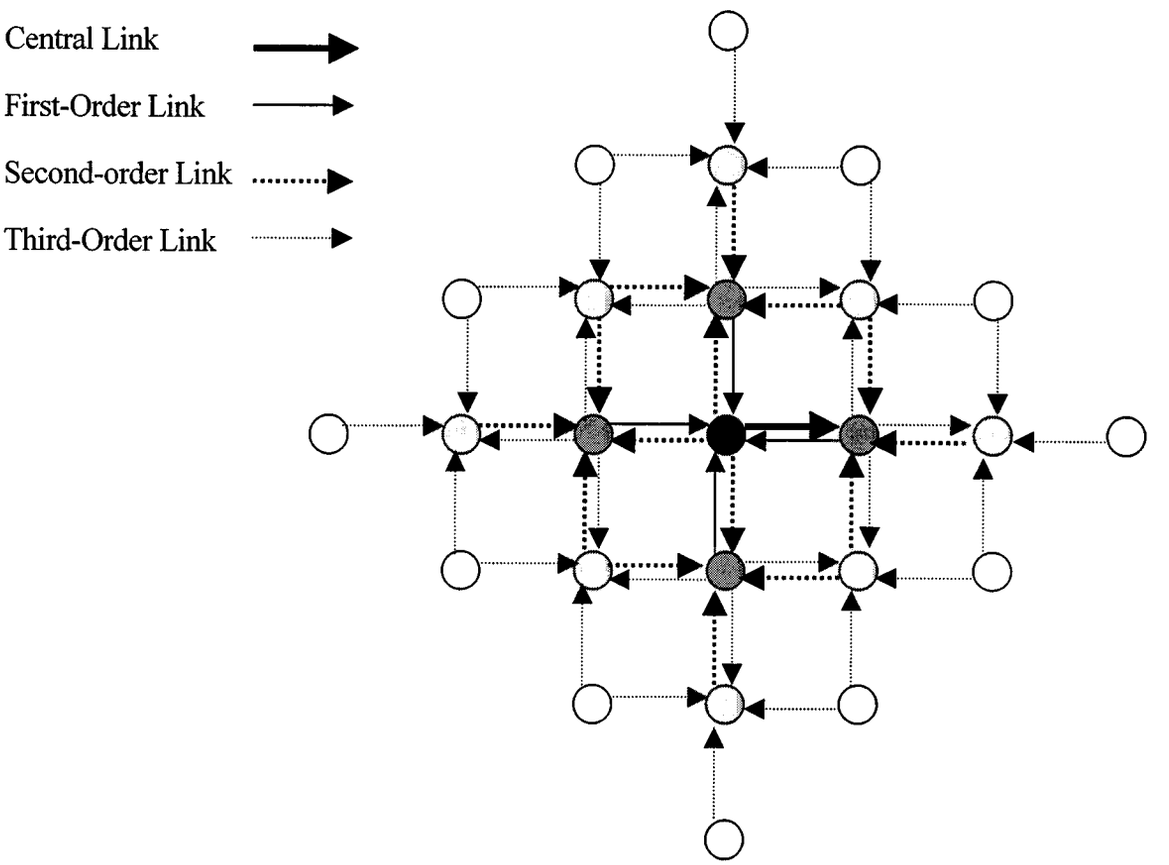

Figure 32. "Third-Order" Neighborhood

[1] Each link in the network model has a direction of travel associated with it, in which travel proceeds from the link's start node to its end node.

It is noted that, if a neighborhood contains more than one bridge in addition to the bridge on the central link, only one additional bridge is closed at a time. In this process, the closure of a given pair of bridges cannot be repeated in multiple neighborhoods containing the two bridges; i.e., any pair of bridges can be closed only once.

The total number of system states in this set depends on the network topology. If all bridges are located within their tenth-order neighborhood, the number of system states is ${}_nC_2$ (where n is number of bridges), as computed using equation 30. However, if a given m^{th}-order neighborhood does not contain any bridges, the combinatorial, reciprocal effect on link flows is assumed to be small.

B.3.5.2(d) Partial Closures of Pairs of Bridges.

This set of system states is formed by partially closing one central bridge and its link in the system model, plus one additional bridge on links within a "tenth order neighborhood" of the first bridge. In this, the link at each partially closed bridge is assumed to have half of its pre-earthquake traffic capacity. Like the previous set of system states, the total number of system states in this set is ${}_nC_2$.

B.3.5.3 Test Cases

AMs developed from the above training cases are tested by applying them to test cases not used to develop the AM matrix. Traffic flows predicted by the AM are compared to target UE traffic flows computed for these test system states. As noted above, these comparisons are assumed to be adequate if the correlation coefficient between the predicted and target traffic flows equals or exceeds 0.98.

In addition, test cases may be based on earthquake-induced system states developed as described in chapter 2, additional randomized choice system states, or other user-defined system states, which are defined as follows

- *Randomized-Choice System States.* Under this option, the network analysis software randomly selects a user-specified number of additional sets of training cases and number of links damaged per case. In this, for a given number of links containing bridges that is defined by the user, the software randomly establishes the degree of damage.

- *User-Defined System States.* If this option is selected, the user can modify the traffic state for any links in the system, and then develop target UE traffic flows for the resulting system state. These user defined test states may be estimates of earthquake induced system states.

APPENDIX C
SCENARIO EARTHQUAKES FOR DEMONSTRATION SRA

C.1 OVERVIEW

In a SRA of a system with spatially dispersed components, individual scenarios are required to evaluate correlation effects of earthquakes, i.e., the simultaneous effects (including systemic consequences of damages) of individual earthquakes on components located at diverse sites. For reasons discussed in section 4.2, scenario earthquake modeling in this SRA methodology is based on an adaptation of the models developed by Frankel et al., (1996) as part of the United States Geological Survey (USGS) National Hazard Mapping Program.

Thus far, this adaptation has been carried out for one region of the country -- the portion of the Central United States (CUS) in the vicinity of Shelby County, Tennessee. This appendix summarizes the adaptation process for this region, as a means for illustrating the process and guiding the future development of scenario earthquakes for other regions of the United States.

The Frankel et al. work for the CUS uses four different spatially smoothed models based on historical seismicity data, plus a special model for the New Madrid Seismic Zone (NMSZ). These models are summarized below.

C.2 HISTORICAL SEISMICITY MODELS

To develop scenario earthquakes for the demonstration SRA of the Shelby County highway-roadway system, a large seismicity zone that encompasses Shelby County was defined. This zone (denoted here as zone A) extends from -87.0 to -92.0 degrees longitude and from 34.0 to 38.0 degrees latitude (see figure 33). It has been divided into 1,763 microzones, with dimensions of about 11.1 km in both length and width.

Three different models were weighted to establish the earthquake activity within each microzone, based on historical seismicity data from a USGS catalogue that is an updated and improved version of the Seeber-Armbruster earthquake catalogue (Seeber and Armbruster, 1991). These models were developed from earthquakes with the following magnitude cutoffs and completeness times: (1) magnitude 3+ earthquakes since 1924; (2) magnitude 4+ earthquakes since 1860; and (3) magnitude 5+ earthquakes since 1700. In addition, a fourth model (model 4) by Frankel et al. that represents background seismicity over a larger zone (denoted as zone B) was weighted with the above three models to establish earthquake activities. Zone B extends from -80.0 to -112.0 degrees longitude and from 30.0 to 40.0 degrees latitude.

The number of earthquakes shown in the USGS catalog to exceed the respective minimum magnitude of models 1 through 3 respectively were counted and, based on the starting and end date of the model (e.g., 71 years for model 1), were converted to a frequency of occurrence. However, within a special aerial zone that covers about 20 percent of zone A, Frankel et al. used a different approach for estimating frequencies of earthquake occurrence which: (a) considers the

historic seismicity database for this zone; and (b) assumes that the earthquakes from this database are uniformly distributed throughout the zone. Zone C is shown as dotted lines in figure 33.

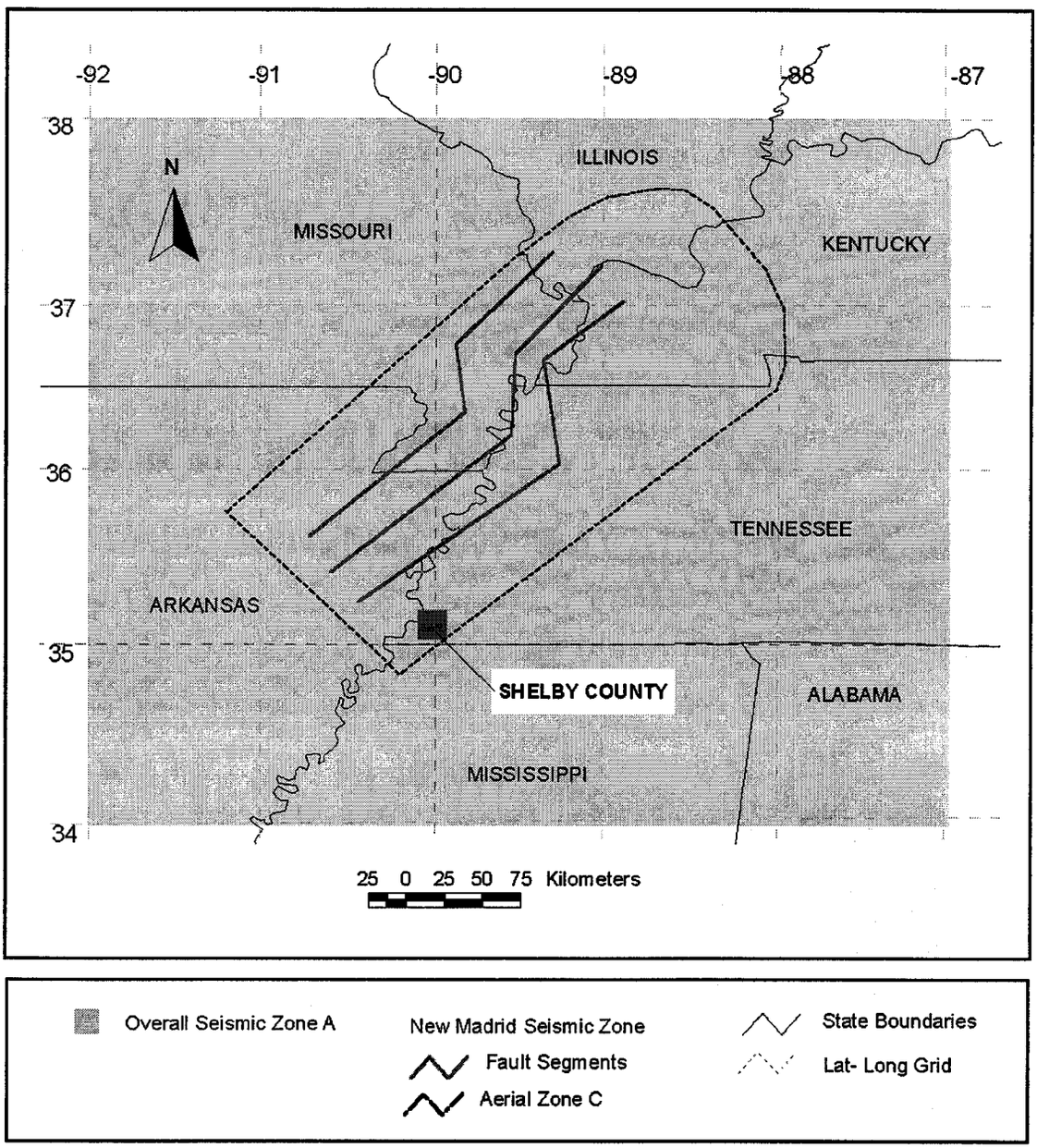

Note: Zone A (overall seismicity zone) and zone C (aerial zone within New Madrid Seismic Zone, NMSZ) as shown above are described in section C.2, and the modeling of the fault traces within the NMSZ is described in section C.3. A large background seismicity zone extending from -80.0 to -112.0 longitude and from 30.0 to 40.0 latitude (that is also described in section C.2 and is referred to as zone B) is not shown in this figure.

Figure 33. Seismic Zones for Central United States (after Frankel et al., 1996)

Then, to further account for uncertainties in the locations of earthquakes as estimated for each of the 1,763 microzones within zone A, a relatively flat gaussian model was used to redistribute

and smooth the earthquake locations among the microzones. Given this redistribution of earthquake occurrences for each of models 1-3, and assuming a threshold magnitude of 5.0 for the onset of earthquake damage, a "b" value of 0.95 in the Richter magnitude-frequency relationship was assumed (based on a derivation by others) to estimate the frequency of occurrence of earthquakes with magnitude ≥ 5.0 in each microzone (for each of these models). For model 4, a uniform distribution was used to allocate potential earthquakes with magnitudes ≥ 5.0 among all of the microzones.

Based on a method of adaptive weighting described in Frankel et al., the above four models were combined to derive frequencies of occurrence of earthquakes of magnitude ≥ 5.0 in each microzone. Next, these frequencies were summed to determine the corresponding frequency of occurrence within the overall seismicity zone. Using this frequency and the frequencies in each microzone, a conditional cumulative probability matrix was then developed for the overall seismicity zone. This two-column matrix contains microzones (numbered) in one column, and cumulative conditional probabilities (from 0 to 1) in the other column. In addition, a Poisson model was used to convert the frequency of occurrence of earthquakes with magnitudes ≥ 5.0 in the overall seismicity zone to a corresponding probability of occurrence.

At this stage, a natural way to develop these scenarios for purposes of analyzing system performance and for eventually compiling information on loss distributions and their variability over a time dimension is to employ a "walk-through" analysis (Daykin et al., 1994). The first step of this analysis was to select an appropriate time frame over which the analysis would be carried out (e.g., one or more time frames of 10 years, 50 years, 100 years, etc.). Then, for each year in each time frame (starting with year 1 and then repeating the process for each successive year), successive uniform random number generators were applied with the appropriate cumulative conditional probability distribution to evaluate: (a) whether or not at least one earthquake of magnitude ≥ 5.0 has occurred somewhere in the large seismicity zone during the year; (b) if so, whether or not a second earthquake has occurred in the zone during the year; and (c) for each earthquake that has occurred in the zone during the year, the microzone where the earthquake is located. A random number generation technique was also used to estimate the earthquake magnitude, with the likelihood of diverse magnitude levels assumed to be represented by a Richter (lognormal) magnitude-recurrence relationship.

C.3 NEW MADRID FAULT ZONE

The following steps were used to model the New Madrid fault zone: (a) adaptation of the Der Kiureghian and Ang (1977) approach to distribute earthquake occurrences within the fault zone (the fault traces appear to be very long for "characteristic" earthquake modeling); (b) application of estimates of the frequency of occurrence for earthquakes in the zone based on the Frankel et al. approach and other relevant studies (Johnston, 1996, Johnston and Schweig, 1996 and Crone, 1998); (c) conversion of these frequencies to probabilities of occurrence using a Poisson model; and (d) postulation that the fault zone is comprised of three parallel linear faults whose locations are shown in figure 33.

Following this, a walk-through analysis was used to develop a random sequence of earthquakes occurring within the zone during the time period of interest. To illustrate, let us assume that the probability of occurrence of an earthquake with a given magnitude (say magnitude 8.0) within the New Madrid fault zone is 0.002. From this, the walk-through process for each year involves the use of successive random number generators to indicate: (a) whether an earthquake of this magnitude has occurred within the fault zone (by checking whether the random number has a value ≤ 0.002); and (b) if so, which of the three fault traces is the source of the earthquake. Then, subsequent steps involve: (c) estimation of the rupture length along the fault trace, by first using the Wells-Coppersmith (1994) relationship between rupture length and earthquake magnitude to obtain best-estimate rupture lengths, and then by accounting for uncertainties in this relationship through use of the polar method in log space (Taylor et al., 1998) along with a standard deviation of 0.22; and (d) estimation of the rupture center within the fault trace, by applying a random number generator to the difference between the fault trace length and estimated rupture length[1].

The results of this walk-through analysis of earthquakes occurring within the New Madrid fault zone were combined with the results of the walk-though analysis of potential earthquakes from the historical seismicity models (section C.1.1) to estimate the total earthquake activity during each year of the time frame of interest.

C.4 RESULTS

The above approach was used to develop an ensemble of 2,320 earthquakes with moment magnitudes ranging 5.0 to 8.0 that occur over a 50,000 year time frame within the above-indicated region that surrounds Memphis and Shelby County, Tennessee. Figures 34 to 36 show the spatial distribution of these earthquakes, broken down by magnitude range.

[1]In this, the difference between the rupture length and the total length of the fault is computed, and a uniform random number generator is used to indicate where the fault rupture is initiated relative to one end of the fault trace.

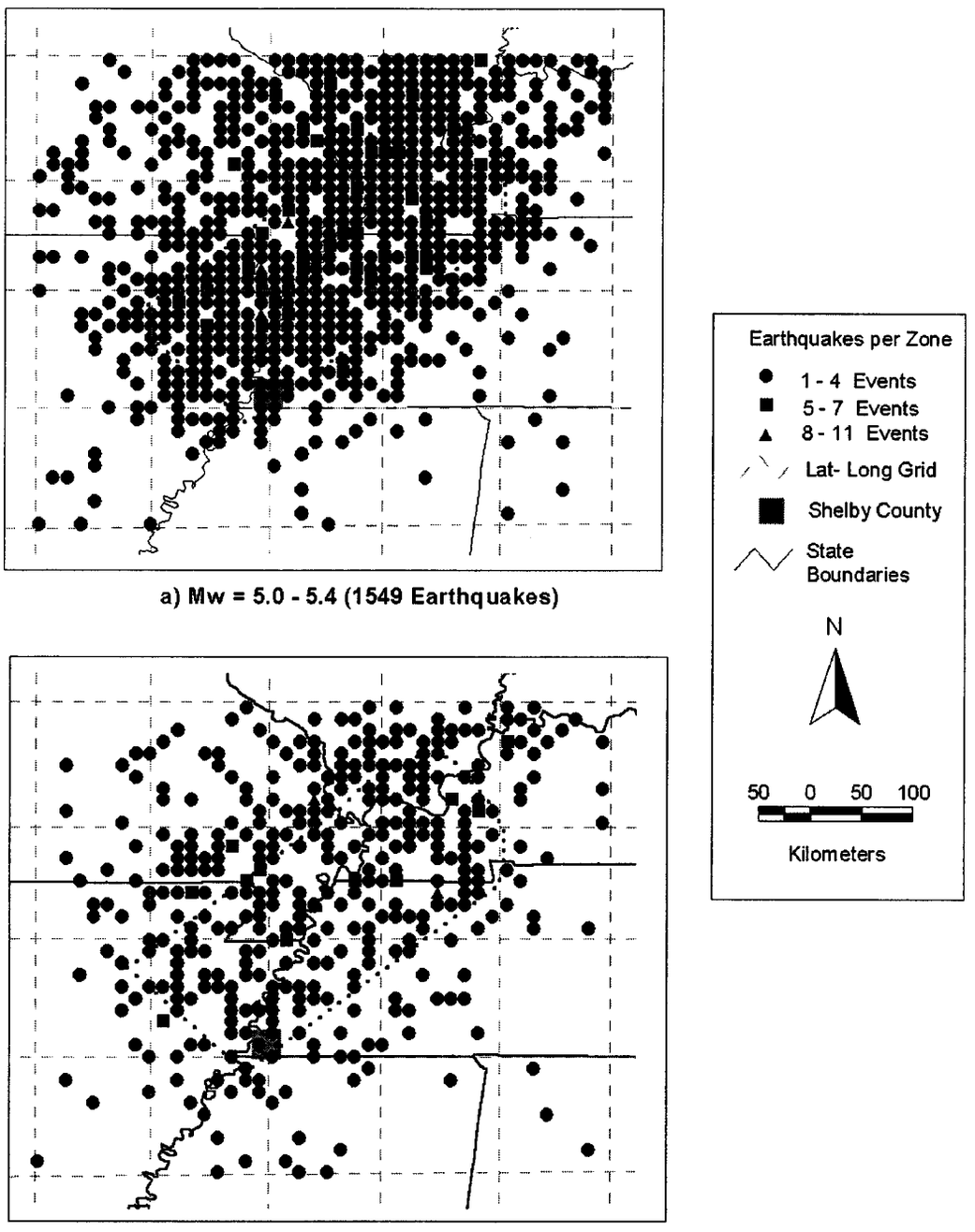

Figure 34. Scenario Earthquakes for 50,000 Year Time Duration (M_w = 5.0 to 5.9)

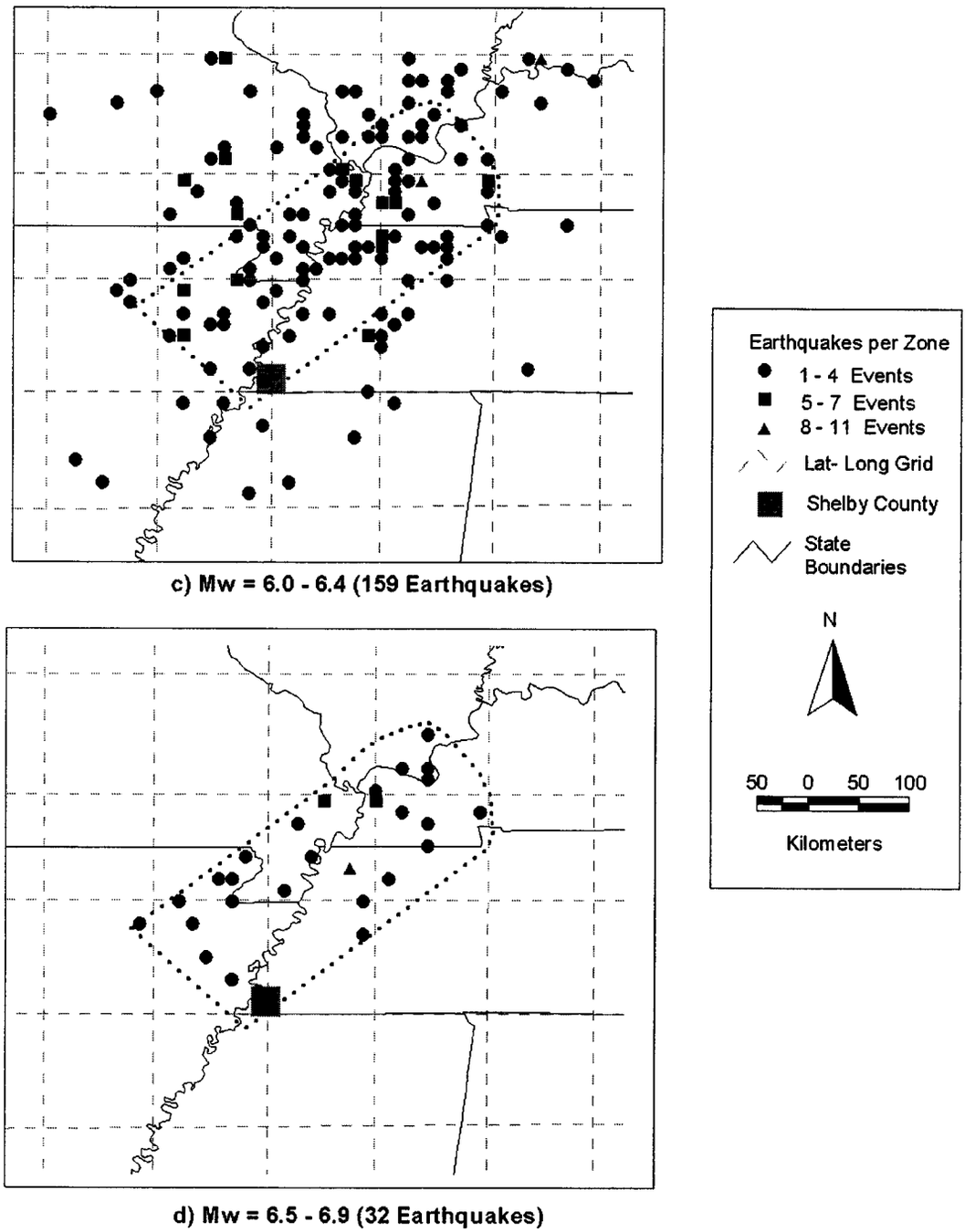

Figure 35. Scenario Earthquakes for 50,000 Year Time Duration (M_w = 6.0 to 6.9)

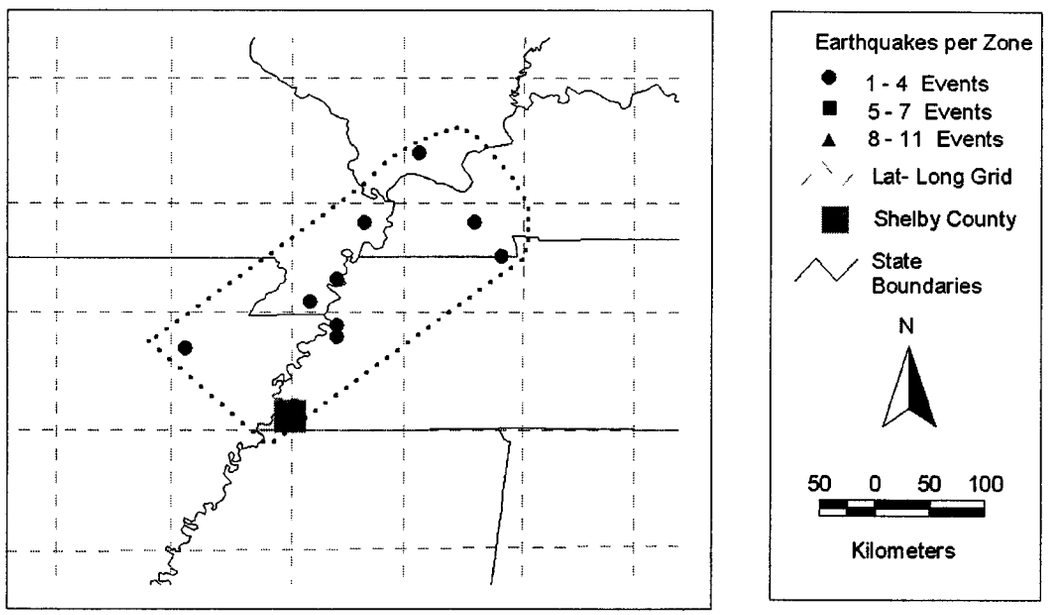

e) Mw = 7.0 - 7.4 (10 Earthquakes)

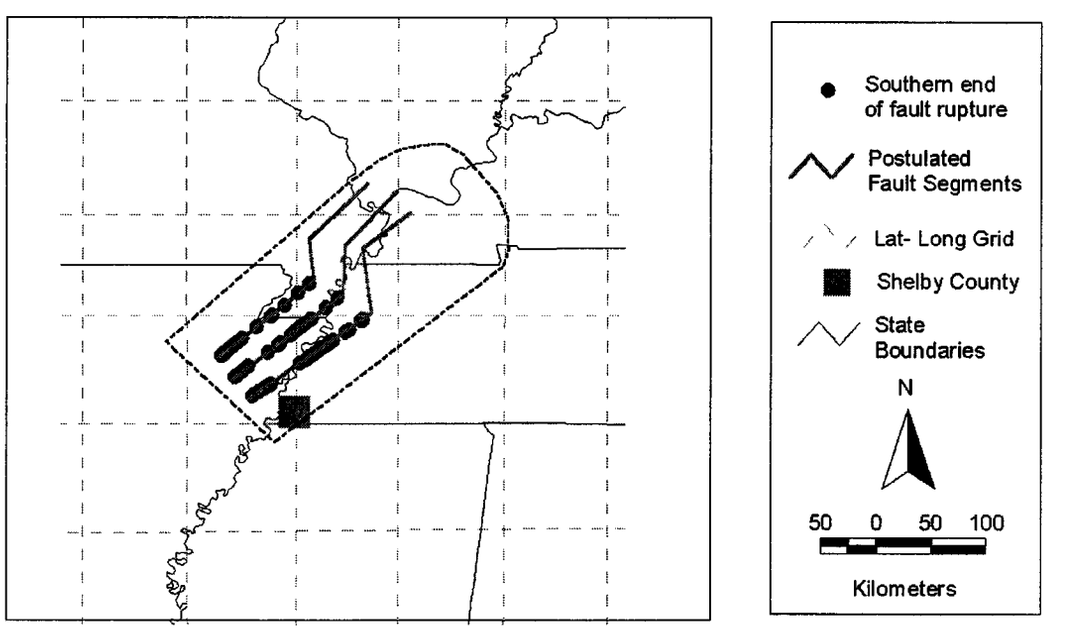

d) Mw = 8.0 (93 Earthquakes)

Figure 36. Scenario Earthquakes for 50,000 Year Time Duration (M_w = 7.0 to 8.0)

APPENDIX D
GROUND MOTION HAZARDS FOR DEMONSTRATION SRA

This appendix outlines a four-step procedure for estimating earthquake ground motions in the Central United States (CUS) that has been used in the demonstration analysis of the Shelby County, Tennessee highway system as described in chapter 7.

D.1 INPUT PARAMETERS

Input parameters for evaluation of ground motion hazards at a specific site due to a given scenario earthquake event consist of : (a) the moment magnitude, M_w, of the earthquake; (b) the location of the earthquake, either within the aerial source zone or along one of the faults in the New Madrid Seismic Zone (NMSZ), using either latitude-longitude coordinates (preferred) or state-plane coordinates; (c) the location of the site of each component within the highway system; and (d) the NEHRP site classification for each component site.

The scenario earthquake's moment magnitude and location (items a and b above) are provided as part of the scenario earthquake development process for the CUS that is described in appendix C. The location of each component in the highway system is provided as part of the overall system input data (see chapter 3).

In addition to bridges, ground motions must be computed at sites of all components at potentially liquefiable sites. For roadways and other components of extended length, the coordinates at which ground motions are computed can be established as follows: (a) divide the entire region containing the highway system into a series of suitably small but finite subzones; (b) for each subzone, obtain all geologic and soils data needed to assess liquefaction hazards, either by compiling existing data or by new testing of soils within the subzone; (c) using preliminary geologic screening that is the first step of the liquefaction hazard evaluation procedure described in appendix E, identify those subzones where liquefaction could occur; (d) for all subsequent scenario earthquakes and simulations, compute the ground shaking at the centroid of each of these subzones; and (e) for the portions of all roadways or other surface or subsurface components of extended length that fall within a given subzone, assess liquefaction hazards using the ground motions computed in step d. The procedure included in the SRA methodology for evaluating liquefaction hazards is described in appendix E.

D.2 EVALUATION PROCEDURE

For each scenario earthquake, the following procedure is used to compute ground motion hazards at the site of each component within the highway system: (1) establish the earthquake's source-site distances; (2) calculate bedrock motions at each component site, using the Hwang and Huo (1997) rock motion attenuation equations; (3) calculate soil amplification factors at each component site, using the Hwang et al., (1997) soil amplification factors for various NEHRP site classifications; and (4) calculate the ground surface motions at the site, as the product of the bedrock motions from step 2 and the soil amplification factors from step 3.

D.2.1 STEP 1 – ESTABLISH SOURCE-SITE DISTANCES

The distance from the source of each earthquake to each component site is established from the coordinates of the earthquake location and the component site locations.

D.2.1.1 Earthquake Location

The earthquake location depends on whether it is centered within an aerial source zone or along one of the faults in the NMSZ (see appendix C). For earthquakes within an aerial source zone, the location is defined by the coordinates of the centroid of the subzone within which the earthquake is centered. For earthquakes along one of the faults within the NMSZ, the earthquake location used to compute source-site distances is equal to the shortest distance from the fault to each component site.

D.2.1.2 Component Location

Source-site distances are computed for all bridges in the highway system, and also for all roadway links for which preliminary geologic screening indicates that the link is located on potentially liquefiable soils

For all bridge components within the system, source-site distances are based on the coordinates of the bridge location that have been provided as input to the SRA procedure. For each roadway link on potentially liquefiable soil sites, source-site distances are computed for the centroid of all soil subzones along the length of the link (see section D.1).

D.2.2 STEP 2 – CALCULATE BEDROCK MOTIONS

D.2.2.1 Deterministic Estimates of Bedrock Motions

Following the procedure by Hwang and Huo (1997), deterministic estimates of bedrock accelerations at each component site are calculated from the following equation:

$$\ln Y = C_1 + C_2 M_w + C_3 \ln[\sqrt{R^2 + H^2} + 0.06\exp^{0.7 M_w}] + C_4 \sqrt{R^2 + H^2} \qquad (44)$$

where

Y = Bedrock spectral acceleration or peak ground acceleration (units of g).
C_1 to C_4 = Regression coefficients given in table 26.
M_w = Moment magnitude of earthquake.
R = Distance from earthquake source to site (section D.2.1.2) including minimum source-site distances for NEHRP soil types D and E given in tables 27 and 28.
H = Focal depth of earthquake (assumed to be 10 km for the CUS).

Table 26. Regression Coefficients for Bedrock Motion Attenuation Equation (Hwang and Huo, 1997)

Period, T (sec.)	C_1	C_2	C_3	C_4
PGA (T=0.0)	-2.904	0.926	-1.271	-0.00302
0.1	-2.312	0.924	-1.233	-0.00317
0.2	-2.968	0.952	-1.219	-0.00240
0.3	-3.461	0.981	-1.208	-0.00210
0.4	-3.911	1.013	-1.195	-0.00199
0.5	-4.344	1.048	-1.180	-0.00200
0.6	-4.764	1.084	-1.165	-0.00203
0.7	-5.176	1.120	-1.149	-0.00211
0.8	-5.578	1.157	-1.134	-0.00219
0.9	-5.970	1.194	-1.117	-0.00231
1.0	-6.362	1.231	-1.100	-0.00243
1.1	-6.733	1.267	-1.084	-0.00257
1.2	-7.103	1.302	-1.069	-0.00267
1.3	-7.447	1.336	-1.054	-0.00279
1.4	-7.791	1.370	-1.039	-0.00290
1.5	-8.135	1.404	-1.024	-0.00302
2.0	-9.652	1.556	-0.961	-0.00354
2.1	-9.910	1.582	-0.951	-0.00362
2.2	-10.167	1.608	-0.941	-0.00369
2.3	-10.425	1.635	-0.932	-0.00377
2.4	-10.682	1.661	-0.922	-0.00384
2.5	-10.940	1.687	-0.912	-0.00392
2.6	-11.162	1.710	-0.905	-0.00367
2.7	-11.384	1.733	-0.897	-0.00342
2.8	-11.606	1.756	-0.890	-0.00317
2.9	-11.828	1.779	-0.882	-0.00292
3.0	-12.050	1.802	-0.875	-0.00267

Table 27. Minimum Source-Site Distances (km) for NEHRP Type D Sites

Period, T (sec)	Moment Magnitude, M_w						
	5	5.5	6	6.5	7	7.5	8
PGA (T=0.0)	5	5	5	15	25	35	50
0.1	10	30	35	45	60	80	100
0.2	5	5	15	25	35	45	65
0.3	5	5	5	5	15	25	40
0.4	5	5	5	5	5	5	5
0.5	5	5	5	5	5	5	5
0.6	5	5	5	5	5	5	5
0.7	5	5	5	5	5	5	5
0.8	5	5	5	5	5	5	5
0.9	5	5	5	5	5	5	5
1.0	5	5	5	5	5	5	5
1.1	5	5	5	5	5	5	5
1.2	5	5	5	5	5	5	5
1.3	5	5	5	5	5	5	5
1.4	5	5	5	5	5	5	5
1.5	5	5	5	5	5	5	5
1.6	5	5	5	5	5	5	5
1.7	5	5	5	5	5	5	5
1.8	5	5	5	5	5	5	5
1.9	5	5	5	5	5	5	5
2.0	5	5	5	5	5	5	5
2.1	5	5	5	5	5	5	5
2.2	5	5	5	5	5	5	5
2.3	5	5	5	5	5	5	5
2.4	5	5	5	5	5	5	5
2.5	5	5	5	5	5	5	5
2.6	5	5	5	5	5	5	5
2.7	5	5	5	5	5	5	5
2.8	5	5	5	5	5	5	5
2.9	5	5	5	5	5	5	5
3.0	5	5	5	5	5	5	5

Table 28. Minimum Source-Site Distances (km) for NEHRP Type E Sites

Period, T (sec)	Moment Magnitude, M_w						
	5	5.5	6	6.5	7	7.5	8
PGA (T=0.0)	5	5	15	15	25	35	50
0.1	15	25	35	45	65	90	90
0.2	5	10	15	25	40	55	75
0.3	5	5	5	10	20	35	45
0.4	5	5	5	5	15	25	35
0.5	5	5	5	5	5	5	20
0.6	5	5	5	5	5	5	5
0.7	5	5	5	5	5	5	5
0.8	5	5	5	5	5	5	5
0.9	5	5	5	5	5	5	5
1.0	5	5	5	5	5	5	5
1.1	5	5	5	5	5	5	5
1.2	5	5	5	5	5	5	5
1.3	5	5	5	5	5	5	5
1.4	5	5	5	5	5	5	5
1.5	5	5	5	5	5	5	5
1.6	5	5	5	5	5	5	5
1.7	5	5	5	5	5	5	5
1.8	5	5	5	5	5	5	5
1.9	5	5	5	5	5	5	5
2.0	5	5	5	5	5	5	5
2.1	5	5	5	5	5	5	5
2.2	5	5	5	5	5	5	5
2.3	5	5	5	5	5	5	5
2.4	5	5	5	5	5	5	5
2.5	5	5	5	5	5	5	5
2.6	5	5	5	5	5	5	5
2.7	5	5	5	5	5	5	5
2.8	5	5	5	5	5	5	5
2.9	5	5	5	5	5	5	5
3.0	5	5	5	5	5	5	5

D.2.2.2 Constraints with Use of Equation 44

Equation 44 applies to far-field motions only. Therefore, lower-bound source-site distances are specified in tables 27 and 28 as a function of earthquake magnitude and natural period, for NEHRP soil types D and E. Distances used in equation 44 to compute ground motions should not be less than these lower-bound values. In addition, upper-bound values of peak bedrock acceleration and spectral acceleration computed by equation 44 are 1.5 g and 3.75 g respectively.

D.2.2.3 Uncertainties

For each simulation to be addressed with each scenario earthquake, bedrock peak accelerations and spectral accelerations are estimated by accounting for uncertainties in the rate of attenuation of the bedrock motions. This estimation procedure is based on the equation:

$$\ln Y' = \ln Y + \varepsilon \tag{45}$$

where

Y = deterministic value of bedrock acceleration (equation 44).
Y' = sample of Y to be derived that includes uncertainty effect.
ε = normally distributed uncertainty function with expected value of 0 and standard deviation of σ (as specified in table 29) .

In this, Y' is estimated by incorporating the following polar method for generating a normally distributed uncertainty factor in log space (Taylor et al., 1998):

1. Using an operational random number generator, select three uniformly distributed random numbers – U_1, U_2, and U_3 – each between 0 and 1.

2. Let $V_1 = 2 * U_1 - 1$ and $V_2 = 2 * U_2 - 1$. Calculate $W = (V_1)^2 + (V_2)^2$.

3. If $W > 1$, start over at Step 1.

4. If $W \leq 1$, calculate $Z = \sqrt{\frac{-2 \ln W}{W}}$

5. Let $X_1 = V_1 * Z$ and $X_2 = V_2 * Z$.

6. If $U_3 < 0.5$, choose $X = X_1$. Otherwise, choose $X = X_2$.

7. For each Y, calculate

$$Y' = \exp^{\ln Y + X\sigma} \tag{46}$$

where σ is given in table 29 and Y' is subject to the upper limits given in section D.2.2.2.

Table 29. Standard Deviation (σ) of Bedrock Motions

Period, T (sec)	Standard Deviation (σ)	Period, T (sec)	Standard Deviation (σ)
PGA (T=0.0)	0.309	1.6	0.435
0.1	0.311	1.7	0.439
0.2	0.326	1.8	0.443
0.3	0.343	1.9	0.447
0.4	0.357	2.0	0.451
0.5	0.365	2.1	0.453
0.6	0.375	2.2	0.454
0.7	0.383	2.3	0.455
0.8	0.388	2.4	0.457
0.9	0.396	2.5	0.459
1.0	0.404	2.6	0.460
1.1	0.410	2.7	0.462
1.2	0.416	2.8	0.463
1.3	0.421	2.9	0.465
1.4	0.426	3.0	0.466
1.5	0.431	--	--

D.2.3 STEP 3 – CALCULATE SOIL AMPLIFICATION FACTORS (SAFs)

D.2.3.1 Deterministic Estimates of SAF

Assuming a NEHRP soil classification A to E is assigned to each component's site, deterministic site-specific estimates of the SAFs for peak ground acceleration and for spectral accelerations at periods of 0.1 to 3.0 sec are computed from equation 47:

$$\ln SAF = aY'(T = 0) + b \tag{47}$$

where

SAF = Deterministic estimate of the site amplification factor.
a, b = Regression coefficients, as given in table 30.
$Y'(T = 0)$ = Sample bedrock peak acceleration, as derived from step 2 (section D.2.2).

D.2.3.2 Uncertainties

For each simulation, $SAFs$ are estimated (including uncertainties) from equation 48:

Table 30. Regression Coefficients for Soil Amplification Factors
(Hwang et al., 1997)

Period, T (sec)	NEHRP Site A		NEHRP Site B		NEHRP Site C		NEHRP Site D		NEHRP Site E	
	a	b	a	b	a	b	a	b	a	b
PGA (T=0.0)	0	0.336	0	0.463	-0.963	0.771	-2.705	1.001	-3.014	1.187
0.1	0	0.351	0	0.463	-0.928	0.736	-4.038	1.046	-4.457	1.112
0.2	0	0.372	0	0.554	-0.625	1.025	-2.741	1.226	-3.239	1.462
0.3	0	0.372	0	0.577	0.171	0.840	-1.972	1.296	-2.158	1.592
0.4	0	0.365	0	0.582	-0.238	0.925	-1.645	1.462	-2.022	1.792
0.5	0	0.351	0	0.577	-0.154	1.020	-0.741	1.399	-1.306	1.779
0.6	0	0.344	0	0.565	0.097	1.021	-0.424	1.390	-0.817	1.753
0.7	0	0.329	0	0.542	0.260	0.955	-0.481	1.459	-0.571	1.751
0.8	0	0.322	0	0.525	0.401	0.863	-0.173	1.484	-0.094	1.722
0.9	0	0.300	0	0.495	0.281	0.793	0.082	1.439	0.330	1.615
1.0	0	0.285	0	0.470	0.253	0.727	0.411	1.351	0.728	1.479
1.1	0	0.274	0	0.445	0.220	0.672	0.727	1.218	1.001	1.324
1.2	0	0.262	0	0.419	0.188	0.616	1.042	1.085	1.274	1.168
1.3	0	0.249	0	0.396	0.122	0.581	1.036	1.002	1.236	1.075
1.4	0	0.236	0	0.374	0.055	0.547	1.030	0.918	1.199	0.981
1.5	0	0.223	0	0.351	-0.011	0.512	1.024	0.835	1.161	0.888
1.6	0	0.213	0	0.337	-0.012	0.484	0.961	0.788	1.070	0.837
1.7	0	0.203	0	0.322	-0.012	0.456	0.898	0.741	0.979	0.787
1.8	0	0.193	0	0.307	-0.013	0.429	0.834	0.693	0.889	0.736
1.9	0	0.183	0	0.292	-0.013	0.400	0.771	0.646	0.798	0.686
2.0	0	0.173	0	0.278	-0.014	0.373	0.708	0.599	0.707	0.635
2.1	0	0.168	0	0.269	-0.047	0.363	0.625	0.578	0.617	0.614
2.2	0	0.163	0	0.259	-0.081	0.353	0.542	0.556	0.528	0.593
2.3	0	0.158	0	0.250	-0.114	0.343	0.460	0.535	0.438	0.571
2.4	0	0.153	0	0.240	-0.147	0.333	0.377	0.513	0.349	0.550
2.5	0	0.148	0	0.231	-0.181	0.324	0.294	0.492	0.259	0.529
2.6	0	0.145	0	0.225	-0.183	0.315	0.261	0.473	0.229	0.509
2.7	0	0.141	0	0.218	-0.184	0.306	0.228	0.455	0.199	0.488
2.8	0	0.138	0	0.212	-0.186	0.296	0.196	0.436	0.168	0.468
2.9	0	0.134	0	0.205	-0.187	0.287	0.163	0.416	0.138	0.447
3.0	0	0.131	0	0.199	-0.189	0.278	0.130	0.399	0.108	0.427

$$\ln SAF' = \ln SAF + \varepsilon \quad (48)$$

where

SAF = deterministic value of soil amplification factor (from equation 47).
SAF' = sample of Y to be derived that includes uncertainty effects.
ε = normally distributed uncertainty function with expected value of 0 and standard deviation of σ (as specified in table 31).

In this, each SAF' value is estimated by incorporating the following polar method for generating a normally distributed uncertainty factor in log space (Taylor et al., 1998):

1. Using an operational random number generator, select three uniformly distributed random numbers – U_4, U_5, and U_6 -- each between 0 and 1.

2. Let $V_4 = 2 * U_4 - 1$ and $V_5 = 2 * U_5 - 1$. Calculate $W = (V_4)^2 + (V_5)^2$.

3. If $W > 1$, start over at step 1.

4. If $W \leq 1$, calculate $Z = \sqrt{\frac{-2 * \ln W}{W}}$

5. Let $X_4 = V_4 * Z$ and $X_5 = V_5 * Z$.

6. If $U_6 < 0.5$, choose $X = X_4$. Otherwise, choose $X = X_5$.

7. Calculate SAF' using equation 49, where σ is given in table 31.

$$SAF' = \exp^{\ln SAF + X\sigma} \quad (49)$$

D.2.4 STEP 4 – CALCULATE GROUND SURFACE MOTIONS

The ground surface motion at each site is computed for each earthquake and simulation as:

$$Y'' = Y' SAF' \quad (50)$$

where

Y'' = ground surface motion (peak acceleration or spectral acceleration at each natural period), including uncertainties.
Y' = bedrock peak acceleration or spectral acceleration at each natural period, including uncertainties (section D.2.2.3). As before, the peak ground acceleration < 1.5 g, and all spectral accelerations < 3.75 g.
SAF' = soil amplification factor for peak acceleration or spectral acceleration at each natural period, including uncertainties (section D.2.3.2).

Table 31. Standard Deviations (σ) of Soil Amplification Factors (Hwang et al., 1997)

Period, T (sec)	NEHRP Site A	NEHRP Site B	NEHRP Site C	NEHRP Site D	NEHRP Site E
PGA (T=0.0)	0.070	0.127	0.222	0.323	0.273
0.1	0.071	0.143	0.237	0.533	0.427
0.2	0.073	0.174	0.166	0.393	0.374
0.3	0.073	0.196	0.128	0.319	0.314
0.4	0.072	0.215	0.098	0.274	0.266
0.5	0.072	0.214	0.098	0.233	0.244
0.6	0.071	0.246	0.098	0.217	0.222
0.7	0.070	0.241	0.089	0.203	0.199
0.8	0.069	0.237	0.082	0.208	0.188
0.9	0.068	0.230	0.091	0.202	0.173
1.0	0.067	0.208	0.072	0.184	0.171
1.1	0.060	0.195	0.077	0.186	0.179
1.2	0.052	0.182	0.082	0.188	0.186
1.3	0.051	0.173	0.082	0.193	0.189
1.4	0.051	0.165	0.083	0.199	0.192
1.5	0.050	0.156	0.083	0.204	0.196
1.6	0.050	0.149	0.083	0.201	0.189
1.7	0.049	0.141	0.083	0.198	0.182
1.8	0.049	0.134	0.083	0.194	0.175
1.9	0.048	0.126	0.083	0.191	0.168
2.0	0.048	0.119	0.083	0.188	0.161
2.1	0.045	0.115	0.081	0.184	0.162
2.2	0.043	0.112	0.080	0.180	0.164
2.3	0.040	0.108	0.078	0.175	0.165
2.4	0.038	0.105	0.077	0.171	0.167
2.5	0.035	0.101	0.075	0.167	0.168
2.6	0.037	0.098	0.074	0.164	0.165
2.7	0.039	0.095	0.072	0.162	0.162
2.8	0.042	0.091	0.071	0.159	0.160
2.9	0.044	0.088	0.069	0.157	0.157
3.0	0.046	0.085	0.068	0.154	0.154

APPENDIX E
LIQUEFACTION HAZARD EVALUATION FOR SRA OF HIGHWAY SYSTEMS

E.1 INTRODUCTION

This appendix describes the adaptation of the Youd (1998) liquefaction hazard evaluation procedure for incorporation into the hazards module of this highway system SRA methodology.

Fundamental to the implementation of this process is the compilation of necessary soils and geologic data for the site soil materials throughout the highway system. In what follows, the necessary data for implementing each step of the process will be listed as part of the documentation of that step.

E.2 EVALUATION PROCEDURE

Evaluation of liquefaction hazards consists of the following steps: (1) initial screening based on geologic and soils data only, to initially establish which sites in the system have a low potential for liquefaction and therefore can be eliminated from further analysis; (2) further screening of the remaining sites through very simplified and conservative assessment of the ground shaking hazard in each cell due to each scenario earthquake and simulation, to identify additional sites for which the liquefaction potential is very low for that particular earthquake and simulation; (3) further evaluation of the liquefaction susceptibility at each remaining site, using the Seed-Idriss (1982) procedure; (4) for each bridge site and each roadway site with liquefiable soils and gently sloping ground or a free face condition, use of the latest models by Youd and his associates (Youd et al., 1999) to estimate lateral spread displacements; and (5) use of the Tokimatsu-Seed (1987) procedure to estimate liquefaction-induced vertical settlements.

Step 1 (initial screening) is carried out by the user prior to initiating the SRA methodology. However, this important step is summarized in this appendix in order to guide potential users in its implementation. The hazards module contained in the SRA software will include steps 2 through 5 only, which are carried out for each scenario earthquake and simulation.

E.2.1 STEP 1 – INITIAL SCREENING

Step 1 provides initial screening of the sites within the highway system by the user. Under this step, sites will be identified that have a low potential for liquefaction based on geologic and soils information, and can therefore be eliminated from further evaluation after Step 1.

E.2.1.1 Input Data Requirements

The input data for this step consists of: (a) locations and properties of Quarternary geologic units in the area; (b) highest average or likely depth to unconfined ground water table, either permanent and perched; (c) soil boring log data consisting of penetration resistance, Atterberg limits, clay content, and natural moisture content; and (d) soil classifications, by either the AASHTO, Unified, or NEHRP classification systems.

E.2.1.2 Screening Procedures

- ***Step 1-a. Geologic Analysis.*** Geologic units and depositional processes are evaluated in order to identify those sites along the highway system that can be classes as low-hazard sites. These sites are eliminated from further liquefaction analysis. This evaluation is based on comparisons of the geologic input data to geologic screening criteria that are shown in table 32 and are based on analysis of geologic conditions at sites of past liquefactio (Youd and Perkins, 1978).

- ***Step 1-b. Water Table Analysis.*** For those cells not eliminated by step 1-a, water-table depths at these sites are evaluated. Based on recommendations fromYoud (1998), sites with water table depths that exceed 15 m are eliminated from further liquefaction analysis.

- ***Step 1-c. Evaluation for Extra-Sensitive Clays.*** A check is made for potential loss of strength in clays with large fractions of colloidal-sized particles in which loss of strength is usually caused be leaching of salts from interstitial water. These clays are found in only a few areas of the U.S. (Alaska, St. Lawrence river valley, and saline lakes of the Great Basin or in esturine sediments along coastal rivers or bays). Clays are classed as extra-sensitive if all of the following conditions are met: (a) liquid limit < 40%; (b) moisture content > 0.9 times the liquid limit (liquidity index > 0.6); (c) a corrected penetration resistance $(N_1)_{60} < 5$, or a corrected and normalized cone penetration resistance < 1 MPa. Only UCS soil types CL or ML and AASHTO soil types A-4, A-2-4, A-6, and A-2-6 meet these criteria. If the soils at a site do not meet all of these conditions, they are classed as non-sensitive.

- ***Step 1-d. Soil Classification Evaluation.*** Fine grained soils are classed as potentially liquefiable if they meet all of the following conditions: (a) clay fraction (percent finer than 0.005 mm) < 15%; (b) liquid limit (LL) > 35%; and (c) moisture content (MC) < 0.9LL. Fine grained soils that do not meet all of these conditions are classed as non-liquefiable.

E.2.1.3 Prior Liquefaction Evaluations by Others

In addition to screening based on geologic and subsurface soils data, the user should also review prior liquefaction evaluations carried out by others in the region containing the highway system. These may be: (a) prior liquefaction evaluations at sites near the highway system; (b) liquefaction hazard maps for the quadrangles or regions where the system is located; and (c) reports of liquefaction occurrences along or near the system during past earthquakes. Such prior evaluations should be used in this initial screening step to supplement interpretations of geologic and soils data as described in section E.2.1.2. Also, they may facilitate interpretation of the results from steps 2 through 5 of the procedure, as described in the remainder of this appendix.

E.2.2 STEP 2 – FURTHER SCREENING

Step 2 is a supplementary screening process that is the first step to be included in the liquefaction evaluation under the hazards module of the SRA methodology. It is carried out for each scenario earthquake and simulation, to identify those sites remaining after the step 1

geologic screening that have a low potential for liquefaction under this particular earthquake and simulation and therefore can be eliminated from further evaluation after step 2.

Table 32. Estimated Susceptibility of Sedimentary Deposits to Liquefaction during Strong Seismic Shaking (Youd and Perkins, 1978)

Type of Deposit	General Distribution of Cohesionless Sediments in Deposits	Likelihood that Cohesionless Sediments when Saturated would be Susceptible to Liquefaction (by Age of Deposit)			
		<500 years	Holocene	Pleistocene	Pre-Pleistocene
(a) Continental Deposits					
River Channel	Locally Variable	Very High	High	Low	Very Low
Flood Plain	Locally Variable	High	Moderate	Low	Very Low
Alluvial Fan and Plain	Widespread	Moderate	Low	Low	Very Low
Marine Terraces and Plains	Widespread	–	Low	Very Low	Very Low
Delta and Fan Delta	Widespread	High	Moderate	Low	Very Low
Lacustrine and Playa	Variable	High	Moderate	Low	Very Low
Colluvium	Variable	High	Moderate	Low	Very Low
Talus	Widespread	Low	Low	Very Low	Very Low
Dunes	Widespread	High	Moderate	Low	Very Low
Loess	Variable	High	High	High	Very Low
Glacial Till	Variable	Low	Low	Very Low	Very Low
Tuff	Rare	Low	Low	Very Low	Very Low
Tephra	Widespread	High	High	?	Very Low
Residual Soils	Rare	Low	Low	Very Low	Very Low
Sebka	Locally Variable	High	Moderate	Low	Very Low
(b) Coastal Zone					
Delta	Widespread	Very High	High	Low	Very Low
Esturine	Locally Variable	High	Moderate	Low	Very Low
Beach					
High Wave Energy	Widespread	Moderate	Low	Very Low	Very Low
Low Wave Energy	Widespread	High	Moderate	Low	Very Low
Lagoonal	Locally Variable	High	Moderate	Low	Very Low
Fore Shore	Locally Variable	High	Moderate	Low	Very Low
(c) Artificial					
Uncompacted Fill	Variable	Very High	–	–	–
Compacted Fill	Variable	Low	–	–	–

E.2.2.1 Input Data

The input data needed to carry out step 2 are: (a) the moment magnitude of the scenario earthquake (M_w); (b) the peak horizontal acceleration of the site-specific ground motions at each site (PGA) for the given earthquake and simulation, in units of g; and (c) the AASHTO or NEHRP site classification for the soils at each site.

E.2.2.2 Evaluation Procedure

Table 33 provides conservative estimates of threshold PGAs leading to onset of liquefaction in very susceptible natural soil deposits for a range of scenario earthquake magnitudes and site conditions. If, for a given scenario earthquake and simulation, the PGA at a given site falls below these threshold PGA values (for the soil profile type representative of the site), the site is classed as non-liquefiable and is eliminated from further analysis for that scenario earthquake and simulation.

Table 33. Minimum Earthquake Magnitudes and Peak Horizontal Ground Accelerations with Allowance for Local Site Amplification, that are Capable of Generating Liquefaction in Very Susceptible Natural Deposits (Youd, 1998)

Earthquake Moment Magnitude, M_w	Liquefaction Hazards at Bridge Sites	
	AASHTO Soil Types I and II (Stiff Site Conditions which correspond to NEHRP Soil Types B and C respectively)	AASHTO Soil Type III (Soft Site Conditions which correspond to NEHRP Soil Type D or E)
$M_w < 5.2$	Very low hazard for PGA < 0.4 g	Very low hazard for PGA < 0.1g
$5.2 \leq M_w < 6.4$	Very low hazard for PGA < 0.1 g	Very low hazard for PGA < 0.05 g
$6.4 \leq M_w < 7.6$	Very low hazard for PGA < 0.05 g	Very low hazard for PGA < 0.025 g
$M_w \geq 7.6$	Very low hazard for PGA < 0.025 g	Very low hazard for PGA < 0.025 g

E.2.3 STEP 3 – LIQUEFACTION SUSCEPTIBILITY EVALUATION

For those sites not eliminated by steps 1 and 2, step 3 uses Seed-Idriss methods (1982) to carry out more detailed evaluations of liquefaction potential for each scenario earthquake and simulation.

E.2.3.1 Input Data

Two sets of input parameters are needed. The first depends on the particular scenario earthquake and simulation being considered and consists of: (a) the moment magnitude of the earthquake, M_w, and (b) the peak horizontal acceleration at the ground surface, PGA. The second set of input parameters describes the soil materials in each layer and the depth of the water table below the ground surface. For the i^{th} layer, the input parameters are the thickness T_i, measured standard penetration resistance N_{mi}, total unit weight γ_i, and fines content (in percent), F_i.

E.2.3.2 Evaluation Procedure

The following procedure computes the factor of safety against liquefaction in each saturated soil layer as the ratio of the liquefaction capacity of the layer (denoted as CRR) to the earthquake demands on layer (denoted as CSR). Layers with a factor of safety less than 1.0 are presumed to liquefy during the earthquake. For sites with liquefiable layers, lateral spread displacements and vertical settlements are computed as described in steps 4 and 5 of this appendix.

E.2.3.2(a) Step 3-1. Estimate Depth-Dependent Stress Reduction Factor, r_d.

In the absence of estimates of r_d provided by the user, the following default values are used to define r_d as a function of the depth below the ground surface, z, in meters (Youd, 1998)

$$r_d = 1.0 - 0.00765z \quad \text{for} \quad z \le 9.2m \tag{51}$$

$$r_d = 1.174 - 0.0267z \quad \text{for} \quad 9.2m \le z < 23m \tag{52}$$

$$r_d = 0.744 - 0.008z \quad \text{for} \quad 23m \le z \le 30m \tag{53}$$

$$r_d = 0.50 \quad \text{for} \quad z > 30m \tag{54}$$

Equations 51 to 54 are used to compute r_d at the mid-thickness of each layer that is either entirely above or entirely below the water table. If the site contains a layer j where the top of the water table is within the layer, r_d is computed at the mid-thickness of the portion of the layer that is below the water table.

E.2.3.2(b) Step 3-2. Compute Total Overburden Pressure, σ_{vo}.

The total overburden pressure, σ_{vo} of a given layer will depend on its unit weight and thickness, as well as the unit weight and thickness of all overlying layers. It is computed at the mid-thickness of each layer either entirely above or entirely below the water table. If the top of

the water table is within the thickness of a given layer, the total overburden pressure is computed at the mid-thickness of that portion of the layer that is below the water table.

E.2.3.2(c) Step 3-3. Calculate Effective Overburden Pressure, σ_{vo}'.

The effective overburden pressure of a given layer, σ_{vo}', will depend on the depth of the water table and the thickness and unit weight of the layer and all overlying layers. As for the total overburden pressure, the effective overburden pressure is computed at the mid-height of each potentially liquefiable layer that is totally below the water table. In addition, if the top of the water table is within the height of the layer, the effective overburden pressure is computed at the mid-thickness of the saturated portion of the layer.

E.2.3.2(d) Step 3-4. Calculate Demand Cyclic Stress Ratio, CSR.

The demand cyclic stress ratio, CSR, is computed as:

$$CSR = 0.65\frac{PGA * \sigma_{vo}}{g * \sigma_{vo}'} r_d \tag{55}$$

where PGA is the peak ground acceleration at the ground surface, g is the acceleration of gravity (981.5 cm/sec^2, or 32.2 ft/sec^2), r_d has been computed using one of equations 51 through 54 in step 3A, and σ_{vo} and σ_{vo}' have been computed in steps 3-2 and 3-3.

E.2.3.2(e) Step 3-5. Calculate Cyclic Resistance Ratio, CRR(M_w).

Substep 3-5-1. Use equation 56 (Youd, 1998) to calculate corrected penetration resistance, $(N_1)_{60}$, that accounts for overburden pressure and hammer energy ratio.

$$(N_1)_{60} = N_m C_N C_E \tag{56}$$

where

N_m = measured standard penetration resistance.

C_N = correction factor for overburden pressure = $\sqrt{\frac{100}{(\sigma'_{vo})*}}$ (57)

$(\sigma'_{vo})*$ = effective overburden pressure in units of kPa.

C_E = correction factor for hammer energy ratio = 0.85 (which is the average of the range of values for C_E (0.5 to 1.2) given in Youd (1998).

Youd (1998) provides additional correction factors for borehole diameter, rod length, and samplers with or without liners. However, these additional factors are neglected here, because these details of the standard penetration tests will usually not be known for most of the conventional (and older) bridges, roadways, and other highway system components in many parts of the country.

Substep 3-5-2. Compute corrected penetration resistance that accounts for fines content, $(N_1)_{60cs}$.

From Youd (1998):

$$(N_1)_{60cs} = \alpha + \beta(N_1)_{60} \tag{58}$$

where α and β are coefficients determined from equations 59 and 60:

$$\begin{aligned} \alpha &= 0 && \text{for} \quad F_i \le 5\% \\ \alpha &= \exp[1.76 - (\frac{190}{F_i^2})] && \text{for} \quad 5\% < F_i < 35\% \\ \alpha &= 5.0 && \text{for} \quad F_i \ge 35\% \end{aligned} \tag{59}$$

and

$$\begin{aligned} \beta &= 1.0 && \text{for} \quad F_i \le 5\% \\ \beta &= 0.9 + \frac{(F_i)^{1.5}}{1000} && \text{for} \quad 5\% < F_i < 35\% \\ \beta &= 1.2 && \text{for} \quad F_i \ge 35\% \end{aligned} \tag{60}$$

In the above expressions for α and β, F_i is the fines content in the ith layer (in units of percent) as measured from laboratory gradation tests on retrieved soil samples.

Substep 3-5-3. Use equation 61 (Youd, 1998) to compute baseline value of CRR (denoted as $CRR_{7.5}$) that corresponds to constant moment magnitude of 7.5 and fines content < 5%.

$$CRR_{7.5} = \frac{a + cx + ex^2 + gx^3}{1 + bx + dx^2 + fx^3 + hx^4} \tag{61}$$

where

$x = (N_1)_{60cs}$ = standard penetration resistance corrected to a clean sand equivalent value, and also corrected for overburden pressure and hammer energy ratio (see step 3-5-2 above).

and

a = 0.048, b = - 0.1248, c = - 0.004721, d = 0.009578, e = 0.0006136, f = - 0.0003285, g = - 1.673 x 10^{-5}, and h = 3.714 x 10^{-6}.

Substep 3-5-4. For moment magnitude M_w of scenario earthquake, use equation 62 to calculate magnitude scaling factor, MSF (Youd, personal communication, 1999).

$$MSF = (\frac{M_w}{7.5})^{-2.56} \quad (62)$$

Substep 3-5-5. Use equation 63 to compute cyclic resistance ratio as function of moment magnitude of scenario earthquake, $CRR(M_w)$.

$$CRR(M_w) = CRR_{7.5} * MSF \quad (63)$$

E.2.3.2(f) Step 3-6. Compute Factor of Safety against Liquefaction.

Equation 64 is used to compute the factor of safety against liquefaction (FS):

$$FS = \frac{CRR(M_w)}{CSR} \quad (64)$$

As the factor of safety decreases, the potential for liquefaction increases. For this adaptation, it is assumed that if the factor of safety is greater than 1.0, then no liquefaction will occur. Otherwise, the site is assumed to have liquefied, and liquefaction-induced lateral-spread and vertical displacements are calculated (see steps 4 and 5).

E.2.4 STEP 4 – CALCULATION OF LATERAL SPREAD DISPLACEMENT

As noted in Youd (1998), the most common cause of liquefaction-induced bridge damage has been lateral ground displacement. This highway system SRA methodology uses the empirical approach developed by Bartlett and Youd (1995) with subsequent modifications by Youd et al, (1999)

E.2.4.1 Input Data

Two sets of input data are needed. The first set depends on the particular scenario earthquake being considered, and the second set describes the soil properties at the site.

E.2.4.1(a) Earthquake-Dependent Data

This set of input data consists of: (a) the moment magnitude of the earthquake, M_w, and (b) the horizontal distance from the seismic energy source to the site, in kilometers, R. For sites west of the Rocky Mountains, the distance R can be taken as the actual distance from the scenario earthquake to each site along the highway system. For sites east of the Rocky Mountains, R is defined in terms of an equivalent distance R_{eq}. The following procedure has been developed to estimate R_{eq} for each scenario earthquake and for each site along the highway system, n accordance with figure 5-2 of Youd, 1998.

- From the moment magnitude of the scenario earthquake (M_w) and the peak ground acceleration at a given site, (PGA), equation 65 is used to compute the parameter b:

$$b = M_w - 12 * PGA \tag{65}$$

- This computed value of b is used with table 53 to estimate the value of R_{eq} for the given site and scenario earthquake. Where this computed value of b falls between two values of b_{eq} in table 34, linear interpolation is used to obtain the corresponding value of R_{eq}.

Table 34. Determination of R_{eq} for Sites East of Rocky Mountains

R_{eq} (km)	b_{eq}
1	2.5
5	2.7
10	3.0
20	4.0
30	4.4
40	4.9
50	5.2
60	5.5
80	5.9
100	6.3
150	6.8
200	7.2

- To illustrate this process, assume that M_w = 5.5 and PGA = 0.1 g. For this case, equation 65 leads to a value of b = 4.3, and table E-3 shows that R_{eq} is about 28 km. It is noted that the limiting R_{eq} values given in figure 5-2 of Youd (1998) range from 1 km to 200 km.

E.2.4.1(b) Site Soils Data

The input site soils data consists of: (a) S = the ground slope, in percent; and (b) W = the ratio of the height (H) of the free face to the distance (L) from the base of the free face to the point in question, in percent (see equation 66 and figure 37)

$$S = \frac{1}{X} * 100{,}0 \qquad \text{and} \qquad W = \frac{H}{L} * 100.0 \tag{66}$$

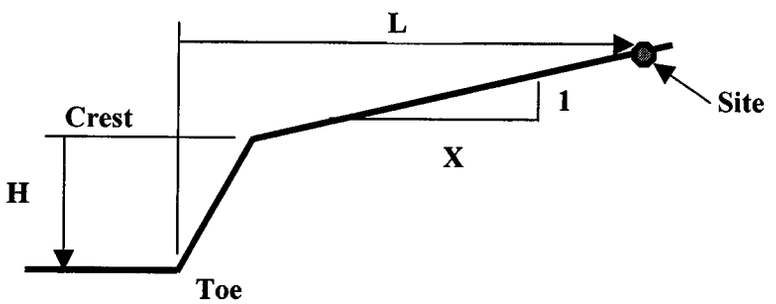

Figure 37. Definition of Slope, S, and Free-Face Ratio, W

E.2.4.1(c) Layer Screening and Grouping

Before beginning the displacement calculations, the user determines if any layers in the site have fines contents and mean grain sizes that are very different from the other layers. If so, these are grouped into separate sets of sublayers (each with similar fines contents and mean grain sizes). For each sublayer in each set, the user then specifies the thickness T_i, fines content F_i (i.e., fraction of the sediment sample passing a No. 200 sieve), and mean grain size D_{50_i}.

The lateral spread displacement calculations are carried out only for those layers or sublayers that contain saturated granular soils with $(N_1)_{60cs} < 15$. The user identifies these layers by providing the following input parameters for each layer:

- *Soil Material (CODE1)*: The user sets CODE1 = 0 if the soil material in the layer is not granular, and CODE1 = 1 if the soil material is granular.

- *Water Table (CODE2)*: The user sets CODE2 = 0 if the bottom of layer is at or above the water table, and CODE2 = 1 if the bottom of layer is below the water table.

- *Corrected Blowcount Values $(N_1)_{60cs}$ (CODE3)*: The user sets CODE3 = 0 if $(N_1)_{60cs} \geq 15$, and CODE3 = 1 if $(N1)_{60cs} < 15$.

After these parameters are specified for a given layer, a composite code parameter $CODE_{ch}$ = CODE1*CODE2*CODE3 is computed for that layer. If $CODE_{ch} = 1$, the layer is included in the lateral spread displacement calculations. If $CODE_{ch} = 0$, the layer is not included.

E.2.4.2 Best Estimate Calculations

The SRA methodology uses the following steps to calculate the best-estimate incremental lateral-spread displacement value for each group of sublayers:

- Use equation 67 to calculate the cumulative thickness of all sublayers within the group:

$$T_{15} = \sum_{i=1}^{L} T_i \tag{67}$$

where T_i is the thickness of the i[th] sublayer, and L is the a number of sublayers in the group.

- For all sublayers in T_{15}, use equation 68 to compute the fines content F_{15} (fraction of the soil sample passing a No. 200 sieve) and the average mean grain size in millimeters $D_{50_{15}}$:

$$F_{15} = \frac{\sum_{i=1}^{L} F_i T_i}{T_{15}} \quad \text{and} \quad D_{50_{15}} = \frac{\sum_{i=1}^{L} D_{50_i} T_i}{T_{15}} \tag{68}$$

where, as noted above, F_i, D_{50_i}, and T_i are the fines content, mean grain size, and thickness respectively in the i[th] sublayer within T_{15}, and L is the total number of such sublayers.

- Use equations 69 through 71 to compute the best-estimate value of lateral spread displacement (in meters), D_H, for sites with free face conditions (W < 20%) or with ground slope conditions (W ≥ 20%) (Youd et al., 1999):

For free-face conditions:

$$\log D_H = -18.172 + 1.586M_w - 1.522\log_{10} R^* - 0.011R + 0.553\log_{10} W + 0.546\log_{10} T_{15} + 3.989\log_{10}(100 - F_{15}) - 0.934\log_{10}(D50_{15} + 0.1mm) \tag{69}$$

For ground slope conditions:

$$\log D_H = -17.700 + 1.586M_w - 1.522\log_{10} R^* - 0.011R + 0.344\log_{10} S + 0.546\log_{10} T_{15} + 3.989\log_{10}(100 - F_{15}) - 0.934\log_{10}(D50_{15} + 0.1mm) \tag{70}$$

where, in equations 69 and 70

$$R^* = R + R_o \quad \text{and} \quad R_o = 0.89M_w - 5.94 \tag{71}$$

Note that, when applied to an individual group of sublayers as described above, these equations yield a best-estimate incremental value of D_H for the group.

- Repeat the above calculations for each group of sublayers. Then, sum these incremental D_H values computed for each group to obtain the total best-estimate D_H value for the site, for this particular scenario earthquake and simulation (Youd, personal communication, 1999).

E.2.4.3 Incorporation of Uncertainty

In the above analysis procedure for lateral spread displacement, there are numerous uncertainties in the various input parameters and correction factors. Since progress in incorporating these uncertainties is likely to be slow (Youd and Power, personal communication, 1999), these uncertainties will be ignored for now. Only modeling errors in the development of the lateral spread displacement calculation procedure are incorporated, as summarized below.

This calculation procedure is basically a linear regression model in which the dependent variable is treated in logarithmic terms. This model is considered to be of the form:

$$Y_i = \alpha_i + \sum \beta_i X_i + \varepsilon_i \qquad (72)$$

where α_i is the intercept coefficient (should all X_i's be 0),
β_i's are slope coefficients,
Y_i is the independent variable for the i^{th} trial,
X_i's are the dependent variables for the i^{th} trial, and
ε_i is an error term with a mean value of 0 and a variance of σ^2.

On page 5-14, Bartlett and Youd (1992) derive 0.207 as the standard deviation for equation 70. They also apply a fairly complex statistical procedure (involving a variance-covariance matrix for the independent variables) to derive confidence levels for various estimates. (See pp. 5-14ff).

Therefore, for incorporating uncertainty as derived from the model itself (and ignoring other uncertainties), it is assumed that the uncertainty for the model has a gaussian (normal) distribution with a variance of $(0.207)^2 = 0.0428$. The following steps are carried out to incorporate uncertainties on this basis:

- Start with the estimate of total D_H for the given scenario earthquake, simulation, and site in question, computed as the sum of the incremental D_H values computed using equation 68 or 69 for each sublayer.

- For each simulation, obtain three uniform random numbers $U_{j,1}$, $U_{j,2}$, and $U_{j,3}$ with values between 0 and 1.

- Use the following steps to develop a standardized normal distribution N(0,1), that is a normal distribution with a mean of 0 and a variance of 1 (Taylor et al., 1998):

  Step 4-1. Compute $V_{j,1} = 2 * U_{j,1} - 1$ and $V_{j,2} = 2 * U_{j,2} - 1$. From this, compute $Z = (V_{j,1})^2 + (V_{j,2})^2$

  Step 4-2. If $Z \geq 1$, start over with two new uniform random numbers $U_{j,1}$, $U_{j,2}$. Otherwise, if $Z < 1$, compute $Y_{j,1} = \sqrt{\frac{-2 * \ln Z}{Z}}$

  Step 4-3. Compute $X_{j,1} = V_{j,1} * Y_{j,1}$ and $X_{j,2} = V_{j,2} * Y_{j,2}$.

- The end results of steps 4-1 to 4-3 are two normally distributed samples $X_{j,1}$ and $X_{j,2}$, which can be used in steps 4-4 and 4-5 below to develop a single sample estimate of permanent ground displacement.

  Step 4-4. If $U_{j,3} < 0.5$, set $X = X_{j,1}$. Otherwise, set $X = X_{j,2}$.

  Step 4-5. Compute $\log_{10} D_H' = \log_{10} D_H + 0.207 * X$, where D_H' is the value of the lateral spread displacement including uncertainties, and D_H is the best-estimate displacement value (section E.2.4.2). From this, $D_H' = 10^{\log_{10} D_H'}$.

E.2.5 STEP 5 – CALCULATION OF GROUND SETTLEMENT

The Tokimatsu-Seed (1987) procedure is used in the SRA methodology to compute liquefaction-induced ground settlement. The input data needed for this procedure, and how the procedure is incorporated into the SRA methodology, are described below.

E.2.5.1 Input Data

The input data needed to estimate ground settlement using the Tokimatsu-Seed procedure is the same as those required for the application of the Seed-Idriss procedure for estimating liquefaction potential (see section E.2.3), plus estimates of layer thicknesses. In addition, it is necessary to identify those layers within the site that are to be included in the settlement calculations. In this, it is noted that, because of dilatency, moderately dense sands do not easily deform in shear but can still densify somewhat. Therefore, it is reasonable that the criteria for including layers in the settlement calculations and the lateral spread displacement calculations (section E.2.4.1.(c)) should be different. Saturated granular soils with corrected blowcounts of $(N1)_{60cs} \geq 15$ are too dense to significantly deform in shear, but may settle with volumetric strains up to 2 percent (Youd, personal communication, 1999). Accordingly, the SRA methodology includes all saturated granular layers in the ground settlement calculations for the site, regardless of their corrected blowcount values. The methodology screens all layers in the site for this purpose by considering the CODE1 and CODE2 parameters previously input by the

user where, as noted in section E.2.4.1(c), CODE1 = 1 if the soils in the layer are granular and = 0 otherwise, and CODE2 = 1 if the soils in the layer are saturated (i.e., below the water table) and = 0 otherwise. Then, a composite parameter $CODE_{cv}$ = CODE1*CODE2 is computed for the layer. If $CODE_{cv}$ = 1, the layer is included in the settlement calculations whereas, if $CODE_{cv}$ = 0, the layer is not included in the calculations.

E.2.5.2 Evaluation Procedure

The following four-step process is used to replicate the Tokimatsu-Seed results (i.e., figure 38) in the SRA methodology. In this, the volumetric strain in each layer, VS (in percent). is computed as a function of the layer's demand cyclic stress ratio, CSR, (see equation 55) and its corrected penetration resistance $(N_1)_{60cs}$ (equations 56 and 58). The layer's volumetric strain is multiplied by the layer thickness to obtain the vertical settlement of that layer. The total ground settlement at the site is then computed as the sum of all of the layer settlements. The four steps that comprise this process are described below.

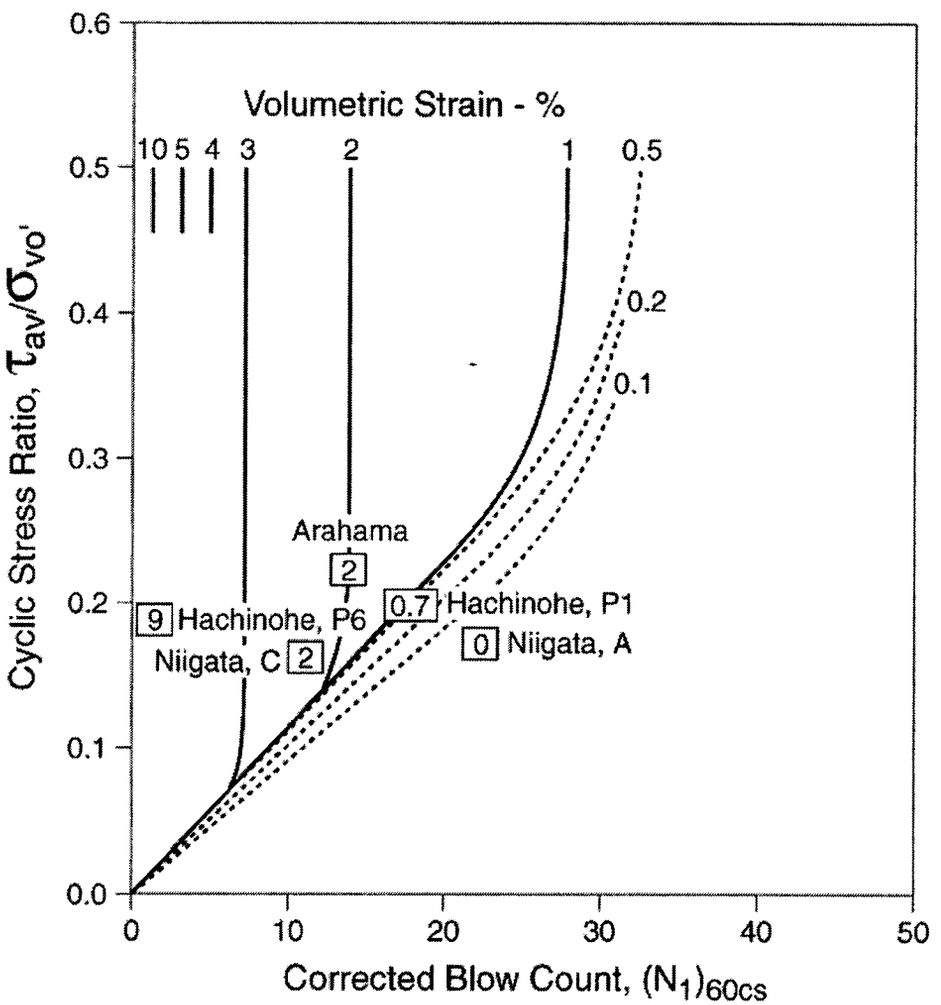

Figure 38. Tokimatsu-Seed Calculation of Liquefaction-Induced Volumetric Strains (Tokimatsu-Seed, 1987)

E.2.5.2(a) Step 5-1. Check if Volumetric Strain (VS) in Layer (in percent strain) is Nonzero .

- If $(N_1)_{60cs} \geq 35$, $VS = 0.0\%$. Otherwise go to step 5-2.

E.2.5.2(b) Step 5-2. Analysis of Layer in Vertical Line Regime of Figure 38 for 2% ≤ VS ≤ 10%.

Substep 5-2-1. Check to see if layer is somewhere in this vertical line regime.

- If $(N_1)_{60cs} > 13$, go to step 5-3 (i.e., layer is in curved line regime of figure 38).
- $(N_1)_{60cs} \leq 13$. Check if $CSR \geq 0.01 * (N_1)_{60cs}$. If so, layer is in vertical line regime. Go to substep 5-2-2 to determine VS. Otherwise go to step 5-3.

Substep 5-2-2. Check if layer is in vertical line regime for VS = 10%.

- If $(N_1)_{60cs} < 1$, $VS = 10\%$. Otherwise go to substep 5-2-3.

Substep 5-2-3. Check if layer is in vertical line regime for VS between 5 and 10 percent.

- If $(N_1)_{60cs} < 3$, use equation 73 to compute VS. Otherwise, go to substep 5-2-4.

$$VS = 12.5 - 2.5 * (N_1)_{60cs} \tag{73}$$

where $1 \leq (N_1)_{60cs} < 3$ and $10\% \geq VS > 5\%$.

Substep 5-2-4. Check if layer is in vertical line regime for VS between 3 and 5 percent.

- If $(N_1)_{60cs} < 7$, use equation 74 to compute VS. Otherwise, go to substep 5-2-5.

$$VS = 6.5 - 0.5 * (N_1)_{60cs} \tag{74}$$

where $3 \leq (N_1)_{60cs} < 7$ and $5\% \geq VS > 3\%$.

Substep 5-2-5. Layer is in vertical line regime for VS between 2 and 3 percent. Use equation 75 to compute VS.

$$VS = 4.16667 - 0.16667 * (N_1)_{60cs} \tag{75}$$

where $7 \leq (N_1)_{60cs} < 13$ and $3\% \geq VS > 2\%$.

E.2.5.2(c) Step 5-3. Analysis for CSR and $(N_1)_{60cs}$ within Curved Line Regimes of Figure 38.

For a layer somewhere in the curved line regimes, use the following substeps to obtain VS.

Substep 5-3-1. Check if layer is along curve for VS = 1%.

- Calculate $y = 0.000036*[(N_1)_{60cs}]^3 - 0.00118*[(N_1)_{60cs}]^2 + 0.0202*(N_1)_{60cs}$ (76)
- If $CSR < y$, go to substep 5-3-2. Otherwise, $VS = 1\%$.

Substep 5-3-2. Check if layer is along curve for VS = 0.5%.

- Calculate $y = 0.000023*[N_1)_{60cs}]^3 - 0.0075*[N_1)_{60cs}]^2 + 0.016167*(N_1)_{60cs}$ (77)
- If $CSR < y$, go to substep 5-3-3. Otherwise, $VS = 0.5\%$.

Substep 5-3-3. Check if layer is along curve for VS = 0.2%.

- Calculate $y = 0.0000153*[(N_1)_{60cs}]^3 - 0.00051*[(N_1)_{60cs}]^2 + 0.013567*(N_1)_{60cs}$ (78)
- If $CSR < y$, go to substep 5-3-4. Otherwise, $VS = 0.2\%$.

Substep 5-3-4. Check if layer is along curve for VS = 0.1%.

- Calculate $y = 0.000018*[(N_1)_{60cs}]^3 - 0.00059*[(N_1)_{60cs}]^2 + 0.0131*(N_1)_{60cs}$ (79)
- If $CSR < y$, then $VS = 0.1\%$. Otherwise, $VS = 0.0\%$.

E.2.5.2(d) Step 5-4. Estimate Total Settlement at Site.

At this point, we assume that: (a) there are I layers at the site, for a volumetric strain VS_i (in units of percent) has been computed for the i^{th} layer; and (b) the i^{th} layer has a thickness T_i. Then, the total settlement at the site is computed from the following substeps:

Substep 5-4-1. Assuming one-dimensional consolidation, estimate the incremental change of thickness of the i^{th} layer $(\Delta T)_i$ as follows:

$$(\Delta T)_i = \frac{(VS)_i T_i}{100} \tag{80}$$

where the above division by 100 is because $(VS)_i$ has been computed in units of percent.

Substep 5-4-2. Compute total settlement of at the site, Z, as the sum of the incremental changes of thickness of all of the layers at the site:

$$Z = \sum_{i=1}^{I} (\Delta T)_i \tag{81}$$

APPENDIX F
DAMAGE STATE FRAGILITY CURVES FOR BRIDGES

F.1 BACKGROUND

This appendix describes the two alternative procedures used in the SRA methodology to obtain damage state fragility curves for bridges commonly found in highway systems. The first is a "rapid pushover" method developed by Mander and his associates (Dutta and Mander, 1998, Mander and Basoz, 1999 and FHWA, 1995a) for application to bridges nationwide. The second procedure is based on the elastic demand-capacity method (FHWA, 1995a). It was developed by Jernigan (1998) and Jernigan and Hwang (1997) specifically for bridges in the Shelby County highway system, and has been used in the demonstration SRA of the Shelby County, Tennessee highway system that is described in chapter 7.

In addition to these approaches, the SRA methodology enables the users to specify their own fragility curves for any bridge in the system. As discussed in chapter 5, the development of such curves could be time consuming and is therefore recommended primarily for use at bridges with unusual configurations that may not be fully represented by the fragility curve procedures described in this appendix. Appendix G further addresses user-specified fragility curves.

F.2 RAPID PUSHOVER METHOD

The rapid pushover method has recently been incorporated into the SRA methodology. It has the following features for modeling of large numbers of commonly occurring bridges: (a) it provides rapid estimation of bridge damage states; (b) it uses simplified but rational engineering procedures that are based on principles of mechanics; and (c) its input data for each bridge are readily available through the National Bridge Inventory database (FHWA, 1995b). Because of these features, the rapid pushover method is the preferred approach for use in the SRA methodology. This method, which was summarized in chapter 5, is further described in the remainder of this section.

F.2.1 CAPACITY EVALUATION

The rapid pushover method uses the approach outlined below to establish the spectral acceleration leading to the onset of each of the five damage states for each of several different "standard bridge" classifications (see tables 5 and 35). A "standard bridge" is defined as a long bridge with no skew and no three-dimensional (3D) effects from deck-arching membrane action. The standard bridge types that are considered are: (a) simply-supported bridges on multi-column bents; (b) discontinuous box girder bridges on single-column bents (unique to California); (c) continuous reinforced- or prestressed-concrete bridges; (d) continuous steel bridges; (e) single-span bridges; and (f) major bridges, whose span length exceeds 150 m.

- The analytical formulation in Mander and Basoz (1999) first establishes a pushover-type capacity curve for each standard bridge type. This curve is represented by an equivalent five-

percent damped spectral acceleration vs. spectral displacement (which can be related to drift). The spectral displacements (drifts) at the onset of each damage state are also defined.

•

Table 35. Summary of Bridge Damage States and Failure Mechanisms (Mander and Basoz, 1999)

Damage State	Failure Mechanism
1. No Damage	First Yield
2. Slight Damage	Cracking, Spalling
3. Moderate Damage	Bond, Abutment Backwall Collapse
4. Extensive Damage	Pier concrete Failure
5. Collapse	Deck Unseating, Pier Collapse

- As noted above, the objective of the capacity evaluation for each bridge is to estimate that level of spectral acceleration that leads to the onset of each damage state shown in table 35. This is accomplished by using a five-percent damped NEHRP spectrum shape for the soil conditions at the bridge site together with the foregoing capacity spectrum, as summarized below. The NEHRP spectral accelerations are equal to 2.5 x PGA at short periods, and are equal to PGA/T at longer periods, where T is the natural period.

- The NEHRP spectrum is scaled by different PGA values until it intersects the capacity spectrum at the spectral displacement (drift) that represents the onset of that damage state. The PGA value that scales the NEHRP spectrum such that the onset of the i^{th} damage state first occurs represents the median PGA for that damage state. Median PGAs for an assumed NEHRP rock (type B) site condition and for each damage state are shown in tables 36 and 37 for each of the six standard bridge classifications.

- From the shape of the NEHRP spectrum, five-percent damped spectral accelerations are obtained as a function of the median PGA for the i^{th} damage state at the m^{th} bridge (denoted as $PGA_{i,m}$). If the spectral displacement (drift) for the i^{th} damage state occurs within the short period portion of the NEHRP spectrum, the spectral acceleration at a period of 0.3 sec is used to characterize the onset of that damage state for that standard bridge type. It is obtained as $C(0.3)_{i,m} = 2.5 * PGA_{i,m}$. If the spectral displacement (drift) for the i^{th} damage state occurs within the longer period portion of the NEHRP spectrum, the spectral acceleration at a period of 1.0 sec. is used to characterize the onset of the damage state for that standard bridge type. It is obtained as $C(1.0)_{i,m} = PGA_{i,m}$.

- The median spectral acceleration leading to the onset of each damage state for the actual bridge being investigated is obtained from the corresponding median spectral acceleration for the appropriate standard bridge type by correcting the standard bridge accelerations to account for skew and 3D effects. This correction is summarized later in this section.

Table 36. Median PGAs: Conventionally Designed "Standard" Bridges on Rock Site (Mander and Basoz, 1999)

Bridge Type	NBI Class	Damage State	Median PGA, g	
			Non-California	California
Multi-Column Bents and Simply Supported Superstructure	101-106	2	0.26	0.33
	301-310	3	0.35	0.46
	501-506	4	0.44	0.56
		5	0.65	0.83
Single Column Bents and Box Girder Superstructure	205-206	2	Not applicable	0.35
	605-606	3		0.42
		4		0.50
		5		0.74
Continuous Concrete Superstructure	201-207	2	0.60*	
	601-607	3	0.79	
		4	1.05	
		5	1.38	
Continuous Steel Superstructure	402-410	2	0.76*	
		5	1.04	
Single Span	All	2	0.80*	
		3	0.90	
		4	1.10	
		5	1.60	
Major Bridges		2	0.40	
		3	0.50	
		4	0.60	
		5	0.80	

*Short period motions govern; therefore use demand and capacity at 0.3 sec. to assess damage state.

Table 37. Median PGAs: Seismically Designed "Standard" Bridges on Rock Site (Mander and Basoz, 1999)

Bridge Type	NBI Class	Damage State	Median PGA, g	
			Non-CA (after 1990)	CA (after 1975)
Multi-Column Bents and Simply Supported Superstructure	101-106	2	0.45	0.45
	301-310	3	0.76	0.76
	501-506	4	1.05	1.05
		5	1.53	1.53
Single Column Bents and Box Girder Superstructure	205-206	2	0.54	0.54
	605-606	3	0.88	0.88
		4	1.22	1.22
		5	1.45	1.45
Continuous Concrete Superstructure	201-207	2	0.91*	0.91*
	601-607	4	1.05	1.05
		5	1.38	1.38
Continuous Steel Superstructure	402-410	2	0.91*	0.91*
		4	1.05	1.05
		5	1.38	1.38
Single Span	All	2	0.80*	0.80*
		3	0.90	0.90
		4	1.10	1.10
		5	1.60	1.60
Major Bridges		2	0.60	0.60
		3	0.80	0.80
		4	1.00	1.00
		5	1.60	1.60

*Short period motions govern; therefore use demand and capacity at 0.3 sec. to assess damage state.

- Table 36 shows that, for conventionally designed continuous steel bridges, only damage states 2 and 5 will occur. For these bridge types, damage state 2 is caused by high forces where the pushover capacity spectrum intersects the flat-top portion of the demand spectrum. There is no intermediate structural damage at damage states 3 or 4, and the next damage state occurs when incipient unseating occurs (damage state 5). This means that the probabilities of occurrence of damage states 1, 2, and 5 sum to 1.0, and the probabilities of occurrence of damage states 3 and 4 are zero. A similar situation is observed in table 37 for seismically designed continuous steel bridges, for which the probability of occurrence of damage state 3 is zero, and the probabilities of occurrence of the remaining damage states sum to 1.0.

F.2.2 DEMAND GROUND MOTIONS

In the SRA methodology, the demand ground motions are provided as five-percent damped spectral accelerations at natural periods ranging from 0.0 sec. (which corresponds to the PGA) to 3.0 sec. These ground motions are estimated from models incorporated into the hazards module. They include effects of local soil conditions at the site, and are provided for each scenario earthquake and simulation. The representation of the ground motions for different scenario earthquakes includes effects of uncertainties in earthquake magnitude and location, and the representation of ground motions for different simulations includes effects of uncertainties in ground motion attenuation rate and local soil conditions.

In the rapid pushover method as applied in this SRA methodology, the ground motion model contained in the hazards module is used to estimate the demand spectral accelerations at periods of 0.3 sec. and 1.0 sec. for each bridge site and each scenario earthquake and simulation. For subsequent estimation of liquefaction hazards for each earthquake and simulation, the model also estimates the PGA at each bridge. As noted above, these ground motion estimates include effects of uncertainties and local soil conditions at the site.

F.2.3 APPLICATION PROCEDURE

The following steps are used to apply the rapid pushover method in the SRA methodology:

- Preceding the seismic risk analysis for each scenario earthquake and simulation, the process outlined in section F.2.1 is used to establish equivalent five-percent damped spectral accelerations for each bridge that represent the onset of each damage state for that bridge. In this, the uncertainties in these spectral accelerations are represented by a lognormal distribution with a standard deviation of 0.35. This standard deviation corresponds to that estimated in Mander and Basoz (1999) for representing uncertainties in bridge material properties and analysis procedures only. The additional standard deviation given in Mander and Basoz (1999) to represent uncertainties in input ground motions is excluded, since these uncertainties are already considered in the ground motion model contained in the hazards module.

- For each scenario earthquake and simulation, the ground motion model from hazards module estimates five-percent-damped demand spectral accelerations at periods of 0.3 sec. and 1.0

sec. at each bridge site. These are denoted as $D(0.3)_{j,k,m}$ and $D(1.0)_{j,k,m}$ for the j^{th} scenario earthquake, the k^{th} simulation, and the site of the m^{th} bridge.

- For the m^{th} bridge, the demand spectral acceleration (from the j^{th} scenario earthquake and the k^{th} simulation) is compared to the spectral acceleration leading to the onset of each damage state at that bridge (including effects of uncertainties), in order to determine the bridge's damage state for this particular earthquake and simulation. Depending on whether the short-period response or the long-period response governs for this bridge and damage state, the spectral accelerations at periods of either 0.3 sec or 1.0 sec are compared.

F.2.4 INPUT DATA

F.2.4.1 Bridge Location

An alphanumeric parameter named STATE is specified to delineate between California and non-California bridges. This is a two-digit parameter that denotes the state where the bridge is located. Bridges in California are noted as STATE = CA.

F.2.4.2 National Bridge Inventory (NBI) Bridge Type (ITYPE)

The parameter, ITYPE, represents the general type of bridge being analyzed as represented in the National Bridge Inventory (NBI) database (FHWA, 1995b). It is a three-digit number that corresponds to item 43 in the NBI database. The first (single-digit) number denotes the material type, and the second (2-digit) number indicates the type of construction. The ITYPE parameter establishes the path followed by the SRA methodology for computing the median PGA for the onset of each damage state for a "standard" bridge. This is carried out for each bridge type described below.

F.2.4.2(a) Simply Supported Bridge

If the input value of ITYPE falls in any of the following ranges -- 101-106, 301-306, 501-506, or 701-706 -- the bridge is recognized as being simply supported. In this, the first (single digit) number represents the material type and indicates that the bridge is simply supported (ss), i.e. 1 = reinforced concrete ss, 3 = steel ss, 5 = prestressed concrete ss, and 7 = wood or timber ss. The second (two-digit) number represents the type of bridge design or construction, i.e., 01 = slab, 02 = stringer/multi-beam or girder, 03 = girder and floor beam system, 04 = tee beam, 05 = multiple box beam or girders, and 06 = single or spread box beam or girders.

F.2.4.2(b) California Type Bridges with Single Column Bents and Box Girder Superstructure

This bridge type denotes bridges from California that have a box-girder superstructure and a substructure consisting of single-column bents. These bridges are continuous over the bents, but may have joints within the various spans.

To denote such bridges, it is necessary to first set the input parameter STATE = CA. Then, if ITYPE has a value of 205-206 or 605-606, the bridge is considered to fall in this category. In this, the first (single digit) number represents the material type for the continuous spans, i.e., 2 = continuous reinforced concrete and 6 = continuous prestressed concrete. The second (two digit) number (i.e., the type of bridge superstructure construction) is either 05 = multiple box beam or 06 = single box beam for this bridge type.

F.2.4.2(c) Continuous Bridges

This bridge type represents any non-California continuous bridge structure (to differentiate it from the California "continuous" bridges addressed in section F.2.4.2(b)). Therefore, this bridge type would be identified as follows: (a) STATE ≠ CA; and (b) a value of the parameter ITYPE that is in the ranges of *201-207* or 601-607 (for continuous concrete superstructures) or 401-410 (for continuous steel superstructures.

F.2.4.3 Number of Spans in Main Bridge (NSPAN)

The parameter NSPAN defines the number of spans in the main portion of the bridge. It is a three-digit number that corresponds to item 45 of NBI database. If NSPAN = 1, then the bridge is recognized as having a single span.

F.2.4.4 Total Length of Maximum Span (SPNMAX)

The parameter SPNMAX is the total length of the maximum span of the bridge. It is a five-digit number that corresponds to item 48 of NBI database. If SPNMAX ≥ 150 meters, the software proceeds to the subroutine that computes the median peak ground acceleration for the onset of each damage state for major bridges. As previously noted, such bridges can also be represented using separate user-specified fragility curves.

F.2.4.5 Year of Construction (YEAR)

The parameter YEAR represents the year that the bridge was constructed. It is a four-digit number that corresponds to item 27 of the NBI database. The rapid pushover method uses this parameter to infer whether or not the bridge has been seismically designed.

F.2.4.6 Skew Angle (ANGLE)

The parameter ANGLE is the skew angle of the bridge, in degrees, between the centerline of a pier and a line normal to the roadway centerline. It is a two-digit number that corresponds to Item 34 of the NBI database. For a right bridge with no skew, ANGLE = 90 degrees. If the bridge is curved has a variable skew, the average skew is recorded. Sometimes the NBI database will show that ANGLE = 99 degrees, which signifies a major variation in skews of the substructure units across the length of the bridge.

F.2.4.7 Deck Width (BDECK)

The parameter BDECK is the width of the deck, in meters. It is a four-digit number that corresponds to item 52 of the NBI database, This quantity is used in the computation of the replacement value of the bridge.

F.2.4.8 Structure Length (SLGTH)

The parameter SLGTH is the total length of the roadway supported by the bridge structure, and is given as a six-digit number to the nearest tenth of a meter (i.e. 000355 = 35.5 m). This corresponds to item 49 of the NBI database.

F1.4.9 Demand Ground Motion and Soil Amplification Factors

The demand ground motions at each bridge site are obtained by applying the ground motion model in the hazards module for each scenario earthquake and simulation. These are termed $D(0.3)_{j,k,m}$ and $D(1.0)_{j,k,m}$ for the j^{th} scenario earthquake, the k^{th} simulation, and the site of the m^{th} bridge (see section F.2.3). To estimate potential liquefaction hazards at the m^{th} bridge site, the peak ground acceleration at the site, denoted as $D(0.0)_{j,k,m}$, is also obtained (appendix H).

The rapid pushover method also uses the soil amplification factor (SAF) at the bridge site in the computation of the bridge's damage state. This is because the median PGAs for each damage state and standard bridge classification are given in tables 36 and 37 for a NEHRP spectrum on rock site conditions. Since the intersection of the demand and capacity spectra (on which these median PGA values are based) will depend on the soil conditions associated with the NEHRP spectrum, the SAFs are used in the damage state calculations.

These SAFs are provided for each bridge site, scenario earthquake, and simulation, and include effects of uncertainties in these factors. They are denoted as $S(0.3)_{j,k,m}$ and $S(1.0)_{j,k,m}$ for natural periods of 0.3 sec. and 1.0 sec. respectively, and for the j^{th} earthquake, k^{th} simulation, and m^{th} bridge. It is these factors that are specified as input to the rapid pushover method.

F.2.5 MEDIAN SPECTRAL ACCELERATION CAPACITY LEADING TO ONSET OF i^{th} DAMAGE STATE AT m^{th} BRIDGE

Once the above input data are provided, the following steps are used to compute the median PGA for each bridge type. These steps are repeated for each damage state at each bridge.

F.2.5.1 Step 1 – Bridge Type and Location

In step 1, the previously defined input parameter ITYPE is used to define the bridge type for each bridge in the highway system, and the input parameter STATE is used to identify whether or not the bridge is located in California.

F.2.5.2 Step 2 – Typical vs. Seismic Design

In step 2, the input parameter YEAR is used to establish whether the bridge was seismically designed. Seismically designed bridges are: (a) California bridges built after 1975; or (b) bridges outside of California built after 1990. Conventionally designed bridges are California or non-California bridges whose year of construction precedes those given above.

F.2.5.3 Step 3 – Median PGA for Standard Bridge

In step 3, tables 36 or 37 are used to obtain the median PGA for each damage state of the "standard bridge" type that corresponds to the m^{th} bridge. Table 36 is used for conventionally designed bridges, and table 37 is used for seismically designed bridges. These tables each list the median PGA for each damage state, in terms of the NBI bridge type and whether the bridge is located in California. This quantity is termed $PGA_{i,m}$ for the i^{th} damage state at the m^{th} bridge.

F.2.5.4 Step 4 – Conversion from Median Peak Acceleration Capacity to Median Spectral Acceleration Capacity for Standard Bridge

In step 3, the median PGA from step 3 is converted to the median spectral acceleration at the onset of each damage state for the m^{th} bridge's standard bridge type (see section F.2.1). Depending on whether short periods or long periods govern the bridge response, the median spectral acceleration at the onset of the i^{th} damage state is computed as:

$$C(0.3)_{i,m} = 2.5 * PGA_{i,m} \quad \text{(if short periods govern)} \tag{82}$$

or

$$C(1.0)_{i,m} = PGA_{i,m} \quad \text{(if longer periods govern)} \tag{83}$$

The asterisks in tables 36 and 37 show those damage states and bridge types at which the bridge's short-period response will govern. The asterisks show that the short period response governs only for damage state 2 and, for this damage state, only for bridge types 201-207 and 601-606 (continuous concrete bridges), 402-410 (continuous steel bridges), and all single-span bridges. For these bridge types only, equation 82 is used to obtain the median spectral acceleration leading to the onset of damage state 2. For all other bridge types and damage states, the long period response of the bridge will govern, and equation 83 is used to obtain the median spectral acceleration leading to the onset of these damage states.

F.2.6 ESTIMATION OF MEDIAN SPECTRAL ACCELERATIONS FOR ONSET OF EACH DAMAGE STATE AT ACTUAL BRIDGES (ASSUMING ROCK SITE CONDITIONS)

It now remains to convert the above median spectral accelerations for the onset of each damage state for each standard bridge type to the corresponding median spectral accelerations for the actual bridges in the highway system. This is accomplished by modifying the standard bridge results for rock site conditions to account for skew and three-dimensional (3D) effects.

F.2.6.1 Damage States 3, 4, and 5

For damage states 3, 4, and 5, which are always governed by long period response, the median spectral acceleration leading to the onset of the i^{th} damage state at the m^{th} bridge (denoted as $C'(1.0)_{i,m}$) are computed for rock site conditions as

$$C'(1.0)_{i,m} = K_{skew} * K_{3D} * C(1.0)_{i,m} \tag{84}$$

where K_{skew} and K_{3D} are factors for modifying the standard bridge's median spectral acceleration to account for the skew and 3D deck-arching membrane action (which occurs when the bridge's lateral displacements are sufficiently large). The parameter K_{skew} is computed as

$$K_{skew} = \sqrt{\sin(ANGLE)} \tag{85}$$

where ANGLE is the skew angle of the actual bridge. The parameter K_{3D} depends on the number of spans, the total structure length, the bridge type, and whether the bridge is seismically designed, and is obtained from table 38.

Table 38. Modification Rules for Modeling Three-Dimensional Effects (Mander and Basoz, 1999)

Bridge Type	NBI Class	Conventionally Designed Bridges	Seismically Designed Bridges (non-CA bridges built after 1990 or CA bridges built after 1975)
Concrete, Simply Supported Superstructure	101-106 501-506	$1+0.25/(NSPAN-1)$	$1+0.25/(NSPAN-1)$
Concrete, Continuous Superstructure	201-206 601-607	$1+0.33/NSPAN$	$1+0.33/(NSPAN-1)$
Steel, Simply Supported Superstructure	301-310	$1+0.09/(NSPAN-1)$; $L \geq 20m$ $1+0.20/(NSPAN-1)$; $L < 20m$	$1+0.25/(NSPAN-1)$
Steel, Continuous	402-410	$1+0.05/NSPAN$; $L \geq 20m$ $1+0.10/NSPAN$; $L < 20m$	$1+0.33/(NSPAN-1)$
Single Span	All	1.0	1.0

Note that, in table 38, L is the average span length, which is computed from equation 84 as:

$$L = \frac{SLGTH}{NSPAN} \tag{86}$$

where *SLGTH* and *NSPAN* are the total structure length and the number of spans, respectively.

F.2.6.2 Damage State 2

F.2.6.2(a) Bridges Governed by Short Period Response

For those bridges that are shown in tables 36 and 37 to be governed by short period response at damage state 2, the median spectral acceleration at the onset of this damage state ($C'(0.3)_{2,m}$) is equal to the median spectral acceleration for the corresponding standard bridge type, i.e.

$$C'(0.3)_{2,m} = C(0.3)_{2,m} \tag{87}$$

F.2.6.2(b) Bridges Governed by Long Period Response

For those bridges that are shown in tables 36 and 37 to be governed by long period response at damage state 2, the median spectral acceleration at the onset of this damage state ($C'(1.0)_{2,m}$) is equal to the median spectral acceleration for the corresponding standard bridge type, i.e.

$$C'(1.0)_{2.m} = C(1.0)_{2,m} \tag{88}$$

Note that in equations 87 and 88, the correction factors for skew and 3D effects are not included. This is because, at damage state 2, the structural displacements are too small for these corrections to be significant.

F.2.7 ESTIMATION OF DAMAGE STATE FOR ACTUAL BRIDGE

Now that the median spectral acceleration leading to the onset of the i^{th} damage state has been developed for the m^{th} bridge and rock site conditions, it remains to establish the actual damage state of that bridge for the j^{th} scenario earthquake and the k^{th} simulation, and including the actual soil conditions at the bridge site. This is carried out as part of the seismic risk analysis for each scenario earthquake and simulation from the following steps.

F.2.7.1 Step 1 – Input Demand Spectral Accelerations

Under step 1, the demand ground motions at the m^{th} bridge site, as obtained by applying the ground motion model contained in the hazards module for the j^{th} scenario earthquake and k^{th} simulation, are input into the damage state estimation procedure. These demand ground motions are specified as spectral accelerations at periods of 0.0 sec., 0.3 sec., and 1.0 sec. The

spectral accelerations at period p are denoted as $D(p)_{j,k,m}$, where p = 0.0, 0.3, and 1.0. As previously noted, they already include effects of uncertainties in attenuation rates and soil amplification factors.

F.2.7.2 Step 2 – Develop Random Variate X

Under this step, a random variate X is determined by applying the following substeps:

- *Substep 2-1:* Select three uniformly distributed random numbers U_1, U_2, and U_3 -- each between 0 and 1.
- *Substep 2-2:* Let $V_1 = 2U_1 - 1$ and $V_2 = 2U_2 - 1$.
- *Substep 2-3:* Calculate $W = (V_1)^2 + (V_2)^2$.
- *Substep 2-4:* If $W > 1$, return to substep 2-1 and select new uniformly distributed random numbers U_1, U_2, and U_3. Otherwise, if $W \leq 1$, calculate

$$Z = \sqrt{\frac{-2\ln W}{W}}$$

- *Substep 2-5:* Let $X_1 = V_1 * Z$ and $X_2 = V_2 * Z$.
- *Substep 2-6:* If $U_3 < 0.5$, set $X = X_1$. Alternatively, if $U_3 \geq 0.5$, set $X = X_2$. In this, we will use one value of X for all damage states addressed in the subsequent steps 3 to 6 (see below).

F.2.7.3 Step 3 – Evaluate whether Bridge is in Damage State 5

F.2.7.3(a) Substep 3-1. Compute Capacity including Structural Uncertainties and Local Soil Conditions

Under this substep, the quantity Q_5 is calculated as

$$Q_5 = \ln C'(1.0)_{5,m} + 0.35X \tag{89}$$

where 0.35 is the structural uncertainty estimated in Mander and Basoz (1999). The spectral acceleration at the onset of damage state 5 (including effects of structural uncertainties and uncertainties in the soil amplification factor) is termed $C''(1.0)_{5,j,k,m}$ and is computed as

$$C''(1.0)_{5,j,k,m} = \frac{\exp(Q_5)}{S(1.0)_{j,k,m}} \tag{90}$$

where $S(1.0)_{j,k,m}$ is the NEHRP soil amplification factor (Dobry et al., 2000) at the m^{th} bridge site for the j^{th} scenario earthquake and the k^{th} simulation (as obtained from the ground motion model in the hazards module, and including effects of uncertainties in the soil amplification factor).

F.2.7.3(b) Substep 3-2. Compare Demand to Capacity for Damage State 5

This substep checks whether $D(1.0)_{j,k,m}$ (which is the demand spectral acceleration at the m^{th} bridge site due to the j^{th} scenario earthquake and k^{th} simulation) $\geq C''(1.0)_{5,j,k,m}$ (the capacity spectral acceleration for this bridge site, earthquake, and simulation as obtained in substep 3-1). If so, the bridge is in damage state 5. Otherwise, the method proceeds to step 4.

F.2.7.4 Step 4 – Evaluate whether Bridge is in Damage State 4

F.2.7.4(a) Substep 4-1. Compute Capacity including Structural Uncertainties and Local Soil Conditions

Under this substep, the quantity Q_4 is calculated as

$$Q_4 = \ln C'(1.0)_{4,m} + 0.35X \tag{91}$$

where 0.35 is the structural uncertainty estimated in Mander and Basoz (1999). The spectral acceleration at the onset of damage state 4 (including effects of structural uncertainties and uncertainties in the soil amplification factor) is termed $C''(1.0)_{4,j,k,m}$ and is computed as

$$C''(1.0)_{4,j,k,m} = \frac{\exp(Q_4)}{S(1.0)_{j,k,m}} \tag{92}$$

where $S(1.0)_{j,k,m}$ is the NEHRP soil amplification factor (Dobry et al., 2000) at the m^{th} bridge site for the j^{th} scenario earthquake and the k^{th} simulation (as obtained from the ground motion model in the hazards module, and including effects of uncertainties in the soil amplification factor).

F.2.7.4(b) Substep 4-2. Compare Demand to Capacity for Damage State 4

This substep consists of checking whether $D(1.0)_{j,k,m}$ (which is the demand spectral acceleration at the m^{th} bridge site due to the j^{th} scenario earthquake and k^{th} simulation) $\geq C''(1.0)_{4,j,k,m}$ (the capacity spectral acceleration for this bridge site, earthquake, and simulation as obtained in substep 4-1). If so, the bridge is in damage state 4. Otherwise, the rapid pushover method proceeds to step 5.

F.2.7.5 Step 5 – Evaluate whether Bridge is in Damage State 3

F.2.7.5(a) Substep 5-1. Compute Capacity including Structural Uncertainties and Local Soil Conditions

Under this substep, the quantity Q_3 is calculated as

$$Q_3 = \ln C'(1.0)_{3,m} + 0.35X \tag{93}$$

where 0.35 is the structural uncertainty estimated in Mander and Basoz (1999). The spectral acceleration at the onset of damage state 3 (including effects of structural uncertainties and uncertainties in the soil amplification factor) is termed $C''(1.0)_{3,j,k,m}$ and is computed as

$$C''(1.0)_{3,j,k,m} = \frac{\exp(Q_3)}{S(1.0)_{j,k,m}} \tag{94}$$

where $S(1.0)_{j,k,m}$ is the NEHRP soil amplification factor (Dobry et al., 2000) at the m^{th} bridge site for the j^{th} scenario earthquake and the k^{th} simulation (as obtained from the ground motion model in the hazards module, and including effects of uncertainties in the soil amplification factor).

F.2.7.5(b) Substep 5-2. Compare Demand to Capacity for Damage State 3

This substep consists of checking whether $D(1.0)_{j,k,m}$ (which is the demand spectral acceleration at the m^{th} bridge site due to the j^{th} scenario earthquake and k^{th} simulation) $\geq C''(1.0)_{3,j,k,m}$ (the capacity spectral acceleration for this bridge site, earthquake, and simulation as obtained in substep 5-1). If so, the bridge is in damage state 3. Otherwise, the rapid pushover method proceeds to step 6.

F.2.7.6 Step 6 – Evaluate whether Bridge is in Damage State 2

If the bridge structure is asterisked in tables 36 or 37, the rapid pushover method proceeds to section F.2.7-6(a). Otherwise, the method proceeds to section F.2.7-6(b).

F.2.7-6(a) Bridges where Long Period Response Governs

Compute Capacity including Structural Uncertainties and Local Soil Conditions. Under this substep, the quantity Q_2 is calculated as

$$Q_2 = \ln C'(1.0)_{2,m} + 0.35X \tag{95}$$

where 0.35 is the structural uncertainty estimated in Mander and Basoz (1999). The spectral acceleration at the onset of damage state 2 (including effects of structural uncertainties and uncertainties in the soil amplification factor) is termed $C''(1.0)_{2,j,k,m}$ and is computed as

$$C''(1.0)_{2,j,k,m} = \frac{\exp(Q_2)}{S(1.0)_{j,k,m}} \tag{96}$$

where $S(1.0)_{j,k,m}$ is the NEHRP soil amplification factor (Dobry et al., 2000) at the m^{th} bridge site for the j^{th} scenario earthquake and the k^{th} simulation (as obtained from the ground motion model in the hazards module, and including effects of uncertainties in the soil amplification factor).

Compare Demand to Capacity for Damage State 2. This substep checks whether $D(1.0)_{j,k,m}$ (which is the demand spectral acceleration at the m^{th} bridge site due to the j^{th} scenario earthquake and k^{th} simulation) $\geq C''(1.0)_{2,j,k,m}$ (the capacity spectral acceleration for this bridge site, earthquake, and simulation as obtained in substep F.2.7.6-a1). If so, the bridge is in damage state 2. Otherwise, the bridge is in damage state 1.

F.2.7-6(b) Bridges where Short Period Response Governs

Compute Capacity including Structural Uncertainties and Local Soil Conditions. Under this substep, the quantity Q_2 is calculated as

$$Q_2 = \ln C''(0.3)_{2,m} + 0.35X \tag{97}$$

where 0.35 is the structural uncertainty estimated in Mander and Basoz (1999). The spectral acceleration at the onset of damage state 2 (including effects of structural uncertainties and uncertainties in the soil amplification factor) is termed $C''(1.0)_{2,j,k,m}$ and is computed as

$$C''(0.3)_{2,j,k,m} = \frac{\exp(Q_2)}{S(0.3)_{j,k,m}} \tag{98}$$

where $S(1.0)_{j,k,m}$ is the NEHRP soil amplification factor (Dobry et al., 2000) at the m^{th} bridge site for the j^{th} scenario earthquake and the k^{th} simulation (as obtained from the ground motion model in the hazards module, and including effects of uncertainties in the soil amplification factor).

Compare Demand to Capacity for Damage State 2. This substep checks whether $D(0.3)_{j,k,m}$ (which is the demand spectral acceleration at the m^{th} bridge site due to the j^{th} scenario earthquake and k^{th} simulation) $\geq C''(0.3)_{2,j,k,m}$ (the capacity spectral acceleration for this bridge site, earthquake, and simulation as obtained in the prior substep). If so, the bridge is in damage state 2. Otherwise, the bridge is in damage state 1.

F.3 FRAGILTY CURVES BASED ON ELASTIC CAPACITY-DEMAND METHOD

This section summarizes a bridge modeling approach that is based on the elastic capacity-demand method (FHWA, 1995a). This approach was used by Jernigan (1998) and Jernigan and Hwang (1997) to develop fragility curves for commonly occurring bridges in the Shelby County, Tennessee highway system, and was used in prior demonstration SRAs of this system (Werner et al., 1998). These fragility curves are included in the SRA methodology. The nine steps used to develop these curves are summarized below.

F.3.1 STEP 1 – STRUCTURAL ATTRIBUTE DATABASE

The Shelby County highway system contains 382 bridges (excluding culverts and the I-40 and I-55 crossings of the Mississippi River, which are modeled by user-specified fragility curves as described in appendix G). For each bridge, a GIS database of structural attributes relevant to seismic response was developed. This database is summarized in table 39.

Table 39. Structural Attributes in Database for Bridges in Shelby County, Tennessee (Jernigan et al., 1996, Jernigan, 1998, and Jernigan and Hwang, 1997)

File	Description	Attributes
B-1	Relevant Information from NBI Data Base	Bridge ID number, route, location (log mile), feature crossed by bridge, maximum span length, total length, roadway width, bridge width, average daily traffic, year built, skew angle, superstructure types (main span and approach span), number of main spans, and number of approach spans.
B-2	Abutment Attributes	Bridge ID number, abutment type (material, type, and fixity), abutment bearing and expansion type, seat width, foundation type, and whether seismic retrofit was implemented.
B-3	Bent File No. 1	Bridge ID number, bent type and material, superstructure to substructure connectivity, bent bearing and expansion type, seat width, number of columns per bent, maximum column height, and minimum column height.
B-4	Bent File No. 2	Bridge ID number, column fixity (to bent cap and to pile cap or footing), column size (at top and bottom), column shape, vertical reinforcement, transverse reinforcement, and foundation type.

F.3.2 STEP 2 – GROUPING OF BRIDGES

Each bridge in the highway system was assigned to one of the following groups: (a) group 302-11 -- simply-supported steel stringer, multi-beam, or girder bridge on multi-column bents; (b) group 302-31 -- simply-supported steel stringer, multi-beam, or girder bridge on pile bents; (c) group 402-11 -- continuous steel stringer, multi-beam, or girder bridge on multi-column bents; (d) group 502-11 -- simply supported reinforced or prestressed concrete stringer, multi-beam, or girder bridge on multi-column bents; (e) group 602-11 -- continuous reinforced or prestressed concrete stringer, multi-beam, or girder bridge on multi-column bents; and (f) single span bridge.

F.3.3 STEP 3 – BRIDGE MODELS FOR EACH GROUP

Bridge models for each group were developed by: (a) identifying several structural attributes as key parameters that would impact the seismic response of bridges in that group; (b) establishing a range of plausible values of each parameter for the group; (c) selecting a random combination of ten values for each parameter in the group; (d) combining the values to develop ten bridge models for the group; and (e) selecting as-built bridge drawings that best fit each model for the group.

F.3.4 STEP 4 – STEEL AND CONCRETE MATERIAL PROPERTIES

The variability of the strength of concrete and reinforcing steel was modeled by using results of past experimental studies (Mirza et al., 1979, Priestley et al., 1996, Mirza and McGregor, 1979) to estimate probability distributions for these strengths. This led to the following distributions; (a) the actual compressive strength of concrete with a 28-day nominal compressive strength of 20, 670 kPa (3,000 psi) was assumed to be normally distributed with a mean strength of 31,000 kPa (4,500 psi) and a standard deviation of 6,200 kPa (900 psi); (c) the yield strength of Grade 40 reinforcing steel was assumed to be lognormally distributed with a mean value of 336,230 kPa (48,800 psi) and a standard deviation of 36,000 kPa (5,220 psi). Then, a set of concrete-strength and steel yield-strength values that fit these distributions was generated.

F.3.5 STEP 5 – DEMAND SPECTRUM

A seismic force factor, SFF, was used to model the variability in the demand spectrum and in the seismic response of the bridge structures. This factor was assumed to be lognormally distributed with a mean value of 1.0 and a coefficient of variation of 0.5. It is related to the AASHTO design spectral accelerations, $S_a(T)$ as follows:

Short Period Segment of Spectrum: $$S_a(T) = SFF * 2.5 * PGA \tag{99}$$

Long Period Segment of Spectrum: $$S_a(T) = SFF * \frac{1.2 * PGA * S}{T^{2/3}} \tag{100}$$

where *PGA* is the peak ground acceleration, *S* is the site coefficient (assumed in Jernigan (1998) and Jernigan and Hwang (1997) to be 1.2 for all sites in Shelby County), and *T* is the fundamental period of the bridge. Sample values of SFF that fit the above distribution were generated.

F.3.6 STEP 6 – BRIDGE SAMPLES

Fifty bridge samples were obtained for each group, by using five random values of concrete strength, steel yield strength, and SFF for each of the 10 bridge models established for the group.

F.3.7 STEP 7 – DYNAMIC ANALYSIS

Each bridge sample was dynamically analyzed by the Single-Mode or Multi-Mode Spectral Method (FHWA, 1995a) and the SEISAB computer program. Input motions consisted of the AASTO design spectrum scaled to PGA values ranging from 0.06 g to 0.48 g. These input motions were oriented along both the longitudinal and transverse axes. Results of the analyses of the bridge response to these two orthogonal input motions were combined by using the 100%-30% rule.

F.3.8 STEP 8 – DAMAGE STATES

The dynamic analyses of each of the 50 bridge samples for each group were used to estimate damage states for each sample due to each set of earthquake motions. Tables 40 and 41 show the bridge damage types and damage states considered in this process.

Table 40. Damage Types for Fragility Curves from Elastic Capacity-Demand Method (Jernigan, 1998 and Jernigan and Hwang, 1997)

Bridge Element	Type of Damage
Expansion Joints and Bearings	• Excessive Displacement (Inadequate Seat Width) • Excessive Force
Columns, Walls, and Footings	• Excessive Column Moment • Excessive Footing Moment • Inadequate Anchorage of Longitudinal Reinforcement • Inadequate Splice Length in Longitudinal Reinforcement • Inadequate Transverse Confinement Steel in Plastic Zone • Excessive Column Shear • Excessive Footing Rotation
	• Excessive Displacement

Table 41. Damage States for Fragility Curves from Elastic Capacity-Demand Method (Jernigan, 1998 and Jernigan and Hwang, 1997)

Damage State	Description	Capacity-Demand Ratio for Onset of Damage State
Minor Damage	Minor cracking and spalling of abutment, cracks in shear keys at abutments, minor cracking and spalling at hinges, minor spalling of column (requiring no more than cosmetic repair), and/or minor permanent movement at bearings.	--
Repairable Damage	Moderate damage to columns (cracking, hinging, spalling). joints (cracked shear keys, bent bolts at bearings, rocker bearing failure etc. without unseating), and/or abutments (cracked shear keys, and cracked end walls or wing walls).	0.5
Irrepairable Damage	Total loss of column structural integrity at sufficient number of bents so that overall collapse mechanism is formed.	0.33

F.3.9 STEP 9 – FRAGILITY CURVES

Damage state results for the 50 samples for each bridge group were used to develop fragility curves for the onset of repairable or significant damage for that group. The fragility curves for each group that are built into the SRA methodology are shown in figures 39 through 44.

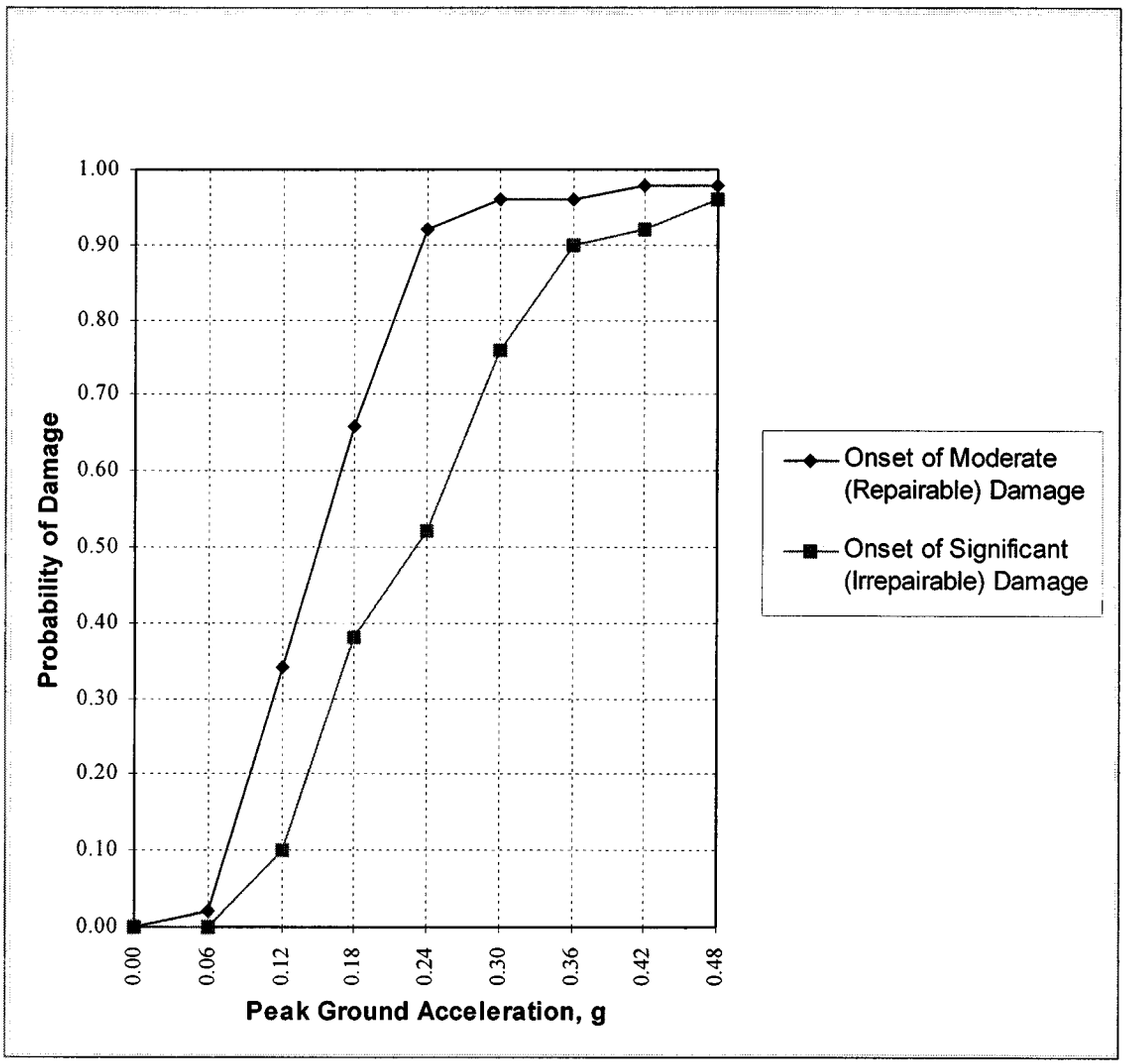

Figure 39. Damage State Fragility Curves for Bridge Type 302-11
(Simply-Supported Steel Bridge on Multi-Column Bents)
(Jernigan, 1998 and Jernigan and Hwang, 1997)

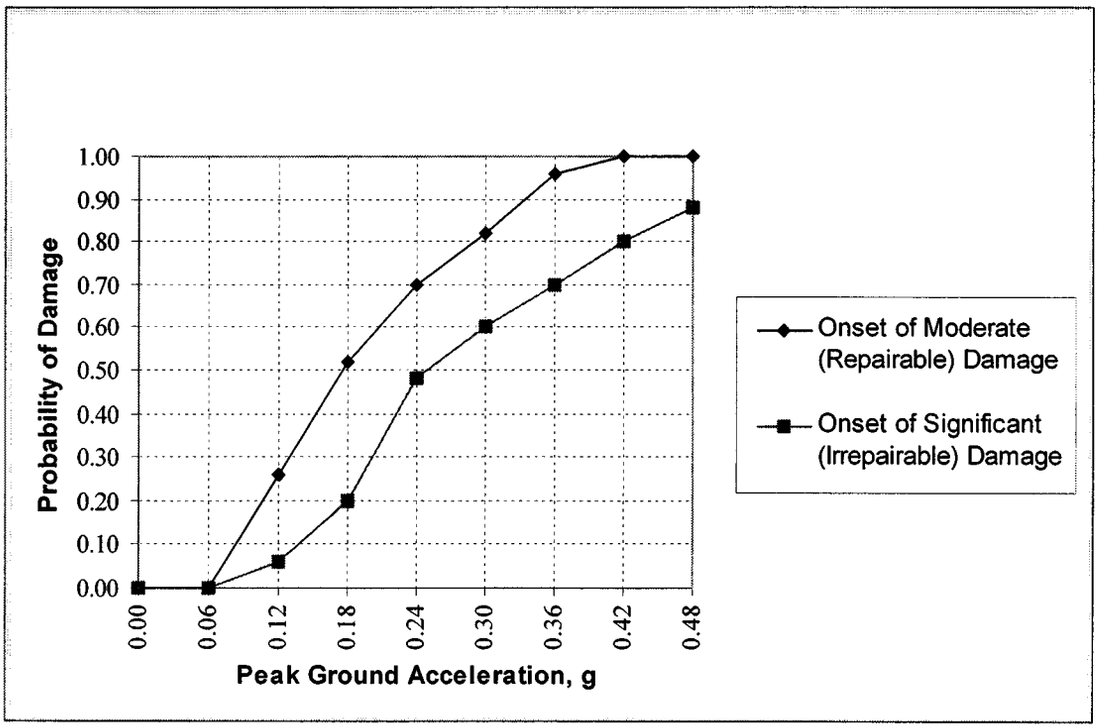

Figure 40. Damage State Fragility Curves for Bridge Type 302-31
(Simply-Supported Steel Bridge on Pile Bents)
(Jernigan, 1998 and Jernigan and Hwang, 1997)

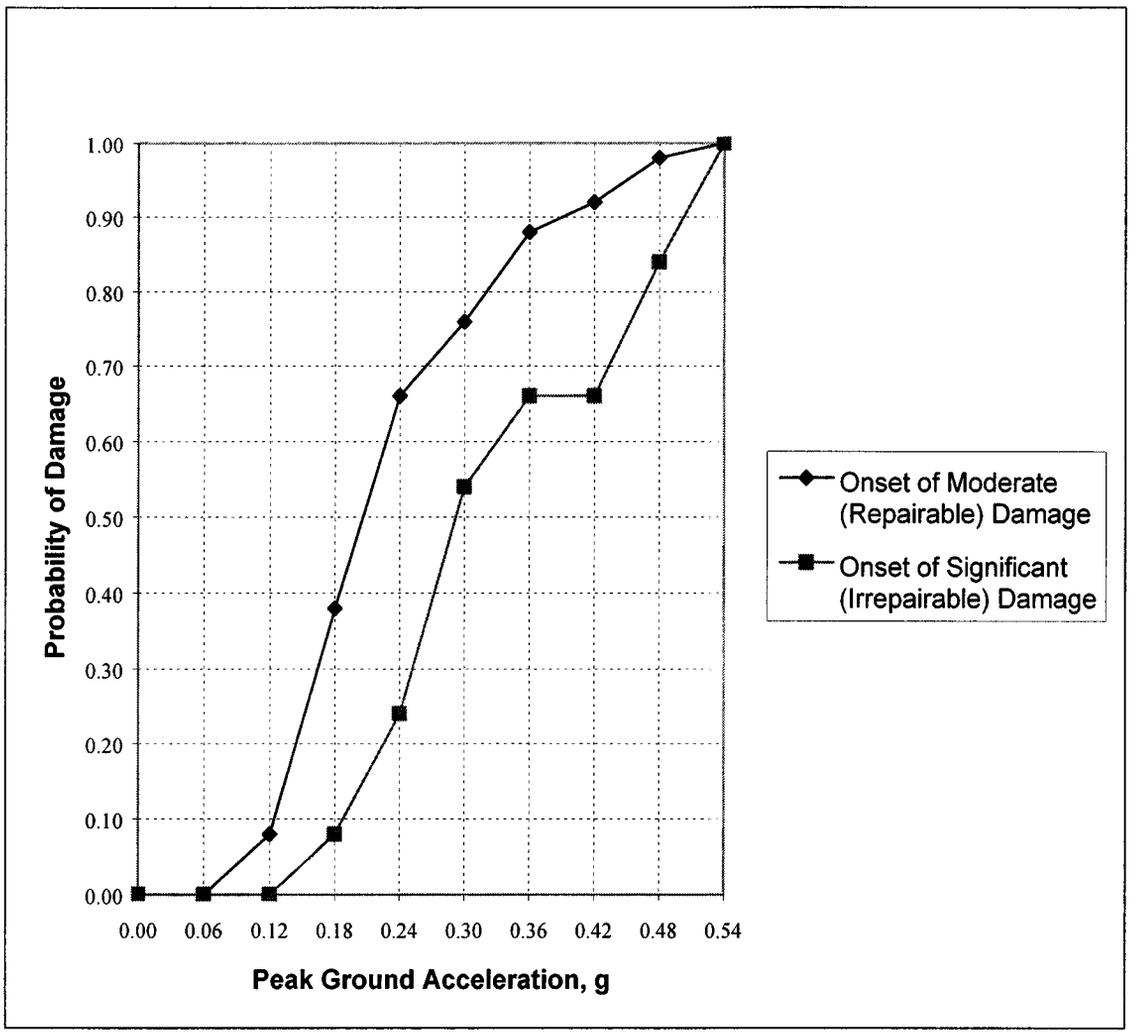

Figure 41. Damage State Fragility Curves for Bridge Type 402-11
(Continuous Steel Bridge on Multi-Column Bents)
(Jernigan, 1998 and Jernigan and Hwang, 1997)

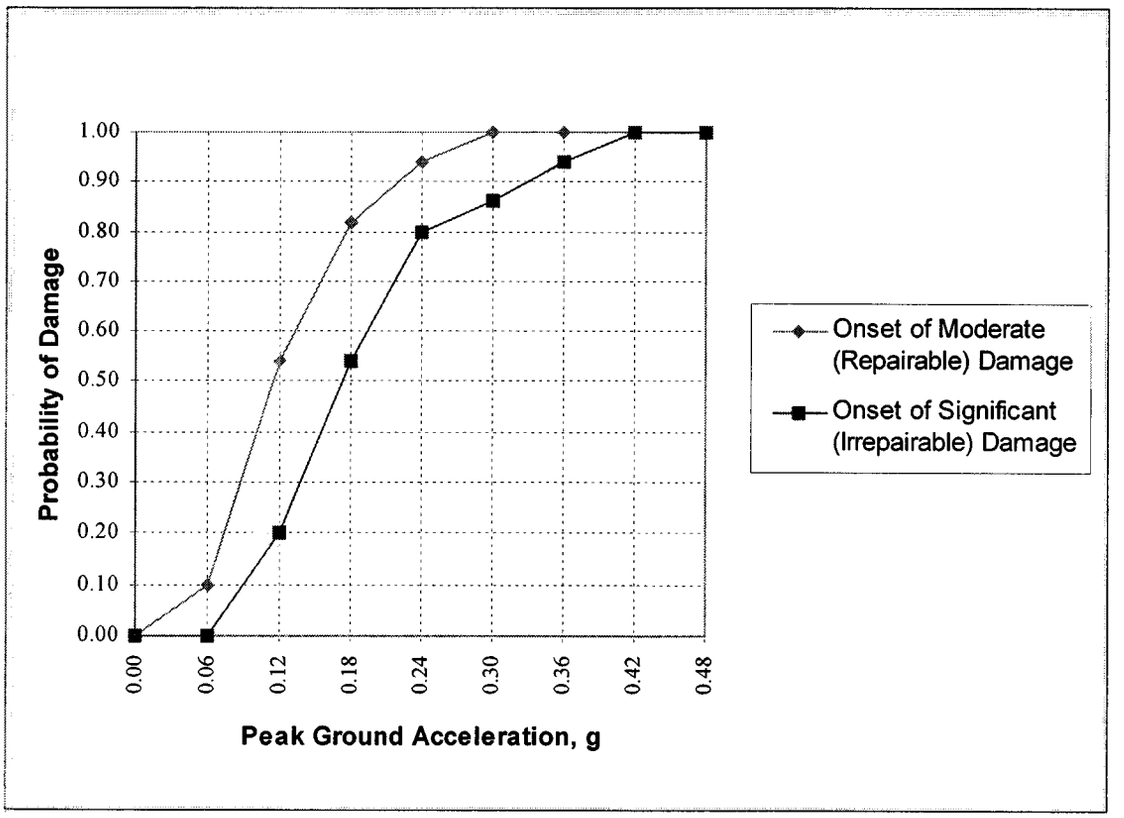

Figure 42. Damage State Fragility Curves for Bridge Type 502-11
(Simply-Supported Concrete Bridge on Multi-Column Bents)
(Jernigan, 1998 and Jernigan and Hwang, 1997)

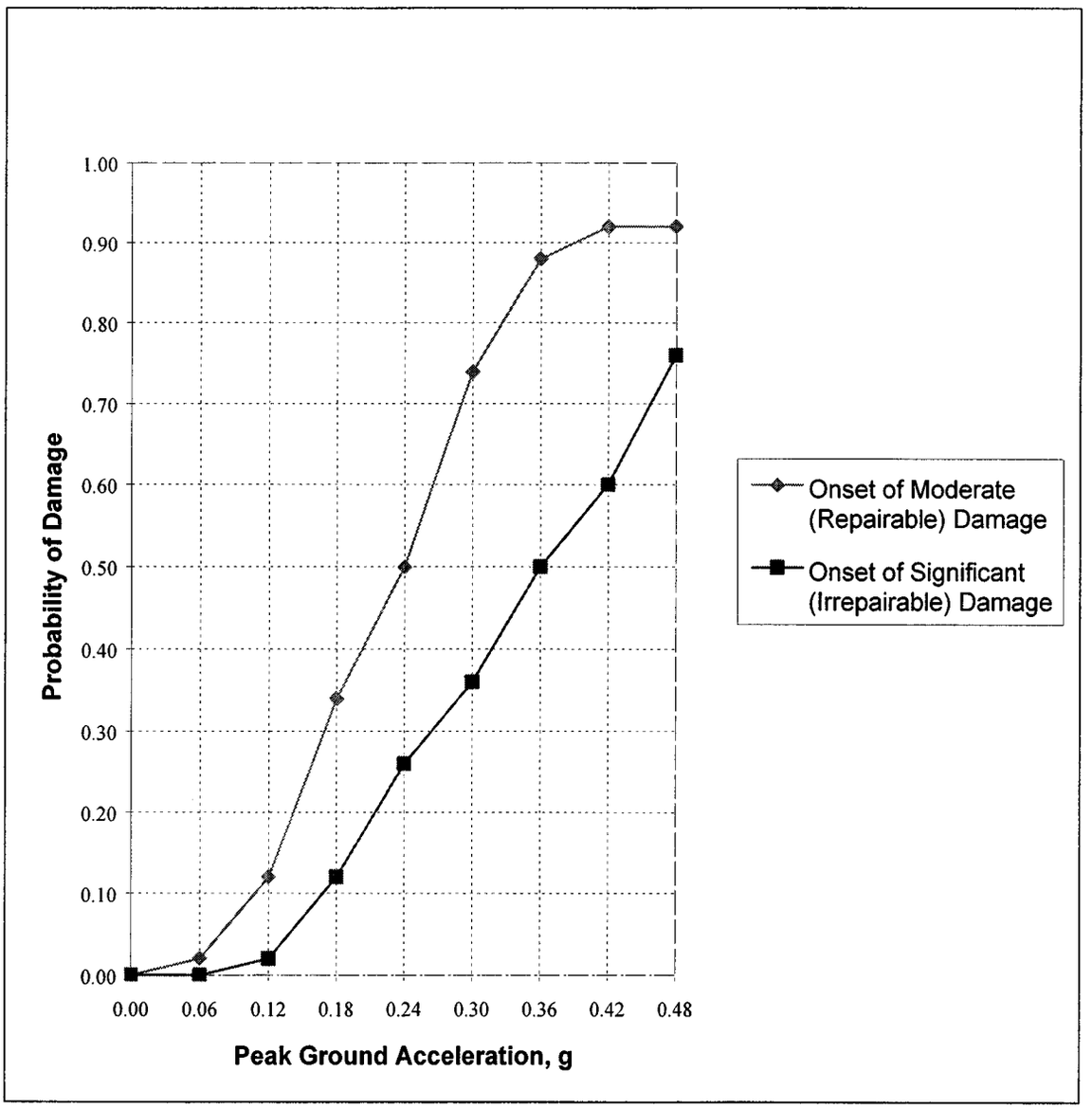

Figure 43. Damage State Fragility Curves for Bridge Type 602-11
(Continuous Concrete Bridge on Multi-Column Bents)
(Jernigan, 1998 and Jernigan and Hwang, 1997)

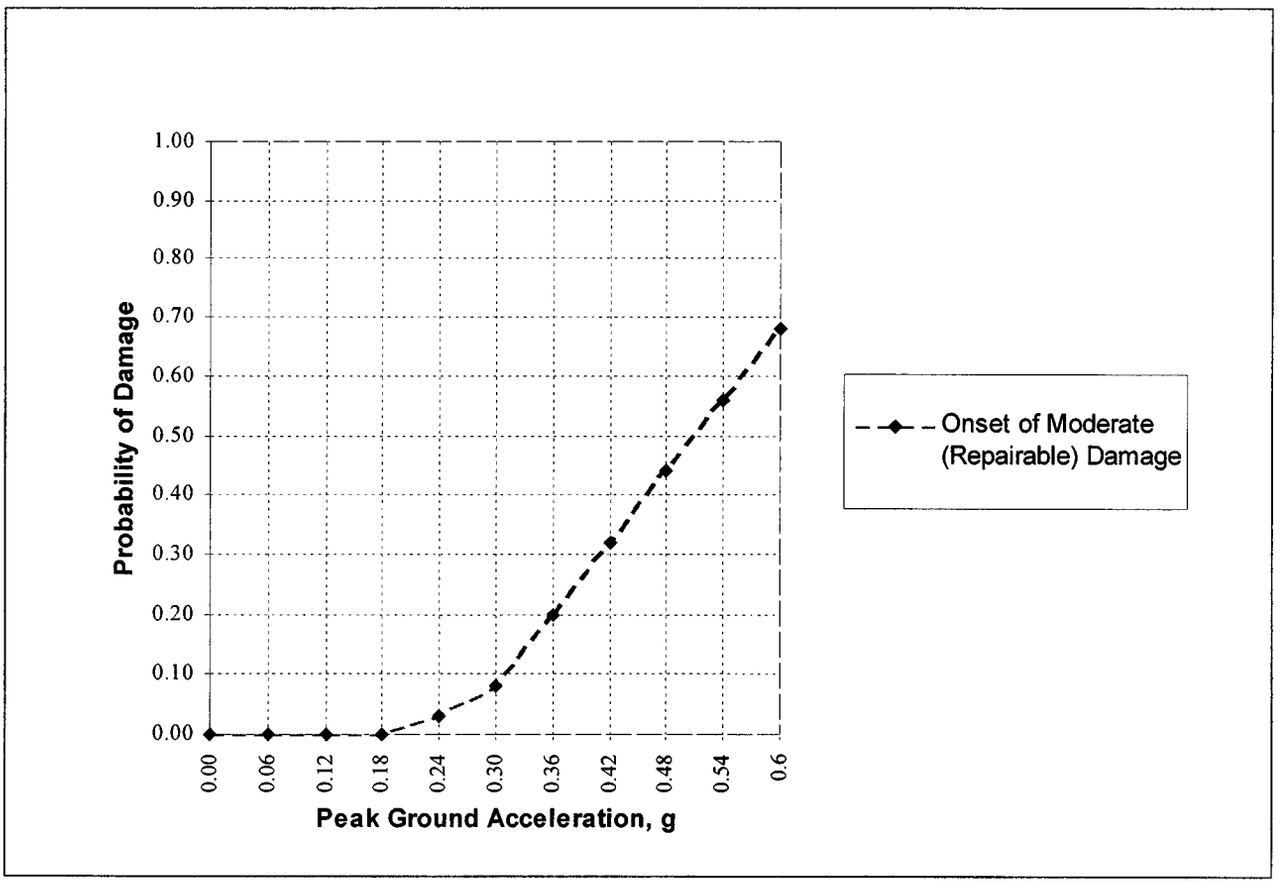

Figure 44. Damage State Fragility Curves for Single-Span Bridges (Jernigan, 1998 and Jernigan and Hwang, 1997)

APPENDIX G
USER-SPECIFIED FRAGILITY CURVES FOR I-40 AND I-55 CROSSINGS OF MISSISSIPPI RIVER

G.1 BACKGROUND

The SRA methodology provides the user with an option to provide user-specified fragility curves for any bridges in the highway system that are of vital importance and/or have unique configurations and geometries that may not be fully represented by the modeling procedures for more commonly occurring bridges that are described in appendix F. This appendix describes the development of user-specified fragility curves for two important long-span bridges in the Shelby County, Tennessee highway system that cross the Mississippi River along Interstate 40 (I-40) and Interstate 55 (I-55) in Memphis. These models have been included in the demonstration SRA of the Shelby County highway system that is described in chapter 7.

G.2 SCOPE

The development of user-specified bridge fragility curves will involve estimation of bridge damage states using detailed engineering evaluation procedures, estimation of traffic states and repair costs for each damage state, and development of the fragility curves. The implementation of these tasks for the I-40 and I-55 crossings of the Mississippi River are summarized below.

G.2.1 Task 1 – Damage States

Under task 1, existing information from past seismic analyses was used to estimate damage states for the I-40 and I-55 crossings (including main spans and approach spans). New seismic analysis was not conducted within in the scope of this work. The resulting damage state estimates were based on each bridge's current condition and configuration, without seismic retrofit. They are given as a function of the level of ground shaking at the site, represented in terms of peak ground acceleration (PGA), and are denoted as "minor", "repairable", and "irrepairable" levels of damage.

Two types of damage state estimates were developed for each bridge. The first, termed structural "element" damage states, considered the structural characteristics and detailing of each bridge's individual structural members, abutments, bearings, and foundations. The second type of damage state, termed "bridge system" damage states, considered the extent, location, and type of element damage throughout the bridge and the redundancy of the damaged elements. Estimation of the overall bridge system damage states was essential for subsequent estimation of bridge traffic states and repair costs under task 2.

The element and system damage-state estimates for the I-40 crossing were based on past experience of the engineers involved in the current seismic retrofit design of the bridge for the Tennessee Department of Transportation. Early in that retrofit project, a detailed seismic analysis of the as-built bridge was performed, in order to identify vulnerable elements requiring seismic retrofit (Imbsen and Associates, 1993). Because the I-40 crossing contains several

distinct "groups" of segments with differing structural characteristics, separate damage states were estimated for each group.

There has been no seismic analysis of the I-55 crossing of the Mississippi River, whose configuration is very different from that of the I-40 crossing. Therefore, damage state estimates for this bridge were based solely on experience and judgment.

G.2.2 Task 2 – Traffic States and Repair Costs

Once the system damage states are established for the I-40 crossing, corresponding traffic states and repair costs were estimated, also as a function of PGA. These estimates were provided for each group along the length of the bridge. For the I-55 crossing, composite traffic states were estimated for the entire bridge, also as a function of PGA. These estimates were based on engineering judgment and past experience with similar bridges. Repair costs for this bridge, which were not estimated during this current effort, will be estimated in the future.

G.2.3 Task 3 – Fragility Curves

Task 3 used the following steps to develop fragility curves for each bridge: (a) engineering estimates of central tendency and dispersion of threshold PGA values for the onset of each traffic state estimated under task 2; (b) review and testing of alternative probability distributions, to assess their ability to represent the estimates from step 1; (c) use of a Beta distribution to develop fragility curves for each bridge; (d) aggregation and simplification of these curves to develop composite fragility curves for each bridge; and (e) review of these curves and, from this review, inclusion of any needed revisions.

G.3 DAMAGE STATE, TRAFFIC STATE, AND REPAIR ESTIMATES FOR I-40 CROSSING

G.3.1 BRIDGE DESCRIPTION

The crossing of the Mississippi River along I-40 is a vital transportation link for interstate traffic. It extends from the St. Francis Levee in Arkansas to Route 240 in Memphis Tennessee. The bridge's main span is a steel tied-arch structure on massive caisson foundations. The total length of the bridge is comprised of several different structural groups, which extend from group A (the westernmost approach to the bridge in Arkansas) to group I (the easternmost approach to the bridge in Memphis). The structural characteristics of each group are as follows (Imbsen and Associates, 1993):

- *Groups A, B, and C.* Precast prestressed girders on concrete caps and columns with four spans of welded steel plate girders over an underlying railroad.

- *Group D.* Welded steel plate girders on concrete columns.

- *Group E.* Welded steel box girders on concrete columns.

- *Group F.* Steel tied arch bridge (two-spans) on large concrete columns (with webwalls) over the Mississippi River.

- *Groups G, H, and I:* Welded steel plate girders on concrete columns and caps.

G.3.2 PRIOR SEISMIC ANALYSIS

As noted earlier, a seismic analysis of the current configuration of the I-40 crossing (groups A through G only) had been carried out by the engineers performing a seismic retrofit of this bridge, during the initial phase of this retrofit design project. The purpose of the analysis was to identify vulnerable elements of the bridge that would be the focus of the seismic retrofit program. The seismic analysis consisted of the following steps (Imbsen and Associates, 1993 and Liu et al., 1994):

- *Seismic Hazard.* Site-specific ground motions were developed corresponding to Design Earthquake Motions (with a probability of exceedance of 10 percent in 50 years) and Contingency Earthquake Motions (with a probability of exceedance of 10 percent in 250 years). Soil amplification effects of the deep soil deposits along the bridge were considered. Design spectra and spatially varying support motion time histories were developed.

- *Structural Models.* Three-dimensional elastic models of the various groups were developed. The models included effects of soil-structure interaction at the abutments and at the foundations along the length of the bridge.

- *Seismic Analysis.* A global analysis of the seismic response of each of the bridge groups was carried out. From this, seismic vulnerabilities were evaluated, retrofit measures were developed, and construction costs were estimated.

G.3.3 EVALUATION PROCEDURE

Damage states, traffic states, and repair costs for the various groups that comprise the I-40 crossing of the Mississippi River were estimated using the following steps.

G.3.3.1 Structural Element Damage States

Results from the prior seismic analysis of the I-40 crossing were used to establish elastic capacity-demand (c/d) ratios for individual structural elements within each group, as a function of PGA. These c/d ratios were interpreted using the damage states shown in table 42, in order to establish structural element damage states.

G.3.3.2 Bridge System Damage States

The element damage states for each PGA level were interpreted for the overall structural system within each bridge group, considering the redundancy of the various elements within the group, and the extent, locations, distribution, and types of damage to these elements.

Table 42. Element-Level Damage States for I-40 Crossing of Mississippi River

Structural Element	Damage State					
	Slight to Minor		Repairable		Irrepairable	
	C/D	Description	C/D	Description	C/D	Description
Columns (Flexure)	1.0 - 0.50	No immediate closure or repair needed.	0.50-0.33	Moderate cracks, hinging, or spalling. Column still structurally sound.	< 0.33	Column structurally unsafe due to severe damage. Replacement required.
Columns (Shear)	1.0 - 0.75	Minor cracking. No immediate closure or repair needed. Repairs cracks by epoxy injection.	0.75-0.50	Cracks widened, but column still has shear capacity. Can epoxy grout cracks.	< 0.50	Loss of concrete shear capacity. Replace column.
Bent Caps with Adequate Shear Reinforcement (Shear)	1.0 - 0.75	Minor cracking. Repair by epoxy injection of cracks (2 days). No immediate repair needed.	0.75-0.50	Cracks widened, but bent cap still has shear capacity.	< 0.50	Loss of concrete shear capacity. Extensive repair or replacement of bent cap.
Bent Caps with Inadequate Shear Reinforcement (Shear)	1.0 - 0.75	Minor cracking. No closure or immediate repair needed.	--	--	< 0.75	Loss of shear capacity. Replace bent cap.
Bent Caps (Flexural)	1.0 - 0.50	No closure or immediate repair needed.	0.50-0.33	Moderate cracks, hinging, or spalling. Bent cap still structurally sound.	< 0.33	Loss of flexural capacity. Extensive repair or replacement of bent cap.
Web Wall[1] (Shear)	1.0 - 0.50	No closure or immediate repair needed.	0.50-0.33	No closure or immediate repair needed.	< 0.33	No closure or immediate repair needed.
Footing (Rocking)	1.0 - 0.50	Minor rocking. No closure or immediate repair needed.	0.50-0.33	Moderate rocking. No closure or immediate repair needed.	< 0.33	Extensive rocking No closure or immediate repair needed.
Bearing	<1.0	Lift bridge. Install new dowels and bearings. No closure needed.	-	-	-	-
Seat Width (Deck Unseating and Dropping)	-	-	-	-	<1.0	Replace fallen deck span Repair expansion joint and bearing damage.

[1]Note that the function of a web wall is to provide lateral stability for wind. It is not a vertical load carrying member.

G.3.3.3 Traffic States

The bridge system damage states for each PGA level were used to assess the functionality of the bridge group, and the ability of the group carry traffic while repairs proceeded.

G.3.3.4 Repair Costs

Repair costs were estimated using repair-cost data previously developed the design of seismic retrofit measures for the I-40 crossing (Imbsen and Associates, 1993). These data were used to establish group-specific unit repair costs for columns, bearings, and other structural elements. Because of differences in structural characteristics of the various groups along the bridge, these unit costs differed from one group to the next. Once the group-specific unit costs were established, the total repair costs at each PGA level in each group were obtained by: (a) counting the total number of each type of structural element in each damage state; and (b) multiplying these by the unit repair costs for that element and damage state.

G.3.3.5 Uncertainties

For each bridge group, threshold PGAs for the onset of each damage state that were estimated from the foregoing procedure were considered to correspond to mean values. Uncertainties in these values were represented in terms of coefficients of variation (CVs) whose estimated values were guided by the following considerations:

- Because the capacity-demand seismic analysis procedure is linear elastic and does not directly account for nonlinear behavior, uncertainties will be least for minor damage (with the least amount of nonlinear behavior) and will be greatest for extensive damage (where nonlinear response will be significant).

- Damage-state assessments using the capacity-demand method are probably conservative, for reasons discussed in FHWA (1995a). Therefore, the uncertainty distributions should be skewed to right; i.e., the median should be to the left of the mean.

- Intuitively, uncertainties will be smallest for simple and regular bridges, and will increase as the complexity and irregularity of the bridge increases. To reduce such uncertainties for the box-girder (group E) and tied-arch segments (group F) of the I-40 crossing, the bridge engineers for the seismic retrofit of this bridge had performed detailed three-dimensional dynamic analyses of these segments.

- For system damage states dominated by damage to concrete members, uncertainties associated with more non-ductile damage modes (e.g., shear damage) will be larger than uncertainties associated with more ductile damage modes (e.g., flexural damage).

- For system damage states dominated by damage to steel members, uncertainties will be less than uncertainties in damage states dominated by damage to concrete members, because of lower uncertainty in steel material properties.

In addition, to guide the designation of CV values for the threshold PGA for each damage level and bridge group, correlations between CV value and estimated uncertainty in the results were established. These correlations are shown in table 43.

Table 43. Use of Coefficient of Variation to Represent Level of Uncertainty in Results

Coefficient of Variation (CV)	Associated Level of Uncertainty
0.2	High degree of confidence in results. Significant amount of supporting test data.
0.4 - 0.5	Reasonable confidence in results. Limited if any test data.
1.0	High uncertainty in results (for complex nonlinear systems). No supporting test data.
>1.0	Extremely high uncertainty for highly nonlinear and very complex systems. No supporting test data.

G.3.4 RESULTS

The results of this process for each of the bridge groups within the I-40 crossing of the Mississippi River are shown in tables 44 and 45. In this, it is noted that group A was not directly included in this evaluation, because its structural characteristics are very similar to those of group B. Therefore, the mean values and CVs of the threshold accelerations for the onset of each damage state for group B are assumed to apply to group A as well, which means that the fragility curves for groups A and B are also assumed to be identical. However, the repair costs shown in table 45 for group A have been assumed to be about 40 percent of the costs for group B, because of the shorter length of group A.

G.4 DAMAGE STATE AND TRAFFIC STATE ESTIMATES FOR I-55 CROSSING

G.4.1 BRIDGE DESCRIPTION

The I-55 crossing is made of the following structures: (a) five cantilever truss spans with span length ranging from 109.7 m. to 242.0 m. (360 ft. to 794 ft.); (b) two Warren truss spans, each with a span length of 132.6 m. (435 ft.); (c) two deck truss spans, each with a length of 52.7 m. (173 ft.); (d) eight steel I-girder spans, each with a length of 25.9 m. (85 ft.); and (e) concrete T-beam trestle spans, with lengths of about 10.7 m. to 18.0 m. (35 ft. to 59 ft.).

Table 44. Uncertainty Estimates for Various Bridge Groups in I-40 Crossing of Mississippi River (page 1 of 3)

Group		Onset of System Damage and Traffic States								
Number	Description	Initial Damage with No Closure to Traffic			Partial Closure to Traffic			Complete Closure to Traffic		
		Description	Mean PGA	CV of PGA	Description	Mean PGA	CV of PGA	Description	Mean PGA	CV of PGA
B	44-span bridge with total length of 765 m (2,510 ft). Superstructure consists of prestressed concrete I-girders, except at piers 55-58 (railroad track overcrossing), where superstructure consists of steel plate girders. Bridge supported on two-column concrete bents with concrete cap and pile foundation. Bronze expansion bearings and fixed elastomeric bearings.	Shear failure of bearing dowel bars at piers 55-58. Minor shear cracking of bent caps at piers 54-57. Moderate flexural cracking of short columns at pier 56. Closed for inspection for 3 days, and then partially open for 1-2 weeks during repairs.	0.10 g	-0.2 +0.2	Bearing dowel bars at piers 54-58 sheared off. Bent caps at piers 55 and 65 lose concrete component of shear strength. Moderate- to-extensive flexural damage to columns in piers 54-57 and 65 (over railway). Closed for inspection/shoring for 3 days. Then, partially open to traffic for 2-4 weeks during repairs.	0.20 g	-0.4 +0.6	Bearing dowels at piers 54-58 and 62-63 sheared off. Some shear damage to bent caps at nearly all piers, with extensive bent cap damage at piers 49-55, 58, 59, and 65. Moderate flexural damage to columns at piers that cross railway. Closed for 1-2 months during repairs (primarily for bent caps.)	0.30 g	-0.5 +0.8
C	18-span prestressed concrete girder bridge with length of 365.8 m (1,200 ft). Deck has two equal-length continuous sections extending from piers W4 to W12 and from piers W12 to W21. Deck supported on 2-column bent piers with web-wall between two columns. Batter pile foundations at columns. Rocker bearings at pier W21, self-lubricated bearings at piers W4 and W12, and fixed elastomeric bearings at all other piers.	Bearings at pier W4 have shear failure of anchor bolts . Minor shear cracking of web wall at pier W4. No closure to traffic.	0.05 g	-0.2 +0.2	At several pier locations, shear failure of anchor bolts minor shear of flexural cracking of bent caps, and moderate-extensive shear damage to columns, and extensive shear damage to web walls. Closed for 1 week for inspection /shoring. Then, partially open to traffic for 2-4 weeks during repairs. More extensive damage of type described above. Closed for inspection/shoring for 1 week. Then partially open to traffic for 4-8 weeks during repairs.	0.10 g 0.15 g	-0.3 +0.6	Extensive flexural and/or shear damage to columns at 7 piers. Complete loss of all columns at 3 piers, leading to loss of deck span. Bent caps fail in shear at piers W11 and W13, and have moderate flexural damage at other piers. Bearing and web wall damage at piers. Relative movement of deck and abutments. Closed for 3-6 months during repairs. More extensive damage of type described above, leading to total loss of bridge. Closed for 5-10 months during replacement.	0.20 g 0.25	-0.5 +0.9

Table 44. Uncertainty Estimates for Various Bridge Groups in I-40 Crossing of Mississippi River (page 2 of 3)

Group		Onset of System Damage and Traffic States								
Number	Description	Initial Damage with No Closure to Traffic			Partial Closure to Traffic			Complete Closure to Traffic		
		Description	Mean PGA	CV of PGA	Description	Mean PGA	CV of PGA	Description	Mean PGA	CV of PGA
D	Steel-girder bridge with 7 spans of 42.7 m (140 ft) length (total length 298.7 m (980 ft)) that extends from piers W21 to W28. Each pier has two 2.1-m (7-ft) diameter columns (with no bent caps) whose heights range from 14.0-18.3 m (46-60 ft) and with 8.5-m (28-ft) high web walls between columns. Batter pile foundations at columns. West end of bridge continuous with Group C and east end continuous with Group E. Rocker bearings at piers W21, W22, W27, and W28, and fixed steel bearings at all other piers.	Shear failure of bearing anchor bolts at all piers. Minor rocking of foundations. No closure to traffic.	0.15 g	-0.2 +0.2	Shear failure of anchor bolts and pintles at bearings. Minor to moderate flexural cracking of columns, minor shear cracking of web walls, and rocking of foundations. Group closed for 3 days for inspection/shoring. Then, partially open to traffic for 2-4 weeks during repairs. More extensive damage of type summarized above. Partially open to traffic for 2-4 weeks during repairs.	0.25 g 0.30 - 0.35 g	-0.3 +0.5 -0.3 +0.5	Extensive flexural damage of all columns at pier W21, leading to loss of deck span. Moderate flexural cracking of columns at other piers, minor shear cracking of web walls, shear failure of anchor bolts and pintles at bearings, and moderate-extensive rocking of pier foundations. Group closed for 3-6 months to replace fallen deck span and repair structural damage.	0.40 g	-0.4 +0.8
E	Main approach structure from Arkansas, just west of tied arch main structure (Group F). Steel box-girder structure has 5 continuous spans with total length of 566.9 m (1,860 ft). Box-girder supports steel floor beam and stringer system and concrete deck. Substructure contains piers with 2 large-diameter concrete columns. Rocker bearings at piers W28 and A that are free to move longitudinally. Steel pile foundation with piles not positively connected to concrete footing .	Bearings at pier W28 have shear failure of anchor bolts . Minor shear cracking of web wall at pier W28. No closure to traffic.	0.15 g	-0.2 +0.2	Possible toppling of rocker bearings at piers W28 and A, causing superstructure to drop and sit on top of pier. Shear failure of other bearings. Minor shear cracking of columns at all piers, and moderate rocking of foundations. Group fully closed to traffic for 1 week for inspection/shoring. Then, partially closed to traffic for 2-4 weeks during structural repairs.	0.35 g	-0.3 +0.5	Extensive damage throughout group. Shear failure of all bearings and extensive rocking of all foundations. Extensive shear cracking of nearly all columns at all piers, possibly leading to loss of deck span. Group fully closed to traffic for 4-8 months during structural repair or replacement.	0.50 g	-0.4 +0.8

Table 44. Uncertainty Estimates for Various Bridge Groups in I-40 Crossing of Mississippi River (page 3 of 3)

Group		Onset of System Damage and Traffic States								
Number	Description	Initial Damage with No Closure to Traffic			Partial Closure to Traffic			Complete Closure to Traffic		
		Description	Mean PGA	CV of PGA	Description	Mean PGA	CV of PGA	Description	Mean PGA	PGA COV
F	Bridge spanning Mississippi River is tied-arch steel structure, with two 274.3-m (900-ft) spans, for total length of 548.6 m (1,800 ft). Structure supported laterally by portal frames with non-redundant truss members and non-redundant bottom lateral braces. Rocker bearings at piers A and C and fixed bearings at pier B. Massive piers consists of two concrete columns with partial- or full-height web walls on deep caisson foundations.	Minor damage to bottom lateral braces that will not affect group's load-carrying capacity. Threshold of local buckling along vertical elements of portal frames. Repairs can be made under traffic with no closure.	0.15 g	-0.2 +0.2	Inelastic deformation due to buckling of some vertical elements of portal frames. Buckling of some non-redundant bottom lateral braces, and tensile damage to other brace elements. Full closure to traffic for up to one week for inspection/shoring. Then, partial closure for 2-4 weeks during repairs.	0.25 g	-0.3 +0.5	Toppling of rocker bearings at pier A, causing superstructure to drop onto pier. (Repairs complicated due to lack of jacking surface.) Major damage to bottom lateral braces. Extensive plastic hinging of portal frame members, requiring installation of temporary bracing above roadway. Closed for 2-4 months during repairs.	0.40 g	-0.5 +0.8
G	12-span steel girder bridge with total length of 676.3 m (2,219 ft), and span lengths ranging from 28.5-71.9 m (93.5-236 ft). Extends from piers C to E12. West end continuous with Group F and east end continuous with Group I. Piers consist of two-column bents with web wall between columns. Heights and stiffnesses of piers vary markedly over length of group. Rocker bearings at piers C, E3, E6, and E12, and fixed bearings at all other piers. Steel or prestressed-concrete pile foundations.	Minor-moderate rocking of foundations. Shear damage to anchor bolts at bearings. Minor flexural cracking of columns. No closure to traffic.	0.10 g	-0.2 +0.2	Shear damage to anchor bolts at bearings and to bent caps. Minor-moderate flexural damage to bent caps and to columns. Minor-moderate foundation rocking. Fully closed to traffic for inspection and shoring for 3 days. Then, partial closure for 2-4 weeks during structural repairs. Same damage types as above, except more extensive. Full traffic closure for 1week, and partial closure for 4-8 weeks during structural repair.	0.15 g 0.20 - 0.25 g	-0.4 +0.6	Extensive column flexural damage at most piers, together with extensive shear or flexural damage to bent caps, leading to possible loss of deck span. Extensive rocking of foundations. Fully closed to traffic for 3-6 months during structural repairs or replacement. Same damage types as above, except more extensive. Fully closed to traffic for 5-10 months during structural repairs or replacement.	0.30 g 0.35 g or more.	-0.5 +0.8

Table 45. Repair Costs for I-40 Crossing of Mississippi River

PGA	Repair Costs (Thousands of Dollars)							
	Group A	Group B	Group C	Group D	Group E	Group F	Group G	Total
0.05 g	$10	$10	$13	$60	$0	$0	$0	$93
0.10 g	$100	$250	$115	$80	$0	$580	$0	$1,125
0.15 g	$150	$380	$1,149	$80	$34	$580	$890	$3,263
0.20 g	$420	$1,300	$2,632	$80	$67	$580	$3,215	$8,294
0.25 g	$600	$1,520	$4,841	$370	$105	$580	$6,260	$14,276
0.30 g	$1,800	$4,640	$6,371	$1,820	$7,574	$580	$11,220	$34,005
0.35 g	$1,800	$4,840	$7,420	$1,820	$8,774	$1,146	$13,560	$39,360
0.40 g	$2,600	$6,450	$7,420	$2,400	$8,774	$6,822	$15,735	$50,201
0.45 g	$2,700	$6,510	$7,420	$2,400	$8,774	$6,822	$15,735	$50,361
0.50 g	$2,700	$6,520	$7,420	$2,400	$8,774	$7,505	$15,735	$51,054

G.4.2 EVALUATION PROCEDURE

In the absence of any seismic analysis of the I-55 crossing (either previously or within the scope of the present effort), experience and judgment were used to estimate damage states for this bridge. Once system damage states were estimated, corresponding traffic states and uncertainties were estimated using procedures similar to those outlined for the I-40 crossing in sections G.3.3.3 through G.3.3.5.

G.4.3 RESULTS

From the foregoing procedure, the seismic vulnerabilities of the I-55 crossing have been evaluated as follows:

- The connections of the bearings to the piers are generally insufficient for transferring seismic inertia load. At low levels of shaking, there is sufficient friction to prevent excessive displacements; however, at PGA levels on the order of 0.25 g, the displacements may be large enough to cause the span to drop, leading to closure of the bridge for about one month.

- Particularly at the common pier between the concrete T-beam span and the steel girder span (pier A10), the upper section of the pier is susceptible to damage from pounding of the steel I-girder and the "half" pier section. Brittle damage from this pounding could occur at PGA levels on the order of 0.25 g, resulting in closure of the bridge for approximately 1-2 months.

- The tall bearings at the truss spans are susceptible to topping at PGA levels on the order of 0.25 g. It is estimated that repair of this damage, which would involve the installation of a jacking frame to jack up the bridge and repair/replace the bearings, would close the bridge for approximately one month.

- In the cantilever spans, the most vulnerable components are the hanger members from which the truss systems are suspended. These non-redundant members are designed only for vertical loads and are very vulnerable to lateral loads. These hangers are very similar to the hangers in the existing truss system in the Benicia-Martinez Bridge east of the San Francisco Bay area. Non-symmetric truck traffic loads imposed on this bridge during widening caused minor torsional vibrations that were nevertheless sufficient to damage the hangers. It is estimated that the seismic-induced transverse loads would cause moderate damage to the hangers at the I-55 crossing at PGA levels of about 0.15 g, and would fail the hangers (with loss of the truss span) at PGA levels of about 0.25 g.

- Rocking response is expected for the un-reinforced masonry piers and foundations, which would tend to reduce the severity of ground shaking. Rocking instability is not expected to be a problem. However, at a higher level of shaking (with PGAs on the order of 0.4 g), it is estimated that the integrity of the masonry piers would become questionable, and that extensive damage to the piers would occur.

- For the concrete trestle spans, the substructure concrete bents (columns, caps, and struts) are very vulnerability for brittle shear failure. These may occur at a relatively low PGA level (with extensive damage at PGA levels on the order of 0.25 g). The detailing and construction of these bents are viewed to be such that they are more vulnerable than any of the vulnerable elements of the I-40 crossing described earlier.

Damage states, traffic states, and estimated uncertainties for the I-55 crossing are provided in table 46. Repair costs for this bridge will be developed in the future.

G.5 FRAGILITY CURVE DEVELOPMENT

G.5.1 PROCEDURE

The iterative procedure used to develop the fragility curves for the I-40 and I-55 crossings of the Mississippi River consists of the six steps summarized below. This procedure has been designed primarily for critical bridge structures where either no seismic response has yet been carried out (e.g., the I-55 crossing) or for which linear elastic methods have been used to evaluate seismic vulnerabilities, even under levels of shaking where the seismic response extends well into the nonlinear range (e.g., the I-40 crossing).

Table 46. Damage States and Traffic States for I-55 Crossing of Mississippi River

Damage State and Traffic State		Threshold PGA	
Traffic State	Damage	Mean Value	Coefficient of Variation
Partial Closure to Traffic	Minor damage to connection of bearings to piers, concrete trestle span bents, and masonry piers, for which repairs can be made without restriction of traffic. Moderate damage to hangers of suspended truss spans, for which repairs can be made with closure of outside lane in each direction, over duration of one week.	0.15 g	-0.3, +0.3
Partial Closure to Traffic	Moderate damage to hangers of suspended truss spans (as noted above). Falling of spans at concrete trestle spans and steel I-girder spans onto bent cap, due to inadequate seat length. Closure of outside lane in each direction for two weeks, to jack up bridge and repair or replace bearings.	0.20 g	-0.3. +0.6
Complete Closure to Traffic	Extensive damage due to dropping of spans at concrete trestle spans and steel I-girder spans onto cap beam, brittle damage at pier A10, toppling of tall bearings at truss spans, and brittle failure at substructures of trestle and I-girder spans. By themselves repair of these damage modes would close bridge for up to two months. However, much more severe damage possibly leading to replacement of bridge (and closure for one-two years) would result from failure of non-redundant hangers from which truss systems of cantilever spans are suspended, which could cause dropping of span into river. Also, possible significant damage to un-reinforced masonry piers.	0.25 g	-0.3, +0.9

G.5.1.1 Step 1 – Expert-Opinion Estimate of Central Tendency and Dispersion

Step 1 involved the use of experienced bridge engineers to estimate: (a) the central tendency of the threshold peak ground acceleration (PGA) for each damage state (e.g., the median or mean values); and (b) the dispersion of these threshold PGAs (i.e., the variation relative to the mean). The dispersion can be represented using the following parameters (Benjamin and Cornell, 1970 and Ayyub and McCuen, 1997).

- *Standard Deviation.* The standard deviation is defined as the square root of the weighted average of the squared deviations from the mean. The standard deviation, and to a lesser extent the mean value, controls the slope of the fragility curve -- which is a key measure of the uncertainty in the threshold PGA for the damage state represented by that curve.

- *Coefficient of Variation (CV).* The CV is defined as the ratio of the standard deviation to the mean. It is useful for comparing the dispersion of random variables with different units or mean values. Table 42 shows approximate correlations of CV with the estimated uncertainty in the results.

- *Coefficient of Skewness (CS).* The CS is a measure of the asymmetry of the distribution. It is defined as the ratio of the third central moment about the mean to the cube of the standard deviation. The CS is important for this application to the I-40 and I-55 crossings, for which it is expected that the mean value of the threshold PGAs will fall below the median (i.e., have a negative CS), to a degree that will depend on the degree of damage to the bridge (see section G.5.2.1).

The implementation of this step for the I-40 and I-55 crossings of the Mississippi River has been described in sections G.3 and G.4.

G.5.1.2 Step 2 – Evaluation of Distribution Families

Step 2 evaluated alternative families of probability distributions, to determine whether they are capable of fitting the expert-opinion estimates of central tendency and dispersion from step 1. For this application, over twenty distribution families were tested. Of these, only the beta, gamma, lognormal, and extreme-value distributions judged to be plausible for modeling the expert-opinion estimates. In this application, the beta distribution has been truncated and shifted to meet some of the testing objectives addressed under step 3.

G.5.1.3 Step 3 – Testing of Distribution

Under step 3, the following "fitting" or "performance" criteria have been used to assess the ability of the beta distribution to represent the engineer's estimates from step 1: (a) check that the mean value and coefficient of variation specified by the user are reasonably represented; (b) check that the resulting standard deviation leads to a slope of the fragility curve that is consistent with the bridge engineer's assessment of the uncertainty in the threshold PGA for the given damage state, relative to that for the other damage states and other bridge groups; (c) check that

the general shape and skewness of the density function is plausible; and (d) check the transitivity for each threshold PGA (which, in this case, involves checking for each PGA that the probability of being in a lower damage and traffic state exceeds the probability of being in a higher damage and traffic state).

G.5.1.4 Step 4 – Aggregations and Simplifications

Because the I-40 crossing consists of several different structural groups with differing seismic vulnerabilities, steps 1 through 3 were used to develop separate sets of traffic-state fragility curves for each group. These separate curve sets for each group were then aggregated into a single set for the entire bridge based on: (a) the fact that the various bridge groups are arranged in series along the length of the bridge; and (b) the premise that sufficient resources can be mobilized after the earthquake to proceed with repairs of all of the bridge groups simultaneously. Therefore, for a given PGA level, the traffic state for the overall bridge will be governed by the worst-case traffic state for any of the bridge groups at that PGA level.

After the aggregated fragility curves for the I-40 crossing were developed in this way, they were represented as a series of straight line segments for which linear coefficients were determined. This step facilitates programming of the curves into the SRA methodology.

For the I-55 crossings, a single set of damage states and traffic states was established for the entire bridge. Therefore, no aggregation of separate fragility curves was required for this bridge. Like the I-40 crossing, fragility curves were represented as a series of straight line segments to facilitate subsequent programming.

G.5.1.5 Step 5 – Review of Preliminary Results with Bridge Engineers

Fragility curves developed from steps 1 through 4 were provided to the bridge engineers for their review.

G.5.1.6 Step 6 – Revision of Results if Necessary

This step involved any necessary revision of the results from steps 1 to 4, based on the review comments received under step 5.

G.5.2 RESULTS

G.5.2.1 Fragility Curves for Individual Groups within I-40 Crossing

The foregoing procedure was used to establish separate traffic-state fragility curves for each bridge group within the I-40 crossing. These are provided in figure 45. Some comments and elaborations on the development of these curves are as follows:

- The fragility curves for each group were checked to assure that the mean PGA for each damage state is suitably lower than the median value, and that the relative slopes of the curves are reasonably consistent with the bridge engineer's assessment of uncertainties.

- As previously stated, it has been assumed that the mean PGAs estimated from the elastic capacity-demand method are a conservative (i.e., low) estimate of the threshold PGAs leading to the onset of each damage state. Therefore, more samples of the population of threshold PGAs should have values larger than the mean, and fewer should have lower values (i.e., the distribution should have a negative skew). Equivalently, the median threshold PGA value for each damage state should be larger than the mean value. In addition, the differences between the mean and median PGAs for each damage state should increase with increasing severity of the damage state, to reflect the greater degree of uncertainty in the damage assessments for the more severe damage states. This latter condition has been somewhat difficult to achieve with the simple two-parameter probability distributions that has been considered.

- The fragility curves developed for each separate group (figures 45a through 45f) show that for all of the groups, the slopes of the fragility curves and the skewness and spread in the distributions generally do increase with increasing damage state.

- The relative slopes of the corresponding damage states among the various groups are not always consistent with the bridge engineer's estimates of the relative degrees of uncertainty for these groups. For example, the slope of the fully-closed-to-traffic fragility curve for groups A and B (assumed to be identical for these groups, for reasons stated in section G.2.4) is flatter than that for group C, even though IAI estimated larger CVs for group C. This is a consequence of the fact that, as indicated in section G.5.1.1, the standard deviation rather than the CV controls the slope of the fragility curve. The fully-closed traffic state curves for group A and B were developed by using a beta distribution with a mean PGA of 0.3 g and a CV of 0.4. This results in a standard deviation of 0.3 g x 0.4 = 0.12 g. The fully-closed traffic state for group C was modeled using a beta distribution with a mean PGA of 0.2 g and a CV of 0.4. This results in a standard deviation of 0.2 g x 0.4 = 0.08 g, which is actually smaller than the standard deviation for group A and B. For this reason, the group A and B fragility curve has a flatter slope.

G.5.2.2 Aggregated Fragility Curves for Entire I-40 Crossing

The above fragility curves for each group were aggregated and simplified using the procedure described in section G.5.1.4. This procedure is further elaborated below:

- It is assumed that sufficient equipment, materials, and manpower resources will be available after an earthquake so that the repair of the entire bridge can be initiated at once. This assumption leads to a lower bound estimate of the total repair time. The resulting traffic state and repair time for the entire bridge (for each level of ground shaking) corresponds to the most severe traffic state and longest repair time estimated for any of the groups. This is a consequence of the groups being oriented in series along the length of the bridge.

- The first step in this process was to overlay the fragility curves for all of the traffic states for all of the groups. Then, the PGA at which each traffic state (open, partially closed, or fully closed) first occurs among any of the groups was noted. This was taken to be the governing traffic state for the overall bridge at that PGA.

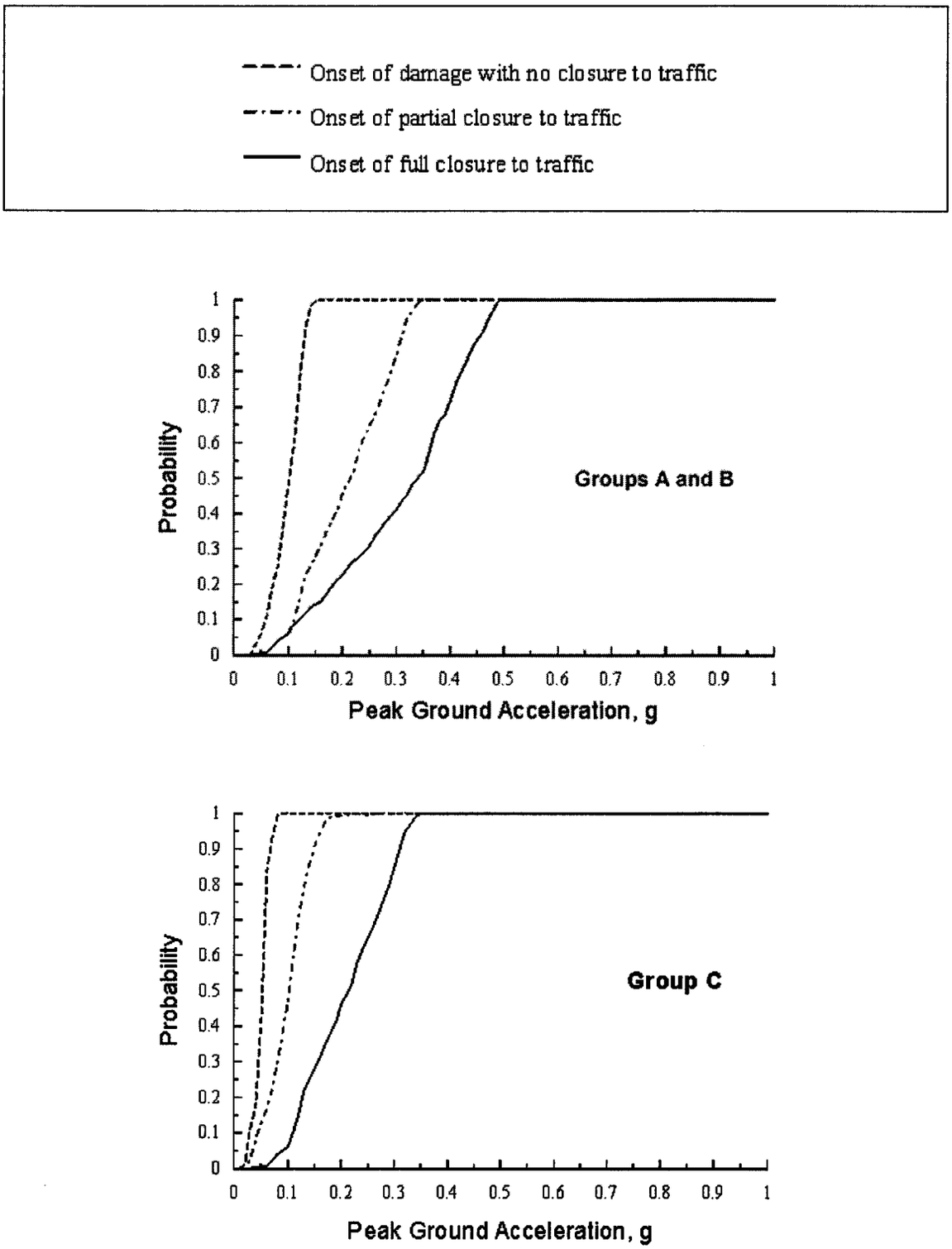

Figure 45. Bridge Group Fragility Curves for I-40 Crossing of Mississippi River

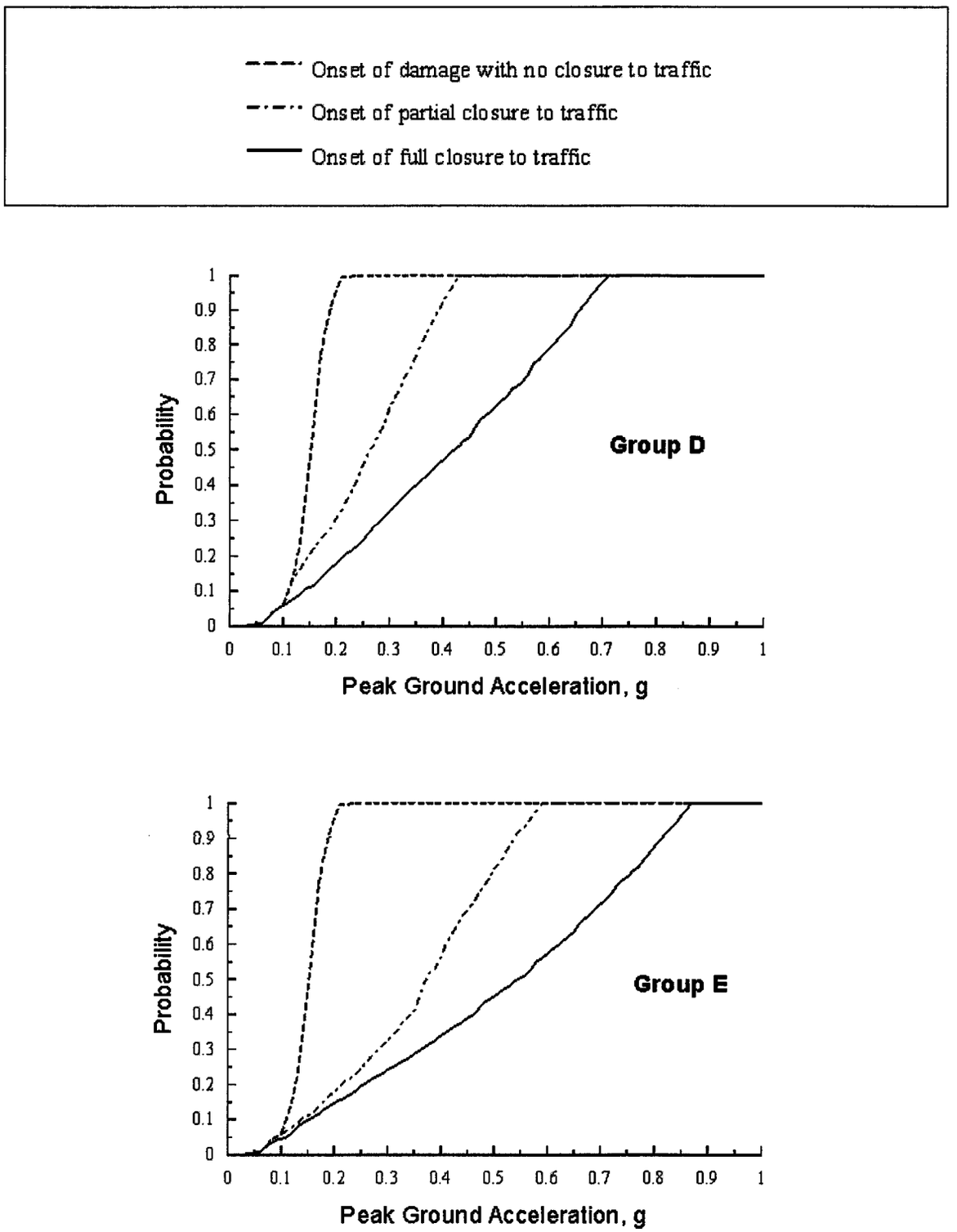

Figure 45. Bridge Group Fragility Curves for I-40 Crossing of Mississippi River (continued)

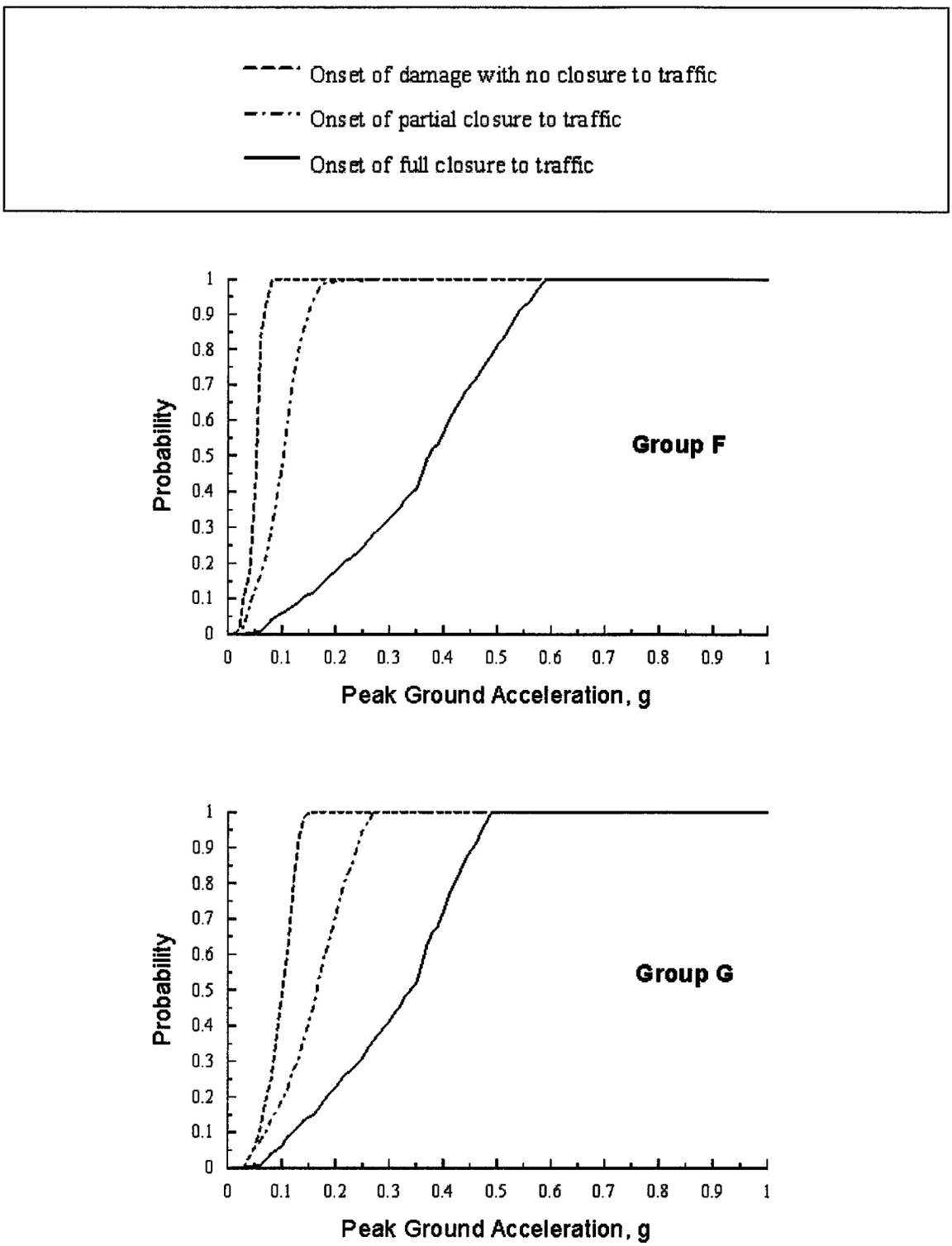

Figure 45. Bridge Group Fragility Curves for I-40 Crossing of Mississippi River (concluded)

- This resulted in the four fragility curves shown in figure 46, which correspond to: (a) the onset of minor damage (with no closure to traffic but with some repair cost); (b) the onset of moderate damage (with partial closure to traffic for 2-4 weeks after the earthquake); (c) the onset of extensive damage (with full closure to traffic for 3-6 months after the earthquake); and (d) the onset of more extensive damage (with full closure to traffic for 5-10 months after the earthquake). All of these governing fragility curves correspond to damage in group C.

- To facilitate the programming of these governing fragility curves, the curves were fitted with a series of straight-line segments. Linear coefficients for each segment are given in table 47.

Table 47. Traffic-State Fragility Curves for I-40 Crossing of Mississippi River (Coefficients A and B in Equation: P = A*PGA + B)

Traffic State	PGA_1(g)	PGA_2(g)	P_1	P_2	A	B
No Traffic Closure	0.00	0.02	0.00	0.00	0.00	0.00
(Onset of Damage, Group C)	0.02	0.05	0.00	0.20	6.67	-0.13
Mean PGA = 0.05 g	0.05	0.06	0.20	0.83	63.00	-2.95
	0.06	0.08	0.83	1.00	8.50	0.32
2-4 Weeks Partial Closure	0.00	0.05	0.00	0.00	0.00	0.00
(Moderate Damage, Group C)	0.05	0.13	0.00	0.80	10.00	-0.50
Mean PGA = 0.10 g	0.13	0.18	0.80	1.00	4.00	0.28
3-6 Months Full Closure	0.00	0.09	0.00	0.00	0.00	0.00
(Extensive Damage, Group C)	0.09	0.13	0.00	0.20	5.00	-0.45
Mean PGA = 0.20 g	0.13	0.34	0.20	1.00	3.81	-0.30
5-10 Months Full Closure	0.00	0.07	0.00	0.00	0.00	0.00
(Extensive Damage, Group C)	0.07	0.475	0.00	1.00	2.50	-0.18
Mean PGA = 0.25 g						

G.5.2.3 Fragility Curves for I-55 Crossing

Table 46 provides the bridge engineer's estimates of mean threshold PGAs and CVs for the onset of minor damage with no closure to traffic, the onset of partial closure, and the onset of complete closure at the I-55 crossing. The corresponding fragility curves were estimating using a beta distribution with the following mean PGAs and CVs: (a) for the onset of the minor damage with no closure to traffic, a mean PGA = 0.15 g and CV = 0.2 was used; (b) for the onset of the damage leading to partial closure to traffic, a mean PGA = 0.20 g and CV = 0.4 was used; and (c) for the onset of the extensive damage leading to full closure to traffic, a mean PGA = 0.25 g and CV = 0.4 was used. These are plotted in figure 47. To facilitate programming of these curves, they were fitted with a series of linear segments with coefficients given in table 48.

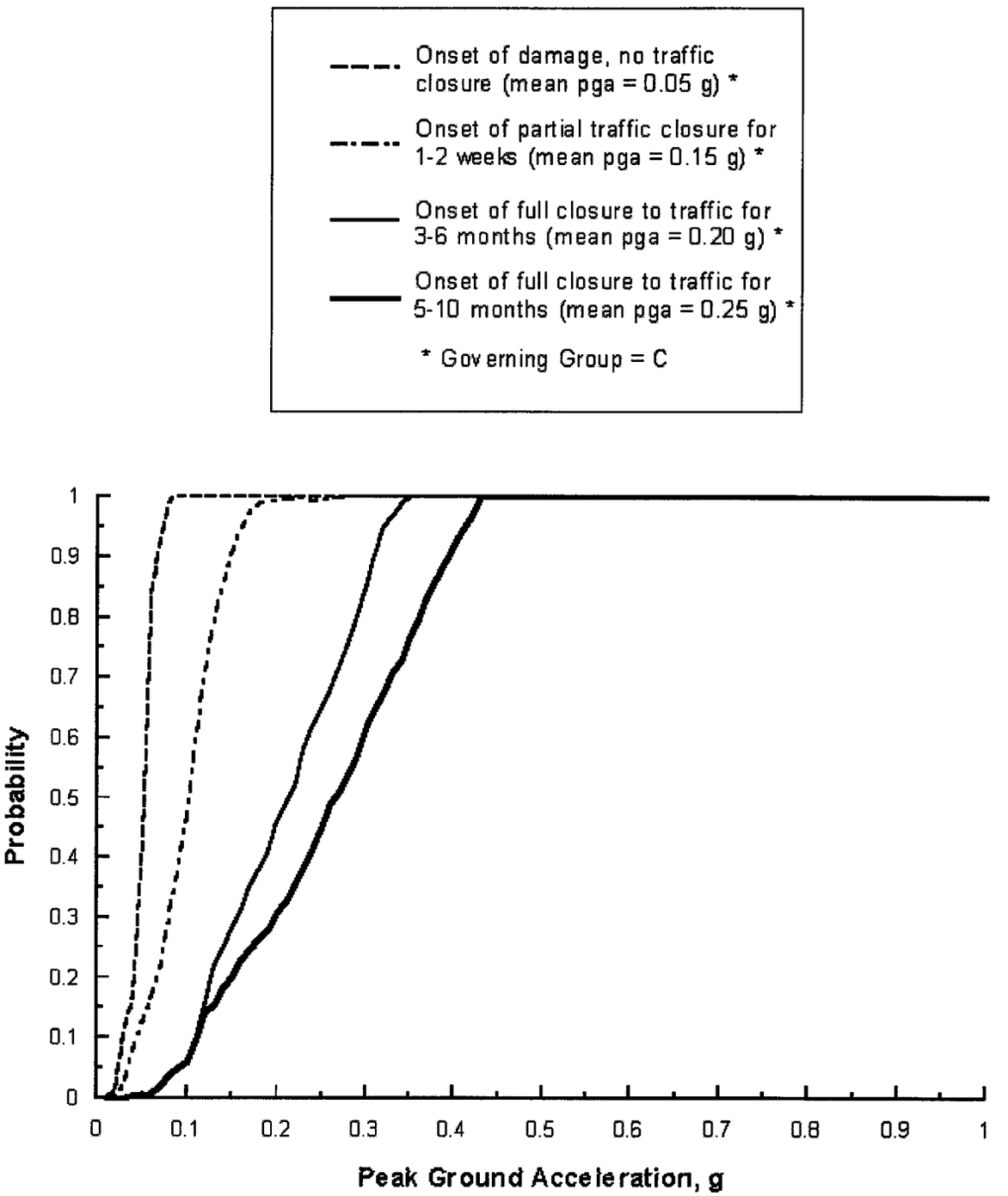

Figure 46. Aggregated Fragility Curves for I-40 Crossing of Mississippi River

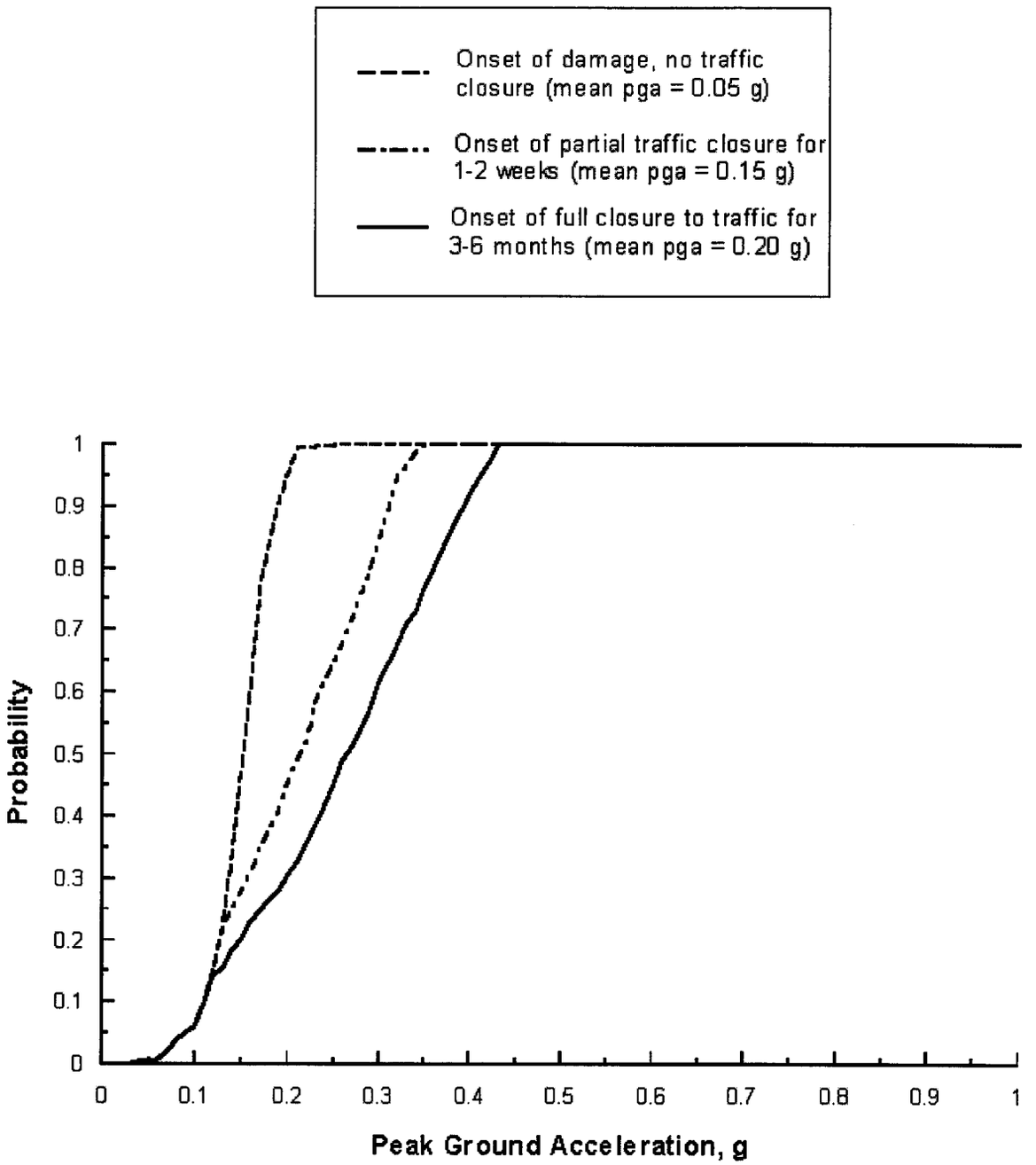

Figure 47. Fragility Curves for I-55 Crossing of Mississippi River

Table 48. Traffic-State Fragility Curves for I-55 Crossing of Mississippi River (Coefficients A and B in Equation: P = A*PGA + B)

Traffic State	PGA_1(g)	PGA_2(g)	P_1	P_2	A	B
No Traffic Closure	0.00	0.07	0.00	0.00	0.00	0.00
(Onset of Damage)	0.07	0.13	0.00	0.20	3.33	-0.23
Mean PGA = 0.15 g	0.13	0.18	0.20	0.80	12.00	-1.36
	0.18	0.23	0.80	1.00	4.00	0.08
1-2 Weeks Partial Closure	0.00	0.07	0.00	0.00	0.00	0.00
Mean PGA = 0.20 g	0.07	0.35	0.00	1.00	3.57	-0.25
Two Years Full Closure	0.00	0.09	0.00	0.00	0.00	0.00
Mean PGA = 0.25 g	0.09	0.45	0.00	1.00	2.78	-0.25

APPENDIX H
FRAGILITY CURVES FOR BRIDGES SUBJECTED TO PERMANENT GROUND DISPLACEMENT

H.1 BACKGROUND

The SRA methodology includes a procedure for obtaining fragility curves for bridges subjected to permanent ground displacement (due to liquefaction, landslide, or surface fault rupture hazards) that is based on the HAZUS algorithm summarized in NIBS (1997).

H.1.1 BRIDGE CLASSIFICATIONS AND DAMAGE STATES

The HAZUS algorithm classes bridges according to whether they are major, continuous, or simply-supported, whether they were seismically designed, and whether they are "high risk" bridges (as defined in section 5.3.3.1 of chapter 5). The algorithm is based on the slight/minor, moderate, extensive, or complete damage states defined in section 5.3.3.2 of chapter 5.

H.1.2 DAMAGE ALGORITHMS AND DEFAULT TRAFFIC STATES

The HAZUS algorithms for estimating bridge damage due to permanent ground displacement are given in table 49. The default traffic states for each damage state are given in table 50.

Table 49. Damage Algorithms for Bridges Subjected to Permanent Ground Displacement (NIBS, 1997)

Bridge Type	Damage State	Median Value of Permanent Ground Displacement, cm. (in.)	Standard Deviation of Permanent Ground Displacement, σ, cm (in)
Seismically Designed*	Slight/Minor	12.7 (5.0)	1.52 (0.6)
	Moderate	20.3 (8.0)	1.52 (0.6)
	Extensive	40.6 (16.0)	1.52 (0.6)
	Collapse	61.0 (24.0)	1.78 (0.7)
Conventionally Designed*	Slight/Minor	12.7 (5.0)	1.52 (0.6)
	Moderate	17.8 (7.0)	1.52 (0.6)
	Extensive	30.5 (12.0)	1.52 (0.6)
	Collapse	45.7 (18.0)	1.78 (0.7)
High Risk (see section 5.3.3.1(c) of chapter 5)	Slight/Minor	10.2 (4.0)	1.52 (0.6)
	Moderate	15.2 (6.0)	1.52 (0.6)
	Extensive	25.4 (10.0)	1.52 (0.6)
	Collapse	35.6 (14.0)	1.78 (0.7)

*For major, continuous, or simply-supported bridges.

Table 50. Default Traffic States for Bridge Damage States given in Table 49

HAZUS Damage State	Repair Procedure		Estimated Traffic State	
	Description	Duration*	Bridge	Underlying Roadway
Slight/Minor	None	None	Fully Open	Fully Open
Moderate	1. Close bridge for inspection and installation of shoring. 2. Repair columns. 3. Repair abutments, bearings, etc.	3 days 3-span bridge: 2-4 weeks 4-span bridge: 2½-5 weeks 5-span bridge: 3-6 weeks	Closed. Partially open to reduced traffic during duration of repairs (see table 11 in chapter 5).	Partially closed (one lane each direction) during cleaning, shoring, column repair operations (2-3 weeks).
Extensive	1. Close bridge for inspection and installation of shoring. 2. Repair columns. 3. Repair abutments, bearings, etc.	1 week 3-span bridge: 4- 8 weeks 4-span bridge: 5 - 10 weeks 5-span bridge: 6 - 12 weeks	Closed. Partially open to reduced traffic during duration of repairs (see table 5-11 in chapter 5).	Partially closed (one lane each direction) during cleaning, shoring, column repair operations (3-4 weeks).
Collapse	Replace Bridge. See table 12 in chapter 5 for summary of repair procedure.	3-span bridge: 3 - 6 months 4-span bridge: 4 - 8 months 5-span bridge: 5 - 10 months	Closed during duration of reconstruction of bridge.	Fully closed during demolition & cleaning (3-6 days). Partially closed (one lane each direction) during cleaning, shoring, column repair operations (4-8 weeks).

*Cut durations in half if critical bridge and repairs are proceeding on basis of incentive bonus and 24-hour per day and 7-days per week schedule as per Caltrans' repair of San Monica Freeway collapses after 1994 Northridge Earthquake.

H.2 INPUT PARAMETERS

The input parameters for this bridge damage state evaluation are as follows:

- *Peak Ground Acceleration (PGA).* The PGA at the bridge site, in units of g, for the given scenario earthquake and simulation.
- *Permanent Ground Displacement (PGD).* The PGD at the bridge site, in units of cm, for the given scenario earthquake and simulation.
- *Bridge Classifications (HAZUS Classification).* The bridge classifications according to type, whether it has been seismically designed, and whether it is high risk, as summarized above and in section 5.3.3.1 of chapter 5.

The PGA and PGD at the bridge site are computed using the seismic hazard models from the hazards module (see chapter 4 and appendices D and E).

H.3 IMPLEMENTATION IN SRA METHODOLOGY

This section outlines the steps for estimating bridge damage states due to permanent ground displacement, based on the HAZUS bridge classifications, damage state definitions, and damage algorithm.

H.3.1 STEP 1 – CHECK FOR ONSET OF BRIDGE DAMAGE

Step 1 screens the *PGD* at the bridge site, as to whether it is sufficient to damage the bridge. In this, if $PGD < 10.2$ cm. (4 in.), it is assumed that the bridge is not damaged by permanent ground displacement.

H.3.2 STEP 2 – CHECK IF BRIDGE DAMAGE STATE = COLLAPSE

Step 2 checks whether or not the bridge is in the collapse damage state due to *PGD*. This consists of the following substeps.

H.3.2.1 Substep 2-1 – Use Damage Algorithm to Obtain Median and Standard Deviation of PGD leading to Onset of Collapse

For the appropriate bridge type, the HAZUS damage algorithm is used to obtain the median value and standard deviation of permanent ground displacement that lead to the onset of collapse (see table 51).

Table 51. Permanent Ground Displacements leading to Onset of Collapse Damage State (NIBS, 1997)

Bridge Structure Type	Median Value of Collapse-Level Displacement, y, cm. (in.), (from table 49)	ln y	Standard Deviation of Collapse-Level Displacement, σ, cm. (in.), (from table 49)
Seismically Designed*	61.0 (24.0)	4.11 (3.18)	1.78 (0.70)
Conventionally Designed*	45.7 (18.0)	3.82 (2.89)	1.78 (0.70)
High Risk	35.6 (14.0)	3.57 (2.64)	1.78 (0.70)

*For major, continuous, or simply-supported bridges.

H.3.2.2 Substep 2-2 – Estimate Value of PGD leading to Onset of Collapse Damage State for this Simulation, Including Uncertainties

The uncertainty equation for this limiting value of *PGD* is represented as follows:

$$\ln y' = \ln y + \varepsilon \tag{101}$$

where

$\ln y'$ is the sample of $\ln y$ to be derived (where y' is the sample value of *PGD* at the onset of the collapse damage state, including uncertainties).

$\ln y$ is the deterministic (median) estimate of the *PGD* at the onset of the collapse damage state, as shown in table 51.

ε is an uncertainty function with an expected value of 0 and a standard deviation of σ, (where σ is given in table 51).

The sample value(s) of y' for this for this normal equation are derived as follows:

a) Pick three uniform random numbers, U_1, U_2, and U_3, each between 0 and 1.

b) Letting

$$V_1 = 2U_1 - 1 \quad \text{and} \quad V_2 = 2U_2 - 1 \tag{102}$$

calculate W as

$$W = (V_1)^2 + (V_2)^2 \tag{103}$$

c) If $W \geq 1$, start over at a). Otherwise, if $W < 1$, let

$$Z = \sqrt{\frac{-2\ln W}{W}} \tag{104}$$

and compute

$$X_1 = V_1 \quad \text{and} \quad X_2 = V_2 Z \tag{105}$$

d) If $U_3 < 0.5$, set $X = X_1$. Otherwise, set $X = X_2$. (Note: retain X in the event that we need to go beyond step 3 for the bridge structure in question.)

e) Calculate the value of PGD leading to the onset of the collapse damage state, including uncertainties. Denoting this value as y', we use equation 101 to calculate

$$\ln y' = \ln y + X\sigma \tag{106}$$

where, as noted above, $\ln y$ and σ are given in table 51. From this, y' is obtained as

$$y' = \exp^{\ln y + X\sigma} \tag{107}$$

H.3.2.3 Substep 2-3 – Determine if Bridge is in Collapse Damage State

In this final substep of step 2, PGD (the permanent ground displacement computed for the given scenario earthquake and simulation) is compared to y' (the value of the permanent ground displacement leading to the onset of collapse for this simulation). If

$$PGD \geq y' \tag{108}$$

the bridge is in the collapse damage state. Otherwise, the bridge is in a less severe damage state, and we proceed to step 3.

H.3.3 STEP 3 – CHECK IF BRIDGE DAMAGE STATE = EXTENSIVE

Step 3 checks whether or not the bridge is in the extensive damage state due to PGD. This consists of the following substeps.

H.3.3.1 Substep 3-1 – Use Damage Algorithm to Obtain Median and Standard Deviation of PGD leading to Onset of Extensive Damage

For the appropriate bridge type, the HAZUS damage algorithm is used to obtain the median value and standard deviation of permanent ground displacement that lead to the onset of extensive damage, and compute the natural logarithm of the median value (see table 52).

Table 52. Permanent Ground Displacements leading to Onset of Extensive Damage State (NIBS, 1997)

Bridge Structure Type	Median Value of Extensive-Damage Level Displacement, y, cm. (in.) (from table 49)	ln y	Standard Deviation of Extensive-Damage Level Displacement, σ, cm. (in.) (from table 49)
Seismically Designed*	40.6 (16.0)	3.70 (2.77)	1.52 (0.60)
Conventionally Designed*	30.5 (12.0)	3.42 (2.48)	1.52 (0.60)
High Risk	25.4 (10.0)	3.23 (2.30)	1.52 (0.60)

*For major, continuous, or simply-supported bridges.

H.3.3.2 Substep 3-2 – Estimate Value of PGD Leading to Onset of Extensive Damage State for this Simulation, Including Uncertainties

As for the prior development for the collapse damage state, the uncertainty equation for this limiting value of PGD is represented as follows:

$$\ln y' = \ln y + \varepsilon \qquad (101)$$

where

$\ln y'$ is the sample of $\ln y$ to be derived (where y' is the sample value of PGD at the onset of the extensive damage state, including uncertainties)

$\ln y$ is the deterministic (median) estimate of the PGD at the onset of the extensive damage state, as shown in table 52.

ε is an uncertainty function with an expected value of 0 and a standard deviation of σ, (where σ is given in table 52).

The sample value(s) of y' for this for this normal equation is derived by repeating the process previously outlined in paragraphs a) through e) of substep 2-2 for the collapse damage state (sec. H.3.2.2). Alternatively, it may be decided to deploy the same value of X that is determined for the collapse state in paragraph d) of substep 2-2, and then compute $\ln y'$ and y' using equations 106 and 107 in paragraph e) of substep 2-2, i.e.

$$\ln y' = \ln y + X\sigma \qquad (106)$$

where, as noted above, $\ln y$ and σ for the extensive damage state are given in table 52, and

$$y' = \exp^{\ln y + X\sigma} \quad (107)$$

H.3.3.3 Substep 3-3 – Determine if Bridge is in Extensive Damage State

In this final substep of step 3, *PGD* (the permanent ground displacement computed for the given scenario earthquake and simulation) is compared to y' (the value of the permanent ground displacement leading to the onset of extensive damage for this simulation). If

$$PGD \geq y' \quad (108)$$

the bridge is in the extensive damage state. Otherwise, the bridge is in a less severe damage state, and we proceed to step 4.

H.3.4 STEP 4 – CHECK IF BRIDGE DAMAGE STATE = MODERATE

Step 4 checks whether or not the bridge is in the moderate damage state due to *PGD*. This consists of the following substeps.

H.3.4.1 Substep 4-1 – Use Damage Algorithm to Obtain Median and Standard Deviation of PGD leading to the Onset of Moderate Damage

For the appropriate bridge type, the HAZUS damage algorithm is used to obtain the median value and standard deviation of permanent ground displacement that lead to the onset of moderate damage, and compute the natural logarithm of the median value (see table 53).

Table 53. Permanent Ground Displacements leading to Onset of Moderate Damage State (NIBS, 1997)

Bridge Structure Type	Median Value of Moderate-Damage Level Displacement, y, cm. (in.) (from table 49)	ln y	Standard Deviation of Moderate-Damage Level Displacement, σ, cm. (in.) (from table 49)
Seismically Designed*	20.3 (8.0)	3.01 (2.08)	1.52 (0.60)
Conventionally Designed*	17.8 (7.0)	2.88 (1.95)	1.52 (0.60)
High Risk	15.2 (6.0)	2.72 (1.79)	1.52 (0.60)

*For major, continuous, or simply-supported bridges.

H.3.4.2 Substep 4-2 – Estimate Value of PGD leading to Onset of Moderate Damage State for this Simulation, Including Uncertainties

This substep is identical to substeps 2-2 and 3-2 of the procedure for evaluating whether the bridge is in the collapse and extensive damage states (see sections H.3.2.2 and H.3.3.2). The end result of this step is the PGD value leading to the onset of the moderate damage state, including uncertainties, for this simulation. As before, this quantity is denoted as y'.

H.3.4.3 Substep 4-3 – Determine if Bridge is in Moderate Damage State

In this final substep of step 4, PGD (the permanent ground displacement computed for the given scenario earthquake and simulation) is compared to y', as obtained in substep 4-2. If

$$PGD \geq y' \tag{108}$$

the bridge is in the moderate damage state. Otherwise, the bridge is in a less severe damage state, and we proceed to step 5.

H.3.5 Step 5: Check if Bridge Damage State = Slight/Minor

Step 5 checks whether or not the bridge is in the slight/minor damage state due to PGD. From table 49, it is seen that traffic on the bridge is unaffected if the bridge is in this damage state. Therefore, the ability of the system to accommodate traffic flows after an earthquake is will be the same, regardless of whether the bridge is undamaged or is in the slight/minor damage state. However, some moderate repair costs will be incurred if the bridge damage is slight/minor, and this will affect overall economic losses due to damage to the highway system. For this reason, the use of step 5 to assess whether the bridge is undamaged or has suffered slight/minor damage is necessary, and is carried out as summarized below.

H.3.5.1 Substep 5-1 – Use Damage Algorithm to Obtain Median and Standard Deviation of PGD leading to Onset of Slight/Minor Damage

For the appropriate bridge type, the HAZUS damage algorithm is used to obtain the median value and standard deviation of permanent ground displacement that lead to the onset of slight/minor damage, and compute the natural logarithm of the median value (see table 54).

H.3.5.2 Substep 5-2 – Estimate Value of PGD leading to Onset of Slight/Minor Damage State for this Simulation, Including Uncertainties

This substep is identical to substeps 2-2, 3-2, and 4.2 of the procedure for the collapse, extensive, and moderate damage states (see sections H.3.2.2, H.3.3.2, and H.3.4.2). Therefore, the end result of this step is the PGD value leading to the onset of the slight/minor damage state, including uncertainties, for this simulation. As before, this quantity is denoted as y'.

Table 54. Permanent Ground Displacement leading to Onset of Slight/Minor Damage State (NIBS, 1997)

Bridge Structure Type	Median Value of Slight/Minor Damage-Level Displacement, y, cm. (in.) (from table 49)	ln y	Standard Deviation of Slight/Minor-Damage Level Displacement, σ, cm. (in.) (from table 49)
Seismically Designed*	12.7 (5.0)	2.54 (1.61)	1.52 (0.60)
Conventionally Designed*	12.7 (5.0)	2.54 (1.61)	1.52 (0.60)
High Risk	10.2 (4.0)	2.32 (1.39)	1.52 (0.60)

*For major, continuous, or simply-supported bridges.

H.3.5.3 Substep 5-3 – Determine if Bridge is in Slight/Minor Damage State

In this final substep of Step 5, *PGD* (the permanent ground displacement computed for the given scenario earthquake and simulation) is compared to y', as obtained in substep 5-2. If

$$PGD \geq y' \tag{108}$$

the bridge is in the slight/minor damage state. Otherwise, the bridge is undamaged.

MULTIDISCIPLINARY CENTER FOR EARTHQUAKE ENGINEERING RESEARCH

A National Center of Excellence in Advanced Technology Applications

University at Buffalo, State University of New York
Red Jacket Quadrangle ▪ Buffalo, New York 14261-0025
Phone: 716/645-3391 ▪ Fax: 716/645-3399
E-mail: mceer@acsu.buffalo.edu ▪ WWW Site: http://mceer.buffalo.edu

University at Buffalo *The State University of New York*

ISSN 1520-295X